A non-invasive analysis of the structure and function of human multi-segmental muscle

Darryl John McAndrew
University of Wollongong

A NON-INVASIVE ANALYSIS OF THE STRUCTURE AND FUNCTION OF HUMAN MULTI-SEGMENTAL MUSCLE

A thesis submitted in fulfilment of the

requirements for the award of the degree

DOCTOR OF PHILOSOPHY

from

UNIVERSITY OF WOLLONGONG

By

DARRYL JOHN MCANDREW *B.Sc. (UoW)*

SCHOOL OF HEALTH SCIENCES

2008

Certification

I, Darryl John McAndrew, declare that this thesis, submitted in fulfilment of the requirements for the award of Doctor of Philosophy, in the School of Health Sciences, University of Wollongong, is wholly my own work unless otherwise referenced or acknowledged. The document has not been submitted for qualifications at any other academic institution.

Darryl John McAndrew

15 December 2008

Acknowledgments

I would like to acknowledge the help given by all those in the former Department of Biomedical Science (now School of Health Sciences) and Graduate School of Medicine. In particular I would like to thank my primary supervisor Dr. Mark Brown, and my secondary supervisor Associate Professor Peter McLennan for their supervision and guidance, both in the production of this thesis and in my professional development throughout my employment with the University. I also wish to thank Mr. Mario Solitro and Mr Mark Andrews, who without their technical support this research would not have been possible. Thanks also to my fellow postgraduate students Dr. James Wickham, Dr. Mark Gorelick, Mr. Nick Rosser, Ms. Katherine Phillips and Ms. Laurel Snelson for their valued input and assistance during the data collection and to all persons who acted as the subjects involved in this thesis.

To Mum and Dad, I thank you for your never ending support, encouragement and belief, not only through my university years but through my entire upbringing. Without your support I may not have taken the education path and ended up where I am today.

Finally, and without doubt most importantly, I would like to thank my beautiful wife Susan, whose endless love and commitment has kept me sane during this project. For her patience during the long hours spent on this endeavour and for putting up with my frequent fits of despair, I shall be forever grateful. To Cooper and Miles, my children, thank you for providing the urge that was greatly needed to get the manuscript finished.

Thesis Organisation

Chapter 1 provides a general introduction to the thesis and specifically states the research objectives.

Chapter 2 reviews the relevant literature, including an overview of muscle fibre types, spatial distribution and contractile physiology, evidence for functional differentiation and research that specifically investigated non-invasive measurements of contractile properties.

Chapter 3 details the techniques used to determine the Tensiometric, Mechanomyographic and Myoelectric measures of muscle performance.

Chapter 4 describes experiments that validated the Laser-MMG technique for the detection of changes in muscle contractile properties induced by physiological modulators of muscle performance (temperature and fatigue). Confirmation of the Laser-MMG technique to detect the contractile properties of multiple muscle segments contained within a single animal muscle is also contained within.

Chapter 5 describes two experiments that examined the contractile properties of muscle segments within human multi-segmental muscles, for the purpose of matching contractile properties to functional roles. This chapter has been published in the Journal of Musculoskeletal Research.

Chapter 6 describes an experiment that examined the neuromotor control of 14 superficial muscle segments surrounding the shoulder during movements at different speeds.

Chapter 7 provides a summary and synthesis of the results from the three experimental chapters and draws conclusions regarding the spatial distribution of muscle fibres within multi-segmental muscle and their neuromotor control based on the objectives outlined in Chapter 1. Recommendations for future research and acknowledgment of experimental limitations are also made.

Table of Contents

Certification i

Acknowledgments ii

Thesis Organisation iii

Table of Contents iv

List of Figures ix

List of Tables xiii

Abbreviations xiv

List of Publications xv

Abstract xvi

CHAPTER 1 INTRODUCTION 19

CHAPTER 2 LITERATURE REVIEW 27

2.1 Muscle fibre types and contractile physiology 28

2.2 Distribution of muscle fibre types 30

2.3 Activation of muscle 31

2.4 Control of muscle activation 32

2.5 Effect of movement speed on muscle activation patterns 35

2.6 Evidence for functional differentiation within skeletal muscle 36

2.7 Functional role of muscle segments 37

2.8 Muscle coordination / synergy 39

2.9 Non-invasive measurement of muscle contractile properties – Mechanomyography (MMG) 40
2.10 Electromyography (EMG) 44
2.11 Musculoskeletal functional anatomy 45
2.12 Justification of research direction 50

CHAPTER 3 GENERAL METHODS 51

3.1 Introduction 52
3.2 Mechanomyography (MMG) 52
3.2.1 MMG laser sensor 53
3.2.2 Neuromuscular Stimulation 53
3.2.3 Animal muscle preparation 53
3.2.4 Simultaneous measurement of Laser-MMG & Tensiometry (Animal studies) 54
3.2.3 Laser-MMG waveform analysis 56
3.3 Tensiometry 58
3.3.1 Force transducer 58
3.3.2 DC Amplifier 59
3.3.3 Tension waveform analysis 59
3.4 Electromyography (EMG) 60
3.4.1 Surface Electrodes 60
3.4.2 Myoelectric Amplifiers 62
3.4.3 Myoelectric signal analysis 62

CHAPTER 4 VALIDATION OF MECHANOMYOGRAPHY I: SENSITIVITY TO PHYSIOLOGICAL MODULATORS OF MUSCLE CONTRACTILE PROPERTIES 65

4.1 Introduction 66

4.1 Introduction 66

4.2 Aims and Hypotheses 68

4.3 Methods 70

4.3.1 Study A: Laser-MMG response to a change in muscle temperature 70

4.3.2 Study B: Laser-MMG response to a change in muscle fatigue 72

4.3.3 Study C: Laser-MMG response to a change in muscle segment fibre type 74

4.4 Results 78

4.4.1 Study A: Laser-MMG response to a change in muscle temperature 78

4.4.2 Study B: Laser-MMG response to a change in muscle fatigue 86

4.4.3 Study C: Laser-MMG response to a change in muscle segment fibre type 93

4.5 Discussion 100

4.5.1 Study A - Temperature 100

4.5.2 Study B – Fatigue 102

4.5.3 Study C – Fibre Type 105

CHAPTER 5 VALIDATION OF MECHANOMYOGRAPHY II: QUANTIFICATION OF HUMAN MUSCLE SEGMENT CONTRACTILE PROPERTIES 109

5.1 Introduction 110

5.2 Aims and Hypotheses 112

5.3 Study D: Contractile properties of segments within gluteus maximus 113

5.3.1 Methods – Gluteus Maximus 113
5.3.1.1 Experimental design 113
5.3.1.2 Subjects 113
5.3.1.3 Muscle segment identification 113
5.3.1.4 Equipment 115
5.3.1.5 Experimental set-up 115
5.3.1.6 Percutaneous neuromuscular stimulation 116
5.3.1.7 Laser-MMG data analysis 117
5.3.1.8 Statistical analysis 117
5.3.1.9 Ethics 118
5.3.2 Results – Gluteus Maximus 119
5.3.2.1 General muscle description and summary of results 119
5.3.2.2 Within muscle segment analysis: (medial to lateral portions) 119
5.3.2.3 Between muscle segment analysis: (superior to inferior segments) 120
5.4 Study E: Contractile properties of multi-segmental shoulder muscles 124
5.4.1 Methods – Multi-segmental Muscle 124
5.4.1.1 Experimental design 124
5.4.1.2 Subjects 124
5.4.1.3 Muscle segment identification 124
5.4.1.3 Equipment 129
5.4.1.4 Experimental set-up 129
5.4.1.5 Percutaneous neuromuscular stimulation 129
5.4.1.6 Laser-MMG data analysis 130
5.4.1.7 Statistical analysis 130
5.3.2.9 Ethics 130
5.4.2 Results – Multi-segmental Muscle 131
5.4.2.1 General muscle description and summary of results 131
5.4.2.2 Between segment analysis of contractile properties 136
5.5 Discussion 144

CHAPTER 6 THE INFLUENCE OF FIBER-TYPE ON THE NEUROMOTOR CONTROL OF HUMAN SHOULDER MUSCLE SEGMENTS..... 149

6.1 Introduction 150

6.2 Aims and Hypotheses 152

6.3 Methods – Study F 153

6.4 Results 159

6.5 Discussion 172

6.5 Discussion 173

CHAPTER 7 GENERAL DISCUSSION, LIMITATIONS AND CONCLUSION ... 185

General Discussion 186

Limitations 199

Conclusion 201

REFERENCES 202

APPENDIX A 221

MMG laser site and Microelectrode site identification 221

List of Figures

Figure 3.1 Gastrocnemius muscle of the toad attached to the test rig 54
Figure 3.2 Neuromuscular stimulation 56
Figure 3.3 Quantification of the Laser-MMG waveform 58
Figure 3.4 Quantification of the Tension waveform 60
Figure 3.5 Bipolar microelectrode 61
Figure 3.6 Myoelectric and Force variables 64
Figure 4.1 Diagram of the medial gastrocnemius attached to rat lower limb. 75
Figure 4.2 Parabolic waveforms representing A: Laser-MMG and B: tension in response to electrical stimulation at different thermal states 78
Figure 4.3 Laser-MMG and Tensiometric waveforms A: 15ºC, B: 20ºC, and C: 25ºC 79
Figure 4.4 Changes in max. displacement and tension due to effect of temperature. ... 81
Figure 4.5 Normalised contraction time, relaxation time and sustain time measures for each muscle temperature 82
Figure 4.6 A: Correlation between Laser-MMG Dmax and Tensiometric Tmax for the medial gastrocnemius. 84
Figure 4.7 Correlation between Laser-MMG tc*N* and Tensiometric tc*N* for the medial gastrocnemius. 84
Figure 4.8 Correlation between Laser-MMG tr*N* and Tensiometric tr*N* for the medial gastrocnemius 85
Figure 4.9 Correlation between Laser-MMG ts*N* and Tensiometric ts*N* for the medial gastrocnemius 85
Figure 4.10 Parabolic waveform output from A: Laser-MMG and B: Tensiometry technique pre- and post-fatigue task 86
Figure 4.11 Laser-MMG and Tensiometric waveform output at A: Pre- fatigue and B: Post- fatigue 87
Figure 4.12 Changes in A: maximal displacement and B: maximal tension due to the repetitive stimulation task. 88
Figure 4.13 tc*N*, tr*N* and ts*N* values for the pre- and post-stimulation task A: Laser-MMG and B: Tensiometry. 89

Figure 4.14 Maximal rate of contraction and relaxation for the pre and post stimulation task, measured by A: Laser-MMG and B: Tensiometry. 89
Figure 4.15 Relationship between Dmax and Tmax for the medial gastrocnemius. 90
Figure 4.16 The relationship between Tensiometry and Laser-MMG for A: tc*N* B: tr*N* 91
Figure 4.17 The correlation between Tensiometry and Laser-MMG for A: maximal rate of contraction B: maximal rate of relaxation 92
Figure 4.18 Pictures taken through Image Pro software of proximal and distal muscle segments. 93
Figure 4.19 Muscle fibre types 94
Figure 4.20 Waveforms from the distal and proximal muscle segments of the medial gastrocnemius when measured by the A: Laser-MMG. B: Tensiometry.... 94
Figure 4.21 Laser-MMG and Tensiometric waveform output from A: distal muscle segment. B: proximal muscle segment 95
Figure 4.22 Differences in A: Dmax and B: Tmax for the distal & proximal segments. 96
Figure 4.23 tc*N*, tr*N* and ts*N* of the distal and proximal segments normalised for the degree of A: displacement and B: tension..... 97
Figure 4.25 Relationship between Dmax and Tmax for the medial gastrocnemius..... 98
Figure 4.26 Relationship for A: tc*N*; B: tr*N* and C: ts*N* when measured by the Laser-MMG and the Tensiometer for the medial gastrocnemius..... 99
Figure 5.1 Posterior view of the left hip, identifying the location of superficial cranial-, middle- and caudal- muscle segments of the gluteus maximus muscle..... 114
Figure 5.2 The Laser-MMG technique..... 116
Figure 5.3 Representative MMG waveforms from the three segments of the gluteus maximus (medial portions). 121
Figure 5.4 Maximal displacement (Dmax) values for each segment (all subjects)..... 121
Figure 5.5 Normalised contraction time (tc*N*), relaxation time (tr*N*), and sustain time (ts*N*) of the cranial, middle and caudal segments. 122
Figure 5.6 Illustration of lateral view of the shoulder musculature showing the muscle segments within the three superficial shoulder muscles. 125
Figure 5.7 Schematic representation of the pectoralis major muscle showing the Laser-MMG recording sites 126

Figure 5.8 Schematic representation of the deltoid muscle showing the Laser-MMG recording sites 127
Figure 5.10 Dmax values for each muscle segment. 133
Figure 5.11 Normalised contraction time (tc*N*) for each muscle segment. 134
Figure 5.12 Normalised relaxation time (tr*N*) and sustain time (ts*N*) for each muscle segment. 135
Figure 5.13 Dmax values for all muscle segments 136
Figure 5.14 tc*N* values for all muscle segments 137
Figure 5.15 tr*N* values for all muscle segments 138
Figure 5.16 ts*N* values for all muscle segments 138
Figure 5.17 Maximal rates of contraction for all muscle segments 139
Figure 5.18 Maximal rates of relaxation for all muscle segments 139
Figure 5.19 The average maximal displacement (Dmax) of each pectoralis major segment (all subjects) 141
Figure 5.20 The average maximal displacement (Dmax) of each segment of the deltoid (all subjects). 142
Figure 5.21 The average maximal displacement (Dmax) of each segment of the latissimus dorsi (all subjects). 143
Figure 6.1 PVC arm cast 154
Figure 6.2 The force/time program display 155
Figure 6.3 View of the pectoralis major, deltoid and latissimus dorsi muscles showing the electromyographic microelectrodes attached to a subject 156
Figure 6.4 Experimental set-up 156
Figure 6.5 Muscle segment On*N* at all MT 162
Figure 6.6 Muscle segment OnN%MT at all MT 163
Figure 6.7 Muscle segment Pk*N* at all MT 165
Figure 6.8 Muscle segment Dur*N*% at all MT 165
Figure 6.9 Muscle segment iEMG*N*% at all MT 166
Figure 6.10 Electromyographic intensity (iEMG*N*%) of muscle segments averaged across all speeds of movement. 167

Figure 6.11 Muscle segment On, Pk, Dur and Off for the 700ms MT (medium speed of movement). 168
Figure 6.12 Onset (On*N*) time for all muscle segments during the 700ms MT condition (medium speed of movement)..... 169
Figure 6.13 Segment onset, peak and duration compared to force onset, peak and duration for the 1500 ms MT (slow)..... 174
Figure 6.14 Segment onset, peak and duration compared to force onset, peak and duration for the 300 ms MT (fast)..... 175
Figure 6.15 Illustration showing a muscle segments contraction time (tc*N*) and order of electromyographic activation (Onset) during the 700ms MT condition.... 181

List of Tables

Table 2.1 A selection of studies from the literature reporting fibre-type composition of the medial gastrocnemius muscle of the rat. 46

Table 4.1 Summary table of results for each measurement technique and muscle temperature..... 80

Table 4.2 Summary table for each measurement technique and muscle condition 87

Table 4.3 Summary table of results from the Laser-MMG and Tensiometry methods for each muscle segment. 95

Table 5.1 Group mean data for Laser-MMG variables..... 119

Table 5.2 MMG variables for the three muscle segments..... 120

Table 5.3 Segment mean values for each MMG variable. 132

Table 6.1 Muscle segment mean values for each EMG variable at the slow (1500 ms), medium (700 ms) and fast (300 ms) MT. 160

Abbreviations

Abbreviation	Term
Cm	centimetre
CNS	central nervous system
CSA	cross sectional area
ºC	degrees Celsius
Dur	electromyographic duration
Dur*N*%	normalised electromyographic duration
Dmax	maximum displacement
EMG	electromyography
Fall	maximal rate of relaxation
FcOn	force onset
FcOff	force offset
FcPk	force peak
FDT	force development time
FT	fibre type
iEMG*N*%	normalised integrated EMG
Int	electromyographic intensity
Kg	kilogram
kHz	kilohertz
MDL	muscle displacement laser
mm	millimetre
MMG	mechanomyography
ms	millisecond
MT	movement time
mv	millivolt
MVC	maximum voluntary contractions
On	electromyographic onset
On*N*	normalised electromyographic onset
Pk	electromyographic peak
Pk*N*	normalised electromyographic peak
Rise	maximal rate of contraction
Tc	contraction time
tc*N*	normalised contraction time
TEN	Tensiometry
Tmax	maximum Tension
Tr	relaxation time
tr*N*	normalised relaxation time
Ts	sustain time
ts*N*	normalised sustain duration

List of Publications

The publications listed below are associated with the research conducted as part of this thesis.

Published Articles

McAndrew, D.J., Gorelick, M. and Brown, J.M.M. (2006). Muscles within muscles: A mechanomyographic analysis of muscle segment contractile properties within human gluteus maximus. *Journal of Musculoskeletal Research* **10**(1): 23-35.

McAndrew, D.J., Rosser, N. and Brown, J.M.M. (2006). Mechanomyographic measures of muscle contractile properties are influenced by the duration of the stimulatory pulse. *Journal of Applied Research.* **6**(2): pp 142-152

Conference Proceedings

McAndrew, D.J. and Brown, J.M.M. (2004). Muscles within muscles, inter- and intra-muscle segment coordination. *Proceedings of the Australian Association of Exercise and Sports Science Inaugural Conference*, Brisbane, Australia.

McAndrew, D.J., Gorelick, M. and Brown, J.M.M. (2004). Muscle belly displacement as a measure of fatigue. *Proceedings of the Australian Association of Exercise and Sports Science Inaugural Conference*, Brisbane, Australia.

McAndrew, D.J., Rosser, N., Gorelick, M., Phillips, K. and Brown, J.M.M. (2005). Mechanomyography for non-invasive clinical diagnosis in musculoskeletal rehabilitation. *Proceedings of the 4th International Cyberspace Conference on Ergonomics*, Johannesburg, South Africa.

McAndrew, D.J., Gorelick, M. and Brown, J.M.M. (2006). Mechanomyography for clinical decision making in exercise physiology practice. *Proceedings of the Australian Association of Exercise and Sports Science Conference,* Sydney, Australia.

Abstract

The Central Nervous System (CNS) exerts extensive control over muscle activation in order to produce accurate voluntary movement, such as the complex movements of the human shoulder joint. Muscles surrounding multi-planar joints are selectively activated depending upon the movement performed, and within the radiate musculature of the shoulder, individual muscle segments exist that are capable of exhibiting specific myoelectric intensity and temporal activation patterns. The aim of this thesis was to assess the influence of inter-segment variations in contractile properties on the strategies employed by the CNS when producing voluntary movements. Experiments were designed to test the hypothesis that muscle segment neuromotor coordination (as determined by electromyographic analysis) would be sensitive to the contractile properties of individual muscle segments. A key component was the variation in isometric contraction speed ranging from slow to ballistic.

Mechanomyography (MMG), which is the measure of a muscle's physical dimensional change during contraction, is founded on the premise that the temporal aspect of muscle displacement is reflective of motor unit contractile properties and consequently the muscle fibre type composition. A series of studies were completed to establish the validity of the new Laser-MMG technique for quantifying contractile properties. The results confirmed: 1) the sensitivity of the Laser-MMG technique to modulators of physiological performance (thermal state, fatigue state, and fibre type composition variation between segments); and 2) that the contractile properties of muscle fibres varied between the individual segments of the muscles following maximal percutaneous neuromuscular stimulation (PNS). Most notably, 'slow-twitch' contractile properties were found in muscle segments that have a greater role in producing movement in the coronal plane, while 'fast-twitch' contractile properties were associated with segments having more efficient moment arms to produce movement in the sagittal plane. Furthermore, each of the muscles investigated was associated with a distinctive anatomical distribution of muscle fibre types. Muscle segment contractile properties were heterogeneous and their arrangement appears to reflect the most common or important joint movements. Moreover, the muscle segments located at the

periphery of all three shoulder muscles exhibited faster contractile properties than those located in the middle of the muscle. It appears that this internal arrangement may be a consistent organisational characteristic of radiate muscles.

Muscle segments within the pectoralis major, deltoid and latissimus dorsi muscles were found to be independently controlled by the CNS through manipulation of the myoelectric activation patterns, in particular: onset time; and discharge rate. The lower segments of the pectoralis major and the latissimus dorsi were identified as prime mover segments, initiating the movement and contributing the greatest myoelectric intensity. The immediately superior segments were classified as assistant movers, activating after the prime movers and contributing less to the overall movement. Furthermore, similarities in neuromotor coordination were identified between adjacent segments of individual muscles. The sequential "wave of segment activation" identified within each whole muscle appeared to ignore the anatomical boundaries between muscles, suggesting that the CNS coordinates individual muscle segments rather than the whole muscle as one unit in order to complete a motor task. This further complicates the process of controlling motor tasks as there appear to be no defined limits of muscles to which discrete functions can be applied.

Coordination between prime mover segments of agonist muscles was identified, with the lower segments of pectoralis major and latissimus dorsi showing no significant difference in any of the temporal myoelectric measures. The similarity in neuromotor coordination between these segments may be the result of a common drive, suggesting that the CNS uses a simple strategy of combining the segments into one functional unit.

No gross disordering of the muscle segments' onset was identified within any of the investigated muscles, with regard to movement speed. However, the pectoralis major exhibited altered relative timing between the segments. This was particularly evident during the fast movement. The sequential "wave of activation" present during the slow movements became disordered as muscle contraction speed was increased. During fast contraction, the assistant mover segments within pectoralis major were activated later than the prime mover segments changing the relative timing of their activation. This indicates

that the CNS may initially prioritise the activation of only the most essential muscle segments to commence the movement during ballistic movements, perhaps due to the imposed time constraints. This form of change in relative timing can be interpreted as a direct reflection of the differences in muscle segment fibre type composition and hence the neuromotor control of the muscle segments involved in producing the movement. Most notably, variation to the control of muscle segment excitation and contraction onset exist in the more centrally located muscle segments that exhibit slower segment contractile properties. This finding appears logical when coupled with the finding of homogeneous myoelectric peak activity. The CNS must manipulate the onset of these slower contracting segments, especially during fast movements, in order to allow enough time for all segments to achieve a uniform peak of muscle activity that occurs just prior to peak force.

The variations and coordination of contractile properties, myoelectric properties and electromyographic burst patterns between adjacent muscle segments within the same skeletal muscle confirms the notion that for CNS control, individual muscle segments are considered as sub-volumes of muscle tissue that require individual neuromotor control – that they are, in effect, muscles within muscles.

Chapter 1

Introduction

Numerous studies have confirmed that single human skeletal muscles can be subdivided into smaller independently controlled muscle segments during a motor task (Paton and Brown 1994, 1995; Wickham and Brown 1998). This phenomenon has been termed 'functional differentiation' (Pare', Stern and Schwartz 1981) and suggests that the central nervous system (CNS) has the ability to 'fine tune' the activation of motor unit sub-populations within single skeletal muscles to maximise the efficiency of force production across a joint. This contention is supported by observations that single muscles are sub-divided into neuromuscular compartments (English, Wolf and Segal 1993); motor units form 'task groups' within single muscles for specific joint movements (Loeb 1985); skeletal muscles show anatomical segmentation (Williams, Warwick, Dyson and Bannister 1995); and that there is a non-uniform distribution of fast- and slow-twitch muscles fibres throughout a muscle's belly (Johnson, Polgar, Weightman and Appleton 1973; Wang and Kernell 2000).

Although the 'function' of muscle segments within single skeletal muscles has been extensively assessed (Brown, Solomon and Paton 1993; Johnson and Bogduk 1994; Manueddu, Blanc and Taillard 1989; Soderberg and Dostal 1978), there has been little effort to quantify the contractile properties and muscle fibre type distributions that may be found within single skeletal muscle segments. Given that individual muscle segments have been shown to have large and absolute differences in moment arms (Ettema, Styles and Kippers 1998; Wickham, Brown and McAndrew 2004), it is possible that each muscle segment may have its own unique distribution of fast- and slow-twitch muscle fibres to support its role in producing torque across a joint. Some evidence does presently exist, which shows that muscle fibre concentrations vary within single muscles. For example, the cadaveric study of Johnson, Polgar *et al.*, (1973) has shown that the ratio of fast- to slow-twitch muscle fibres may vary between the anatomical heads of a muscle (e.g. medial and lateral heads of the rectus femoris) or in a superficial to deep direction. However, there is little evidence to show how muscle fibre type varies within the many segments of a multi-segmental muscle. At present, we simply do not know in detail how muscle fibre types vary throughout such muscles and how this variation is related to the function of each individual muscle segment. Optimally, an assessment of muscle segment fibre type could

be accomplished by a multi-site biopsy technique. However, ethical considerations would preclude the application of this particular invasive technique in human subjects. Alternatively and in recognition of the contracting properties of different fibre types, muscle segment fibre type distributions could be estimated indirectly by measuring the contractile properties (e.g. contraction time) of each muscle segment. Such an analysis could be performed invasively, utilising Tensiometry, by measuring the development of force at the tendon. However, a more practical measurement solution has been provided by the development of a non-invasive technique that shows considerable promise for the 'in-clinic' measurement of muscle physiological status.

This technique, mechanomyography (MMG), provides a means to determine muscle contractile properties without resorting to surgical procedures. The MMG technique measures the lateral displacement of a muscle's belly following maximal neuromuscular stimulation (percutaneous or direct) (Orizio, Baratta, Zhou, Solomonow and Veicsteinas 2000; Orizio, Liberati, Locatelli, De Grandis and Veicsteinas 1996). The rise and fall of the stimulated muscle's belly has been found to be highly related to the development of tension longitudinally within the muscle's tendons, albeit phase-lagged in time (Orizio, Gobbo, Diemont, Esposito and Veicsteinas 2003). Importantly, there is evidence to suggest that the MMG technique even has the ability to non-invasively estimate muscle fibre composition within single muscles. For example, Dahmane, Valencic *et al.* (2001) have reported a correlation co-efficient of 0.93 between muscle contraction time, as determined by MMG, and the percentage of type I muscle fibres estimated by an invasive biopsy technique in human subjects. A similar finding has also been reported more recently utilising a rat model (Gorelick 2005). Further suggested applications of the MMG technique include the measurement of neuromuscular fatigue (Kouzaki, Shinohara and Fukunaga 1999), the detection of injury site in chronic low back pain patients (Gorelick 2005), the diagnosis of neuromuscular disorders (Akataki, Mita, Itoh, Suzuki and Watakabe 1996) and the control of external prostheses (Barry, Leonard, Gitter and Ball 1986). In addition, MMG has also been shown to be reflective of electromyographic (EMG) measures of muscle activation during a change in the force of muscle contraction (Esposito, Orizio and Veicsteinas 1998; Yoshitake, Shinohara, Ue and Moritani 2002).

The development of the MMG as a practical tool for assessing muscle contractile properties provides an opportunity to examine, in detail, the physiological properties of multiple segments which may be found within a single muscle, and across a group of muscles forming a functional muscle group. For the first time it is now possible to characterise the physiological "profiles" of individual muscle segments which have distinct origins and insertions and unique moment arms but function as a coordinated group within a single muscle or a muscle group. Importantly, such data may be correlated with that from other neurophysiological techniques (e.g. EMG) to gain a greater insight into how the CNS controls muscle segments of similar, and different, physiological profiles during the production of a range of motor skills. Fundamentally, such an analysis would determine how the CNS controls the intensity and timing of multiple muscle segments, which vary in their physiological (e.g. fibre type) and biomechanical (e.g. moment arms) properties and their anatomical locations (e.g. origin and insertion), both within single muscles and uniquely, across a muscle group.

To support this analysis, a major focus of the thesis was to determine and correlate the physiological properties (through Laser-MMG techniques) and function (through electromyographic techniques) of individual muscle segments within three major superficial muscles surrounding the shoulder joint. Selection of the pectoralis major, deltoid and latissimus dorsi for analysis recognises that they are all large multifunctional shoulder muscles, which are ideal to study as they all have wide origins and narrow insertions (Williams, Warwick *et al.* 1995) with multiple muscle segments, each with a unique moment arm (Wickham, Brown *et al.* 2004).

It is already well known that individual muscle segments within multifunctional muscles, such as those investigated here, are selectively activated (e.g. timing and intensity) by the CNS to produce the wide range of movements available across the multi-axial shoulder joint (Brown, Wickham, McAndrew and Huang 2007; Scheving and Pauly 1959; Shevlin, Lehmann and Lucci 1969; Wickham and Brown 1998; Wickham, Brown *et al.* 2004). For example, the anterior deltoid and the 'clavicular' and 'sternal' heads of the pectoralis major combine to produce horizontal flexion of the shoulder (Kapandji 1982). Horizontal

extension is accomplished through the actions of the middle and posterior heads of the deltoid as well as the latissimus dorsi (Crouch 1985; MacConaill and Basmajian 1977). Shoulder abduction is performed primarily by the middle deltoid with both the anterior and posterior heads assisting (Kapandji 1982). To produce shoulder adduction, the pectoralis major and the latissimus dorsi act in synergy as prime movers (Williams, Warwick *et al.* 1995). Additionally the latissimus dorsi, acting alone, may produce medial rotation of the shoulder joint due to its insertion on the anterior aspect of the humerus (Jenkins 1998) while the clavicular-, but not the sternal-, head of the pectoralis major may produce shoulder flexion. Finally, the extensive studies of Wickham, Brown *et al.* (1998; 2004) and Brown, Wickham *et al.* (2007), investigating the neuromotor coordination of individual segments within these three muscles, have concluded that muscle segments may be individually controlled by the CNS to "fine tune" torque production during the performance of both isometric and isotonic movements.

From this brief analysis, it is clear that the CNS has the capacity to control discrete segments of an individual shoulder muscle, in coordination with segments of other shoulder muscles, to produce movements around the shoulder joint. Although it is obvious that individual muscle segments of single skeletal muscles have the capacity for more independent action during a motor task, it still remains unclear how fast- and slow-twitch muscle fibres are distributed within particular muscle segments of individual shoulder muscles. Furthermore, we have yet to gain a good understanding of how the spatial distribution of muscle fibres within each multifunctional muscle influences neuromotor coordination by the CNS. Simply stated, we do not presently have a robust understanding of how the spatial distribution of fast- and slow-twitch muscle fibres, within individual muscle segments, influences the CNS when controlling motor tasks about the shoulder joint.

There is recent evidence to suggest the presence of a distinct superficial spatial arrangement of muscle fibre types across the surface of the deltoid muscle. Utilising a Laser-MMG technique, Gorelick and colleagues (Gorelick 2005; 2007) have suggested that type I slow-twitch muscle fibres are concentrated in the multipennate medial head of the deltoid with an

increasing proportion of type II fast-twitch fibres located in the more medial muscle segments of the anterior and posterior heads. This exciting recent discovery has yet to be confirmed and it remains unknown whether these findings are applicable to other multifunctional muscles, both around the shoulder and elsewhere within the musculoskeletal system.

Therefore the primary aim of this thesis was to use non-invasive assessment techniques (Laser-MMG and EMG) to determine how muscle fibre type concentrations, as inferred by their contractile properties, vary between individual muscle segments and to assess how a muscle segment's fibre type might influence its neuromotor control. The overall objective of the study was to gain further insight into how muscle segment contractile properties vary across the surface of a multifunctional muscle and how such variations may reflect changes in muscle segment function, biomechanical attributes and fibre type composition.

Although MMG techniques have been utilised for decades (Emanuel 1972), it is only recently that laser sensors have been incorporated to measure the lateral displacement of the muscle belly. While Laser-MMG techniques (as utilised here) have obvious advantages over those utilising mechanical sensors, little information currently exists to validate their use. Therefore, to establish the utility and validity of the Laser-MMG technique to assess muscle segment contractile properties in human muscles, a series of animal and human validation studies were conducted. The initial experiment, utilising an animal model, determined the ability of the Laser-MMG technique to detect changes in muscle contractile properties due to altered temperature and fatigue state. In this experiment, the contractile properties determined by the Laser-MMG technique were compared to those obtained by the 'gold standard' invasive Tensiometry technique. A second experiment, also involving an animal cohort, then determined whether the Laser-MMG technique could identify differences in muscle segment contractile properties within a muscle (rat gastrocnemius) that had known segmental differences in the proportion of fast- and slow-twitch muscle fibres.

Having confirmed the suitability of the Laser-MMG technique to assess muscle segment contractile properties '*in vitro*' in an animal model, the technique was then applied '*in vivo*' to a cohort of human subjects. In these experiments, the Laser-MMG technique was able to show significant ($p<0.05$) muscle-segment related changes in muscle contractile properties in the gluteus maximus and also in three superficial muscles surrounding the shoulder joint. These experiments suggested that muscle segment contractile properties, and by inference muscle fibre type, varied within different segments of the gluteus maximus and the three superficial shoulder muscles investigated here. Finally, the influence of muscle segment contractile properties on neuromotor coordination was determined. The coordination of 14 muscle segments, within three superficial shoulder muscles, was assessed to determine whether the speed of a motor task (e.g. slow to fast) influenced how the CNS coordinated muscle segments with different proportions of fast- and slow-twitch muscle fibres. The aim of this final experiment was to determine whether the CNS had to account for variations in muscle segment fibre type distributions when coordinating muscle segments during a shoulder adduction task.

The present thesis tests the following hypotheses:-

1. Both Laser-MMG and Tensiometry techniques will detect temperature and fatigue related modulation of muscle physiological conditions.

2. Both Laser-MMG and Tensiometry techniques will detect differences in muscle contractile properties due to variations in muscle fibre type concentrations.

3. Muscle segments that perform the same function across a joint will possess similar fibre type compositions and hence contractile properties (as determined by Laser-MMG analysis) that will be consistent with their function across the associated joint.

4. Muscle segment neuromotor coordination (as determined by electromyographic analysis) within three superficial shoulder muscles, during a shoulder isometric adduction task performed from slow to fast speeds, will be sensitive to the contractile properties of individual muscle segments.

Specifically, the aims of the thesis were to:-

1. Develop the application of a Laser-MMG technique to *in vitro* animal muscle investigations **(Chapter 4)**,
2. Determine the sensitivity of the Laser-MMG technique to measure whole-muscle or muscle-segment contractile properties through determining the influence of the known modulators of muscle fibre performance; temperature and fatigue, in comparison to established Tensiometry measures **(Chapter 4)**,
3. Examine the gluteus maximus and three superficial shoulder muscles to establish the spatial variation of muscle segment contractile properties within whole skeletal muscle and, by inference, the distribution of muscle fibre types within each muscle segment **(Chapter 5)**,
4. Determine the function (electromyographic analysis) of each of 14 muscle segments throughout the three superficial shoulder muscles and to establish the effect of movement time (slow to fast) on the pattern of activation of muscle segments with varying contractile properties **(Chapter 6)** and
5. Discuss overall the findings of the experimental studies, interpret their significance and propose new directions for further investigation **(Chapter 7)**.

Chapter 2

Literature Review

2.1 Muscle fibre types and contractile physiology

Skeletal muscle is composed of two main muscle fibre types; type I (slow-twitch) and type II (fast-twitch). Type II fibres can be subdivided into type IIA (fast-twitch oxidative), type IIB (fast-twitch glycolytic) and type IIX (undifferentiated fibres), on the basis of their metabolic and contractile properties (Brooks, Fahey, White and Baldwin 2000; Burke, Levine and Zajac 1971; Burke and Tsairis 1973; Close 1972; Loughlin 1993). The physiological properties of muscle fibre types, including their contractile properties and susceptibility to fatigue, differ in many ways (Burke and Tsairis 1973). Type I fibres have a predominantly oxidative metabolism, making them more resistant to fatigue than type IIB fibres which are optimised for glycolytic metabolism. Additionally, the type IIB fibres possess an ability to produce faster contraction rates and generate greater forces than the type IIA and type I fibres.

Muscles that function across an individual joint and are closely associated may have vastly different whole muscle contraction velocities. Each muscle's contraction properties appear to be adapted (by the CNS) to its role in joint movement (Close 1965). For example, within the cat triceps surae muscle group, contraction times (time to peak force) are as short as 20 ms in the medial gastrocnemius and as long as 130 ms in the soleus muscle. This marked difference in contraction time is attributed to different fibre type compositions within these two muscles (Burke and Tsairis 1973). The slow-twitch soleus muscle was observed to be the sole muscle active during quiet standing (Hodgson 1983), indicating its role as a postural muscle.

Properties such as muscle mass, fibre length and fibre pennation angle may give rise to variations in contractile properties such as maximal force and contraction velocity (Sacks and Roy 1982; Spector, Gardiner *et al.* 1980). In general, the overall contraction velocity of a muscle fibre is a function of the number of sarcomeres that are arranged in series (Brooks, Fahey *et al.* 2000). The more sarcomeres that are arranged in parallel to each other, the greater the capacity for maximum force production (Barrata 1995; Brooks, Fahey *et al.* 2000).

Muscle fibre composition and contractile properties can be determined through a variety of invasive and non-invasive techniques (Henriksson-Larsen, Lexell and Sjostrom 1983; Johnson, Polgar *et al.* 1973; Lexell, Henriksson-Larsen and Sjostrom 1983a, 1983b; Lexell, Taylor and Sjostrom 1985; Nonaka, Mita, Akataki, Watakabe and Yabe 2000). Invasive techniques include Tensiometry, intra-muscular EMG and, most commonly, muscle biopsy followed by histochemical tissue analysis (Johnson, Polgar *et al.* 1973; Lexell, Henriksson-Larsen *et al.* 1983a, 1983b). These techniques may have detrimental effects on the subject, including pain, muscle wastage, development of scar tissue and infection (Linder, Dag, Marti-Korff, Quiroz-Rothe, Rivero and Drommer 2002). In addition, there are a number of associated technical limitations in all invasive techniques (Esposito, Orizio *et al.* 1998; Miyamoto and Oda 2003; Orizio 1993). For example, muscle biopsy is a poor estimator of whole-muscle fibre type composition due to the large variability in the spatial distribution of fibre types throughout a muscle (Lexell, Taylor *et al.* 1985).

Muscle contractile properties have been investigated using electromyographic parameters of amplitude, frequency and rate of activation, however, the surface electromyographic technique cannot reliably determine a muscle's fibre type distribution (Brooks, Fahey *et al.* 2000). Although Tensiometry techniques are well established, their application is invasive and completely unsuited to a clinical environment. It is clear that, from the variety of assessment techniques available (biopsy, EMG, Tensiometry), no completely satisfactory non-invasive method currently exists to reliably estimate muscle fibre type distributions throughout a muscle. However, evidence now exists to suggest that the MMG technique may have utility as a non-invasive measurement of muscle fibre type composition. For example, a high correlation ($r = 0.93$) has been identified between muscle contractile properties detected by MMG and muscle fibre composition determined through biopsy of cadaveric specimens (Dahmane, Valencic *et al.* 2001).

2.2 Distribution of muscle fibre types

In both animals and humans, the proportion of a muscle's two main fibre types (Type I and Type II) has been found to vary considerably from one muscle to another (Jennekens, Tomlinson and Walton 1971; Johnson, Polgar *et al.* 1973). Predominantly tonic/postural muscles (e.g. cat soleus (Hodgson 1983)) generally have a high percentage of type I fibres; phasic/dynamic muscles (e.g. cat gastrocnemius (Hodgson 1983)) in contrast have a high percentage of type II fibres; muscles with both dynamic and postural roles have no overall predominance of either type (Johnson, Polgar *et al.* 1973).

In addition to muscle-to-muscle differences in muscle fibre type, wide variations exist within the same muscle between individual subjects (Johnson, Polgar *et al.* 1973; Sandstedt 1981; Sandstedt, Nordell and Henriksson 1982), with deviations as high as 40% reported (Mahon, Toman, William and Bagnall 1984; Sandstedt, Nordell *et al.* 1982). Fibre type discrepancies also exist between muscle segments and within muscles as a function of depth (Johnson, Polgar *et al.* 1973; Lexell, Henriksson-Larsen *et al.* 1983a, 1983b; Lexell, Taylor *et al.* 1985; Loughlin 1993; Mannion 1999; Sandstedt 1981), with type II fibres generally located superficially and type I located deeper. This distribution of fibre types is thought to be functionally advantageous, on the basis of several, not mutually exclusive, factors. These factors include: a) biomechanical properties; fast-twitch muscle fibres being located superficially may allow for longer moment arms, enhancing their force development capacity (Wang and Kernell 2000); b) heat conservation; vascular rich slow-twitch muscle fibres located deep within the muscle would prevent the unnecessary loss of large amounts of heat and in turn, decrease the amount of energy required to maintain heat during cold exposure (Loeb 1987); and c) dynamic adaptation of speed and power; increased shortening speed and power is possible when muscle fibres are heated (Bennett 1984), as would occur in the deeply located slow-twitch muscle fibres thus augmenting their contribution to the overall rate and force of the muscle contraction.

Furthermore, muscle fibres in rats exhibit proximo-distal regionalisation (Wang and Kernell 2000). Investigations have shown a reduction in the density of type I muscle fibres in the more distal regions of the rat medial gastrocnemius. This is thought to be due to the

thermoregulatory role of the type I fibres (locating heat generating muscle fibres proximally enhances core temperature stability) and their recruitment patterns (active in all contractions, therefore always generating heat) (De Ruiter, De Haan and Sargeant 1996; Wang and Kernell 2000).

The fact that motor units / muscle fibres exhibit such striking differences in terms of speed of contraction and biochemical profiles suggests that their involvement in muscle activity is unlikely to be random but rather suited to the task demanded of them (Martini, Timmons and McKinley 2000; McComas 1996). Real-life muscle activity may partly determine the types of fibres that will comprise an individual muscle (Martini, Timmons *et al.* 2000). Therefore, the possibility exists that multifunctional muscles, those muscles that can contribute to a range of joint movements, may exhibit a variety of muscle fibre types located within anatomical muscle segments that may each have their own unique role in the production of force across a joint. Based on the observation that a muscle's maximal contraction speed is reflective of fibre type, individual muscle segments could also be characterised by their contraction speed dependent upon their fibre type compositions.

2.3 Activation of muscle

A motor unit consists specifically of an alpha-motor neuron and all the muscle fibres it innervates (Bern and Levy 1990; Brooks, Fahey *et al.* 2000). All the muscle fibres within a single motor unit have nearly identical biochemical properties and physiological phenotypes (Brooks, Fahey *et al.* 2000; Burke and Tsairis 1973) and so have relatively similar metabolic, regulatory and physiological properties that have a direct influence on the motor unit's contraction velocity, relaxation rate and peak tension (Burke, Levine *et al.* 1971; Burke and Tsairis 1973; LeBozec and Maton 1987; McComas 1996).

The motor unit is the basic building block for the integration and control of movement. Motor units can be very generally classified in two ways, based on size (small or large), and in three ways based on metabolic properties (slow oxidative, fast oxidative and fast glycolytic). The size of the cell body and its axon depends upon whether it is a slow-twitch

or fast-twitch. Pioneering experiments by Burke and colleagues (1978; 1971) established that morphological, histochemical and mechanical properties of motor units were all precisely interrelated i.e. small motor units were associated with small/slow-twitch muscle fibres that produce low force levels and conversely, large motor units with large/fast-twitch muscle fibres produce high force levels. In addition, these studies of the soleus and gastrocnemius muscles of the cat determined that the organisation of the motor unit populations seemed ideally suited to the vastly different functional roles played by these two muscles (soleus/slow-twitch/postural : gastrocnemius/fast-twitch/dynamic). Motor units also vary in the number of muscle fibres that they innervate (innervation ratio). This directly influences the degree of control of the muscle and provides insight to its functional role. A muscle that has a large number of motor units in relation to the number of muscle fibres is more capable of precise, finite movements, than one with a low number of motor units.

The recruitment of motor units is a complex process requiring an extensive neural input to control a muscle's contraction (Martini, Timmons *et al.* 2000). When a muscle is activated by the CNS, the smallest type I motor units are initially recruited as tension first develops longitudinally within the muscle belly (Henneman, Somjen and Carpenter 1965a). As more tension is required from the muscle, larger type I, and then the type II, motor units are recruited in order of their physical size as described by Henneman's "size principal" (Henneman, Somjen *et al.* 1965a). Once activated, motor units of both major types can produce higher levels of force by increasing their rate of firing (a process known as rate coding).

2.4 Control of muscle activation

Traditionally, a "motoneuron pool" is a spinal cord structure that includes all the motoneurons that innervate one muscle. Within the pool, the motoneurons are generally believed to receive synaptic input from the same neurons (Henneman and Mendell 1981), be under a common drive (Hoffer, Sugano, Loeb, Marks, O'Donovan and Pratt 1987) and be progressively recruited in an orderly pattern determined by cell size (Henneman, Somjen

and Carpenter 1965). This premise has been supported experimentally in anatomically simple muscles acting about a single joint (Binder, Bawa, Ruenzel and Henneman 1983; Hoffer, Loeb, Marks, O'Donovan, Pratt and Sugano 1987; Hoffer, Loeb, Marks and Sugano 1983).

The anatomical design and physiological control of multi-articular muscles rejects the traditional idea that a single, homogenous, motoneuron pool innervates a single muscle. A muscle contraction has been shown to rarely activate a single motoneuron pool, with the contraction more likely to involve either a group of muscles working together (multiple motoneurons pools) or alternatively, a sub-section of the muscle activated by a task group (Desmedt and Godaux 1981; Kanda, Burke and Walmsley 1977; Riek and Bawa 1992; Thomas, Schmidt and Hambrecht 1978). A task group is a group of motor units that are activated for the purpose of contributing to a specific task e.g. flexion of the elbow. These motor units may be associated with a single muscle or alternatively numerous muscles that are required to produce the task (movement). Riek and co-workers (1992) suggested that *"if the very essence of the size principle is correct …, then orderly recruitment should hold within every task group. This cannot be considered an exception to the size principle, rather an extension of it"* (Riek and Bawa 1992).

Conducting experiments with forearm muscles, Riek and co-workers (1992) confirmed that motor units are recruited according to size within a task group and that muscles may have either numerous task groups that partially overlap (as in extensor digitorium communis) or an absence of separate task groups (as in extensor carpi radialis). This study implies that the functionality and/or control of each muscle differs, with the extensor digitorium communis capable of producing force in multiple directions through the control of individual digits. In contrast, the extensor carpi radialis is anatomically a much simpler muscle with a narrow single insertion and is only capable of a limited number of force vectors. Moreover, it has been suggested that when a muscle has multiple force vectors, then "….*the mechanical arrangement of muscle units is such that strict orderly recruitment occurs in terms of force for the direction requiring most precision"* (English and Weeks 1984).

Further evidence exists with Brown, Solomen *et al.* (1993) showing that motor units within the two heads of biceps brachii muscle could be recruited differentially when producing elbow flexion with and without the forearm supinated. It was concluded that the CNS drive to the motoneuron pool was determined by the task being performed (flexion, extension, etc). Therefore each task may place a different demand on the motoneuron pool and as such, require different 'task groups' within the motoneuron pool.

The motoneuron pool innervating the cat sartorius muscle has been experimentally identified to consist of at least three functionally separate motoneuron groups (task groups), each of which was independently recruited to perform individual tasks during locomotion (Hoffer, Loeb, Sugano, Marks, O'Donovan and Pratt 1987). Hoffer and co-workers (1987) showed that the sartorius was anatomically divided into anterior and medial muscle segments and that the motor units controlling a single muscular segment were distributed only within the boundaries of a specific area of the motoneuron pool. Through studying gait patterns of the cat, nine of thirteen motoneurons innervating the sartorius were found to be active only during the swing phase. The other four motoneurons were shown to be active only during the stance phase. They concluded that functionally separate task groups were each capable of independent recruitment and suggested that the "*assignment of specific roles to separate populations of motoneurons is a solution to the problem of how to control several functions in a single muscle while retaining most of the central organisational properties of motoneurons pools*" (Hoffer, Loeb *et al.* 1987).

Given this evidence, it is clear that Henneman's 'size principle' would be most appropriately applied to motor units found within 'task groups' or muscle segments, rather than to the entire muscle. Each muscle segment could therefore be thought of as its own independent muscle – a 'muscle within a muscle' (Wickham and Brown 1998). It is also possible that synergies present between whole muscles may be present for individual segments of a muscle and between muscle segments of agonist muscles.

2.5 Effect of movement speed on muscle activation patterns

The neuromotor control of rapid limb movements is known to vary, dependant on the ultimate speed of the movement. Movements lasting less than 400ms are characterised by a sequential three burst pattern (triphasic) of EMG activity (Angel 1977, 1981; Berardelli, Hallett, Rothwell, Agostino, Manfredi, Thompson and Marsden 1996; Gottlieb, Corcos and Agarwal 1989). These movements generally involve myoelectric activity from both the agonist and antagonist muscles working about the joint.

The triphasic pattern reflects firstly a burst of activity from the agonist muscle, followed by activity from the antagonist muscle, with the agonist reactivating at or just prior to the movement termination. The initial burst of activity from the agonist provides the *"driving force"* that sets the limb in motion, the antagonist then *"brakes"* the movement while the second agonist burst of muscle activity works with the antagonist to *"dampen out the oscillations that might occur at the end of the movement"* (Berardelli, Hallett *et al.* 1996).

The pattern of agonist and antagonist muscle bursts were investigated in muscle segments (Wickham, Brown, Green and McAndrew 2004) to determine whether segments displayed either a single-, two- or a continuous- burst pattern during shoulder adduction tasks. Results identified classic triphasic muscle burst patterns in those segments that had larger moment arms and greater relative contributions to the torque development about the joint. The muscle segments identified in the study as prime movers exhibited distinct two-burst patterns (AG1 followed by AG2) whilst the segments identified as antagonists clearly exhibited single-burst patterns. Other muscle segments not involved in the production of the motor task either displayed a continuous burst or were not active. The authors concluded that the classic triphasic muscle burst pattern is best observed between muscle segments identified as primary prime movers and primary antagonists, for the planned motor task.

2.6 Evidence for functional differentiation within skeletal muscle

Within particular muscles, especially those with broad origins and narrow insertions, it has been shown that a number of lines of action, or 'directions of pull', exist onto the tendon of insertion. Biomechanical analysis can deconstruct a joint movement into the many individual lines of action that make up the desired movement. By matching the individual lines of action to muscle fibres that have similar lines of action, muscle activity can be predicted. As a result, many studies have sought to anatomically identify individual compartments or segments within whole muscles (Paton and Brown 1994, 1995; Wickham and Brown 1998; Wickham, Brown *et al.* 2004) and to identify different motor unit activity (by electromyographic analysis) across different segments of the one muscle (Pare', Stern *et al.* 1981). These studies have conclusively shown that individual muscle segments may be independently controlled in the production of a coordinated movement (Riek and Bawa 1992); that a muscle segment's line of action influences its activation timing and intensity (Brown, Wickham *et al.* 2007) and that muscles are in fact 'functionally differentiated'. Functional differentiation has been described in numerous human muscles, including the extensor digitorum communis (Riek and Bawa 1992), the gluteus medius (Soderberg and Dostal 1978), the tensor fascia latae (Pare', Stern *et al.* 1981), the latissimus dorsi (Paton and Brown 1995), the pectoralis major (Paton and Brown 1994), the deltoid (Wickham and Brown 1998) and the biceps brachii (Brown, Solomon *et al.* 1993; Ter Harr Romeny, Denier Van Der Gon and Gielen 1982).

Based on results from the above anatomical and functional studies, it appears that individual muscles may be divided into multiple segments, each with its own particular function. Soderberg, Dostal *et al.* (1978) investigated the anterior, middle and posterior muscle segments of gluteus medius and concluded that selective activation (functional differentiation) of individual segments could occur within muscles with multiple lines of action to the tendon of insertion. The three muscle segments of gluteus medius were capable of asynchronous activation during the walking gait cycle; during hip flexion the anterior, then the middle and finally the posterior segment controlled internal rotation. The order of muscle segments involved in the swing phase of gait was also noted to differ from

those producing the stance phase. The evidence of asynchronous electromyographic activation of segments of a muscle is characteristic of functional differentiation.

In another study, Paton and Brown (1994) proposed that muscle segments within the pectoralis major, with lines of action divergent from the force vector produced by the muscle, would remain electrically quiescent during the initial phase of the movement. The process of eliminating surplus muscle activity essentially consumes less energy, decreases the complexity of movement control and provides for a smoother movement. Their study also found evidence that each functional segment within pectoralis major varied its activation on response to the contraction force and plane of motion. Further evidence of functional differentiation is provided by Pare' and co-workers (1981) in their study of the tensor fascia latae. Near heel strike, the posterolateral fibres were active but the anteromedial fibres were electrically silent. The rationale for this finding was that the anteromedial fibres had a greater mechanical advantage for hip flexion whereas the posterolateral fibres work more efficiently for hip abduction and internal rotation. The line of action for each group of muscle fibres was evident through the different levels of activity within the muscle.

2.7 Functional role of muscle segments

The functional role of an individual muscle during any given movement is well established in the scientific literature. In contrast, limited investigations have focused on identifying and allocating specific functional roles to muscle segments during movements. Functional classifications, previously used to describe whole muscle function, have been applied to muscle segments within the pectoralis major, deltoid and latissimus dorsi (Wickham, Brown *et al.* 2004). Using predetermined criteria, Wickham and colleagues (1998; 2004) characterised the activity of 19 individual muscle segments during different motor tasks as either prime mover, synergist or antagonist segments. Their results show prime mover segments have the earliest onsets, the longest durations of activation, the greatest intensity of electromyographic activation and, through moment arm analysis, the most biomechanically effective line of action. Moreover, synergist segments, identified as those

with progressively more divergent lines of action, displayed increasingly later onsets, shorter durations and lower intensities of electromyographic activation. In contrast, antagonist segments, those with lines of action opposing the direction of the movement, were activated last, had the shortest period of electromyographic activation and inconsistent intensities.

The studies by Wickham and colleagues (1998; 2004) determined how muscle segments were coordinated to produce a variety of movements about the shoulder joint (shoulder extension, flexion, abduction and adduction). Their results offer detailed insight to muscle segment functionality. Specifically, the adduction isometric impulse induced activity from all of the investigated muscles, although only the posterior segments of the deltoid displayed electromyographic activity. The adduction force impulse was initiated by a global activation of all segments within the latissimus dorsi followed by the lower segments of the pectoralis major. Data shows that all latissimus dorsi segments and a single segment of the pectoralis major were activated prior to the onset of force. This was followed by subsequent activation of the upper segments of pectoralis major and the posterior segments of the deltoid. All segments reached electromyographic peak before force peak with the lower latissimus dorsi segments peaking earlier than the remaining segments. Additionally, all the latissimus dorsi and lower pectoralis major segments exhibited longer electromyographic duration compared to the upper pectoralis major and posterior deltoid segments. Latissimus dorsi and the lower segments of pectoralis major displayed greater intensity than the remaining segments. Wickham and colleagues (2004) were subsequently able to apply functional classifications to each of the segments based on the previously discussed criteria.

Overall, and particularly pertinent to this thesis, was the finding that the timing and intensity of each muscle segment was determined by the muscle segment's line of action. Individual muscle segments were also found to be activated in a coordinated pattern that ignored muscle anatomical boundaries. What remains to be investigated, and is the focus of this thesis, is the physiological composition of each muscle segment and whether this

composition influences the coordination present between the segments when movement speeds are altered.

2.8 Muscle coordination / synergy

Muscle coordination is a term which refers to the patterns of whole muscle activity which the CNS utilises to produce a desired movement (Buchanan, Almdale, Lewis and Rymer 1986). To accomplish skilled movement, the CNS must coordinate the activation of numerous muscles/muscle segments and match their lines of action to the desired outcomes of the intended motor task (Buchanan, Almdale *et al.* 1986).

Studies of the relationship between the trapezius (superior fibres) and the serratus anterior (inferior fibres) (Bull, De Freitas and Vitti 1989; Bull, Vitti and De Freitas 1990; Piacentini and Berzin 1989) have shown that the two muscles work synergistically in movements involving scapula rotation. Maton and Gamet (1989) have shown the presence of muscle coordination between the agonistic biceps brachii and the brachioradialis during elbow flexion. In particular, the study by Maton, Gamet *et al.* (1989) observed similar motor unit activation strategies (recruitment order and firing rate) for both muscles during the isometric voluntary sub-maximal contraction, indicating that the CNS may impose the same control strategy on the motor units of both muscles.

Through the study of co-activation in muscles of different fibre types, Kuo and Clamann (1981) found that synergist muscles could play different roles in initiating and sustaining concentric movement. The electrical activity of four pairs of synergistic muscles was investigated during isometric contractions at varying speeds. Synergistic pairs of muscles, in which the muscle fibres were both predominately fast-twitch, became active simultaneously in movements at all speeds. No difference in onset activation of these muscles was found as a function of movement speed. In synergistic muscle pairs composed of fast- and slow-twitch muscles, a slow movement was always initiated by the slow-twitch muscle, whose electrical activity predominated throughout the movement. During a rapid

movement, the fast muscle could be initially most active, but not necessarily initiate the movement. However, movements in intermediate speed could be initiated by the slow-twitch muscles, rather than the fast-twitch muscles. The speed of contraction may therefore be a necessary, but not a sufficient stimulus for the reversal of muscle activation patterns. Individual muscle segment activation, given differences in muscle fibre composition, may therefore vary, but not reverse their roles during the slow, medium and fast speeds of movement.

Given that muscle coordination exists between individual muscles, it is therefore probable that it exists between individual muscle segments within one muscle and even between individual segments of different muscles. To date, there have been few studies which have investigated how individual muscle segments of single muscles are coordinated with those of adjacent or distant muscles that have a role in the production of a specific movement. Muscle segment coordination, contractile properties and biochemical profiles remain undefined, particularly within human subjects. Fortuitously, non-invasive measurement techniques (e.g. MMG) are now available. These techniques have the potential to provide considerable insight into the physiological properties of individual muscle segments and their role in the production of skilled movement.

2.9 Non-invasive measurement of muscle contractile properties – Mechanomyography (MMG)

Recent research has determined that measuring the lateral displacement of a muscle's belly following maximal percutaneous neuromuscular stimulation (PNS) may provide accurate, non-invasive determinations of muscle contractile properties and an indirect estimate of muscle fibre type, at least in superficial muscles (Beck, Housh, Cramer, Weir, Johnson, Coburn, Malek and Mielke 2005; Dahmane, Djordjevic, Simunic and Valencic 2005; Dahmane, Djordjevic and Smerdu 2006; Dahmane, Valencic *et al.* 2001; Orizio, Baratta, Zhou, Solomonow and Veicsteinas 1999). The MMG technique can be applied to measure the lateral displacement of individual contracting muscle fibres (Djordjevic, Valencic and

Jurcic-Zlobec 2001; Valencic and Djordjevic 2001; Valencic, Knez and Simunic 2001) or the lateral displacement of the whole muscle belly (Watakabe, Mita, Akataki and Itoh 2003) following PNS. Although the MMG waveform was originally detected by sensors including microphones, piezoelectric contact devices and accelerometers, more recently it has been suggested that laser sensors provide a more reliable means of detecting a muscle belly's lateral displacement (Orizio, Baratta *et al.* 1999; Watakabe, Mita *et al.* 2003).

The MMG technique has been extensively studied to verify its reliability as a tool to investigate muscle contractile properties and fibre type (Dahmane, Djordjevic *et al.* 2005; Dahmane, Valencic *et al.* 2001; Orizio, Baratta *et al.* 1999, 2000). Orizio and associates (2000; 1999) studied the relationship between muscle force and MMG in the gastrocnemius of cats. The medial gastrocnemius tendon was severed and connected to a force transducer while an MMG detected the lateral displacement of the muscle's belly. An MMG laser sensor was positioned over the muscle, at the site that produced the largest displacement during supra-maximal twitch stimulation. The motor nerves of the medial gastrocnemius were electrically stimulated and the relationship between muscle force and the lateral displacement of its muscle belly, as detected by MMG, was investigated. Results showed that at low firing rates the MMG peak was reached earlier than the force peak, whereas at high firing rates the MMG plateaued earlier with respect to the force plateau, arguing that the properties of the MMG and force are due to different mechanisms. The authors suggested that the relationship between MMG and force be split into two phases; the first one with large geometrical changes to the muscle and low force increments and the second one with small changes to the muscle's lateral displacement and large force increments. This is in agreement with the stress-strain relationship found in soft tissue presenting with a non-elastic response phase (toe-in). The mechanical effect of increasing the motor unit's activation level is firstly the deformation of the muscle, followed by tension generation. They concluded that the force and lateral displacement of a muscle are not linearly related but that MMG was a reliable tool to detect and measure a muscle's contractile properties.

Similar results were obtained by Orizio, Diemont *et al*. (1999) with the human tibialis anterior muscle. These researchers correlated MMG waveforms with muscle force before

and immediately after electrically-induced fatigue as well as during six minutes of recovery. The MMG parameters of peak force, contraction time and half relaxation time were analysed and compared with parameters derived from the muscles force-time curve as determined through Tensiometry. As with previous studies (Orizio, Gobbo, Veicsteinas, Baratta, Zhou and Solomonow 2003), it was concluded that the MMG output reflects aspects of muscle mechanics, in particular the maximal rate of acceleration, as a high correlation was found between MMG and force signals in un-fatigued muscle and during recovery. In addition they indicated that the MMG technique could also be successfully used to follow changes in muscle contractile properties caused by fatigue over the duration of a task.

Other research (Yoshitake, Shinohara *et al.* 2002) has examined whether the MMG waveforms recorded from the skin over a contracting muscle reflect the contractile properties of individual motor units in humans. The muscle's MMG waveforms were detected by a condenser microphone that measured the volume of air displaced by the muscle when it expanded laterally. The oscillations were then transmitted to a thin diaphragm through an air column (Yoshitake, Shinohara *et al.* 2002). The examined muscle (medial gastrocnemius) was stimulated by current delivered through fine-wire bipolar electrodes inserted under the skin and located directly beneath the MMG microphone sensor. This type of electrical stimulation is known as 'intra-muscular micro-stimulation' which, due to its invasive nature, can be painful and uncomfortable for subjects. Results of the study confirmed a significant positive correlation between the MMG duration and twitch duration and that the rate of change in MMG and force was positively correlated across motor units. These results supported a direct relationship between MMG and the contractile properties of individual motor units within the gastrocnemius muscle. Moreover, these results indicated that surface MMG was dependent on the contractile properties of the activated motor units. A major limitation discussed in this study was that the layers of tissue (skin and fat tissues) beneath the transducer can act as a low-pass filter. The extent of this filtering was thought to be subject dependent.

Some MMG techniques may have limited applicability to human populations as they involve invasive surgical techniques. In addition, the relationship between the laser detected MMG waveform and force output in a small portion of muscle cannot be simply extrapolated to be representative of the whole muscle (Orizio, Gobbo *et al.* 2003). The research of Orizio and colleagues (1999; 2003) adopted experimental protocols where a single site on a muscle was chosen by identifying the region that produced the largest surface displacement following electrical stimulation. This site was thought to be representative of the entire muscle. Other evidence however, (Orizio, Baratta, Zhou, Solomonow and Veicsteinas 2000; Zuurbier and Huijing 1993) suggests that there is not a uniform lateral displacement of muscle fibres following electrical stimulation, across the surface of pennate muscles (e.g. deltoid). This is due to regional differences in the distribution of muscle fibre lengths (Zuurbier and Huijing 1993), a non-uniform distribution of the actin and myosin filaments (contractile tissue) (Frangioni, Kwan-Gett, Dobrunz and McMahon 1987) and the differing behaviour of the sarcomeres and aponeurosis along the active muscle (Huijing, Nieberg, vd Veen and Ettema 1994). It is most probable therefore that a single MMG recording site would not be representative of the entire muscle, at least in multifunctional muscles.

The literature and associated methods that have been reviewed in this section aided in the design and development of the laser-based MMG technique which was used here to determine motor unit contractile properties within individual segments of radiate muscles. It is hoped that this non-invasive method will enable the measurement of important contractile properties of muscles, including contraction and relaxation times, which would ultimately allow researchers to understand individual muscle fibre type distributions in different segments of muscles and muscle groups (Djordjevic, Valencic *et al.* 2001). It is also expected that research pertaining to this technique will prove useful for investigating mechanical properties of muscles in the fields of physiology, clinical medicine and rehabilitation (Yoshitake, Shinohara *et al.* 2002).

2.10 Electromyography (EMG)

The electromyographic waveform develops from the motor unit action potential passing from the motor end plate to the sarcolemma and then into the surrounding muscle tissue. It is the movement of ions (Na^+ and K^+) across the sarcolemma that produces the action potential, which then generates an electromagnetic field. The electromagnetic field is detected by surface or in-dwelling electromyographic electrodes thus producing the characteristic electromyographic waveform (Basmajian and DeLuca 1985).

Generally favoured in kinesiological studies due to their non-invasive application, surface electrodes detect the electromagnetic field from numerous motoneurons and therefore represent the summation of many motor unit action potentials. Due to their configuration, surface electrodes are preferred when estimations of whole muscle electromyographic activity are required (Basmajian and DeLuca 1985). The utilisation of surface electrodes can be more problematic when recording from multiple sites within the one muscle or from adjacent sites between two muscles. In this instance, crosstalk between electrode sites is a reality that can contaminate electromyographic waveforms (Basmajian and DeLuca 1985).

Two methods have been suggested for decreasing the surface electrode pickup area in order to reduce electrode cross talk: 1) reducing the active detection area of the electrode and; 2) minimising the distance between the bipolar surface electrode pairs (Winter, Fuglevand and Archer 1994). Using a theoretical model, Winter, Fuglevand *et al.* (1994) estimated the electrode detection area to be 1.8 cm deep when using 49 mm^2 electrodes with a bipolar electrode spacing of 2.0 cm (including 2 mm of skin and fat). Basmajian and Deluca (1985) stipulate using a voltage decrement function when determining the selectivity of a bipolar electrode configuration. However, they also note a 'rule-of-thumb' (Lynn, Bettles, Hughes and Johnson 1978) to simplify the calculation, that being that the inter-electrode distance corresponds roughly to the distance from which muscle fibres will contribute to the detected electrical signal. Other researchers (Koh and Gradiner 1993) have also stated that the detection area of a surface electrode pair is equal to the inter-electrode distance when applied as a radius from each surface electrode. For instance, if a bipolar electrode

pair had an inter-electrode distance of 10 mm, each electrode would detect electrical signals from muscle tissue that was within a 10 mm radius of the surface electrode.

Myoelectric signal detection becomes problematic when recording from muscles with an excessive adipose covering (Solomonow, Baratta, Bernardi, Zhou, Lu, Zhu and Acierno 1994). De la Barrera and Milner (1994) showed that the selectivity of surface electrodes is progressively impeded as skin fold thickness increases - a function of greater filtering and attenuation of the signal. Thus, when recording from small areas of a muscle with a multi-electrode technique, it is advantageous that skin fold thickness be minimised as far as possible.

2.11 Musculoskeletal functional anatomy

Animal Muscles:

Medial Gastrocnemius

The rat gastrocnemius consists of two heads that are considered distinct muscles; the tri-pennate gastrocnemius lateralis and the uni-pennate gastrocnemius medialis (Prodanov, Thil, Marani, Delbeke and Holsheimer 2005). The gastrocnemius muscle originates from the femur and joins tendons with the soleus muscle thereby forming the common calcaneal tendon that attaches to the calcaneus (Hebel and Stromberg 1986). The medial and lateral gastrocnemius muscles are innervated by separate branches of the tibial nerve (Hebel and Stromberg 1986).

The medial gastrocnemius muscle has been used extensively as a model for investigations of fibre type, function and performance due to the clear delineation between muscle segments that contain different fibre type compositions (Table 2.1). The proximal segment of the muscle consists of a mixture of slow oxidative and fast oxidative fibres (25.5% Type I: 74.5% Type II), whereas the distal muscle segment is completely composed of fast-twitch glycolytic fibres (0% Type I: 100% Type II) (De Ruiter 1996; De Ruiter, De Haan and Sargeant 1995a, 1995b; De Ruiter, De Haan *et al.* 1996; Kraemer, Staron, Gordon, Volek, Koziris, Duncan, Nindl, GÃmez, Marx, Fry and Murray 2000; Staron, Kraemer,

Hikida, Fry, Murray and Campos 1999; Wang and Kernell 2000). The proximal muscle segment has smaller motor unit territories, smaller cross-sectional fibre areas, lower force production, greater resistance to fatigue and greater half relaxation times, in comparison to the distal muscle segment (De Ruiter, De Haan *et al.* 1995a, 1996).

Author	Technique	Proximal Segment Fibre Type Composition	Distal Segment Fibre Type Composition	Total Muscle Fibre Type Composition
(Kraemer, Staron *et al.* 2000)	Myosin ATPase Staining	Type I = 25.5% Type II = 74.5%	Type I = 0% Type II = 100%	n/a
(De Ruiter, De Haan *et al.* 1995b)	Myosin ATPase Staining	Type I = 10% Type II = 90%	Type I = 0% Type IIB = 100%	n/a
(Thomas, Sesodia, Erb and Grumbles 2003)	Myosin ATPase Staining	n/a	n/a	Type I = 15% Type II = 85%
(Ustunel, Akkoyunlu and Demir 2003)	Myosin ATPase Staining	n/a	n/a	Type I = 25% Type II =75%
(Rivero, Talmadge and Edgerton 1999)	MHC Content & Immunohistochemical Staining	n/a	n/a	Type I = 24% Type II = 76%
(Kanda and Hashizume 1992)	Myosin ATPase Staining	n/a	n/a	Type I = 17% Type II = 83%
Average		**Type I = 18% Type II = 82%**	**Type I =0% Type II = 100%**	**Type I = 20% Type II = 80%**

Table 2.1 A selection of studies from the literature reporting fibre-type composition of the medial gastrocnemius muscle of the rat.

Human Muscles:

Gluteus Maximus

The gluteus maximus is the largest, most superficial muscle within the gluteal region. The muscle has a characteristic quadrilateral shape with coarse muscular fasciculi lying parallel to one another (Williams, Warwick *et al.* 1995). The muscle has a broad origin arising from the posterior 1/3 of the crest of the ilium, the lateral aspect of the sacrum and the posterior surface of the sacrotuberous ligament (Crouch 1985). Its muscle fibres run in an oblique inferior and posterior direction to insert into the fascia latae and linea aspera (Williams, Warwick *et al.* 1995). Deep fibres also pass obliquely down to insert into the

gluteal tuberosity of the femur (Williams, Warwick *et al.* 1995). The muscle is innervated by the inferior gluteal nerve, arising from spinal nerves L5-S2 (Schuenke, Schulte and Schumacher 2006).

The muscle is said to contribute to hip extension, abduction, adduction (in particular its lower fibres; Jenkins (1998)) and lateral rotation, although it is generally only active when moderate to heavy effort is required (Basmajian and DeLuca 1985; Soderberg and Dostal 1978). Furthermore, Basmajian and DeLuca (1985) report that the muscle has three functional muscle segments (upper, middle and lower) that are independently controlled by the CNS during walking tasks. Somewhat surprisingly however, given the importance of the muscle to hip function, there currently exists relatively little information regarding the detailed anatomy of the muscle and the contractile properties, fibre type distributions and function of the three segments of this muscle.

Pectoralis Major

The pectoralis major is the largest superficial muscle on the anterior aspect of the thorax. It is a thick, flat, radiate muscle consisting of multiple segments found within three general heads, determined from its origin. The upper head originates from the inner two thirds of the anterior border of the clavicle, the middle originates from the whole length of the sternum and the costal cartilages of the first six ribs and the inferior head originates from the aponeurosis of the external oblique abdominal muscle (Crouch 1985). Its insertion is by a flat tendon (approximately 5 cm wide) into the ridge formed by the outer lip of the bicipital groove under the lesser tubercle of the humerus, extending down to the deltoid tuberosity (Williams, Warwick *et al.* 1995). The medial and lateral anterior thoracic nerves, arising from the brachial plexus (C5 – T1 spinal nerves), innervate the muscle (Schuenke, Schulte *et al.* 2006).

As the muscle's tendon approaches the insertion, it twists through 180 degrees with the lower fibres passing beneath, to be inserted cranially. The fibres from the clavicle pass anteriorly and inferiorly across to the attachment on the humerus at a point inferior to the sternal fibres. Due, in part, to the broad origin and the resultant moment arms, the muscle

is commonly divided into a 'clavicular' and a 'sternal' head. The clavicular head is a prime mover for shoulder flexion and an assistant mover for abduction after the arm has been abducted to 90 degrees and the sternal head is a prime mover for extension and adduction (Kapandji 1982). Both parts act strongly in horizontal flexion and are assistant movers in forward flexion. Strong evidence of functional differentiation within this muscle is provided in the work of Brown and colleagues, with at least 5 independent muscle segments identified (McAndrew and Brown 2004; Paton and Brown 1994; Wickham and Brown 1998; Wickham, Brown *et al.* 2004; Wickham 2002; Wickham, Brown *et al.* 2004).

Deltoid

The deltoid is a triangular muscle located on the lateral aspect of the shoulder with its base on the scapulae and acromion and its apex directed inferiorly to the humerus. The origin follows a curved line from the outer third of the anterior border of the clavicle to the top of the acromion process and onto the spine of the scapula (Crouch 1985). Its complex insertion is to the deltoid tuberosity and surrounding areas of the humerus (Wickham and Brown 1998), while the axillary nerve, a continuation of the 5th and 6th cervical nerves, supplies innervation (Schuenke, Schulte *et al.* 2006).

The muscle is historically divided into three 'heads' (or segments): the anterior, middle and posterior (Williams, Warwick *et al.* 1995) . The anterior and posterior heads are of penniform shape while the middle head is multipennate (Wickham 1998). Fick (1911, as cited by Kapandji, 1982) suggests that the anterior (clavicular) head contains two muscle segments (I & II); the middle (acromial) head contains one muscle segment (III); while the posterior (spinal) head contains four muscle segments (IV, V, VI & VII). Kapandji (1982) explained the action of the muscle segments as follows:

"Pure abduction (0 degrees of flexion) utilises the acromial band III, the spinal IV and V and the clavicular band II. Abduction with 30 degrees of flexion contracts band III and II to start the movement with IV, V, and I adding later. Forward flexion and horizontal flexion is obtained by the clavicular head, components I & II. Lateral rotation with abduction is through contraction of the II, IV and V components. Posterior heads V, VI,

and VII are prime movers for horizontal extension and adduction. The deltoid is most active from 90 degrees through to 180 degrees."

Anatomical and electromyographical analysis (Wickham 1998) has confirmed the results of Fick (1911, as cited by Kapandji 1982), identifying seven anatomical and functional muscle segments. Each muscle segment was determined capable of independent action when producing an abduction or adduction movement and identified as an agonist, synergist or antagonist depending on their role during the movement.

Latissimus Dorsi

The latissimus dorsi is a broad triangular muscle situated superficially on the inferior and lateral aspect of the posterior trunk. The origin of this muscle covers the spinous processes of the six lower thoracic and all the lumbar vertebrae, the posterior surface of the sacrum, the crest of the ilium and the lower three ribs (Crouch 1985). The insertion is through a flat tendon (approximately 7.5 cm in length), lying parallel and medial to the insertion of the pectoralis major, attaching to the lower portion of the intertubercular groove (Crouch 1985). The thoracodorsal nerve from the brachial plexus supplies innervation, arising from the sixth, seventh and eighth cervical nerves.

The fibres of the latissimus dorsi converge from their wide origin, similar to the pectoralis major, with its flat tendon twisted 180 degrees just prior to the insertion (Crouch 1985). The muscle is attached to the lower vertebrae and sacrum by a sheet of aponeurotic fibrous tissue called the thoracolumbar fascia. The latissimus dorsi, acting alone, may produce extension of the glenohumeral joint and medial rotation of the shoulder joint due to its insertion on the anterior aspect of the humerus (Jenkins 1998), assist the deltoid with horizontal extension (MacConaill and Basmajian 1977) and, acting together in synergy with the pectoralis major, produce upper limb adduction (Kapandji 1982). As many as 6 functionally independent muscle segments have been identified in the latissimus dorsi through anatomical and electromyographical investigations (McAndrew and Brown 2004; Paton and Brown 1995; Wickham 2002; Wickham, Brown *et al.* 2004).

2.12 Justification of research direction

The preceding review of the relevant literature serves to lay the basis for the proceeding research. The current literature however, fails to report on a number of vital aspects relating to the understanding of the structure and function of multi-segmental human muscle. Justification for the research is based on the following points:

- While investigations utilising various MMG sensors have confirmed the validity of its use in determining motor unit properties, no work has assessed the validity of multiple measurement sites within a single muscle. Study A and B will address the development of the Laser-MMG and validate the technique for determining, in an animal model, motor unit properties under conditions that modulate the physiological performance of the muscle (temperature and fatigue). Study C will address the ability, in an animal model, to determine such properties from multiple distinct sites within a single muscle.

- It has yet to be determined how muscle segment fibre type compositions (the spatial distribution of muscle fibre types) differ across the surface of a multi-segmental human muscle. Study D and E will address this through investigations that aim to determine the contractile properties of muscle segments within human gluteus maximus, pectoralis major, deltoid and latissimus dorsi. Muscle segment contractile properties will be correlated to functional roles.

- Only recently, research has focused on gaining an understanding of the neuromotor control of muscle segments. While previous electromyographic investigations have quantified timing and intensity properties during movements of varied force and direction, the effect of movement speed on neuromotor control is yet to be determined. Study F will assess the effect of movement speed and muscle fibre type composition on the neuromotor control of muscle segments.

Chapter 3

General Methods

3.1 Introduction

This chapter outlines the equipment and methodologies utilised during the data collection phase of the research. Each recording technique was utilised to assess particular properties from the animal and human muscles under investigation. In most experiments described here, a non-invasive Laser-MMG was used to measure muscle contractile properties from the lateral displacement of the muscle belly following neuromuscular stimulation. As described before (Akataki, Mita, Watakabe and Itoh 2003), the lateral displacement of a muscle's belly may provide information on its contractile properties and by inference, its constituent muscle fibre type (Dahmane, Djordjevic *et al.* 2005; Dahmane, Valencic *et al.* 2001). Measurements of muscle contractile properties, using an invasive Tensiometry technique, were also recorded during the animal studies. Tensiometry is the 'gold standard' for the assessment of muscle contractile properties and was used as a comparison to those derived from the Laser-MMG. However, the invasive nature of Tensiometry largely prevents its application to human subjects; a limitation not present with the Laser-MMG technique. Finally, a electromyographic technique was utilised to determine the activation patterns, and therefore function, of muscle segments within three superficial human shoulder muscles.

3.2 Mechanomyography (MMG)

The Laser-MMG (Onspot, Australia) was designed "in-house" to measure the lateral displacement of a muscle's belly following percutaneous neuromuscular stimulation (PNS), utilising a unique laser sensor. Originally designed to measure human muscle function *in vivo*, it was adapted for the *in vitro* assessment of animal muscle in the laboratory. The Laser-MMG consisted of three integral components: (a) the laser sensor, (b) the MMG stimulator and (c) the MMG collection software. All three components were specifically designed to measure muscle contractile properties including maximal displacement, contraction time and time to relaxation.

3.2.1 MMG laser sensor

The laser sensor (Model LG10A65PU) was supplied by Banner Engineering (Australia). It was a self-contained Class 2 visible displacement laser featuring a diffuse sensing beam (670 nm visible red laser; 0.20 mW radiant power output) with a sensing distance of 75 mm to 125 mm, a focal point of 180 mm and a beam size of 0.06 mm x 0.8 mm. The maximum resolution, within the normal operating range, was less than 10 μm. Before each testing session the laser's self test function was executed followed by a calibration against a series of known standard distances (1–10 mm; 0.5 mm increments). This proved the linearity between the sensor's voltage (V) output with displacement (mm). All data from the laser sensor was collected at 10 kHz and stored on a desktop IBM compatible computer.

3.2.2 Neuromuscular Stimulation

Neuromuscular stimulation (direct or PNS) was administered via an MMG stimulator (Onspot-Australia). This unit exceeded Australian design regulations for therapeutic electrical devices (AS/NZS 3200.2.40:1999). The device offered an operating range of 0 V to 180 V (1 volt increments) at a fixed current of 85 mA and a pulse duration range of 50 μs to 500 μs (50 μs increments). Neuromuscular stimulation could be delivered as a single twitch or as a train of pulses depending upon the application. In all animal studies, neuromuscular stimulation was delivered directly to the muscle via direct contact with the MMG electrodes. In contrast, all human studies involved the stimulation of muscle tissue through the skin (PNS) via surface electrodes.

3.2.3 Animal muscle preparation

The Laser-MMG was adapted for both human and animal preparations. For experiments utilising the isolated gastrocnemius muscle, the animal's hind limb was removed immediately following euthanasia via pithing (toad) or following anesthesia with pentobarbital sodium (60 $mg.kg^{-1}$ body weight intra-peritoneal) and rapid exsanguinations (rat), and dissected to reveal the underlying gastrocnemius musculature. After the resting length of the whole muscle was measured *in-situ*, it was rapidly

dissected from the limb and placed in a bath of toad Ringers solution (toad) or Krebs Buffer solution (rat) pre-gassed with carbogen (compressed 5% carbon dioxide in oxygen) (BOC Gases, Australia) and at room temperature (23°C). After the muscle was cleaned and trimmed of any additional connective tissue, its proximal end was attached to a force transducer on the test rig with surgical silk. The muscle's distal end was attached to an anchor point on the test rig via surgical silk (toad) or glue (SupaGlue Gel) to ensure its anatomical shape was maintained (rat) (Figure 3.1).

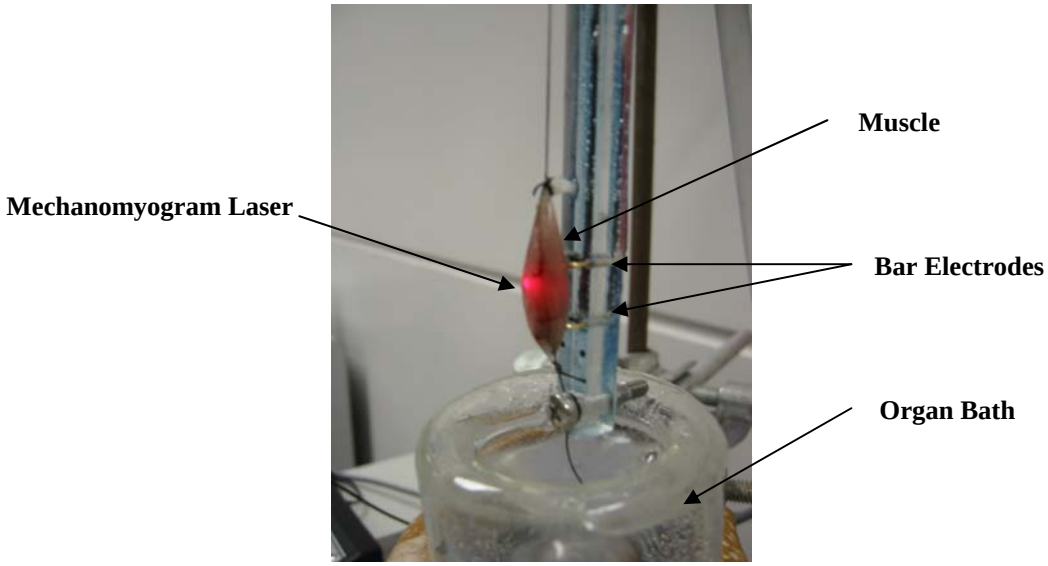

Figure 3.1 Gastrocnemius muscle of the toad attached to the test rig, resting against the bar stimulation electrodes. Seen below the muscle is the organ bath containing gassed Ringers solution. The laser beam (red dot) of the Mechanomyogram is visible on the surface of the muscle belly. The muscle was only lifted clear of the solution in the organ bath when undergoing stimulation.

3.2.4 Simultaneous measurement of Laser-MMG & Tensiometry (Animal studies)

Prior to testing, the Laser-MMG and force transducer were connected to the computer and calibrated for displacement (mm) and tension (g) respectively. The muscle was attached to the testing rig and to the force transducer at a length similar to its *in situ* anatomical length (Figure 3.2). The MMG's laser sensor was orientated perpendicular to the muscle belly at positions appropriate for each study.

Direct neuromuscular stimulations were delivered via two bar electrodes (Fig. 3.1) that were in contact with each end of the muscle belly (toad) or by two 75 μm fine wire electrodes (A-M Systems, stainless steel, Teflon coated, catalogue no. 791000), inserted into either end of the muscular tissue (rat). Each electrode was connected to the MMG stimulator which delivered the stimulation current. The optimal voltage required to maximally stimulate each muscle was assessed by performing a voltage ramp (incrementally stepping up the stimulation voltage until maximal displacement, as measured by the Laser-MMG, was achieved). The optimal muscle length was then determined by stimulating the muscle at maximal voltage whilst making micrometer adjustments to its length above and below its 'resting' length. Once the optimal length was obtained, the muscle was rested for 10 minutes, within the appropriate solution, prior to the experimental trials.

Typically, ten single twitch recordings (one twitch = one trial) were made at each Laser-MMG recording site, predetermined as the site that produced the largest displacement during supra-maximal twitch stimulation (Orizio, Baratta *et al.* 1999). During each trial the muscle was removed from the organ bath for approximately 5 seconds to allow the stimulation and data collection to take place and then returned for 2 minutes prior to the next stimulation. This was necessary because the beam of the laser sensor was unable to penetrate the dual glass layers of the jacket organ bath.

Data from the Laser-MMG and force transducer was recorded simultaneously through a National Instruments® A-D card and an in-house designed collection and analysis program using LabVIEW® software (National Instruments®). Data was stored on a computer for later analysis (Figure 3.2).

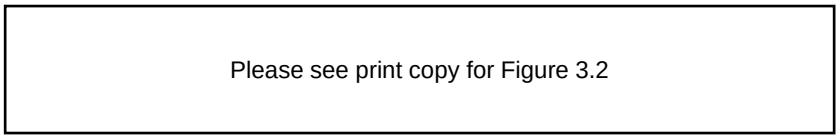

Figure 3.2 Neuromuscular stimulation (a) generated a longitudinal isometric tension (b) which was recorded by a force transducer (c). Simultaneously, the lateral displacement of the muscle's belly (d) was recorded by the Laser-MMG (e). Both the Laser-MMG and force transducer data were stored on a computer. Diagram adapted from Philips (2005).

3.2.3 Laser-MMG waveform analysis

Maximal neuromuscular stimulation of the muscle produced a mono-phasic parabolic Laser-MMG waveform that represented the displacement of the muscle's belly (Figure 3.3). Two phases could be identified within each Laser-MMG waveform: an ascending phase, where the muscle was contracting in response to the stimulation pulse delivered by the neuromuscular stimulation device; and a descending phase, where the muscle was undergoing relaxation. The properties of muscle belly displacement could be determined

by analysing the Laser-MMG waveforms (Figure 3.3). The following parameters were determined from the Laser-MMG waveforms generated during each trial:-

A **Maximal lateral displacement (Dmax) –** maximal lateral displacement of the muscle belly (mm)
B **Contraction time (tc) –** the period of time between 10% and 90% maximal displacement (ms)
C **Relaxation time (tr) -** the period of time between 90% to 10% of maximal displacement (ms)
D **Sustain time (ts) -** the period of time the muscle's displacement was greater than 50% of its maximal value (ms)
E **Maximal rate of contraction (+dD/dt) -** maximal slope of the positive displacement curve (+mm/s)
F **Maximal rate of relaxation (-dD/dt) –** maximal slope of the negative displacement curve (-mm/s)
G **Start time (tstart)** – time from stimulation to 10% maximal displacement (ms)

It is important to note that all time variables (e.g. contraction time, relaxation time and sustain time) were normalised for the amount of displacement achieved and are generally presented throughout the manuscript in this format and not as absolute values. The principal reason for this normalisation process was to ensure that the magnitude of muscle displacement, unique to each muscle, did not influence the time variables. A muscle or muscle segment moving at a constant rate with a larger magnitude of displacement would theoretically take a longer time period to reach its peak. Therefore all time variables were normalised in an attempt to allow for a more accurate comparison between the muscles or muscle segments. The normalised time variables are presented as:

- **Normalised contraction time (tc*N*) –** contraction time / maximal displacement (ms/mm)
- **Normalised relaxation time (tr*N*) –** relaxation time / maximal displacement (ms/mm)
- **Normalised sustain time (ts*N*) –** sustain time / maximal displacement (ms/mm)

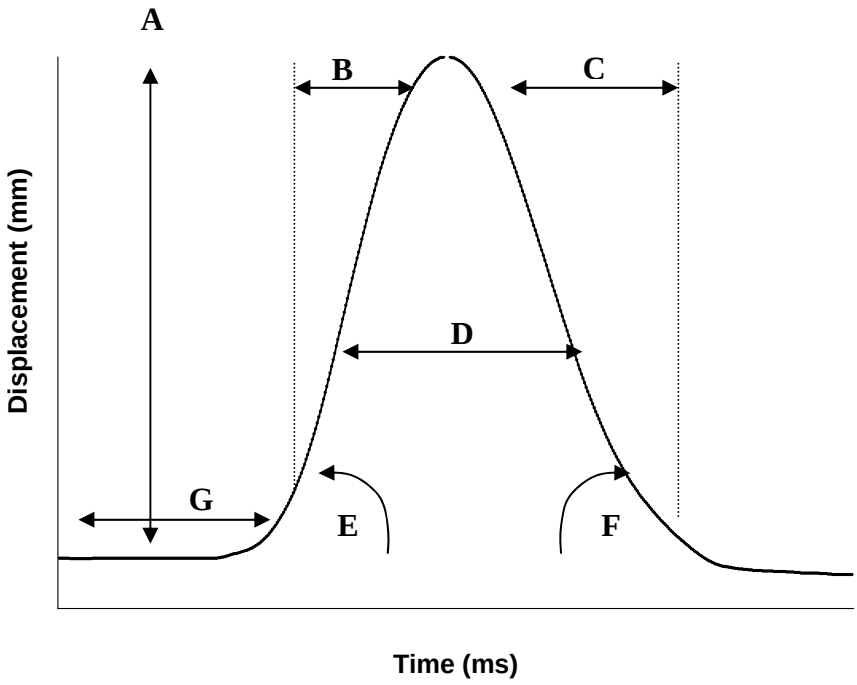

Figure 3.3 Quantification of the Laser-MMG waveform **A:** Maximal displacement (mm) **B:** Contraction time from 10-90% of Dmax (ms) **C:** Relaxation time from 10-90% of Dmax (ms) **D**: Sustain time above 50% Dmax (ms) **E:** Maximal rate of contraction (+mm/s) **F:** Maximal rate of relaxation (-mm/s) **G:** Start time (ms)

3.3 Tensiometry

3.3.1 Force transducer

All tension measurements were recorded using a GRASS® Force Transducer Model FT03C manufactured by Grass Instrument Co, Quincy, Mass., USA. The force transducer operated with a maximum working range of ± 0.2 kg and a displacement rate of 5 mm/kg. Prior to each testing session the transducer was calibrated against a series of known weights (H.B. Selby & Co. LTD). This proved the linearity between the transducers voltage (V) output and tension (g). Force transducer data was recorded at a sampling rate of 1000 Hz.

3.3.2 DC Amplifier

The output of the force transducer was fed through a single channel amplifier (Onspot, Australia) which had both DC offset and gain adjustability. The amplified signal was passed through a breakout box connected to the National Instruments® A-D card.

3.3.3 Tension waveform analysis

Electrical stimulation of the muscle tissue produced a mono-phasic parabolic waveform that represented the tension generated longitudinally through the tendon of the muscle (Figure 3.4). Two phases could be identified within each waveform: an ascending phase, where the muscle was contracting in response to the stimulation pulse delivered by the neuromuscular stimulation device; and a descending phase, where the muscle was undergoing relaxation (Figure 3.4). The properties of tension development were determined by analysing the following parameters that were calculated from the waveforms:

A **Maximal isometric Tension development (Tmax) –** maximal tension development (g)

B **Contraction time (tc) –** the period of time between 10% and 90% maximal tension (ms)

C **Relaxation time (tr) -** the period to time between 90% to 10% of maximal tension (ms)

D **Sustain time (ts) -** the period of time the muscle's tension was greater than 50% of its maximal value (ms)

E **Maximal rate of contraction (+dT/dt) -** maximal slope of the positive tension curve (+g/s)

F **Maximal rate of relaxation (-dT/dt) -** maximal slope of the negative tension curve (-g/s)

G **Start time (tstart)** – time from stimulation to 10% maximal tension (ms)

All time variables (contraction time, relaxation time and sustain time) were normalised for the amount of tension achieved and are generally presented throughout the manuscript in this format and not as absolute values. The normalised time variables are presented as:

- **Normalised contraction time (tc*N*) –** contraction time / maximal Tension (ms/g)
- **Normalised relaxation time (tr*N*) –** relaxation time / maximal Tension (ms/g)
- **Normalised sustain time (ts*N*) –** sustain time / maximal Tension (ms/g)

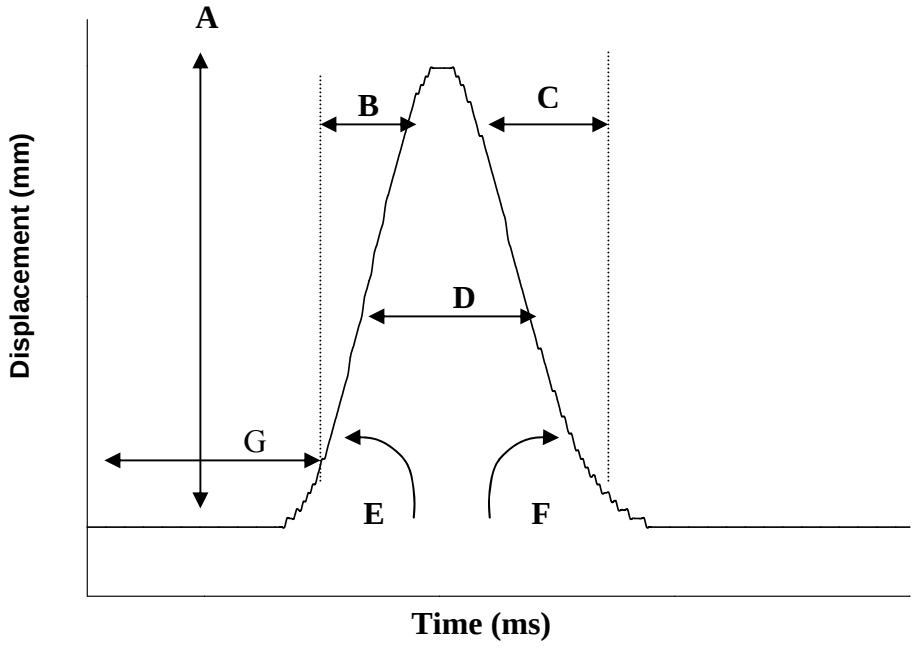

Figure 3.4 Quantification of the Tension waveform **A:** Maximal Tension (Tmax) (g) **B:** Contraction time from 10-90% of Tmax (tc) (ms) **C:** Relaxation time from 10-90% of Tmax (tr) (ms) **D**: Sustain time above 50% Tmax (ts) (ms) **E:** Maximal rate of contraction (+dT/dt) (+g/s) **F:** Maximal rate of relaxation (-dT/dt) (-g/s) **G:** Start time (tstart) (ms)

3.4 Electromyography (EMG)

3.4.1 Surface Electrodes

Fourteen bipolar surface microelectrodes were designed and manufactured specifically for this experiment (Figure 3.5) to minimise electrode pickup area and hence reduce potential electrode crosstalk. The microelectrodes consisted of two 1.6 mm diameter active plates made of 18 carat gold wire (0.7 mm diameter) each of which was heated, expanded and

then filed to a flat electrode surface. A male gold plated computer terminal pin was soldered in parallel to the opposite end of the 12 cm wire and sealed with heat shrink. To produce the base that housed the recording area of the electrode, a 10 mm brass cast was machined into which two wells (6.5 mm inter-electrode distance, 2 mm deep) were drilled. To this cast, rubber-moulding material was applied to create an inverse mould of the microelectrodes. To produce the microelectrode base, 5 minute araldite was combined with ink dye and poured into the mould, surrounding the gold electrodes that were embedded in the rubber base. Different colour ink dyes were used to identify the electrodes for the three different muscles. The finished product consisted of a solid electrode base containing individual wells that housed the flat gold recording electrodes. Through utilising individual recording wells, gel contamination from the opposite recording plate was eliminated and consistent inter-electrode distances across all electrodes / recording sites was achieved. The bipolar microelectrode base was adhered to the skin via double-sided tape. Electrode gel contacted the skin via holes punched through the tape.

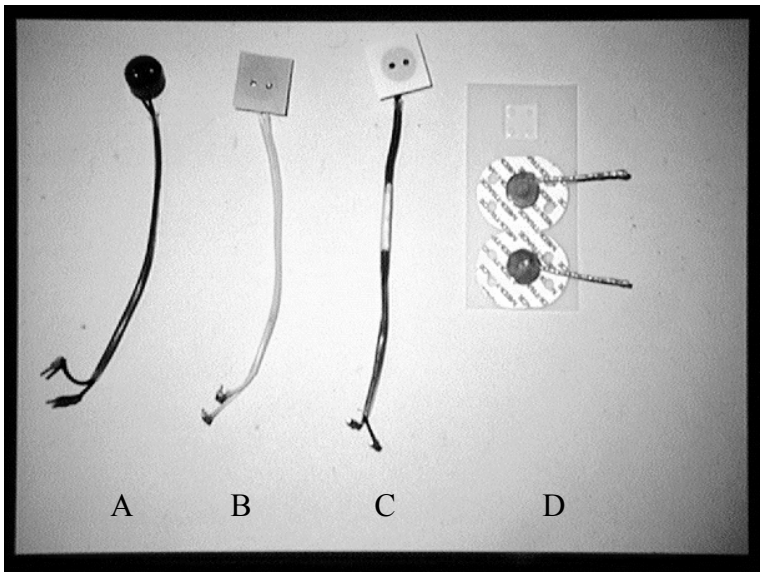

Figure 3.5 Bipolar microelectrode and commercially available unipolar electrodes. A: unprepared microelectrode B: microelectrode with double sided adhesive tape attached C: prepared microelectrode prior to attachment to subject D: commercial electrodes in a bipolar configuration. The microelectrodes designed for this thesis enabled a surface pickup area equal to a sphere of 6 mm radius from each electrode within the microelectrode housing.

3.4.2 Myoelectric Amplifiers

Two 8 channel HUMTEC electromyographic amplifiers collected the raw signals during the experimental trials. Each channel had a selectable sensitivity range of 100 μv to 5000 μv. The differential pre-amplifier leads (x14) had a 90 db common mode rejection ratio. The amplifiers were calibrated to ensure consistency and accuracy prior to data collection by passing sine wave calibration signals (50 Hz, 1 Volt peak to peak) (Kikusui Model 418B) through each pre-amplifier and amplifier, with the collected waveforms saved for later analysis.

3.4.3 Myoelectric signal analysis

Myoelectric signals were pre-amplified (x10) and high-pass filtered, with a cut-off frequency of 10 Hz, prior to collection. The raw electromyographic data was low-pass filtered using a cut-off frequency of 30 Hz, notch filtered for 50 Hz interference and full wave rectified. The temporal properties of the electromyographic waveforms were ascertained via visual inspection of: i) the 1000 Hz low pass raw signal directly from the HUMTEC amplifier, ii) the full wave rectified signal, iii) the low / high / 50 Hz notch filtered electromyographic signal and iv) the threshold detector signal. All signals were displayed simultaneously on the computer screen. The criteria for determining the onset and offset of each electromyographic waveform was based on a minimum threshold detection of 10% of the maximum voltage achieved for that trial and a minimum burst duration of 50 ms.

An electromyographic intensity (amplitude) analysis was performed by scaling all signals to a common amplification level to negate differences in electrode site amplification, removing any sample offsets and by full wave rectifying as per the temporal analysis. An integrated electromyographic (iEMG) value was determined between the electromyographic waveform's onset and offset by subdividing its duration into 10 ms intervals with the resultant values averaged to calculate average mV/ms (its 'discharge rate').

The properties of muscle segment activation were determined by analysing the following parameters that were calculated from the electromyographic waveforms (Figure 3.6):

Temporal parameters (Figure 3.6)

A **Onset (On)**: onset time of electromyographic activity in relation to FcOn (ms)

B **Offset (Off)**: offset time of electromyographic activity (ms)

C **Peak (Pk)**: time of peak electromyographic activity (ms)

D **Duration (Dur)**: duration of electromyographic activity (ms)

E **Force Onset (FcOn)**: initial rise of the force/time curve – identified as 0 ms

F **Force Offset (FcOff)**: final fall of the force/time curve (ms)

G **Force Peak (FcPk**): peak of the force/time curve (ms)

Amplitude parameters (Figure 3.6)

H **Intensity (Int)**: maximal intensity of electromyographic activity (mV)

It is important to note that the duration of muscle segment activation was normalised for the total movement time (TMT) and is generally presented throughout the manuscript in this format and not as absolute values. The principal reason for normalisation was to ensure that the movement time, unique to each TMT, did not influence the time variables. Additionally, the discharge activity for each muscle segment was normalised to a percentage of the value it achieved during a maximum voluntary contraction (Mirka 1991). The time and amplitude variables were normalised in an attempt to allow for a more accurate comparison between the muscles or muscle segments. The normalised time variables are presented as:

- **Normalised Onset (On*N*)**: onset of electromyographic activity in relation to FcOn (ms)
- **Normalised Peak (Pk*N*)**: time of peak electromyographic activity in relation to FcPk (ms)
- **Normalised Duration time (Dur*N*%)**: duration of electromyographic activity expressed as a percentage of the TMT [(Dur/TMT)*100] (%)
- **Normalised iEMG (iEMG*N*%)**: average iEMG expressed as a percentage of that muscle segments average iEMG value recorded during the 100% MVC.

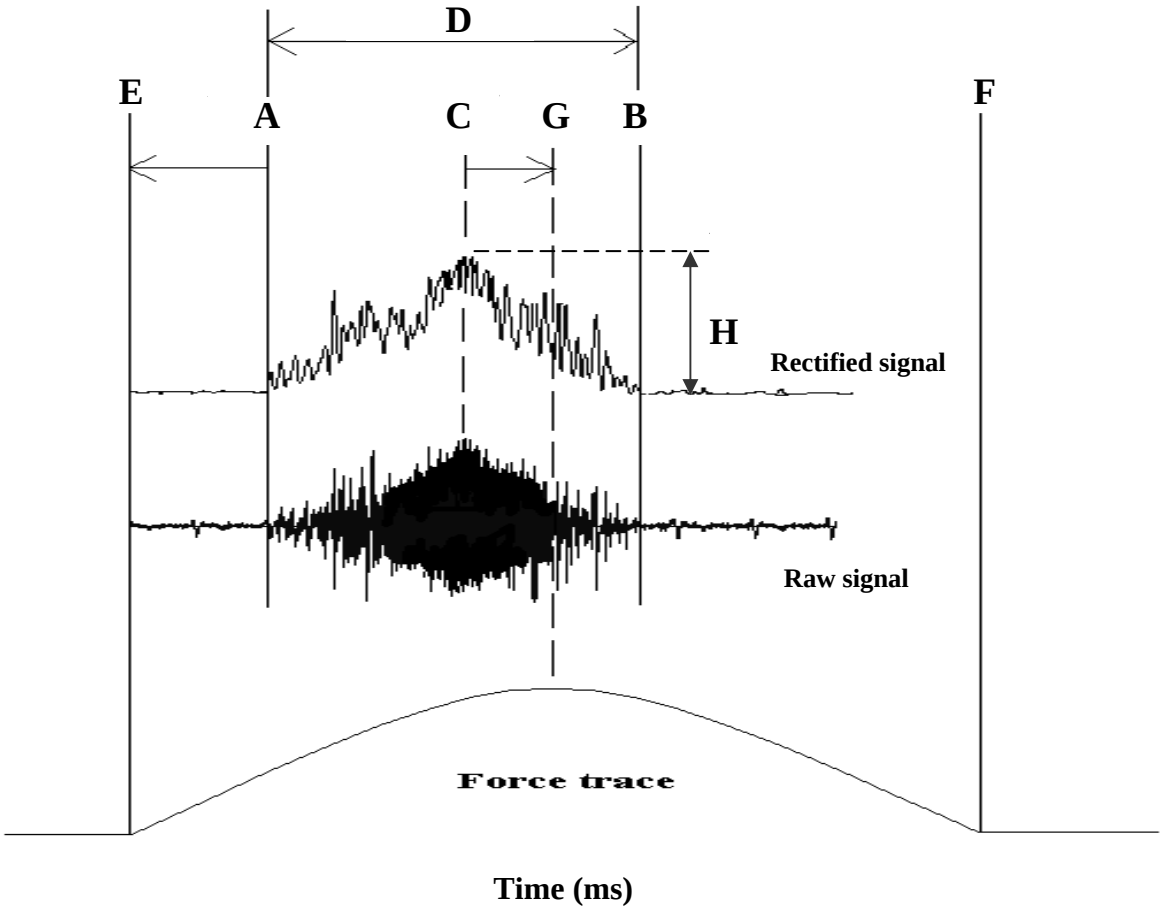

Figure 3.6 Myoelectric and Force variables determined from the signals recorded during each trial. A: Onset (ms) B: Offset (ms) C: Peak (ms) D: Duration (ms) E: Force Onset (0ms) F: Force Offset (ms) G: Force Peak (ms) H: Intensity (mV)

Chapter 4

Validation of Mechanomyography I: Sensitivity to physiological modulators of muscle contractile properties

4.1 Introduction

The contractile properties of muscle can be altered through experimentally induced physiological change. Conditions such as muscle fatigue (Allen, Lannergren and Westerblad 1995) and altered temperature (Bennett 1984) are well known to influence muscle contractile properties as measured within the temporal and amplitude domains of the waveforms recorded from an appropriate measuring device. The contractile properties of muscle are usually investigated by analysis of its force-time waveform and/or its electromyographic activity or mechanical counterpart (MMG). As discussed above, the MMG waveform is a measure of the lateral displacement of the muscle's belly and is generated by the pressure waves developed from the lateral expansion of the activated and shortening muscle fibres (Orizio 1993). As per the force signal, an analysis of the MMG in the temporal domain suggests that it may reflect not only the underlying motor unit recruitment, but also the contractile properties of the activated motor units (Bichler and Celichowski 2001a, 2001b; Esposito, Orizio *et al.* 1998; Yoshitake, Shinohara *et al.* 2002). Additionally, it has been demonstrated that the relative proportions of fast- and slow-twitch motor units within the muscle determines its contractile properties (Bellemare, Woods, Johansson and Bigland-Ritchie 1983) and so may influence features of the MMG waveform such as contraction time and relaxation time (Dahmane and colleagues 2001; 2005). Data from the above mentioned research suggests that MMG analysis has utility for quantifying the magnitude of change in muscle contractile properties induced by different physiological conditions.

For example, altering muscle temperature produces quantifiable changes in a muscle's contractile properties (Asmussen and Gaunitz 1989; Bennett 1984, 1985; Bershitsky and Tsaturyan 2002; Bigland-Ritchie, Thomas, Rice, Howarth and Woods 1992; Prezant, Richner, Valentine, Aldrich, Fishman, Nagashima, Chaudhry and Cahill 1990). In particular, the work of Kimura, Hamada *et al.* (2003) has determined, by using an MMG technique, that experimentally induced hypothermia within the human triceps surae muscle produces a marked slowing in contractile properties including the prolongation of twitch contraction- and relaxation-times.

Likewise, muscle fatigue has a readily detectable effect on the contractile properties of muscle tissue (Bigland-Ritchie and Woods 1984; Esposito, Orizio *et al.* 1998; Perry-Rana, Housh, Johnson, Bull, Berning and Cramer 2002; Yoshitake, Ue, Miyazaki and Moritani 2001). Muscle fatigue is defined as 'any reduction in the force generating capacity regardless of the task performed' (Bigland-Ritchie and Woods 1984). While easily quantified by invasive techniques in an animal model, in the human such techniques (if ethical) are restricted to a limited range of strictly controlled laboratory experiments. Moreover, non-invasive measures of muscle force (e.g. KinCom, Cybex) cannot provide more than an estimate of the force produced by groups of muscles around a joint, and certainly not individual muscles or segments of individual muscles (Abernethy, Wilson and Logan 1995). Investigations therefore have focused on identifying alternative methods to determine changes in muscle tension. Importantly, it is becoming apparent that the non-invasive MMG technique may have utility in determining force production in individual muscle segments around a particular joint. For the MMG technique to have application, and, in particular the Laser-MMG technique developed for this thesis, it needs to undergo a rigorous validation process against what are considered to be the 'gold standard' invasive techniques (e.g. Tensiometry) for quantification of muscle force output.

The three experimental studies presented within this chapter endeavored to determine (validate) whether the Laser-MMG technique could faithfully reflect the contractile properties of muscles which were undergoing change due to alterations in muscle temperature (induced hypothermia) and fatigue. Importantly, the output of the Laser-MMG was compared to that derived from a Tensiometric technique which measured actual force developed longitudinally through the muscle's tendons. The correlation between the outputs of the Laser-MMG and the Tensiometric technique was considered to be an indicator of the validity of the Laser-MMG technique. In addition, because a major focus of the Laser-MMG technique is to assist diagnosis in human populations (Gorelick 2005), to date no *in vitro* studies have been performed in an animal model using this particular technique. Therefore, its applicability to measure contractile properties in animal skeletal muscle is, at present, unknown.

In the following experiments, the simultaneous collection of Tensiometry and Laser-MMG measures allowed for direction and sensitivity comparisons between the techniques and provided confirmation that the muscle, under experimental condition, was behaving in an acceptable, literature-proven manner. This was a vital step in order to establish the Laser-MMG's physiological relevance.

In the context of this thesis, it was important to establish that the Laser-MMG technique possessed the capacity to ultimately be used to differentiate individual human muscle segments based on their fibre type compositions. The three individual studies were designed with the specific aim to determine this capacity. This was achieved through imposing conditions on muscle *in vitro* that negatively impacted on its ability to contract optimally and by comparing the MMG response (output) with that from Tensiometry. In addition, it was valuable to determine whether the Laser-MMG technique was sensitive to differences in muscle fibre type. These important outcomes were achieved by measuring the effects of altered thermal status (Study A) and fatigue (Study B) and by investigating the influence of muscle fibre type concentrations (Study C) on muscle contractile properties in an animal model.

4.2 Aims and Hypotheses

Specifically, this part of the thesis aimed to set up and evaluate a new Laser-MMG technique that would:

1. Pioneer its use in an animal model,
2. Determine the sensitivity of the Laser-MMG technique to the effects of known modulators of muscle fibre contractile performance and
3. Determine the ability to detect the contractile properties of small sub-volumes of muscle with contrasting muscle fibre-type concentrations.

It was hypothesised that measurements from the Laser-MMG would:

1. Mimic the directional trends of simultaneous measures of tension (Tensiometry),

2. Sensitively detect the effects of temperature and repetitive stimulation (fatigue) on muscle contractile properties as does the Tensiometric technique,
3. Sensitively detect differences in muscle contractile properties due to varied fibre type concentrations, as can be detected by Tensiometry and
4. Prove viable in determining the contractile properties of individual muscle segments within the whole muscle.

4.3 Methods

4.3.1 Study A: Laser-MMG response to a change in muscle temperature

4.3.1.1 Experimental design

This experiment compared the output of the Laser-MMG, with that of Tensiometry, following neuromuscular stimulation of *in vitro* muscle at three different temperatures. The aim was to determine whether the Laser-MMG could accurately detect changes in muscle contractile properties (e.g. maximal displacement, contraction- and relaxation-time) due to altered thermal states. The experiment was constructed as a randomised, repeated measures design, developed and conducted in conjunction with Snelson (2003).

4.3.1.2 Animals

The animals consisted of 10 adult cane toads (*Bufo marinus*), previously sacrificed for a first year physiology teaching class. Prior to sacrifice the animals were housed within the University Animal House and were allowed *ad libitum* access to food and water for the duration of their housing.

4.3.1.3 Measurement of Laser-MMG and Tension

The MMG laser beam was orientated perpendicular to the muscle belly, at a position representing 50% of muscle tissue length. Ten single twitch recordings were made at each muscle temperature (15°C/20°C/25°C, randomized order between subjects). Muscles were incubated for 10 minutes at each temperature to ensure consistent and even muscle temperature. The organ bath water jacket temperature and the toad Ringers solution temperature were controlled by small ancillary heating/cooling baths. The experimental setup ensured a short distance between the heating/cooling bath and the organ bath in order to minimise temperature fluctuations. All temperatures were measured at the muscle via a thermometer mounted within the organ bath.

4.3.1.4 Statistical analysis

Only those muscles in which both displacement and tension measurements were obtained, underwent analysis. All data presented as mean ± SEM unless otherwise stated. Twelve variables (6 Laser-MMG & 6 Tension parameters) were determined from each muscle. All statistical analyses were performed using SigmaStat (SPSS Inc. USA). Data was subjected to a normality and equal variance test to confirm the normal distribution and equal spread of the data (all passed).

a) Quantification of temperatures effect on muscle performance

A Repeated Measures Analysis of Variance (RMANOVA) (α=0.05) was conducted in order to identify any significant differences in measurement variables (displacement etc.) for each measurement device (MDL and Tensiometry) related to differing thermal states. A post-hoc analysis (Tukey Test) was used to further identify any significant differences between the experimental temperatures. Data related to the contraction-, sustain- and relaxation-times for each temperature were normalised for the effect of displacement and tension respectively.

b) The relationship between Laser-MMG and Tension

A Pearson's Correlation was carried out to determine the magnitude and direction of the relationship between the Laser-MMG and Tension variables. The power of the performed test was α<0.05.

4.3.1.5 Ethics

Ethical clearance for this experiment was sought and received from the University of Wollongong Animal Ethics Committee.

4.3.2 Study B: Laser-MMG response to a change in muscle fatigue

4.3.2.1 Experimental design

This experiment assessed, in a muscle *in vitro*, the effect of a repetitive stimulation task on muscle contractile properties (e.g. maximal tension/displacement, contraction- and relaxation-times) determined from the output of the Laser-MMG and Tensiometric techniques. A comparison between the techniques was performed to determine the sensitivity of the Laser-MMG technique to that of Tensiometry. This experiment was performed using a randomised, repeated measures design, developed and conducted with Gorelick (2005).

4.3.2.2 Animals

The animals consisted of 12 adult male (aged 10 - 14 weeks) Wistar rats, weighing between 340 g and 510 g (average of 408 g).

4.3.2.3 Measurement of Laser-MMG and Tension

The MMG laser beam was orientated perpendicular to the muscle belly, at a position representing 50% of muscle tissue length. The experimental protocol consisted of a repetitive maximal stimulation task (50 μs pulse duration, 2 Hz, 20 second duration). Single twitch maximal stimulations (50 μs pulse duration) were conducted prior to the task to determine baseline contractile properties and immediately upon completion to quantify the tasks effect.

4.3.2.4 Statistical analysis

Only those muscles in which both displacement and tensions measurements were obtained underwent analysis. All data is presented as mean ± SEM unless otherwise stated. Twelve variables (6 Laser-MMG & 6 Tension parameters) were determined from each muscle. All statistical analyses were performed using SigmaStat (SPSS Inc. USA). Data was subjected to a normality and equal variance test to confirm the normal distribution and equal spread of the data (all passed).

a) Quantification of muscle performance

A paired two sample, two tailed t-test (α=0.05) was conducted in order to identify any significant differences in measurement variables (contraction and relaxation time etc.) between the pre- and post- fatigue trials for each measurement device (MDL and Tensiometry). Data related to the contraction and relaxation times for each muscle was normalized for the effect of displacement and tension respectively.

b) The relationship between Laser-MMG and Tension

A Pearson's Correlation was performed to determine the magnitude and direction of the relationship between the Laser-MMG and Tension variables. The power of the performed test was α<0.05.

4.3.2.5 Ethics

The University of Wollongong Animal Ethics Committee approved all procedures conducted in this experiment.

4.3.3 Study C: Laser-MMG response to a change in muscle segment fibre type

4.3.3.1 Experimental design

This experiment determined the utility of the Laser-MMG to detect differences in muscle contractile properties (e.g. fibre type, contraction speed etc) between two segments of the medial gastrocnemius by comparing the Laser-MMG output of each muscle segment. Additionally, the Laser-MMG output was compared to that of a standard Tensiometry technique during stimulation of each muscle segment to determine the sensitivity of the Laser-MMG technique. This experiment was conjointly designed and conducted with Philips (2005).

4.3.3.2 Animals

The animals consisted of 10 adult male (aged 10 - 16 weeks) pathogen-free Wistar rats weighing between 380 g and 640 g (average 478 g).

4.3.3.3 Muscle preparation

The muscle chosen for analysis was the medial gastrocnemius which was composed of two distinct muscle segments; a darker red 'proximal' segment (25.5% Type I fibres: 74.5% Type II fibres, Kraemer, Staron *et al*. 2000) and a lighter red 'distal' segment (0% Type I fibres: 100% Type II fibres, Kraemer, Staron *et al.* (2000)) (Figure 4.1).

4.3.3.4 Measurement of Laser-MMG and Tension

The MMG laser was positioned in the middle of the muscle segment's belly, perpendicular to the direction of muscle belly movement. Intra-muscular stimulation was applied to either end of the proximal (red) or distal (white) segment of the muscle. These muscle segments could be easily identified by direct observation. The optimal voltage and muscle segment length were specific for the selected active muscle part and determined as previously described (Chapter 3, General Methods). It is known that optimum length differs for rat medial gastrocnemius when different muscle segments are active (De Ruiter, De Haan *et al.* 1995b). The optimal length for the muscle with the distal muscle segment active was about 1.5 mm longer than when the proximal part was active because the distal

segment muscle fibres contain slightly more sarcomeres in series than fibres in the proximal part (Heslinga and Huijing 1990).

On completion of testing, each muscle segment's MMG laser recording site was marked with ink to enable identification when cryostat sectioning, then wrapped in aluminium foil, snap frozen in liquid nitrogen and stored in a -80°C freezer for histochemical analysis.

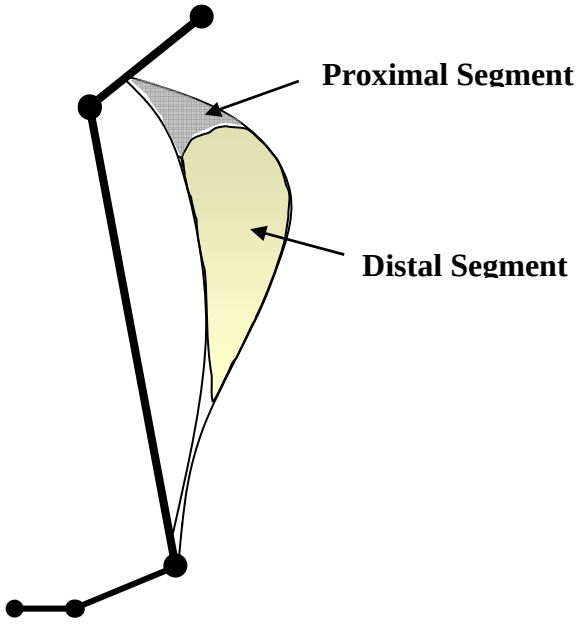

Figure 4.1 Diagram of the medial gastrocnemius muscle attached to the lower limb of the rat. Indicated is the muscle consisting of a darker proximal muscle segment and a lighter distal muscle segment. Differences in shading also reflect differences in muscle fibre types.

4.3.3.5 Histochemical analysis

Prior to cryostat sectioning each muscle was separated into its proximal 'red' and distal 'white' segments. Each muscle segment was mounted on to a specimen holder using Jung tissue freezing medium (Leica Microsystems, GmbH, Germany). Serial cross sections, 10 μm in width, were cut from each muscle segment using a cryostat (Jung CM3000, Leica Instruments, GmbH, Germany) and mounted on gelatine coated glass slides.

Myosin adenosine triphosphatase staining (ATPase, pre-incubation at pH 4.3) was demonstrated using a protocol from the Muscle and Nerve Staining Manual (The Institute of Clinical Neurosciences, Royal Prince Alfred Hospital, Sydney, Australia, (Bonner and Pollard 2003). Using Image Pro Software, a composite digital image of each ATPase preparation was prepared, which enabled the muscle fibres to be classified as type I and type II on the basis of myosin ATPase uptake (Brooke and Kaiser 1970). A standard H & E stain, produced by the Anatomical Pathology Laboratory at Wollongong Hospital, NSW, Australia was also performed to gather architectural information from each muscle segment.

4.3.3.6 Measurement of cross sectional area and muscle fibre number

The analysis was performed using measurements of relative optical density in order to avoid the subjective interpretations of relative staining intensity. The cross sectional area (whole muscle and each muscle segment) and the number of type I (slow-twitch) and type II (fast-twitch) muscle fibres was measured and recorded according to established practice (Guyton and Hall 2000). The proportion of muscle segment cross sectional area devoted to either type I or type II muscle fibres was calculated via Image-Pro Software and expressed as a percentage of the whole cross sectional area for the muscle segment. Additionally the actual number of type I or type II muscle fibres was determined and the results expressed as a percentage of the total number of fibres counted per muscle segment.

4.3.3.7 Statistical Analysis

Data was obtained from proximal and distal muscle segments of the medial gastrocnemius (MG). Only muscles in which both proximal and distal measurements were obtained were analysed. All data is presented as mean ± SEM unless otherwise stated. Twelve variables (6 Laser-MMG & 6 tension) were determined from each of the two segments within each muscle. All statistics were performed using SigmaStat (SPSS Inc. USA). Data was subjected to normality and equal variance tests to confirm the normal distribution and equal spread of the data (all passed).

a) Quantification of muscle segment performance

A paired, two sample, two tailed t-test (α=0.05) was conducted in order to identify any significant differences in measurement variables (contraction and relaxation times etc.) between the proximal (red) muscle segment and the distal (white) muscle segment for each measurement device (Laser-MMG & Tensiometry). Data related to the contraction and relaxation times for each muscle segment were normalised for the effect of displacement and tension respectively.

b) The relationship between Laser-MMG and Tension

A Pearson's Correlation was carried out to determine the magnitude and direction of the relationship between the Laser-MMG and Tension variables. The power of the performed test was α<0.05.

4.3.3.8 Ethics

Ethical clearance for this experiment was sought and received from the University of Wollongong Animal Ethics Committee.

4.4 Results

4.4.1 Study A: Laser-MMG response to a change in muscle temperature

4.4.1.1 Quantification of muscle performance

As a result of electrical stimulation, the muscle generated tension longitudinally through the tendon while its muscle belly displaced laterally as detected by the MMG laser sensor. From a visual inspection of the Laser-MMG waveforms, it was clear that temperature had an effect on the muscles contractile properties (Figure 4.2). In addition, it was apparent that the peak of the Tensiometric waveform generally preceded the peak of the Laser-MMG waveform and that the Tensiometric waveform was completed sooner than the Laser-MMG waveform – the Laser-MMG output appeared 'phase-lagged' in comparison to tension (Figure 4.3). A summary of results for all measurement variables, at each muscle temperature, may be found in Table 4.1.

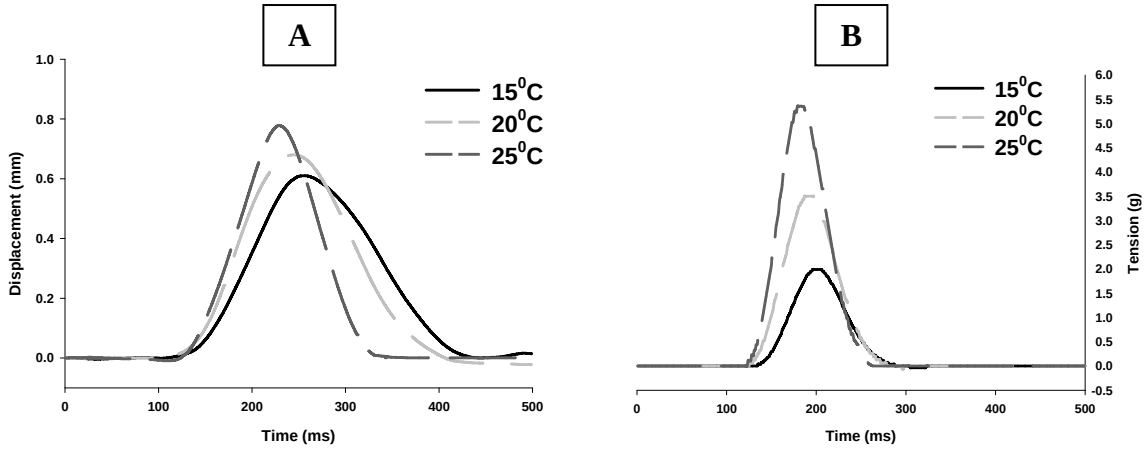

Figure 4.2 Parabolic waveforms representing **A:** the Laser-MMG and **B:** tension in response to electrical stimulation at different thermal states n =1. Figure for descriptive purposes only.

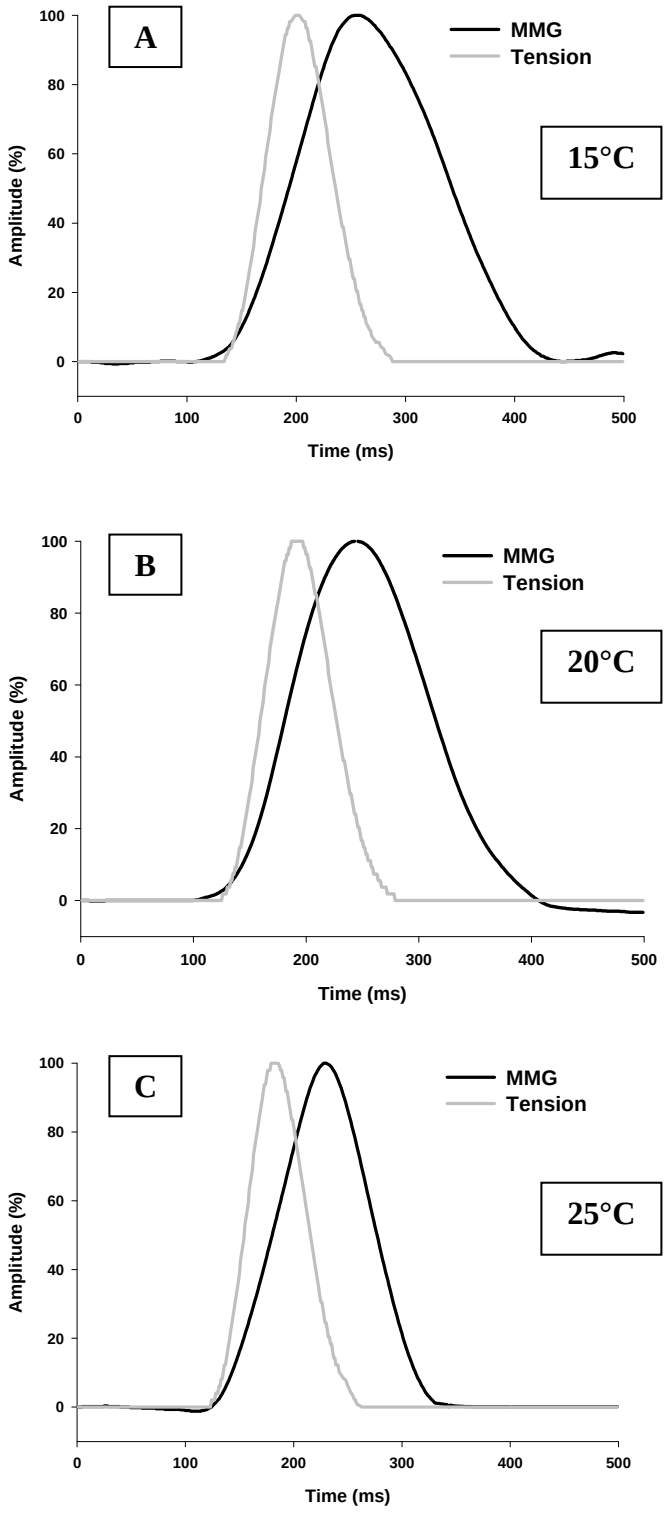

Figure 4.3 Laser-MMG and Tensiometric waveforms at **A**: 15ºC, **B**: 20ºC, and **C**: 25ºC. Data has been normalised to 100% of maximum amplitude to allow comparison of Laser-MMG and Tensiometric outputs n = 1. Figures for descriptive purposes only.

Table 4.1 Summary table of results for each measurement technique and muscle temperature. Presented as group means (±SEM) n = 10. Values within columns sharing a common symbol (*, #, †) are not significantly different ($p<0.05$, 1-way RMANOVA, n = 10). % change indicates the percentage that the second measure differs from the first measure. Correlation coefficient (r^2) represents analysis between Laser-MMG and Tensiometry measures ($p<0.05$).

Laser-MMG	**Dmax (mm)**	**tc (ms)**	**tc*N* (ms/mm)**	**tr (ms)**	**tr*N* (ms/mm)**	**ts (ms)**	**ts*N* (ms/mm)**
15°C	0.61* (0.07)	81.15* (1.41)	153.39* (19.80)	116.34* (3.95)	222.86* (29.26)	143.02* (4.06)	273.22* (34.86)
20°C	0.68# (0.09)	71.58# (0.94)	121.01# (14.64)	98.64# (3.08)	168.02# (22.66)	118.32# (2.87)	201.50# (26.12)
25°C	0.77† (0.10)	61.86† (1.56)	93.02† (11.79)	79.50† (2.61)	120.58† (16.55)	103.28† (1.97)	156.10† (20.39)
% change (15-20°C)	12.64	-11.80	-22.12	-15.21	-24.61	-17.27	-26.25
% change (20-25°C)	12.79	-13.58	-23.13	-19.40	-28.24	-12.70	-22.53
Tensiometry	**Tmax (g)**	**tc (ms)**	**tc*N* (ms/g)**	**tr (ms)**	**tr*N* (ms/g)**	**ts (ms)**	**ts*N* (ms/g)**
15°C	2.18* (0.31)	52.03* (1.49)	27.80* (3.47)	89.61* (2.00)	47.09* (5.21)	113.91* (4.57)	59.35* (6.34)
20°C	3.60# (0.37)	47.40* (1.35)	15.02# (2.29)	68.66# (2.52)	21.53# (3.00)	99.63* (3.71)	30.89# (4.04)
25°C	5.35† (0.54)	36.86# (1.75)	7.54# (0.83)	50.50† (1.20)	10.36# (1.04)	76.83# (5.20)	15.30# (1.30)
% change (15-20°C)	65.12	-8.89	-45.96	-23.37	-54.29	-12.54	-47.95
% change (20-25°C)	48.23	-22.23	-49.84	-26.46	-51.87	-22.89	-50.48
Correlation Coefficient (r^2)	0.67	0.52	0.66	0.41	0.71	0.37	0.70

4.4.1.2 Effect of muscle temperature on performance

Temperature change was found to induce significant change ($p<0.05$) in the maximal displacement (Dmax) of the muscle belly, with the largest displacement (0.77mm) occurring at 25°C and the smallest (0.61 mm) at 15°C (Figure 4.4A & Table 4.1). As the muscle temperature decreased, so too did the degree of displacement ($p<0.05$; $r^2 = 0.45$).

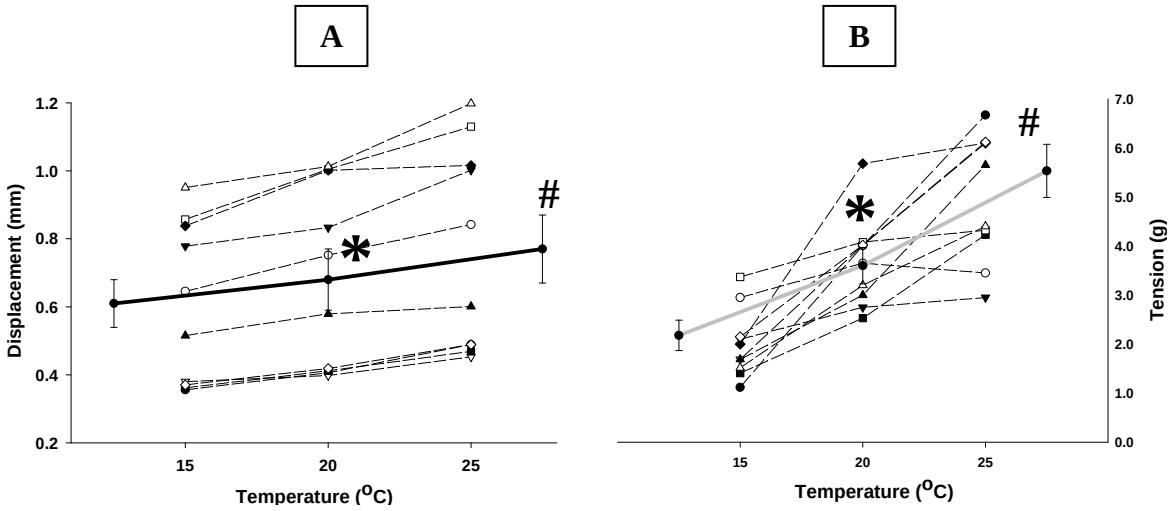

Figure 4.4 Changes in maximal displacement and tension due to the effect of temperature for each subject. **A:** Lateral displacement. **B:** Tension. Solid line indicates group mean ± SEM. Values sharing a common symbol are not significantly different, 1-way RMANOVA, n = 10.

The amount of tension (Tmax) developed at a muscle temperature of 25ºC was significantly greater ($p<0.05$) than that developed 20°C which was also significantly greater ($p<0.05$) than that developed at 15°C (Figure 4.4B & Table 4.1). As with the displacement, when muscle temperature decreased, so too did the amount of tension developed ($p<0.05$; $r^2 = 0.61$).

Temporal measures of the Laser-MMG and Tensiometric output varied as a result of temperature change (Table 4.1). For the Laser-MMG output, significant differences ($p<0.05$) were identified between all muscle temperatures for all measurement variables. Normalised measurement variables tc*N*, ts*N* and tr*N* were consistently reduced in association with an increase in muscle temperature (Figure 4.5A). Significant negative correlations existed for temperature change and Laser-MMG measures of tc*N* ($p<0.05$; $r^2 = -0.49$), tr*N* ($p<0.05$; $r^2 = -0.64$) and ts*N* ($p<0.05$; $r^2 = -0.48$), demonstrating that increases in

muscle temperature (within the experimental range) result in faster displacement properties. Results for Tension measures followed a similar direction, however, significant differences ($p<0.05$) were only found for the 15ºC muscle temperature for all temporal measurement variables (Figure 4.5B). Significant negative correlations also existed for temperature change and Tension measures of tc*N* ($p<0.05$; $r^2 = -0.55$), tr*N* ($p<0.05$; $r^2 = -0.64$) and ts*N* ($p<0.05$; $r^2 = -0.69$).

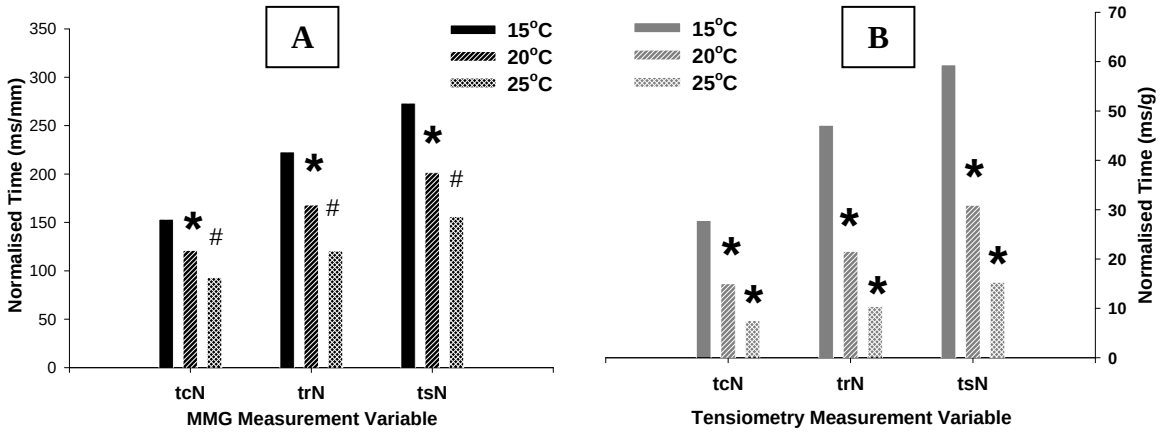

Figure 4.5 Normalised contraction time, relaxation time and sustain time measures for each muscle temperature. **A:** Laser-MMG. **B:** Tensiometry. Columns sharing a common symbol are not significantly different $p<0.05$, 1-way RMANOVA, n = 10.

4.4.1.3 The relationship between Laser-MMG and Tensiometry

A significant positive correlation was identified between maximal displacement and maximal tension when muscle temperature was varied ($p<0.05$; $r^2 = 0.65$) (Figure 4.6A). The relationship between the measurement techniques can be seen in Figure 4.6B for each temperature. To investigate the low correlation between Dmax and Tmax, a voltage ramp was performed with the values plotted against a percentage of the maximal stimulation voltage (Figure 4.6C). It can be clearly seen that Tmax values rise continually up to 100% of maximal stimulation voltage whereas the Dmax values plateau at 70% of maximal stimulation voltage.

A

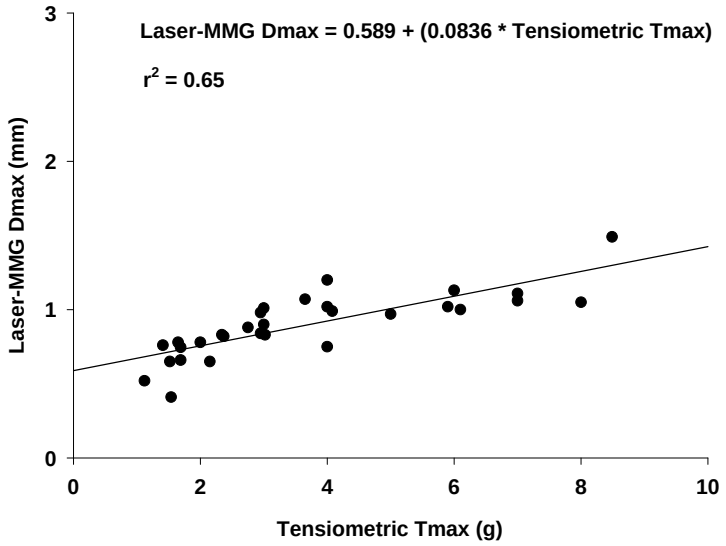
Laser-MMG Dmax = 0.589 + (0.0836 * Tensiometric Tmax)
r2 = 0.65
Laser-MMG Dmax (mm)
Tensiometric Tmax (g)
0
1
2
3
0
2
4
6
8
10

B

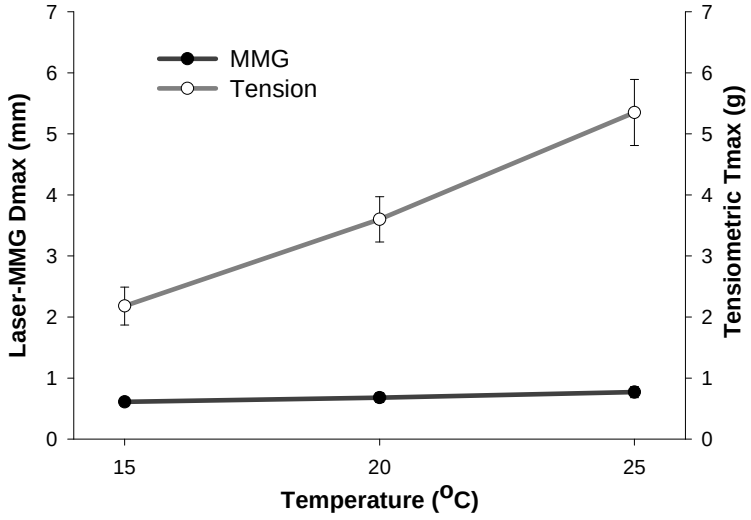
MMG
Tension
Laser-MMG Dmax (mm)
Tensiometric Tmax (g)
Temperature (OC)
0
1
2
3
4
5
6
7
15
20
25

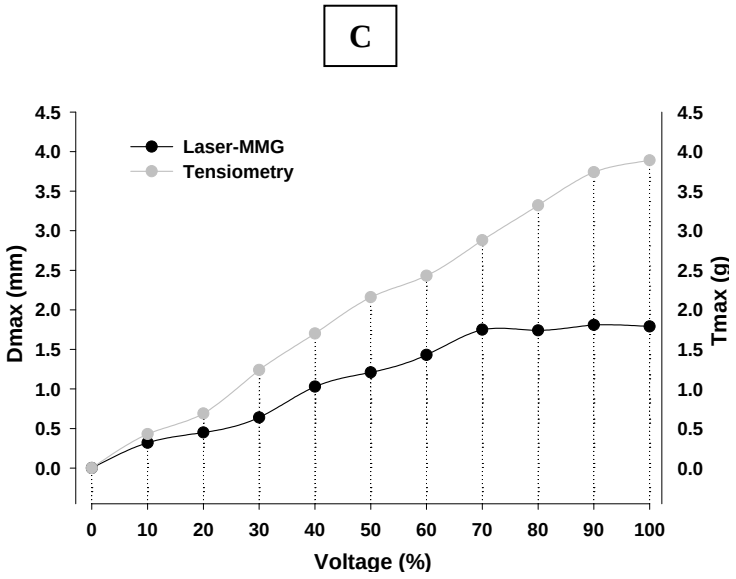

Figure 4.6 **A:** Correlation between Laser-MMG maximal displacement (Dmax) and Tensiometric maximal tension (Tmax) for the medial gastrocnemius. r^2, the coefficient of determination, is shown for the fitted linear regression line. **B:** Graph illustrating the different relationship each measurement technique has with temperature change n = 30 (line of best fit) (Mean group values ± SEM). **C:** Dmax and Tmax values at respective percentage of maximal stimulation voltage (n=1, Figure for descriptive purposes only).

Significant positive correlations of greater strength existed between the Laser-MMG and Tensiometry measures of tc*N* ($p<0.05$; $r^2 = 0.66$) (Figure 4.7), tr*N* ($p<0.05$; $r^2 = 0.71$) (Figure 4.8), and ts*N* ($p<0.05$; $r^2 = 0.70$) (Figure 4.9). The effect of temperature change on Laser-MMG output was significantly related ($p<0.05$) to the change in Tensiometric output.

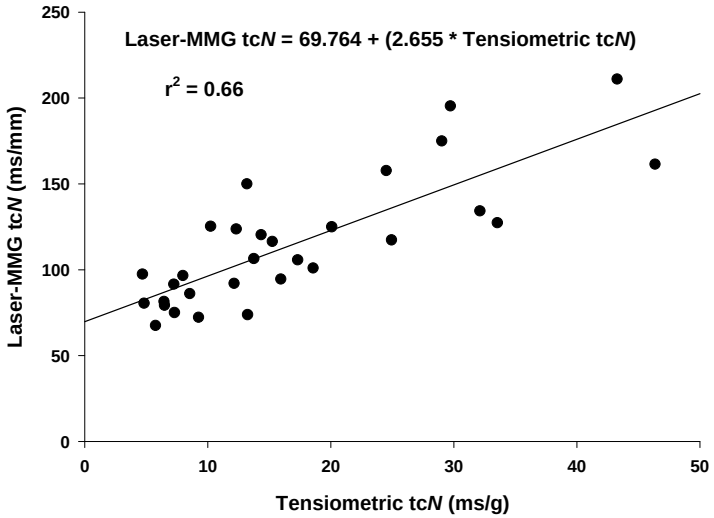

Figure 4.7 Correlation between Laser-MMG normalised contraction time (tc*N*) and Tensiometric normalised contraction time (tc*N*) for the medial gastrocnemius. n = 30. r^2, the coefficient of determination, is shown for the fitted linear regression line.

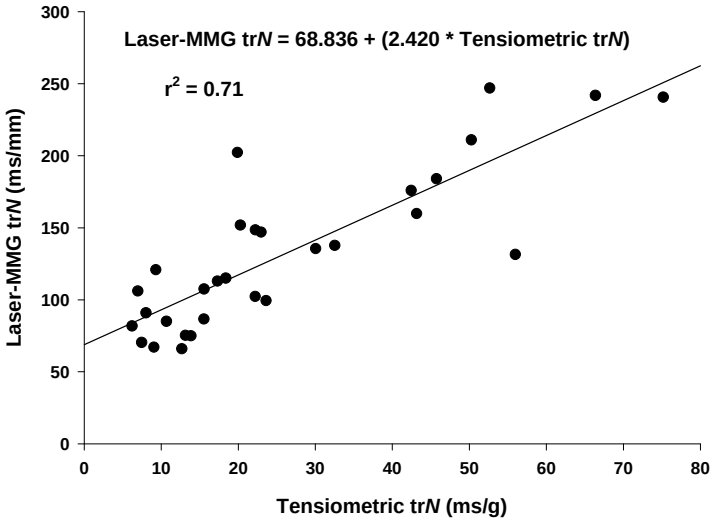

Figure 4.8 Correlation between Laser-MMG normalised relaxation time (tr*N*) and Tensiometric normalised relaxation time (tr*N*) for the medial gastrocnemius n = 30. r^2, the coefficient of determination, is shown for the fitted linear regression line.

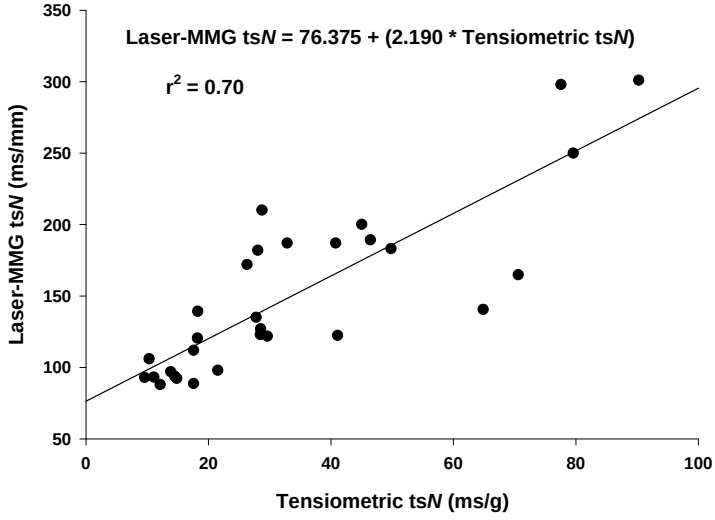

Figure 4.9 Correlation between Laser-MMG normalised sustain time (ts*N*) and Tensiometric normalised sustain time (ts*N*) for the medial gastrocnemius n = 30. r^2, the coefficient of determination, is shown for the fitted linear regression line.

4.4.2 Study B: Laser-MMG response to a change in muscle fatigue

4.4.2.1 Quantification of muscle performance

The electrical stimulation initiated tension development longitudinally through the muscle with a corresponding lateral displacement of the muscle belly. After repetitive stimulation (fatigue), both the Laser-MMG and tension waveforms in response to single twitch stimulation were attenuated (Figure 4.10). Generally, the tension waveform preceded the displacement waveform for all conditions (Figure 4.11). A summary of results for each measurement variable for each muscle condition (pre- and post-fatigue task) can be seen in Table 4.2.

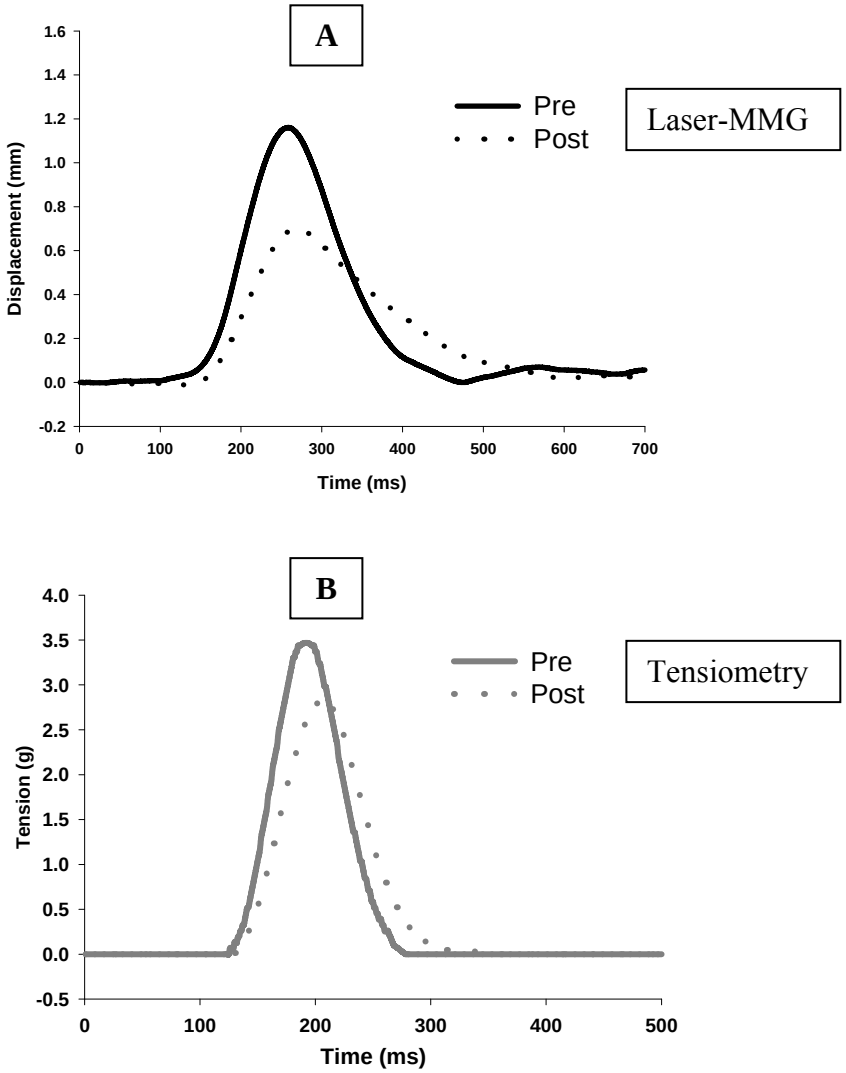

Figure 4.10 Parabolic waveform output from **A:** Laser-MMG and **B:** Tensiometry technique pre- and post-fatigue task n = 1. Figure for descriptive purposes only.

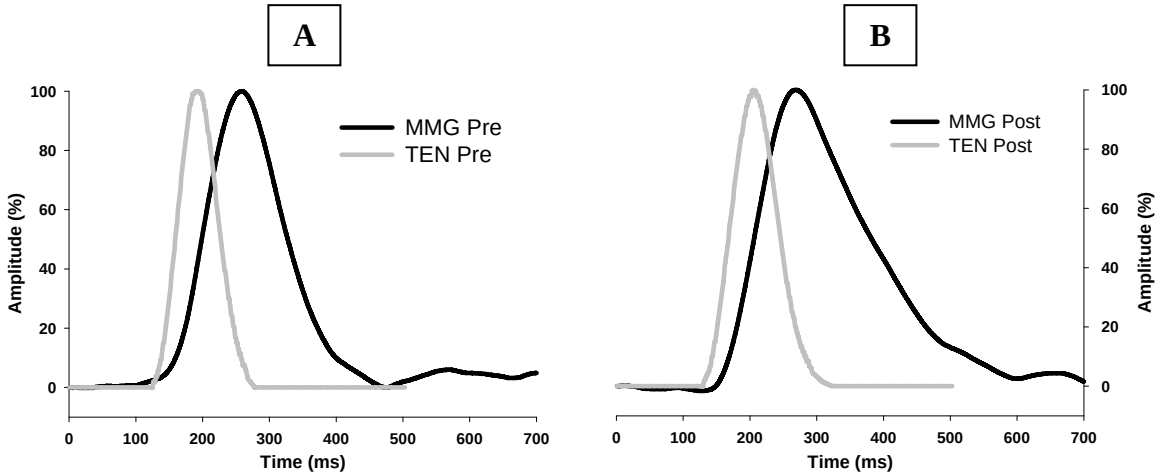

Figure 4.11 Laser-MMG and Tensiometric waveform output at **A:** Pre- fatigue and **B:** Post- fatigue. Data has been normalised to 100% of maximum amplitude to allow comparison of Laser-MMG and Tension outputs n = 1. Figure for descriptive purposes only.

Table 4.2 Summary table for each measurement technique and muscle condition ***** $p<0.05$ vs. pre-fatigue value, paired t-test, n = 12. % change indicates the percentage that the second measure differs from the first measure. Correlation coefficient (r^2) represents analysis between Laser-MMG and Tensiometry measures ($p<0.05$). Group mean data (±SEM).

Laser-MMG	**Dmax (mm)**	**tc (ms)**	**tc*N* (ms/mm)**	**tr (ms)**	**tr*N* (ms/mm)**	**ts (ms)**	**ts*N* (ms/mm)**	**+dD/dt (+mm/s)**	**-dD/dt (-mm/s)**
Pre-Task	1.09 (0.09)	72.33 (2.50)	69.32 (3.28)	101.50 (2.30)	98.85 (6.31)	144.50 (2.89)	141.30 (9.60)	11.03 (0.34)	8.74 (0.40)
Post-Task	0.72***** (0.05)	91.25***** (1.99)	133.22***** (7.90)	134.42***** (3.54)	195.34***** (10.99)	186.10***** (2.88)	273.99***** (18.61)	6.63***** (0.46)	6.43***** (0.33)
% change	-33.94	26.15	92.18	32.43	97.61	28.79	93.91	-39.90	-26.43
Tensiometry	**Tmax (g)**	**tc (ms)**	**tc*N* (ms/g)**	**tr (ms)**	**tr*N* (ms/g)**	**ts (ms)**	**ts*N* (ms/g)**	**+dT/dt (+g/s)**	**-dT/dt (-g/s)**
Pre-Task	3.90 (0.22)	45.58 (1.42)	11.97 (0.51)	75.92 (3.40)	20.57 (1.96)	95.59 (3.59)	25.31 (1.53)	684.69 (27.30)	376.36 (17.19)
Post-Task	2.32***** (0.10)	55.92***** (1.71)	24.41***** (0.91)	106.50***** (1.97)	46.90***** (2.27)	173.25***** (4.95)	75.87***** (3.36)	193.18***** (16.18)	168.18***** (19.04)
% change	-40.50	22.68	103.93	40.28	128.00	81.24	199.76	-71.78	-55.31
Correlation coefficient (r^2)	0.73	0.59	0.65	0.70	0.76	0.71	0.78	0.72	0.83

4.4.2.2 Effect of repetitive stimulation on muscle performance

The measures of Dmax for the medial gastrocnemius were significantly less ($p<0.05$) following the repetitive stimulation task (Figure 4.12A). An identical pattern was observed for the measure of Tmax with the single twitch response after repetitive stimulation being significantly lower ($p<0.05$) than the baseline values (Figure 4.12B). The changes in Dmax and Tmax during the repetitive stimulation task for one subject are shown in Figure 4.12C. During the initial contractions, displacement and tension rose to reach maximum values (100%) after 2 to 5 contractions. Subsequently, displacement (Laser-MMG) declined somewhat faster than tension.

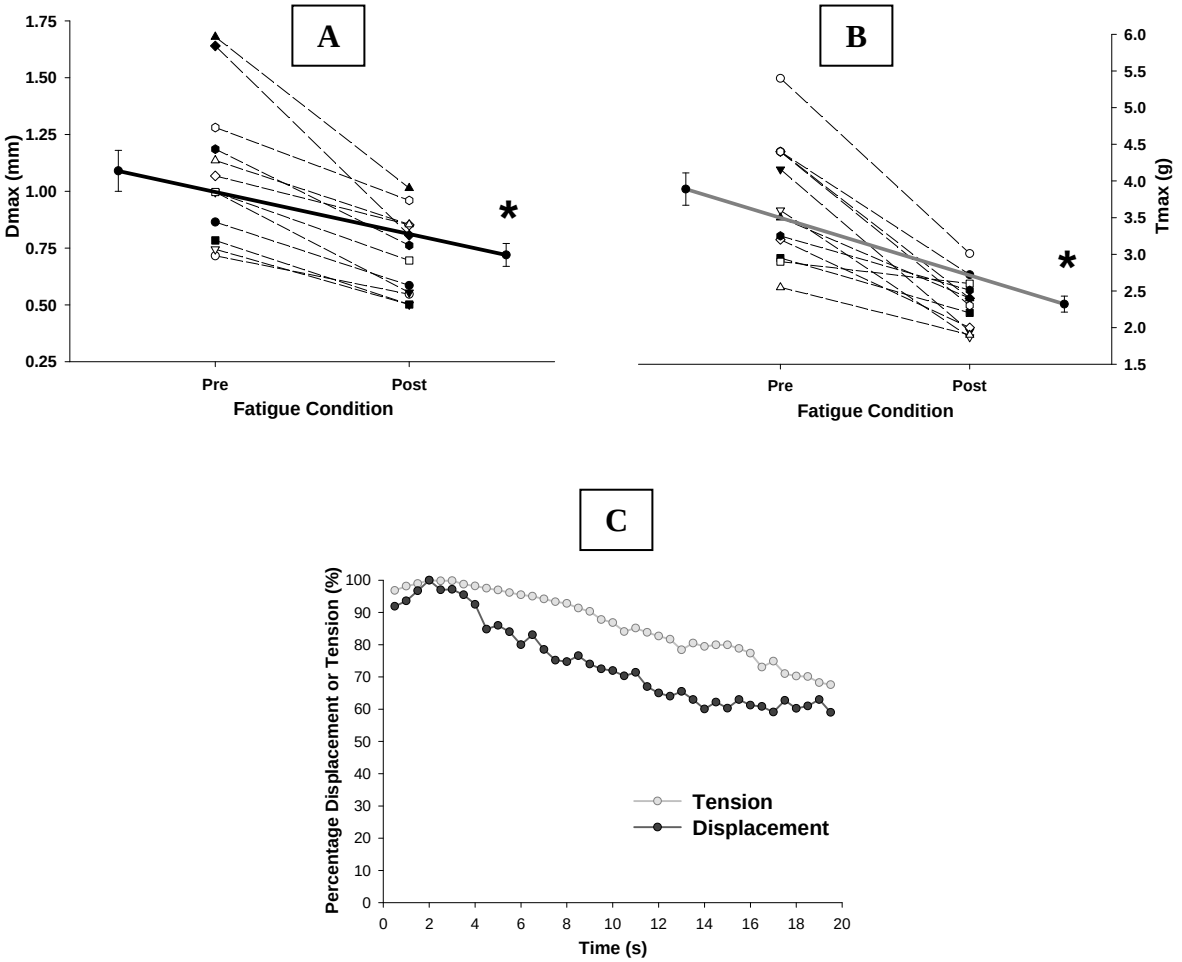

Figure 4.12 Changes in **A:** maximal displacement (Dmax) and **B:** maximal tension (Tmax) due to the repetitive stimulation task. * $p<0.05$, paired t-test n = 12. Individual matched subject data with group mean represented by longer solid line. **C:** changes over time of displacement and tension during the repetitive stimulation task (n = 1, Figure for descriptive purposes only). Each symbol represents the peak value of each contraction relative to the highest peak values recorded during the test.

For both methods of measurement, the repetitive stimulation task induced significant increases ($p<0.05$) in the tc*N*, tr*N* and ts*N* values (Figure 4.13). This indicated that the repetitive stimulation task effectively slowed the overall timing of the muscle contraction in response to the single twitch stimulation. As a result of increasing both the time required to reach maximal values and the time required to relax to baseline values, the overall contraction was significantly elongated ($p<0.05$). The repetitive stimulation also significantly reduced ($p<0.05$) the maximal rate of contraction and relaxation recorded by the Laser-MMG and the Tensiometry ($p<0.05$) (Figure 4.14).

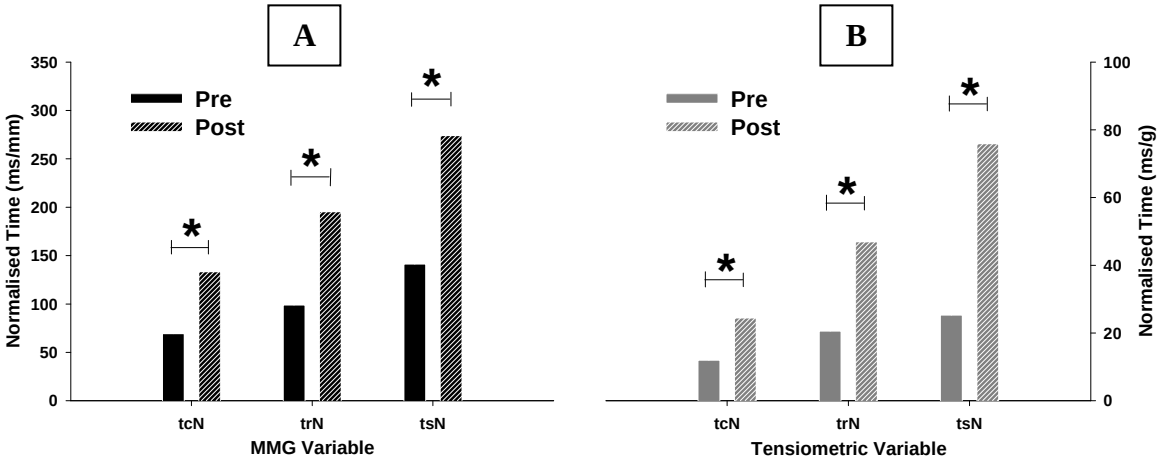

Figure 4.13 Normalised contraction time (tc*N*), relaxation time (tr*N*) and sustain time (ts*N*) values for the pre- and post-stimulation task **A:** Laser-MMG and **B:** Tensiometry. * $p<0.05$, paired t-test, n = 12.

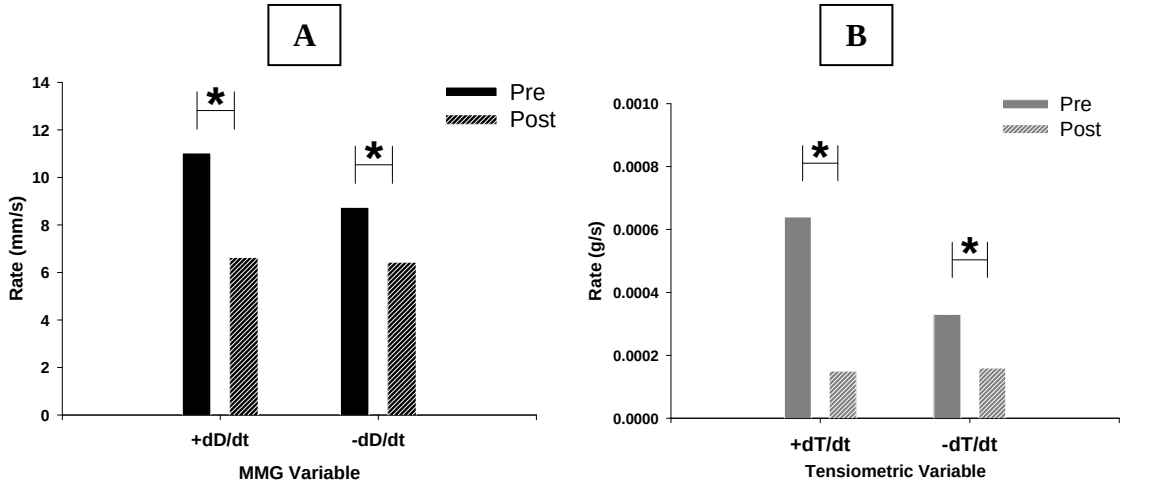

Figure 4.14 Maximal rate of contraction and relaxation for the pre and post stimulation task, measured by **A:** Laser-MMG and **B:** Tensiometry. * $p<0.05$, paired t-test n = 12.

4.4.2.3 The relationship between Laser-MMG and Tensiometry

A significant positive relationship ($p<0.05$; $r^2 = 0.73$) existed between Dmax and Tmax indicating that higher tension values were associated with higher displacement values (Figure 4.15).

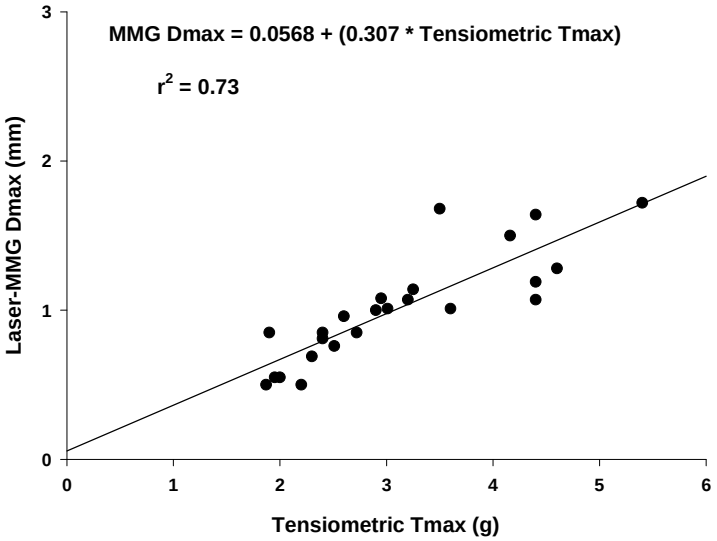

Figure 4.15 Relationship between maximal displacement (Dmax) and maximal tension (Tmax) for the medial gastrocnemius. n = 24. r^2, the coefficient of determination, is shown for the fitted linear regression line.

Laser-MMG and Tensiometry was significantly correlated for tc*N* ($p<0.05$; $r^2 = 0.69$) (Figure 4.16A), tr*N* ($p<0.05$; $r^2 = 0.76$) (Figure 4.16B) and ts*N* ($p<0.05$; $r^2 = 0.78$) (Figure 4.16C).

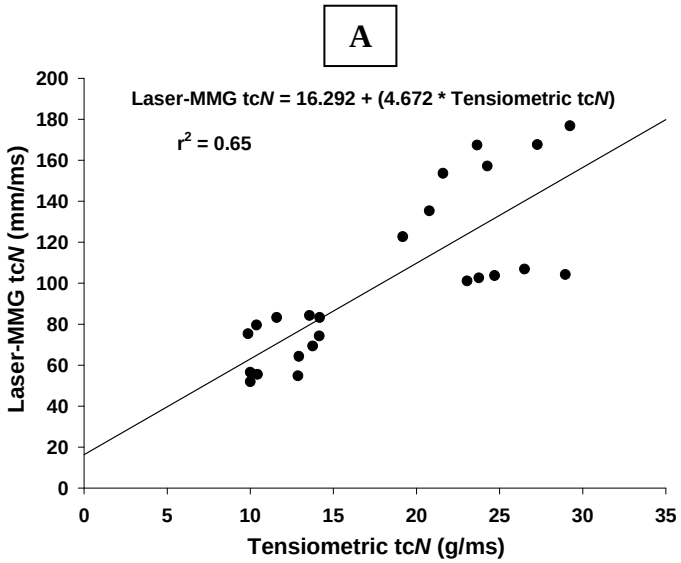

B

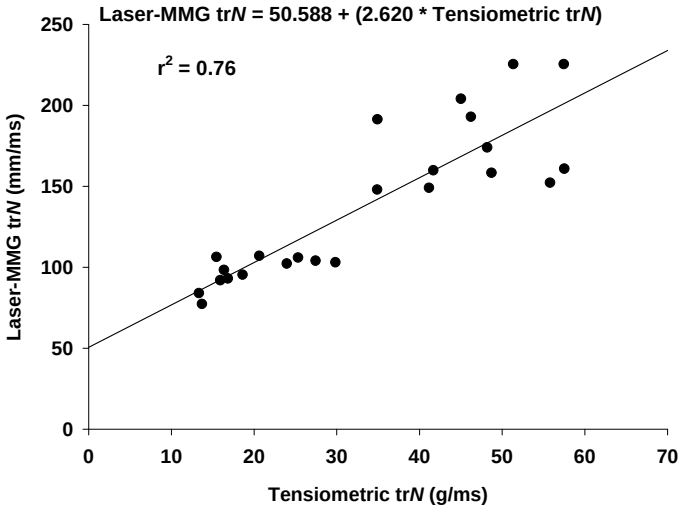

C

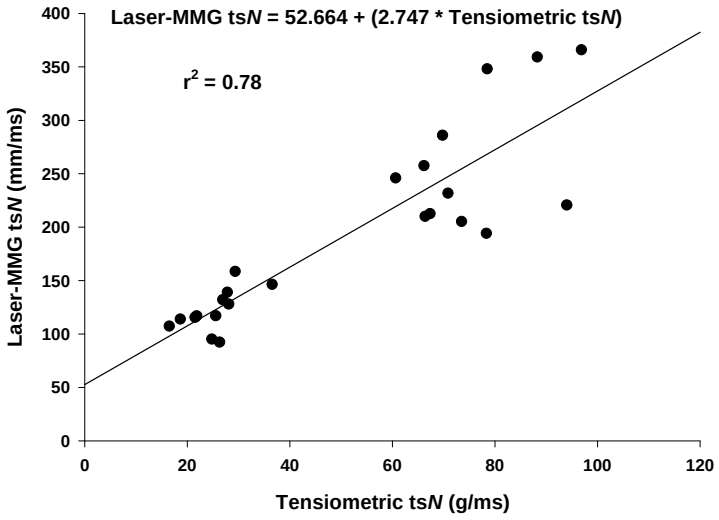

Figure 4.16 The relationship between Tensiometry and Laser-MMG for **A:** normalised contraction time (tc*N*) **B:** normalised relaxation time (tr*N*) **C**= normalised sustain time (ts*N*) n = 24. r^2, the coefficient of determination, is shown for the fitted linear regression line.

Laser-MMG and Tensiometry output were significantly correlated for maximal rate of contraction ($p<0.05$; $r^2 = 0.72$) and relaxation ($p<0.05$: $r^2 = 0.83$) (Figure 4.17).

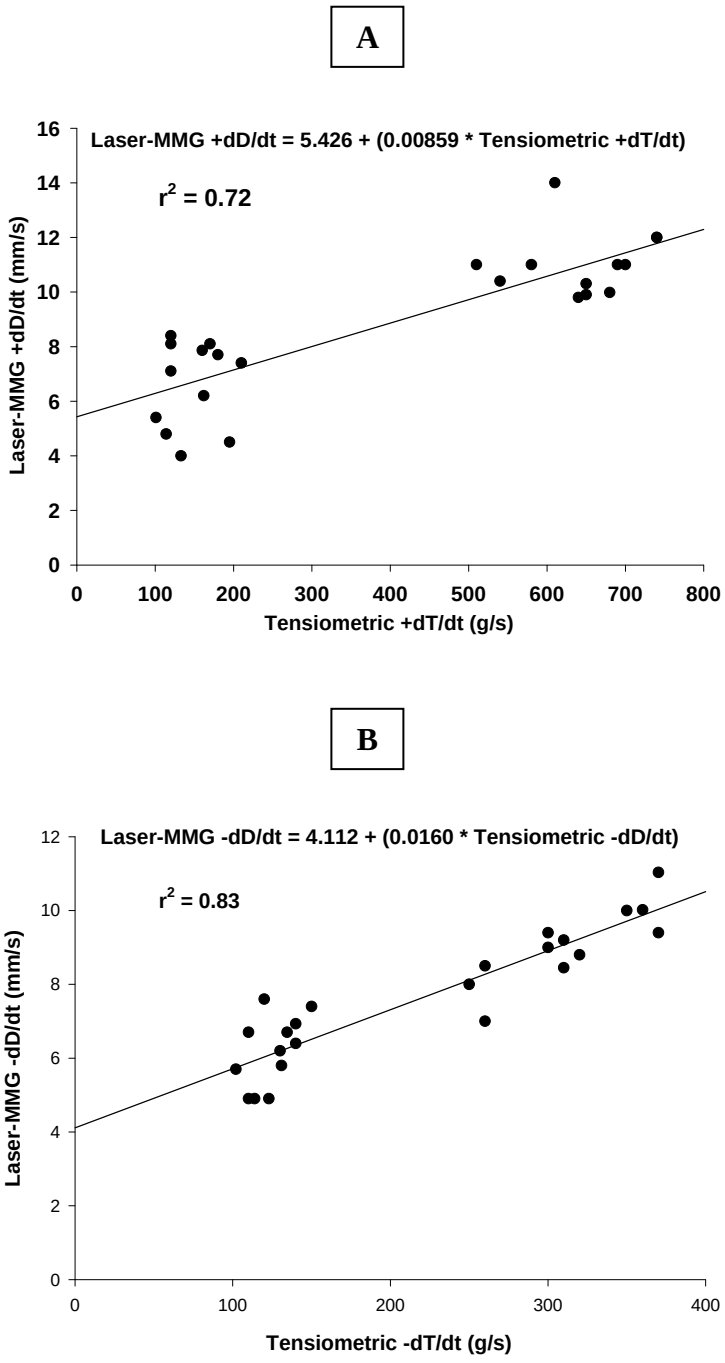

Figure 4.17 The correlation between Tensiometry and Laser-MMG for **A:** maximal rate of contraction. **B:** maximal rate of relaxation n = 24. r^2, the coefficient of determination, is shown for the fitted linear regression line.

4.4.3 Study C: Laser-MMG response to a change in muscle segment fibre type

4.4.3.1 Muscle tissue

Staining for myosin ATPase clearly demonstrated the different morphology of type I and type II muscle fibres (Figure 4.18). Fibre type composition of the proximal and distal muscle segments was assessed by calculating the fibre type percentage (of total fibre number) and cross sectional area. Results indicated the proximal muscle segment to have a mixture of type I and type II fibres (21% type I: 79% type II) as demonstrated by their proportional contribution to muscle cross sectional area (10.08% type I: 89.92% type II). By comparison, the distal muscle segment contained almost exclusively type II fibres (1% type I: 99% type II) with a type II dominance of the cross sectional area (0.5% type I: 99.5% type II) (Figure 4.19).

A B

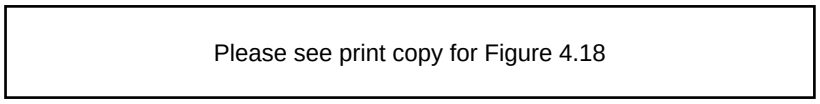

Figure 4.18 Pictures taken through Image Pro software of proximal and distal segments of a Wistar rat medial gastrocnemius muscle. **A**: proximal muscle segment (Myosin ATPase pH 4.3 magnified 100x) **B:** distal muscle segment (Myosin ATPase pH 4.3 magnified 100x). In the image, type I muscles fibres appear darker while type II fibres appear lighter. Figure previously published in Phillips (2005)

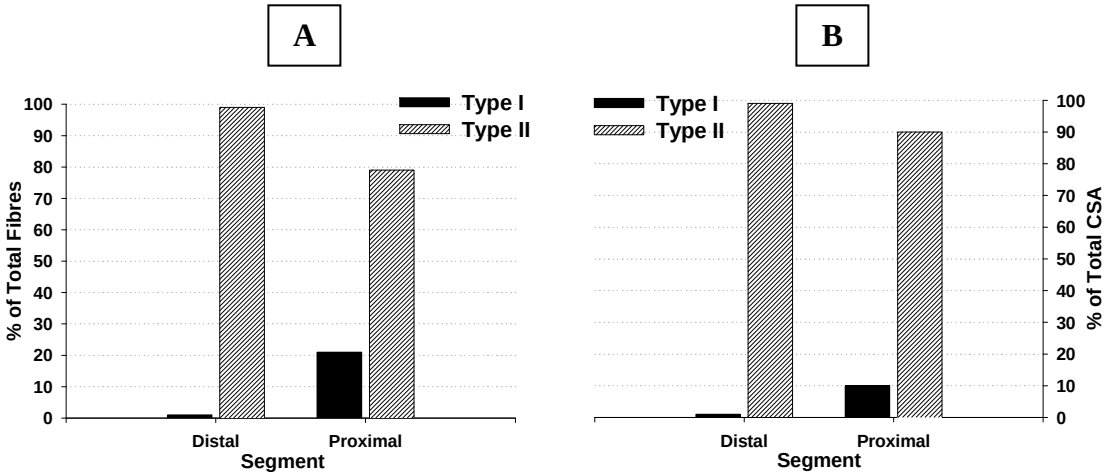

Figure 4.19 Muscle fibre types expressed as **A:** a percentage of the total fibre number for the distal and proximal muscle segments and **B:** a percentage of the total cross sectional area for the distal and proximal muscle segments (n = 10).

4.4.3.2 Quantification of muscle segment contractile properties

In response to electrical stimulation, each muscle segment generated tension with a simultaneous lateral displacement of its muscle belly. The two muscle segments were shown to have different contractile properties when they were assessed by both Laser-MMG and Tensiometric techniques (Figures 4.20, 4.21). A summary of results for each measurement variable for each muscle segment can be seen in Table 4.3.

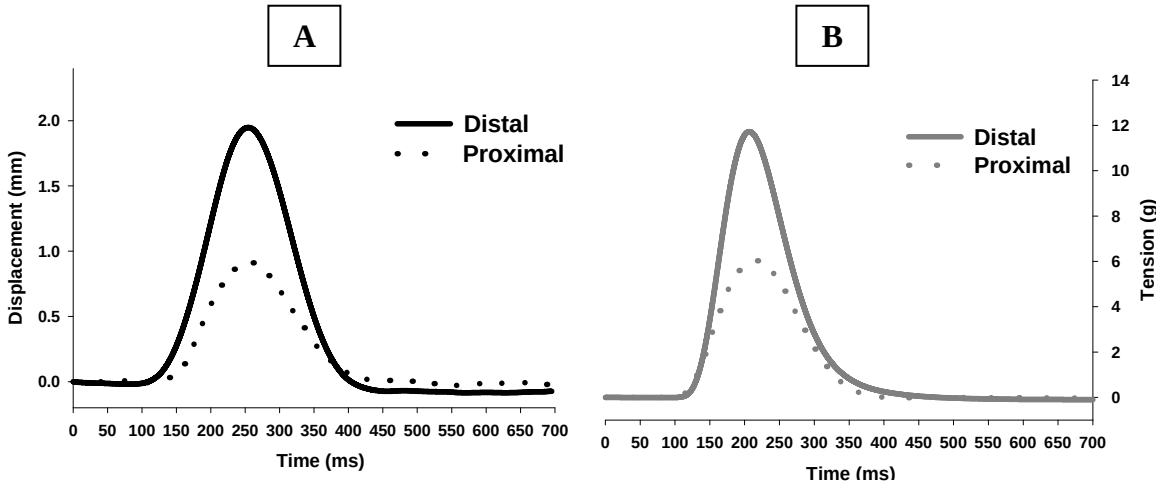

Figure 4.20 Waveforms from the distal and proximal muscle segments of the medial gastrocnemius when measured by the **A:** Laser-MMG. **B:** Tensiometry n = 1. Figure for descriptive purposes only.

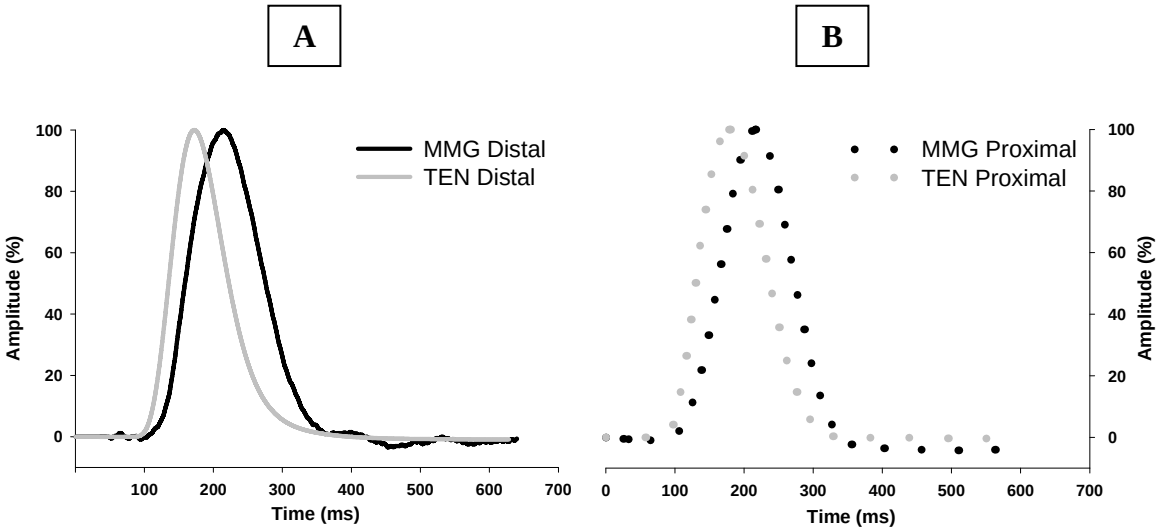

Figure 4.21 Laser-MMG and Tensiometric waveform output from **A:** distal muscle segment. **B:** proximal muscle segment. Data has been normalised to 100% of maximum amplitude to allow the comparison of Laser-MMG and Tensiometric output n = 1. Figure for descriptive purposes only.

Table 4.3 Summary table of results from the Laser-MMG and Tensiometry methods for each muscle segment. The row titled "% difference" indicates the percentage that the proximal measure differs from the distal measure. * indicates $p<0.05$ proximal vs. distal muscle segment, paired t-test, n = 10. Correlation coefficient (r^2) for analysis between Laser-MMG and Tensiometry measures shown when significant ($p<0.05$). Group mean data (±SEM).

Laser-MMG	**Dmax (mm)**	**tc (ms)**	**tc*N* (ms/mm)**	**tr (ms)**	**tr*N* (ms/mm)**	**ts (ms)**	**ts*N* (ms/mm)**	**+dD/dt (+mm/s)**	**-dD/dt (-mm/s)**
Distal Segment	1.65 (0.25)	69.20 (1.93)	43.89 (6.74)	201.48 (31.75)	112.85 (24.75)	134.90 (3.39)	84.11 (11.57)	23.45 (3.38)	10.73 (3.67)
Proximal Segment	0.85* (0.12)	76.33* (1.52)	86.23* (11.54)	264.73 (29.59)	198.07* (22.84)	157.75* (8.55)	159.07* (20.84)	10.24* (1.36)	3.14* (2.05)
% difference	-48.48	10.30	96.47	31.39	75.52	16.94	89.12	-56.33	-70.73
TEN	**Tmax (g)**	**tc (ms)**	**tc*N* (ms/g)**	**tr (ms)**	**tr*N* (ms/g)**	**ts (ms)**	**ts*N* (ms/g)**	**+dT/dt (+g/s)**	**-dT/dt (-g/s)**
Distal Segment	14.58 (0.98)	38.05 (2.28)	3.16 (0.71)	104.44 (9.69)	9.65 (2.94)	91.65 (5.80)	14.95 (6.03)	300.05 (46.67)	118.21 (22.68)
Proximal Segment	7.82* (1.05)	38.56 (1.08)	6.30* (0.67)	135.16* (9.03)	23.56* (2.76)	110.31* (6.64)	20.49 (2.11)	132.08* (19.52)	32.00* (5.53)
% difference	-46.36	1.34	99.36	29.41	144.14	20.37	37.06	-55.98	-72.93
Correlation coefficient (r^2)	0.69	0.21	0.74	0.41	0.84	0.47	0.69	0.60	not significant

4.4.3.3 Distal vs. proximal muscle segments

The maximal displacement (Dmax) of the distal muscle segment (1.65 ± 0.25mm) was significantly higher ($p<0.05$) than that produced by the proximal segment (0.85 ± 0.12mm). Maximal tension values (Tmax) were also significantly higher ($p<0.05$) for the distal segment (14.58 ± 0.99g) than the proximal segment (7.82 ± 1.05g) (Figure 4.22). The Laser-MMG mimicked the directional trend of the Tensiometric measure.

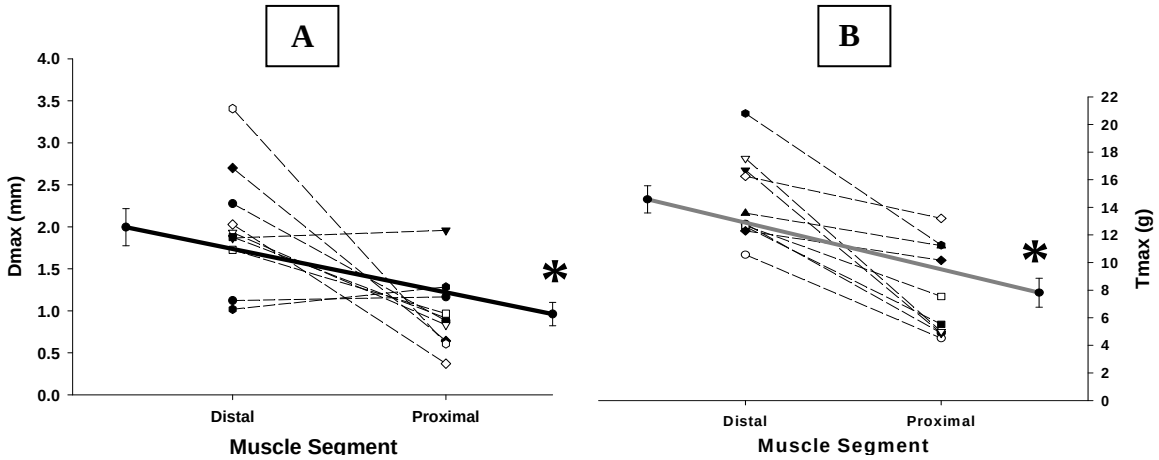

Figure 4.22 Differences in **A:** maximal displacement (Dmax) and **B:** maximal tension (Tmax) for the distal and proximal segments. * $p<0.05$ paired t-test. Individual matched subject data (n = 10) with group mean ± SEM represented by long solid line.

Normalised contraction (tc*N*) and relaxation (tr*N*) times measured by the Laser-MMG and Tensiometer were significantly slower ($p<0.05$) in the proximal segment than in the distal segment (Figure 4.23A). The Laser-MMG measure of ts*N* was significantly longer ($p<0.05$) in the proximal segment than the distal segment. Tensiometry measures of ts*N* failed to reach significance ($p = 0.42$), although trends were similar to the Laser-MMG in direction of change (Figure 4.23B).

The maximal rate of contraction when measured by the Laser-MMG (+dD/dt) and Tensiometer (+dT/dt) differed significantly ($p<0.05$) between muscle segments with the distal segment having a higher rate. The maximal rate of relaxation was also significantly higher ($p<0.05$) in the distal segment for both Laser-MMG and Tensiometry measures.

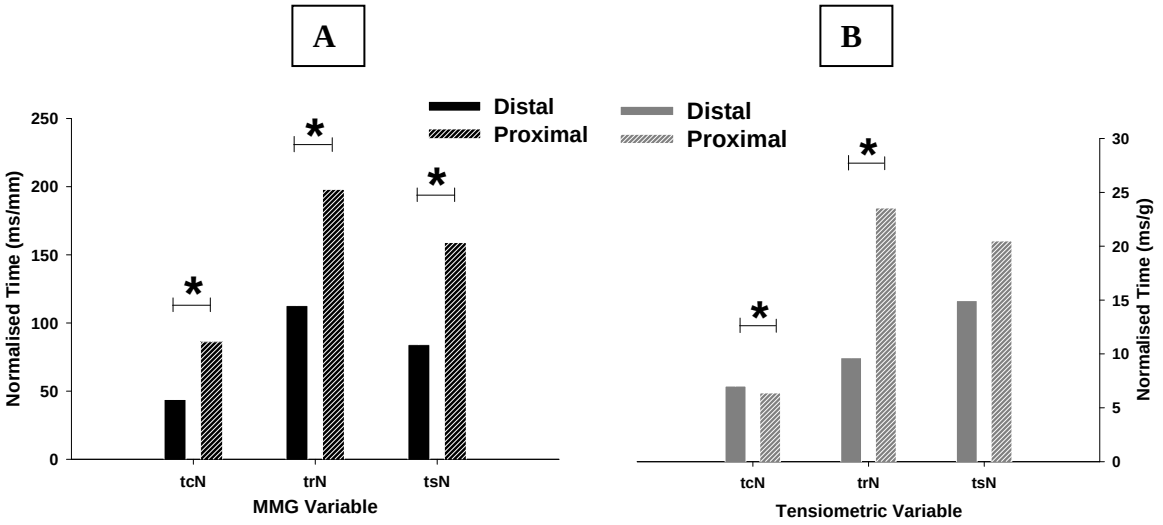

Figure 4.23 Normalised contraction time (tc*N*), relaxation time (tr*N*) and sustain time (ts*N*) of the distal and proximal segments normalised for the degree of **A:** displacement and **B:** tension. * $p<0.05$, paired t-test, n = 10

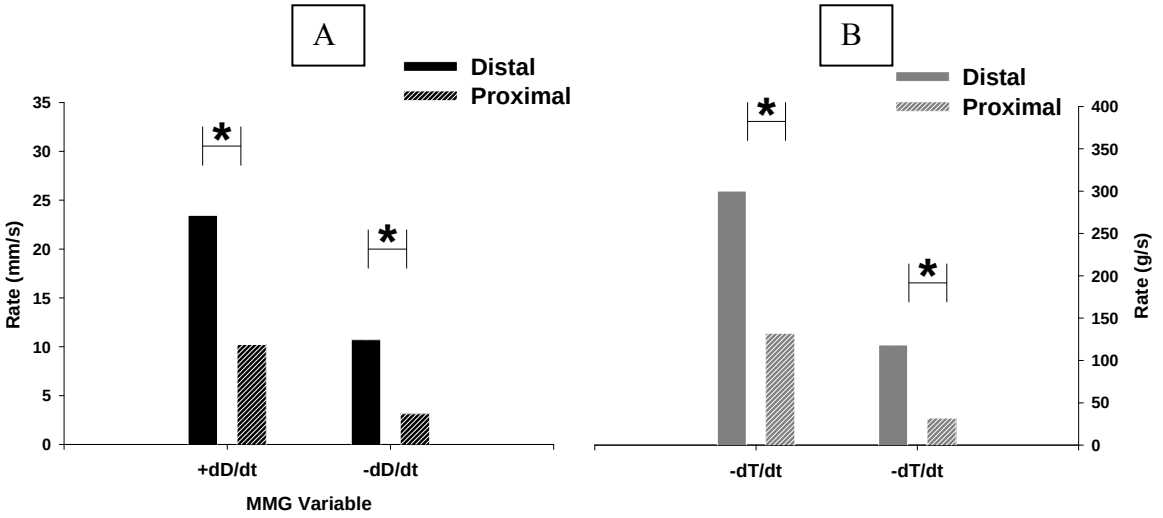

Figure 4.24 Maximal rate of contraction and relaxation of the distal and proximal segment when measured by the **A:** Laser-MMG and **B:** Tensiometry. * $p<0.05$, paired t-test, n = 10.

4.4.3.4 The relationship between Laser-MMG and Tensiometry

A significant positive relationship ($p<0.05$; $r^2 = 0.69$) was identified between Dmax and Tmax (Figure 4.25) indicating that lateral displacement increased simultaneously with tension.

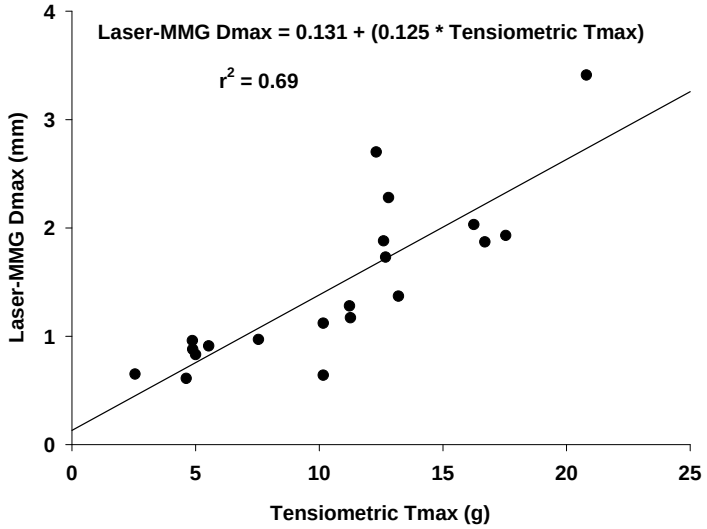

Figure 4.25 Relationship between maximal displacement (Dmax) and maximal tension (Tmax) for the medial gastrocnemius n = 10. r^2, the coefficient of determination, is shown for the fitted linear regression line.

A positive correlation ($p<0.05$; $r^2 = 0.74$) existed for tc*N* when Laser-MMG and Tensiometer measures were compared, indicating that faster displacement development times are associated with faster tension development times (Figure 4.26A). Similar positive correlations were identified between displacement and tension for tr*N* ($p<0.05$; $r^2 = 0.84$) (Figure 4.26B), ts*N* ($p<0.05$; $r^2 = 0.69$) (Figure 4.26C) and maximal rate of contraction ($p<0.05$; $r^2 = 0.60$) but not for maximal rate of relaxation ($p=0.057$).

A

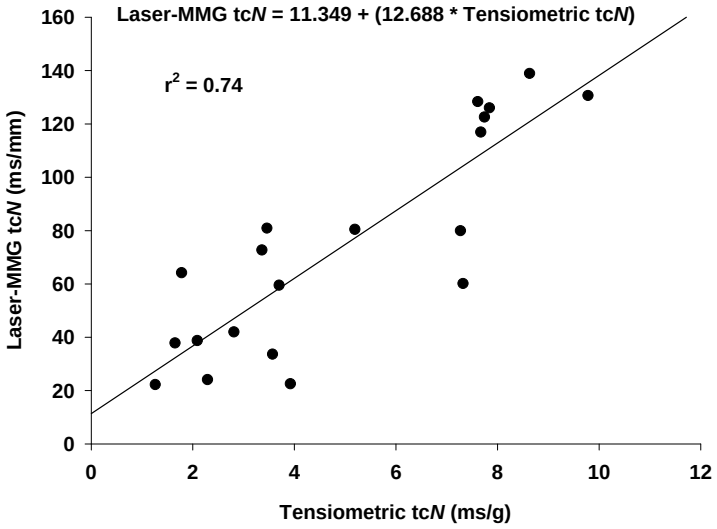

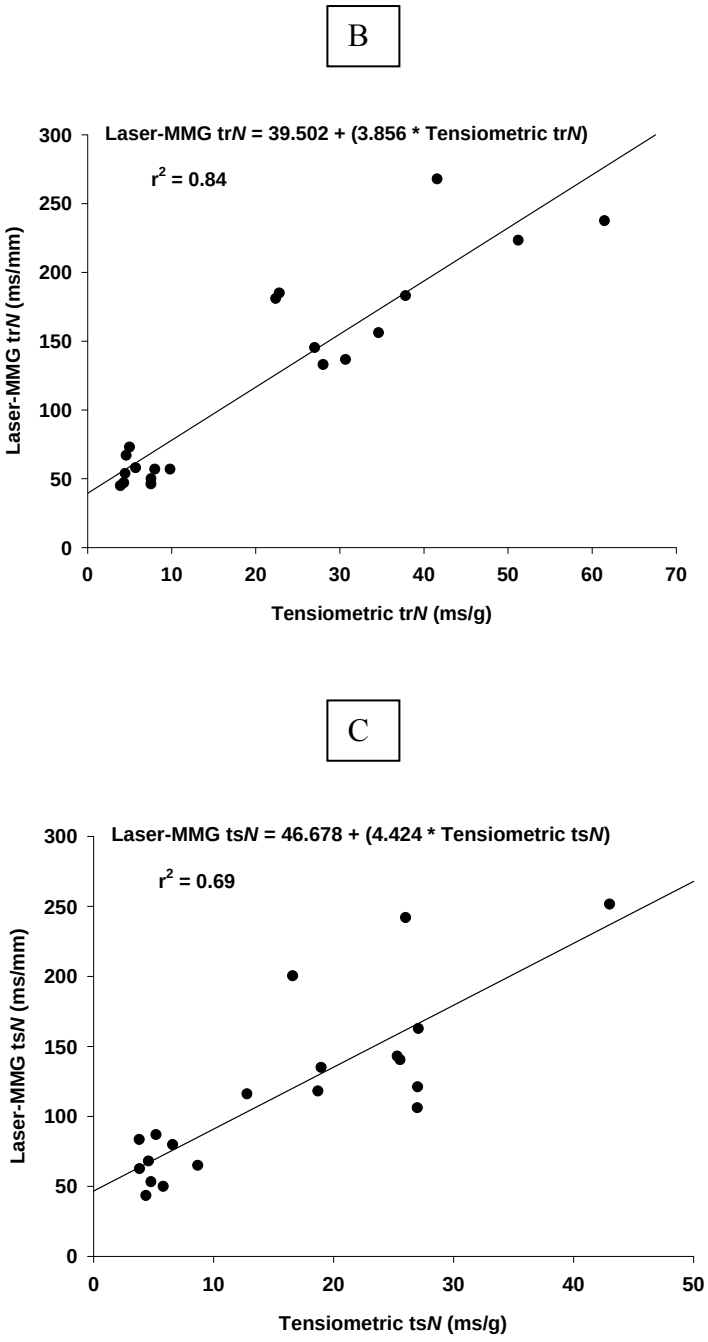

Figure 4.26 Relationship for **A:** tc*N*; **B:** tr*N* and **C:** ts*N* when measured by the Laser-MMG and the Tensiometer for the medial gastrocnemius n = 10. r^2, the coefficient of determination, is shown for the fitted linear regression line.

4.5 Discussion

The studies presented within this chapter investigated the contractile properties of animal muscle when exposed to modulators of performance. The aims of the investigations were to pioneer the use of the Laser-MMG in an animal model, determine the sensitivity of the Laser-MMG technique to the effects of temperature and repetitive stimulation and to determine the ability of the Laser-MMG to detect the contractile properties of small sub-volumes of muscle with contrasting muscle fibre-type compositions. It should be noted that the investigations were not designed to determine the effects of temperature change nor repetitive stimulation on muscle performance *per se*, but rather to quantify their effects for the purpose of technique validation.

The overall results of the three studies reported here clearly support the hypothesis that the Laser-MMG would mimic the directional trends of Tensiometry measures recorded simultaneously and be as sensitive as the Tensiometric technique to the effects of temperature, repetitive stimulation and fibre type on muscle contractile properties. The chosen modulators influenced the muscle's contractile properties and the induced changes in muscle physiology were detectable, to a similar degree, by both the Laser-MMG and Tensiometry techniques. Similarly, the Laser-MMG technique and Tensiometry were able to detect differences in muscle segment contractile properties due to variations in muscle fibre type concentrations. Generally, both recording techniques were useful in characterising contraction time (tc), and normalised contraction time (tc*N*) which are variables closely associated with underlying muscle fibre type (Dahmane, Djordjevic *et al.* 2005).

4.5.1 Study A - Temperature

This study aimed to determine if the Laser-MMG technique was as sensitive as the Tensiometric technique to the effects of temperature on muscle contractile properties. Temperature significantly altered ($p<0.05$) muscle contractile properties as determined by concurrent Laser-MMG and Tensiometry measures. The 25ºC condition resulted in the highest lateral displacement (Dmax) and tension development (Tmax) recorded during the experiment. When muscle temperature was decreased to 20ºC and then 15ºC, both Dmax

and Tmax values diminished significantly ($p<0.05$). In previous studies (Asmussen and Gaunitz 1981, 1989), maximum tension was found to decrease on cooling in soleus and extensor digitorium longus of rats, mice and guinea pigs; a result generally in agreement with those reported here for the toad medial gastrocnemius.

It is well established that skeletal muscle contractions are initiated by an increase in cytoplasmic Ca^{2+} concentration (Guyton and Hall 2000) and involve the cyclic interaction (bind and release) of actin and myosin filaments, exerting force whenever there is an interaction (Guyton and Hall 2000). The number of interactions (cross-bridges) and hence the magnitude of force generated by the muscle, is therefore dependant upon the availability of intra-cellular Ca^{2+}. Fundamentally, the amount of Ca^{2+} determines the number of myosin heads available for cyclic binding, force generation and then detachment. The cross-bridge force generation phase has been proven to be endothermic and temperature is a known mechanism through which Ca^{2+} sensitivity can be modulated (Stephenson and Williams 1985). While the mechanisms are not well identified, changes in dispersion of the myosin heads with changing temperature (Xu, Offer, Gu, White and Yu 2003) and a loss of organisation of the myosin heads with respect to the myosin filament at low temperatures (Malinchik, Xu and Yu 1997), have been shown. There appears to be an optimal proximity of the myofilaments for cross-bridge formation, with high physiological temperatures (above the normal operating range) reducing this proximity by increasing the space between actin and myosin (MacIntosh 2003).

The reduced Tmax values associated with the reduction in muscle temperature seen here are attributed to a decrease in the number of formed cross-bridges. The reduction in Dmax values recorded during the cooler muscle temperatures was, therefore, the result of a decrease in the quantity and quality of overlap between the actin and myosin filaments; a function of the reduction in cross-bridge formation. Through investigating the relationship between Tmax and Dmax at different stimulation voltages (Figure 4.6C), it appears that once the maximal number of cross-bridges are formed, lateral displacement of the muscle belly plateaus. This occurred at approximately 70% of the stimulation voltage required to produce maximal tension. In contrast, increased stimulation voltages above 70% of

maximal continued to elicit a linear increase in maximal tension that was produced by the contractile elements (myofibrils) of the cross-bridge. This phenomenon explains the low correlation between Dmax and Tmax values ($r^2 = 0.69$).

Both phases of the contraction cycle (contraction and relaxation) were elongated by decreasing the muscle temperature. Significantly slower ($p<0.05$) Laser-MMG measures of tc*N*, tr*N* and ts*N* were identified for each step reduction in muscle temperature. Therefore, the Laser-MMG technique was considered highly sensitive to changes to motor unit contractile properties brought about by the small changes in temperature. Tensiometry measures mimicked the directional trend of MMG measures although no significant differences existed between the 20ºC and 25ºC conditions for tc*N*, tr*N* and ts*N*. Based on these results it may be suggested that the Laser-MMG technique was more sensitive than the 'gold standard' Tensiometry technique in detecting changes in muscle physiology due to variations in temperature.

4.5.2 Study B – Fatigue

This study aimed to determine whether the Laser-MMG technique was as sensitive as the Tensiometric technique to the effects of repetitive stimulation on muscle contractile properties. The results identified that both the Laser-MMG and Tensiometric waveforms were altered by the repetitive stimulation task. Significantly less ($p<0.05$) lateral displacement (Dmax) and maximum tension (Tmax), as well as significantly elongated ($p<0.05$) contraction- (tc*N*), relaxation- (tr*N*) and sustain-times (ts*N*), resulted from performance of the repetitive stimulation task. Correspondingly, the maximal rate of contraction and relaxation were significantly lower as a result of fatigue.

A decrement in muscle force production is a commonly accepted effect of fatigue (repetitive stimulation) protocols (Bigland-Ritchie and Woods 1984). Type II muscle fibres are susceptible to repetitive stimulation due to their inability to maintain adequate energy supplies and their reliance on anaerobic metabolism (Guyton and Hall 2000). Reduction in firing rates of large motor units has also been associated with fatigue-inducing tasks (Basmajian and DeLuca 1985). It is often a combination of a reduction in energy levels,

and an inability to maintain high firing rates, that result in the loss of force producing ability. The tension results recorded here indicated that significant reductions ($p<0.05$) in force production were evident as a result of the 20 second stimulation application.

Westerblad, Allen, Bruton, Andrade and Lannergren (1998) report that low frequency stimulation protocols, which mimic prolonged sub-maximal exercise, tend to follow a stereotypical pattern of force decline involving 3 phases. Initially, force declines to about 80%, with further steady declines to about 70% comprising the second phase. Following this, force rapidly declines to about 30-40% of original values. Of interest was that the mechanisms underlying the reduction in force during phase 1 and 2 were different than during phase 3. The force decline during phase 1 and 2 was due to a reduction in myofibrillar force producing capacity. In contrast, force decline during phase 3 was due to impaired Ca^{2+} activation of the myofibrils. Simply, phase 1 and 2 force reduction was due to an impairment of cross-bridges to produce force, whereas during phase 3, the number of activated cross-bridges declined (Westerblad, Allen *et al.* 1998). This pattern of force decline has been noted in single motor unit of cats (Burke, Levine, Tsairis and Zajac 1973) and isolated muscle fibres of the frog (Nagesser, van der Laarse and Elzinga 1993) and mouse (Lannergren and Westerblad 1991). Reductions to 59.5% were obtained in the present investigation, indicating at least the first two phases and the beginning of phase 3 had occurred due to the stimulation task. Whilst Tensiometry has been well proven to be sensitive to such minor alterations in physiological state (Asmussen 1979; Cady, Jones, Lynn and Newham 1989a), of particular interest was the sensitivity of the Laser-MMG to detect fatigue induced changes in the lateral displacement of the muscle belly. Our results show that Dmax values decreased to 66% of pre-task values, an expected result considering that the muscle was only able to activate a reduced number of cross-bridges (phase 3 changes). As noted before, the lateral displacement of the muscle belly is dependent upon the formation of cross-bridges and the overlap of myofibrils. Based on these results it may be suggested that the Laser-MMG measure of maximal displacement mimicked Tensiometry measures of maximal tension both in direction and in magnitude of change, occurring as a result of repetitive stimulation (correlation coefficient of 0.73).

The most noticeable effects of the stimulation task were observed within the measures of tc*N*, tr*N* and ts*N*, with values elongated to approximately 200% of the pre-fatigue values following the fatigue task. De Ruiter and co-workers (De Ruiter 1996; De Ruiter, De Haan *et al.* 1996) assessed fast-twitch muscle unit properties in different rat medial gastrocnemius muscle compartments and observed that the time taken to attain the peak twitch force of the fatigue resistant and fast fatigable distal motor units in the muscle, was half that of slow units located in the proximal compartment. In the present study, whole muscle tc*N* times of 11.97ms/g were recorded during pre-task stimulation twitch trials, which were twice as fast as that recorded from post-task twitches (24.41 ms/g). The short duration low frequency stimulation task employed during this investigation appeared to have reduced the ability of the fast-twitch motor units to respond to the electrical stimulation, contribute to the force development and produce a fast contraction speed. The post-task stimulation tc*N* measures therefore reflect the activity of the fatigue resistant slow-twitch motor units.

Measures of contraction and relaxation time during single-twitch contractions are predominantly influenced by myosin ATPase activity and the reuptake of calcium, respectively, with the latter being acutely impaired by fatigue (Barany 1967; Westerblad, Bruton, Allen and Lannergren 2000). If surface Laser-MMG signals reflect the pressure waves from motor unit activity, then a close correlation should exist between the duration of the surface Laser-MMG waveform and the required time for the muscle fibres to complete a cycle of contraction and relaxation.

The Laser-MMG technique mimicked the directional trends recorded by the Tensiometric technique for contraction and relaxation times and these trends were confirmed by correlation analysis with results of $r^2 = 0.65$ and $r^2 = 0.76$ respectively. Additionally, the strong positive correlation between maximal rate of contraction for the Laser-MMG and Tensiometry techniques ($r^2 = 0.72$) further indicates that muscle belly displacement properties are reflective of tension development properties.

4.5.3 Study C – Fibre Type

This study aimed to establish whether the Laser-MMG technique could be used to detect differences in contractile properties due to variations in muscle fibre type. The results showed that the distal segment (1% slow-twitch) of the medial gastrocnemius of the rat had significantly higher ($p<0.05$) lateral displacement (Dmax), lateral displacement (Tmax), shorter contraction (tc*N*) and relaxation (tr*N*) times and higher maximal rates of contraction and relaxation compared to the proximal segment (21% fast-twitch) as shown by both Tensiometric and Laser-MMG analysis. Furthermore, the measures of Dmax and Tmax were found to be 48% and 46% less (respectively) and tc*N* measures 96% (Laser-MMG) and 99% (Tensiometric) longer in the proximal segment. The detection of similar differences between the proximal and distal segments confirmed that the Laser-MMG was as sensitive as Tensiometry to differentiate between the contractile properties of muscle segments with different fibre-type compositions.

The medial gastrocnemius muscle is highly regionalised with respect to fibre type composition (De Ruiter 1996; De Ruiter, De Haan *et al.* 1995a, 1995b, 1996; Kraemer, Staron *et al.* 2000; Staron, Kraemer *et al.* 1999; Wang and Kernell 2000). In the rat, it consists of a proximal segment, composed of a mixture of fast oxidative and slow oxidative fibres and a distal segment that is completely composed of fast-twitch glycolytic fibres. In the present study, the muscle fibre distribution of the medial gastrocnemius was determined using the techniques of Bonner and Pollard (2003), at the Institute of Clinical Neurobiology within the Royal Prince Alfred Hospital, Sydney, Australia. The present results agreed with those reported previously in the literature and confirmed the fibre type composition of the proximal and distal segments of the experimental muscles.

Muscles of different fibre type composition have been shown to possess different contractile properties, in particular contraction speed (+dT/dt) and contraction time (tc) (Burke and Tsairis 1973). Type I fibres are recognised as having slower contraction velocities and a reduced force production capacity, compared to type II fibres (Barany 1967; Burke and Tsairis 1973; Close 1965). Early investigators observed that the cat soleus muscle, a dominantly slow-twitch muscle (100% type I fibres (Ariano, Armstrong and Edgerton 1973)), had slower contractile properties than the medial gastrocnemius, a muscle

predominantly fast-twitch (14% Type IIa and 61% type IIb fibres (Ariano, Armstrong *et al.* 1973)) fibres (Burke and Tsairis 1973).

Muscle architecture determines, to a large part, the force, velocity and displacement properties of the muscle (Sacks and Roy 1982; Spector, Gardiner *et al.* 1980). Up to 12.6 fold differences in maximal contractile velocity has been attributed to differences in muscle fibre lengths (architecture) compared to a 2.5 fold difference attributed to biochemical (fibre type) differences (Sacks and Roy 1982). The medial gastrocnemius muscle has a continuous, uniform pennate architecture throughout the entire muscle (proximal and distal segments) (Huijing, Van Lookeren Campagne and Koper 1989; Van Leeuwen and Spoor 1993; Woittiez, Huijing and Rozendal 1983; Wolf and Kim 1997). It should be expected therefore, that the influence of variations in architecture on the contractile properties of the muscle's two segments would be negligible in the present study. Variation in fibre type composition therefore, as confirmed by the histochemical analysis, was the major contributor to the different contractile properties of each segment.

As reported previously, the proximal segment has smaller motor unit territories, smaller cross-sectional fibre areas, lower force production, greater resistance to fatigue and greater half-relaxation times in comparison to the distal segment (De Ruiter, De Haan *et al.* 1995a, 1996). These contractile properties are typical of slow-twitch fibres that exhibit similar slow contraction speeds as reported here. The sensitivity of the Laser-MMG to detect changes in contractile properties due to muscle fibre type was a noteworthy finding. Interestingly, this outcome was achieved in spite of the small variation (20%) in muscle fibre type composition present between the two segments investigated.

That the Laser-MMG can identify muscle tissue based on its fibre type is important for future application of the technique to human muscle segment analysis. Muscle injury causes small variations (10-30%) in fibre type composition (Hortobagyi, Dempsey, Fraser, Zheng, Hamilton, Lambert and Dohm 2000; MacDougall, Elder, Sale, Moroz and Sutton 1980; Mannion, Dumas, Cooper, Espinosa, Faris and Stevenson 1997). The Laser-MMG may prove viable in the detection of injury-induced changes in contractile properties and

also in tracking recovery of function during the injury rehabilitation process (Rosser, McAndrew and Iverson 2005). Indeed, evidence suggests that the Laser-MMG technique may also find application in injury site diagnosis (Gorelick 2005) and areas of human science such as training (Gollnick, Piehl, Saubert, Armstrong and Saltin 1972), fatigue and recovery (Allen 2004; Allen, Lannergren *et al.* 1995; Cady, Elshove, Jones and Moll. 1989b; Cady, Jones *et al.* 1989a), identification of scar tissue/injury sites (Burnham, Martin, Stein, Bell, MacLean and Steadward 1997; Mannion, Kaser, Weber, Rhyner, Dvorak and Muntener 2000; Mannion, Weber, Dvorak, Grob and Muntener 1997), quantifying aging effects (Larrson, Sjodin and Karlsson 1978; Lexell, Henriksson-Larsen *et al.* 1983a, 1983b; Sugiura and Kanda 2004), immobilisation (Hortobagyi, Dempsey *et al.* 2000; MacDougall, Elder *et al.* 1980) and the diagnosis of other neuromotor disease states (Mannion, Meier, Grob and Muntener 1998).

The results presented here also suggest that the Laser-MMG may be more sensitive than Tensiometry when identifying contractile properties from segments within a single muscle. Whilst similar directional trends were observed between the two measurement techniques, Tensiometry was unable to detect a similar number of significant differences ($p<0.05$) in contractile properties as identified by the Laser-MMG. Unlike the Laser-MMG technique, Tensiometric analysis failed to detect a significant difference ($p<0.05$) in contraction time (tc) and normalised sustain time (ts*N*) between each segment. One possible explanation for this result is that the neuromuscular stimulation protocol may have resulted in the spread of the stimulatory current from one segment to the next. The tension waveforms recorded may have represented force contributions from both muscle segments. In contrast, the Laser-MMG technique recorded from specific areas within each of the two segments and would have been relatively unaffected by any unintentional spread of the stimulatory current.

The use of this particular experimental design was unavoidable as the anatomical separation of the segments would have altered the structure of the muscle and resulted in the loss of functional muscle tissue. This would have reduced the muscle's ability to maximally contract and therefore disrupted the natural expansion of the muscle belly.

As an overall summary, the results and conclusions from the three encompassing studies (A, B & C) support the stated hypotheses. The Laser-MMG measures: mimicked the directional trends of simultaneous Tensiometry measures; were as sensitive as the Tensiometry measures to the effects of temperature and repetitive stimulation; and showed it as a viable technique for the translation to assessment of the contractile properties of multiple segments within whole human muscles.

Chapter 5

Validation of Mechanomyography II: Quantification of human muscle segment contractile properties

5.1 Introduction

The work described in the previous chapters has established, in an animal model, that differences in contractile properties between muscle segments of different fibre types, or changes in muscle contractile properties within a muscle due to fatigue or temperature modulation, can be reliably determined by a non-invasive Laser-MMG technique.

Previous findings have shown that single skeletal muscles may be subdivided into smaller muscle segments that may be independently controlled (functionally differentiated) by the CNS during particular motor tasks (Brown, Solomon *et al.* 1993; English, Wolf *et al.* 1993; Paton and Brown 1994, 1995; Wang and Kernell 2001; Weeks and English 1985; Wickham and Brown 1998; Wickham, Brown *et al.* 2004). The segments of a single skeletal muscle may be defined by many criteria: their anatomical structure (Segal, Wolf, DeCamp, Chopp and English 1991), the presence of unique moment arms and mechanical lines of action for particular movements (Ettema, Styles *et al.* 1998), different fibre type compositions (Johnson, Polgar *et al.* 1973) and the presence of neuromuscular compartments (Wang and Kernell 2001; Weeks and English 1985).

Multifunctional muscles, in particular those with wide origins and/or insertions, appear to be well suited for functional subdivision into discrete segments (Soderberg and Dostal 1978; Wickham and Brown 1998). Muscles such as the human gluteus maximus, pectoralis major, deltoid and latissimus dorsi offer a large and readily accessible site within which to assess the functionally related variations in muscle segment contractile properties.

In the present chapter, the focus is upon determining whether the Laser-MMG technique has utility to characterise contractile properties of individual muscle segments within human skeletal muscles. As noted previously (Chapter 2), muscle contractile properties and fibre type are traditionally determined through invasive techniques (Johnson, Polgar *et al.* 1973; Lexell, Henriksson-Larsen *et al.* 1983b; Linder, Dag *et al.* 2002; Loughlin 1993). Traditional invasive Tensiometry techniques for measuring muscle force production are

generally restricted to non-recovery animal studies due to the invasive and destructive effect upon the tissue in attaching the force transducer.

The non-invasive MMG technique measures and quantifies either the lateral displacement of contracting muscle fibres (Orizio 1993) or the lateral displacement of the whole muscle belly following maximal stimulation (Djordjevic, Valencic *et al.* 2001; Valencic and Djordjevic 2001). Importantly, recent research has suggested that the MMG technique may provide an accurate determination of muscle force and its contractile properties, and through this, an estimate of muscle fibre type, at least in superficial muscles (Djordjevic, Valencic *et al.* 2001; Orizio, Baratta *et al.* 1999; Orizio, Diemont *et al.* 1999).

In vitro animal studies performed in this thesis have so far demonstrated that the Laser-MMG can detect changes in muscle contractile properties associated with variations in temperature (Study A), muscle fatigue (Study B) and muscle fibre type composition (Study C). Of considerable interest now is whether the Laser-MMG technique can be utilised to determine how the contractile properties vary within and between, human muscles. If detected, variations in muscle contractile properties within a single muscle may suggest that muscle fibre populations are inhomogeneously distributed across the surface of a muscle in a pattern that may reflect the function of individual muscle segments. This work has been given impetus by two recent studies. In the first, Cescon and co-workers (Cescon, Farina, Gobbo, Merletti and Orizio 2004) have reported that MMG waveforms detected at multiple sites within a single muscle and between muscles are dissimilar, reflecting gross differences in architecture and fibre type distribution. In the second, Dahmane and co-workers (Dahmane, Djordjevic *et al.* 2005) have shown, in nine human limb muscles, spatial differences in muscle fibre type distribution when using a combined biopsy and MMG technique.

5.2 Aims and Hypotheses

The aims of the two experiments reported upon here were to:-

1. Characterise the contractile properties of three segments within the gluteus maximus,
2. Characterise the contractile properties of 14 segments across three superficial shoulder muscles and
3. Determine how the function of individual muscle segments influences their contractile properties.

It was hypothesised, based on a Laser-MMG technique, that:-

1. Muscle contractile properties would vary significantly ($p<0.05$) between adjacent and more distant segments of a multifunctional muscle,
2. Slower contractile properties would be found in muscle segments which had a greater postural role while faster contractile properties would be associated with segments having a greater role in joint rotation and,
3. There would be a gradation of muscle segment contractile properties across the surface of a multifunctional muscle.

5.3 Study D: Contractile properties of three segments within gluteus maximus

5.3.1 Methods – Gluteus Maximus

5.3.1.1 Experimental design

The aim of this experiment was to determine the contractile properties of multiple muscle segments within a single human muscle. Within each of the three segments of the gluteus maximus, two MMG recording sites were utilised to assess differences in contractile properties. Statistically significant differences in contractile properties, inferring variations in fibre type composition, were then matched to the known functions of the particular segment.

5.3.1.2 Subjects

Ten healthy young male subjects (mean age 21 years; range 18 to 25 years) volunteered to participate in this investigation. All were free from musculoskeletal injury or pathology to the back, hips and lower limbs.

5.3.1.3 Muscle segment identification

The pelvises of six human cadavers (aged between 72 years to 92 years; fixed and at 5ºC) were examined to obtain normalised anatomical landmarks to identify three gluteal segments (cranial- middle- and caudal-), each with a medial and a lateral portion, within the left gluteus maximus of each specimen (Figure 5.1).

The anatomical borders of each muscle segment were identified via a visual inspection of the muscle's architecture, muscle fibre attachments and fibre directions. The cranial- and caudal-borders of the origin of each of the three segments were determined from a line drawn along the iliac crest between the anterior superior iliac spine (ASIS) and the coccyx. This distance was then normalised as 100% and the borders marked as per Figure 5.1. The cranial- and caudal-borders of the insertions of each segment were then determined from a line drawn from the iliac crest down through the hip joint to the lateral epicondyle of the femur. The location of each border was then marked as per Figure 5.1.

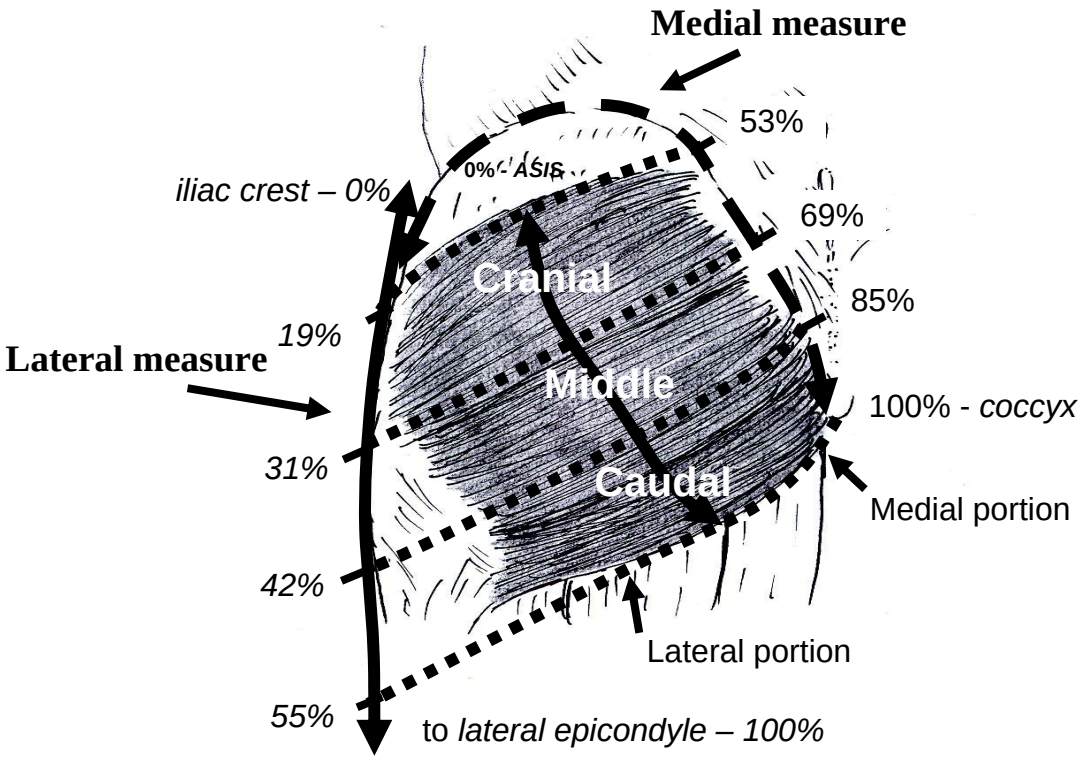

Figure 5.1 Posterior view of the left hip, identifying the location of superficial cranial-, middle- and caudal- muscle segments of the gluteus maximus muscle (summary of the data from 6 specimens). The diagram indicates the medial measure for the origin of the muscle segments (anterior superior iliac spine (ASIS) to the coccyx) and the lateral measure for the insertion of the muscle segments (ASIS to the lateral epicondyle). The physical distance of each measure was divided with the percentages as indicated. This enabled the clear identification of a muscle segments cranial and caudal border. Stimulating electrodes were attached to the medial and lateral portions of the three superficial segments of the muscle. Note that the deep fibres of the gluteus maximus, attached to the gluteal tuberosity, were not analysed in this investigation.

Once the borders of each muscle segment had been delineated, the medial to lateral extent of active muscle tissue, as opposed to aponeurosis, was then determined within each segment of the gluteus maximus. That part of each muscle segment containing actual muscle fibres was then divided equally into a medial and a lateral portion. In this way, three segments (cranial- middle- and caudal-) each with a medial and a lateral portion, were delineated and applied to the subjects of the study (Figure 5.1).

5.3.1.4 Equipment

A detailed description of the equipment is provided in Chapter 3, General Methods.

5.3.1.5 Experimental set-up

All experiments were carried out within the musculoskeletal laboratory at the University of Wollongong at a constant room temperature of 23ºC. Subjects were required to lie prone on a plinth for the duration of the testing session (Figure 5.2). The three segments of the left gluteus maximus were identified, each with a medial and lateral portion, based on the normalised data obtained from the analysis of the cadaveric specimens. All subjects were right leg dominant. The left non-dominant hip was chosen to reduce the effect of specific subject attributes i.e. favoured kicking leg.

The MMG electrode sites were marked either side of the centre of each of the six parts (3 segments x 2 portions) of the gluteus maximus to be tested. The subjects were secured to the plinth by straps across the lower back and mid-thigh region to immobilise the lower back, pelvic region and lower limb (Figure 5.2). The skin at the MMG electrode sites was alcohol washed and abraded to reduce source impedance prior to attachment of the stimulating electrodes (3M; 0.5 cm active plate). The inter-electrode distance was 2 cm with the MMG electrodes arranged parallel to the direction of the muscle fibres (cathode medial). The MMG electrodes were connected to the muscle stimulator to provide percutaneous neuromuscular stimulation (PNS) to the muscle segment. The stimulator delivered a single maximal twitch pulse to the muscle tissue lying immediately under each pair of MMG electrodes. The MMG laser sensor was positioned over the skin between the two MMG electrodes at each of the six MMG recording sites investigated (Figure 5.2). Ten trials were recorded randomly at each of the six MMG recording sites across the surface of the gluteus maximus. The present technique did not permit examination of the deep fibres of the muscle which have their attachment to the gluteal tuberosity of the femur.

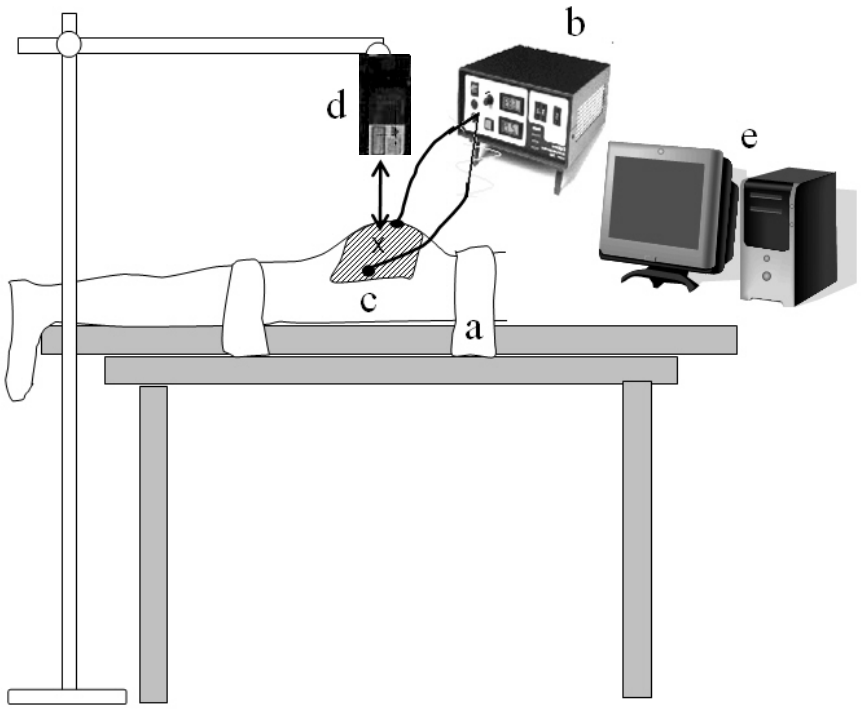

Figure 5.2 The Laser-MMG technique. With the subject lying prone and firmly secured to the plinth (a), a single-twitch PNS was delivered to the gluteus maximus (striped) via a stimulation device (b) utilising MMG electrodes (c). The resultant lateral displacement of the muscle's belly was detected by the Laser-MMG sensor (d) using a laser beam (double arrow). The Laser-MMG sensor was positioned 10 cm from the surface of the muscle (x) and at right angles to the direction of the stimulated muscle's motion. The resultant Laser-MMG waveform (the mechanomyogram) was digitised and stored on a computer (e).

5.3.1.6 Percutaneous neuromuscular stimulation

PNS was administered during each of the 60 trials recorded for each subject by the stimulator. The stimulator had a voltage range of between 0 V and 180 V, a maximum current of 85 mA, and a pulse duration of 300 μs delivered as a single twitch (optimal pulse duration identified previously by McAndrew, Rosser and Brown (2006)). A voltage ramp was used to determine the maximal voltage required to elicit maximal muscle displacement at each of the six MMG recording sites tested across the muscle. This procedure involved a

gradual increase in voltage until no further increase in peak muscle displacement was evident without distortion to the muscle belly displacement curve recorded by the Laser-MMG. In order to avoid muscle fatigue, a 60 second recovery period was enforced between each of the ten trials at each of the six MMG recording sites.

5.3.1.7 Laser-MMG data analysis

The MMG laser sensor was positioned at right angles to the movement of the muscle tissue under investigation to ensure an undistorted record of muscle displacement. Analogue records of muscle belly displacement (the MMG waveforms) were digitally converted at 1 kHz prior to storage and analysis utilising LabVIEW® version 7.0 software.

Maximal PNS of the gluteus maximus produced a parabolic waveform which represented the displacement of the muscle's belly (refer to the General Methods chapter). Ten MMG waveforms were available for analysis from each of the six recording sites across the surface of the gluteus maximus. Two phases within each MMG waveform could be identified: an ascending phase when the muscle was contracting in response to the 300 μs PNS pulse delivered by the stimulator and a descending phase when the muscle was undergoing relaxation (Figure 5.3).

The timing and amplitude of muscle belly displacement, and from this data each muscle segment's contractile properties, were determined by analysis of the MMG waveforms. Please refer to Chapter 3, General Methods, for a detailed description of the measurement variables determined by analysing the MMG waveforms generated at each of the six MMG recording sites.

5.3.1.8 Statistical analysis

The mean and standard error of the mean was calculated for each of the 6 variables determined from each Laser-MMG recording site within the muscle. All statistics were performed using SPSS 13.0 for windows (SPSS Inc. USA). Data was subjected to a normality and equal variance test to confirm the normal distribution and equal spread of the data (all passed). All data presented as mean ± SEM unless otherwise stated.

A Multivariate Analysis of Variance (MANOVA) was conducted to determine between subject differences (10 levels), between muscle segment differences (3 levels – each segment) and between portion differences (2 levels – medial and lateral) in contractile properties. A post-hoc Bonferroni comparison was performed to determine the nature of the main effects (subject, segment, portion) that significantly differed ($p<0.05$) from each other for each Laser-MMG variable.

5.3.1.9 Ethics

The experimental protocol was approved by the University of Wollongong / Illawarra Area Health Service Human Research Ethics Committee.

5.3.2 Results – Gluteus Maximus

5.3.2.1 General muscle description and summary of results

The gluteus maximus was found to have contractile properties that significantly varied ($p<0.05$) between muscle segments across the surface of the muscle but not between the medial and lateral portions of each segment. No significant differences ($p<0.05$) were identified between subjects indicating a homogenous subject group. The effect of subject was subsequently removed from the statistical analysis.

*5.3.2.2 **Within** muscle segment analysis: (medial to lateral portions)*

No significant differences were identified between MMG waveforms derived from the medial and lateral portions within any of the three muscle segments (Table 5.1).

Table 5.1 Group mean data for Laser-MMG variables for the lateral and medial potions of the three muscle segments of the human gluteus maximus muscle. Note that no significant ($p<0.05$) differences were identified between medial and lateral portions of the three segments for any MMG variable ($p<0.05$, MANOVA, n = 10). Group mean data (±SEM).

		Dmax (mm)	**tc*N*** (ms/mm)	**tr*N*** (ms/mm)	**ts*N*** (ms/mm)	**+dD/dt** (+mm/s)	**-dD/dt** (-mm/s)	**tc** (ms)	**tr** (ms)	**ts** (ms)
Cranial segment	**Med.**	6.16 (0.34)	19.13 (1.17)	26.10 (2.89)	37.36 (2.29)	85.0 (10.40)	61.7 (10.32)	114.81 (2.56)	154.92 (21.27)	224.90 (8.30)
	Lat.	5.30 (0.43)	21.93 (1.77)	31.95 (4.51)	40.76 (3.78)	56.31 (8.37)	40.79 (8.85)	109.63 (1.59)	153.33 (13.77)	202.08 (8.35)
Middle segment	**Med.**	11.53 (0.76)	8.74 (0.63)	14.85 (2.56)	17.91 (1.72)	68.4 (9.97)	46.60 (9.67)	96.73 (1.93)	160.54 (22.76)	195.87 (9.43)
	Lat.	9.30 (1.30)	10.31 (0.46)	17.80 (2.27)	18.88 (1.22)	109.25 (13.61)	72.7 (11.21)	94.73 (2.02)	164.88 (22.66)	173.64 (9.18)
Caudal segment	**Med.**	6.74 (0.37)	12.10 (0.46)	25.50 (2.77)	26.36 (1.73)	69.1 (8.88)	40.56 (6.53)	80.02 (1.62)	168.27 (18.19)	172.19 (4.39)
	Lat.	6.08 (0.17)	12.94 (0.40)	32.30 (4.10)	31.02 (1.73)	50.71 (3.78)	24.89 (2.71)	78.15 (1.49)	192.38 (20.51)	186.48 (7.32)

5.3.2.3 ***Between*** *muscle segment analysis: (superior to inferior segments)*

A visual comparison of the MMG waveforms collected from each muscle segment suggested muscle contractile properties were not uniform across the surface of the gluteus maximus muscle (Figure 5.3). Upon further analysis it was found that the middle segment produced the largest magnitude of displacement, occurring at the greatest rate of contraction, with the adjacent cranial and caudal segments exhibiting lower amplitude and slower temporal properties. A summary of results for all MMG variables from each muscle segment can be seen in Table 5.2.

Table 5.2 MMG variables for the three muscle segments. Values within columns sharing the same symbol (* # †) are not significantly different ($p<0.05$, MANOVA, n = 10). Group mean data (±SEM).

	Dmax (mm)	**tc*N*** **(ms/mm)**	**tr*N*** **(ms/mm)**	**ts*N*** **(ms/mm)**	**+dD/dt (+mm/s)**	**-dD/dt (-mm/s)**	**tc (ms)**	**tr (ms)**	**ts (ms)**
Cranial Segment	5.73 (0.28)	20.53* (1.08)	29.02 (2.69)	39.06* (2.18)	70.60 (7.28)	51.23 (7.05)	112.2* (1.58)	180.33 (13.63)	213.40* (6.30)
Middle Segment	10.41* (0.47)	9.87 (0.34)	16.32* (1.70)	18.40 (1.03)	88.51 (9.40)	59.35 (7.81)	95.73# (1.38)	162.71 (15.64)	184.76*† (6.89)
Caudal Segment	6.41 (0.21)	12.52 (0.32)	28.89 (2.53)	28.69 (1.30)	59.94* (5.15)	32.60* (3.88)	79.08† (10.9)	154.12 (9.26)	179.34† (4.47)

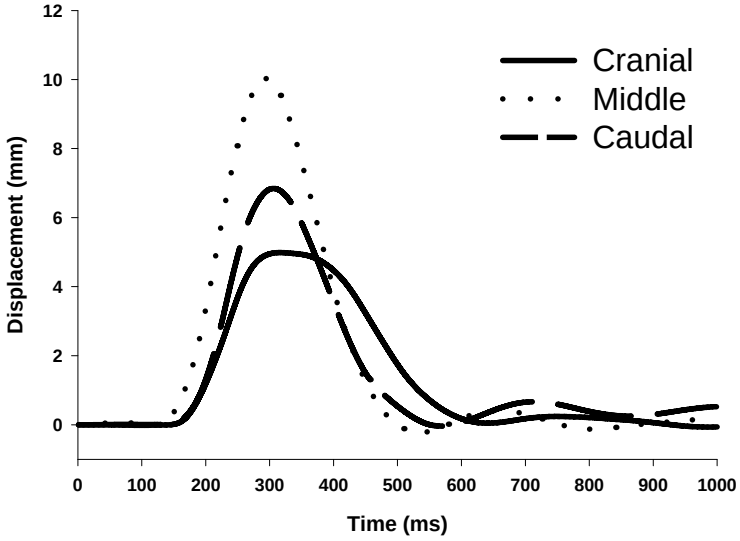

Figure 5.3 Representative MMG waveforms from the three segments of the gluteus maximus (medial portions). Note the obvious difference in the amplitude and timing of whole segment contraction between the muscle's three segments. Data from one subject only.

The maximal displacement (Dmax) of the muscle's middle segment was significantly greater ($p<0.05$) than either the cranial or the caudal segments, however, there was no significant difference ($p<0.05$) in maximal displacement (Dmax) between the cranial and caudal segments (Figure 5.4).

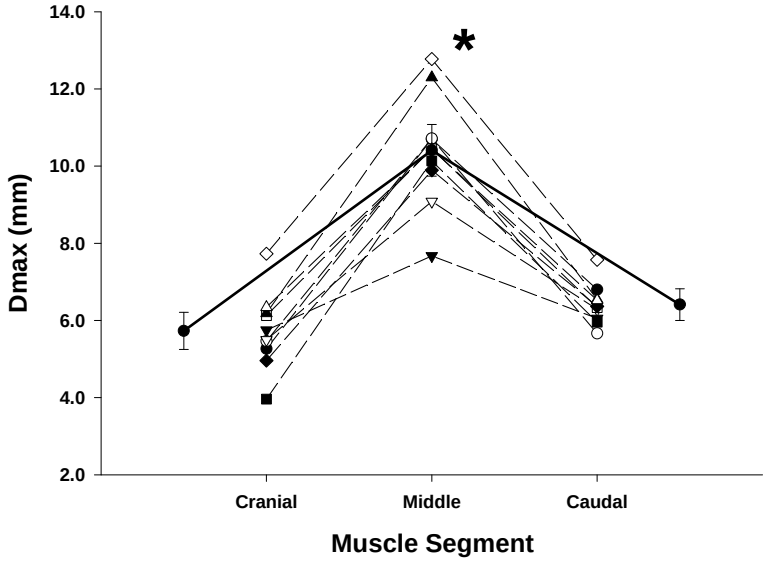

Figure 5.4 Maximal displacement (Dmax) values for each segment (all subjects). * indicates significant difference from cranial and caudal segments ($p<0.05$, MANOVA, $n = 10$). Each symbol represents an individual subject. Solid line indicates group mean (±SEM).

To account for different absolute values of muscle belly displacement recorded from the three segments, contraction time (tc) was normalised to Dmax (now tc*N*) (Figure 5.5). The cranial segment was shown to have the slowest normalised contraction time, taking 20.5 ms for each millimetre of displacement. This was significantly slower ($p<0.05$) than the middle and caudal segments (Table 5.2).

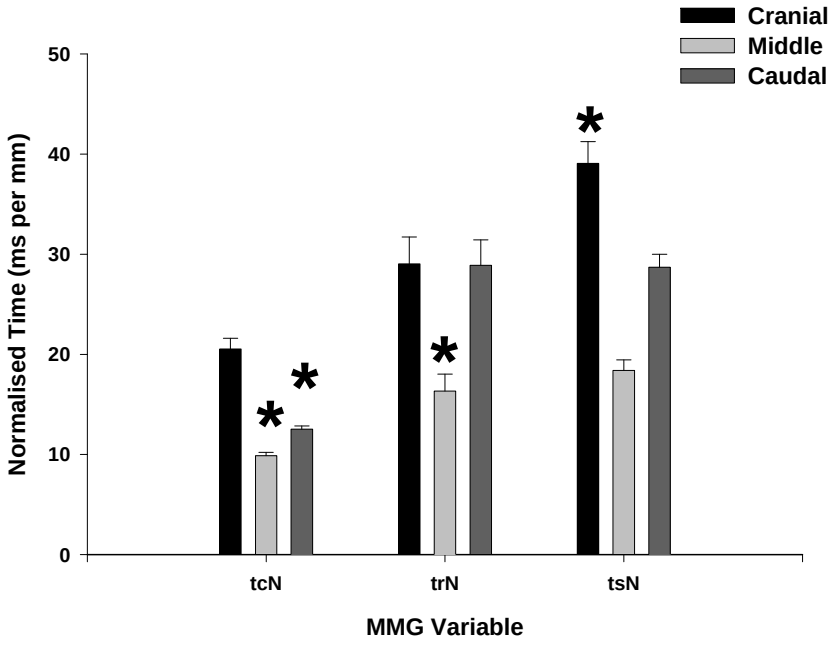

Figure 5.5 Normalised contraction time (tc*N*), relaxation time (tr*N*), and sustain time (ts*N*) of the cranial, middle and caudal segments. * indicates significant ($p<0.05$) difference from all segments ($p<0.05$, MANOVA, n = 10).

The relaxation time (tr) was, on average, 165.72 ms for the three segments. The middle segment had a significantly shorter ($p<0.05$) normalised relaxation time (tr*N*) than either the cranial or caudal segments ($p<0.05$) (Figure 5.5 and Table 5.2).

Sustain time (ts) was, on average, 192.53 ms for the three segments. Normalised sustain time (ts*N*) was shown to be longer ($p<0.05$) in the cranial segment than either the middle or caudal segments (Figure 5.5).

The caudal segment of the gluteus maximus was found to have the slowest maximal rate of contraction (+dD/dt) and relaxation (-dD/dt) with both the cranial and middle segments found to be significantly faster ($p<0.05$) (Table 5.2).

5.4 Study E: Contractile properties of multi-segmental shoulder muscles

5.4.1 Methods – Multi-segmental Muscle

5.4.1.1 Experimental design

The aim of this experiment was to determine the contractile properties of 14 muscle segments from within three superficial muscles surrounding the human shoulder joint. The segments were determined from an analysis of human cadaveric specimens. Laser-MMG variables were calculated from the Laser-MMG waveforms recorded from each segment and statistically compared to identify differences between muscles and segments. This experiment is a continuation of Study D, designed to investigate multiple human muscle segments, within a group of muscles, operating over a common multi-planar joint.

5.4.1.2 Subjects

Twelve healthy young male subjects (mean age 22.3 ± 6.2 yrs, height 179.9 ± 4.7 cm, weight 76.8 ± 7.2 kg) volunteered to participate in this experiment. All were free from musculoskeletal injury or pathology to the shoulder and dominant (right) upper limb. All subjects had low body fat skin fold measurements (avg. 87.3mm ± 21.4mm (sum of nine sites)).

5.4.1.3 Muscle segment identification

Five cadaveric thorax specimens (aged between 72 years to 92 years; fixed and stored at 5ºC) were examined to obtain normalised anatomical landmarks to identify 14 muscle segments within the right superficial shoulder musculature of each subject (5 segments within pectoralis major, 4 segments within deltoid and 5 segments within latissimus dorsi – Figure 5.6).

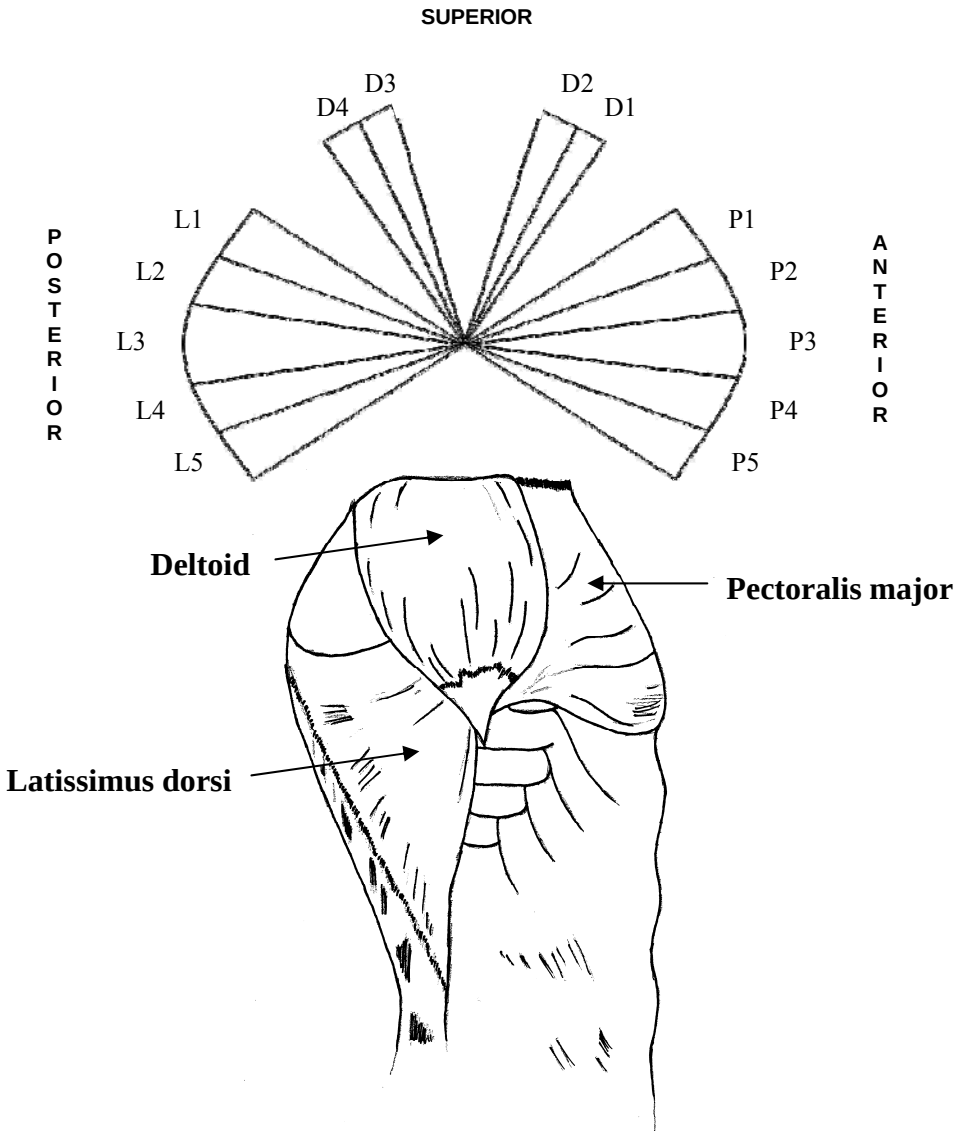

Figure 5.6 Illustration of a lateral view of the right shoulder musculature showing the investigated muscle segments within the three superficial shoulder muscles. Each segment is labelled with an abbreviation of its muscle i.e. P = pectoralis major, D = deltoid, L = latissimus dorsi. The segments of the pectoralis major and latissimus dorsi muscles are numerically labelled from superior to inferior (1-5) whilst the deltoid segments are numbered from anterior to posterior (1-4). The middle head of the deltoid was not examined in this study.

Pectoralis Major (segments P1, P2, P3, P4, P5)

Five MMG recording sites were identified for analysis, one within each of the muscular segments of the pectoralis major (Figure 5.7). A detailed description of the calculations used to determine the muscle segments and the MMG recording sites is contained in Appendix A.

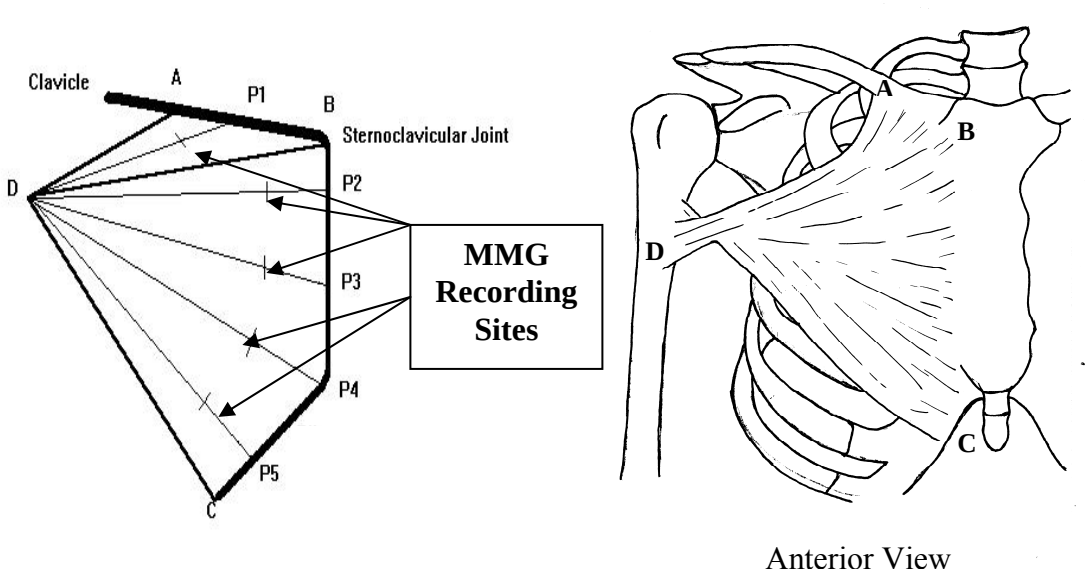

Figure 5.7 Schematic representation of the pectoralis major muscle showing the Laser-MMG recording sites. The diagram is marked with **A**: the origin of the pectoralis major on the clavicle, **B**; the sternoclavicular joint, **C**: the inferior point of the origin of the pectoralis major on the costal cartilage and **D**: the insertion of the pectoralis major on the humerus. These landmarks were used to determine the origin and insertion of the muscle and hence the muscle segment borders. Radiating lines within the left diagram indicate the centre of each muscle segment, which is identified with P1, P2 etc. Bipolar stimulating electrodes were attached to either side of each Laser-MMG recording site within the five segments of the muscle.

Deltoid (segments D1, D2, D3, D4)

Four MMG recording sites were identified within the deltoid: two within the anterior head (2 muscle segments) and two within the posterior head (2 muscle segments) (Figure 5.8). MMG waveforms were not recorded from within the middle segments of the deltoid as technical limitations (i.e. number of available EMG channels) prevented the collection of EMG waveforms in the proceeding study (Study F). Additionally, the anterior and posterior segments were chosen for analysis as the underlying muscle fibres possess similar lines of action to the superior segments of both the pectoralis major and latissimus dorsi. The muscle segments investigated in this study were identical to those identified by Wickham and Brown (1998) during their functional EMG study of the deltoid. A detailed description of the calculations used to determine the muscle segments and the MMG recording sites is contained in Appendix A.

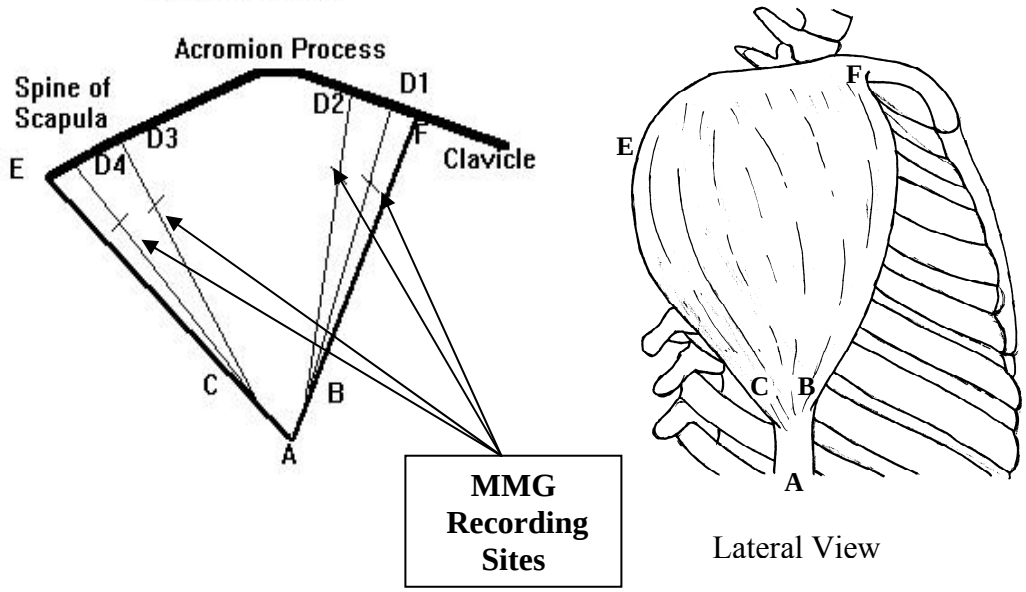

Figure 5.8 Schematic representation of the deltoid muscle showing the Laser-MMG recording sites within the four investigated segments of the muscle. The diagram is marked with **A**: the insertion of the middle deltoid on the humerus, **B**: the insertion of the anterior deltoid on the humerus, **C**: the insertion of the posterior deltoid on the humerus, **D**: the origin of the deltoid on the clavicle and **E**: the origin of the deltoid on the spine of the scapula. These landmarks were used to determine the origin and insertion of the muscle and hence the muscle segment borders. The radiating lines within the left diagram indicate the centre of each muscle segment, which is identified with D1, D2 etc. Bipolar stimulating electrodes were attached to either side of each Laser-MMG recording site within the four investigated segments of the muscle.

Latissimus Dorsi (segments L1, L2, L3, L4, L5)

Five MMG recording sites, each within a single muscle segment of the latissimus dorsi, were identified and analysed (Figure 5.9). A detailed description of the calculations used to determine the muscle segments and the MMG recording sites is contained in Appendix A.

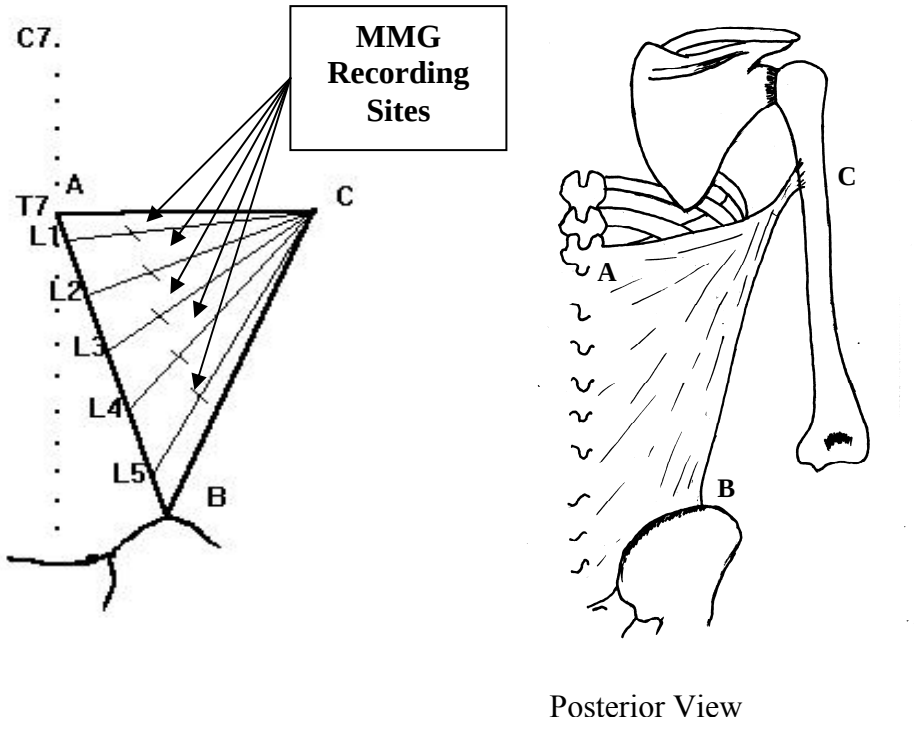

Figure 5.9 Schematic representation of the latissimus dorsi muscle showing the MMG recording sites. The diagram is marked with A: the origin of the latissimus dorsi on vertebrae T7, B: the origin of latissimus dorsi on the iliac crest and C: the insertion of the latissimus dorsi on the humerus. These landmarks were used to determine the origin and insertion of the muscle and hence the muscle segment borders. Radiating lines within the left diagram indicate the centre of each muscle segment, which is identified with L1, L2 etc. Bipolar stimulating electrodes were attached to either side of each MMG recording site within the five investigated segments of the muscle.

5.4.1.3 Equipment

A detailed description of the equipment is provided in Chapter 3, General Methods.

5.4.1.4 Experimental set-up

All experiments were carried out within the musculoskeletal laboratory at the University of Wollongong at a constant room temperature of 23ºC. Subjects were required to lie either prone or supine on a plinth during the testing session (dependent on which muscle was being investigated). The fourteen segments within the shoulder musculature were identified based on the normalised data obtained from the analysis of the cadaveric specimens.

Two MMG electrode sites were marked either side of the Laser-MMG recording site of each of the fourteen segments to be tested. The subjects were secured to the plinth by straps across the abdomen and upper humerus region to immobilise the thorax, shoulder girdle and upper limb. The skin at the stimulating electrode sites was alcohol washed and abraded to reduce source impedance prior to attachment of the stimulating electrodes (3M; 0.5 cm active plate). The inter-electrode distance was 2 cm with the electrodes arranged parallel to the direction of the muscle fibre (cathode medial). The stimulation electrodes were connected to the stimulation device to provide the required current. The MMG laser sensor was positioned over the MMG recording site, perpendicular to the direction of muscle belly movement. The neuromuscular stimulation device delivered a single maximal twitch pulse to the muscle tissue lying immediately beneath each pair of stimulating electrodes. Ten trials were recorded randomly at each of the fourteen MMG recording sites across the surface of the three superficial muscles.

5.4.1.5 Percutaneous neuromuscular stimulation

Refer to Chapter 5 – Study D (Percutaneous neuromuscular stimulation)

5.4.1.6 Laser-MMG data analysis

Refer to Chapter 5 – Study D (Laser-MMG Data Analysis)

For a detailed description of the measurement variables, please refer to Chapter 2 – General Methods.

5.4.1.7 Statistical analysis

Data was collected from the pectoralis major, deltoid and latissimus dorsi muscles of the human subjects. The mean and standard error of the mean was calculated for each of the 6 MMG variables determined from each segment within the three superficial muscles. Statistics were performed using SPSS 13.0 for Windows (SPSS Inc. USA). Data was subjected to a normality and equal variance test to confirm the normal distribution and equal spread of the data (all passed). All data presented as mean ± SEM unless otherwise stated.

A Multivariate Analysis of Variance (MANOVA) was conducted to determine between subject (12 levels) and between muscle segment (14 levels – each segment) differences in contractile properties. A post-hoc Bonferroni comparison was performed to determine the nature of the main effects (subject and segment) that significantly differed ($p<0.05$) from each other for each MMG variable.

5.3.2.9 Ethics

The experimental protocol was approved by the University of Wollongong / Illawarra Area Health Service Human Research Ethics Committee.

5.4.2 Results – Multi-segmental Muscle

5.4.2.1 General muscle description and summary of results

No significant effect ($p<0.05$) for subject was reported, indicating a homogeneous subject sample. The effect of subject was therefore removed from the analysis. Muscle segment MANOVA showed significant differences ($p<0.05$) between segments, most notably between the central and peripheral segments within the pectoralis major and the latissimus dorsi (Table 5.3) for the MMG variables of maximal displacement (Dmax), normalised time (tc*N*, tr*N*, ts*N*), maximal rate of contraction (+dD/dt) and relaxation (-dD/dt), and muscle segment thickness.

All three muscles were found to have segment contractile properties that significantly varied ($p<0.05$) across the surface of the muscle (between segments) (Table 5.3 and Figure 5.10, 5.11 and 5.12). The segments located on the periphery of the pectoralis major and latissimus dorsi muscles exhibited significantly greater ($p<0.05$) displacement and shorter normalised contraction times (tc*N*, tr*N*) than those located more centrally within the muscle.

Table 5.3 Segment mean values for each MMG variable. Mean values that differ by greater than the t-value are significantly different ($p<0.05$) (MANOVA, n = 12). Group mean data (±SEM). Deltoid segments are highlighted in grey to aid differentiation between muscles.

		SEGMENT	Dmax (mm)	tc*N* (ms/mm)	tr*N* (ms/mm)	ts*N* (ms/mm)	+dD/dt (+mm/s)	-dD/dt (-mm/s)	tc (ms)	tr (ms)	ts (ms)
Anterior Segments	Pectoralis Major	PEC 5	2.86 (0.28)	28.98 (4.41)	86.10 (13.26)	68.63 (12.70)	23.99 (3.15)	7.39 (0.70)	73.37 (1.50)	218.97 (13.42)	170.92 (7.16)
		PEC 4	1.66 (0.02)	45.87 (1.13)	82.54 (5.45)	89.61 (6.29)	12.51 (0.90)	7.33 (0.22)	75.95 (1.22)	136.74 (8.79)	148.31 (4.43)
		PEC 3	1.34 (0.02)	51.80 (1.38)	115.15 (6.56)	93.81 (4.24)	10.31 (0.24)	3.51 (0.24)	69.20 (1.48)	153.87 (10.02)	125.86 (4.73)
		PEC 2	1.46 (0.07)	54.37 (3.38)	119.81 (6.92)	126.94 (6.97)	16.07 (0.91)	7.07 (0.46)	79.18 (0.90)	179.99 (12.83)	186.47 (6.46)
		PEC 1	2.52 (0.16)	30.47 (1.43)	81.36 (2.70)	65.04 (4.01)	28.57 (3.74)	9.31 (1.05)	75.01 (1.76)	202.41 (7.91)	160.79 (9.21)
	Deltoid	DELT 1	2.94 (0.22)	27.46 (1.49)	76.87 (5.02)	71.78 (4.51)	32.06 (3.19)	8.39 (0.46)	77.95 (1.25)	216.62 (2.81)	203.28 (3.70)
		DELT 2	2.40 (0.19)	34.24 (2.44)	82.69 (8.31)	77.58 (5.12)	21.63 (2.87)	8.12 (0.76)	78.05 (0.89)	188.68 (10.53)	179.49 (7.79)
Posterior Segments		DELT 3	1.71 (0.04)	43.30 (1.42)	68.32 (3.01)	78.04 (2.05)	17.57 (0.58)	10.57 (0.40)	73.48 (1.13)	116.11 (4.69)	132.67 (1.97)
		DELT 4	2.50 (0.11)	31.71 (0.97)	70.39 (3.71)	74.02 (4.69)	29.05 (0.94)	13.16 (0.40)	78.24 (1.33)	173.65 (7.40)	182.78 (10.34)
	Latissimus Dorsi	LAT 1	2.14 (0.04)	39.06 (0.70)	81.23 (2.47)	65.68 (2.70)	19.77 (3.18)	6.36 (1.12)	83.56 (1.13)	173.46 (3.39)	139.97 (3.90)
		LAT 2	1.61 (0.08)	53.74 (2.69)	131.24 (7.33)	106.55 (7.63)	16.95 (2.14)	5.31 (0.55)	84.66 (2.14)	206.11 (4.45)	168.40 (10.61)
		LAT 3	1.69 (0.03)	47.59 (1.13)	103.03 (3.61)	97.54 (3.98)	12.87 (1.22)	5.29 (0.59)	80.01 (1.23)	173.39 (5.89)	164.25 (6.90)
		LAT 4	1.79 (0.04)	46.07 (0.76)	76.80 (4.12)	78.78 (4.67)	14.35 (1.44)	9.32 (0.97)	82.19 (1.70)	136.09 (5.21)	139.65 (5.75)
		LAT 5	2.15 (0.06)	34.19 (1.09)	90.61 (4.09)	58.08 (2.41)	24.55 (4.46)	7.33 (1.09)	73.00 (0.97)	192.93 (4.52)	123.74 (2.34)
		t-value	0.59	7.45	18.42	17.24	10.71	2.76	6.51	32.96	31.49

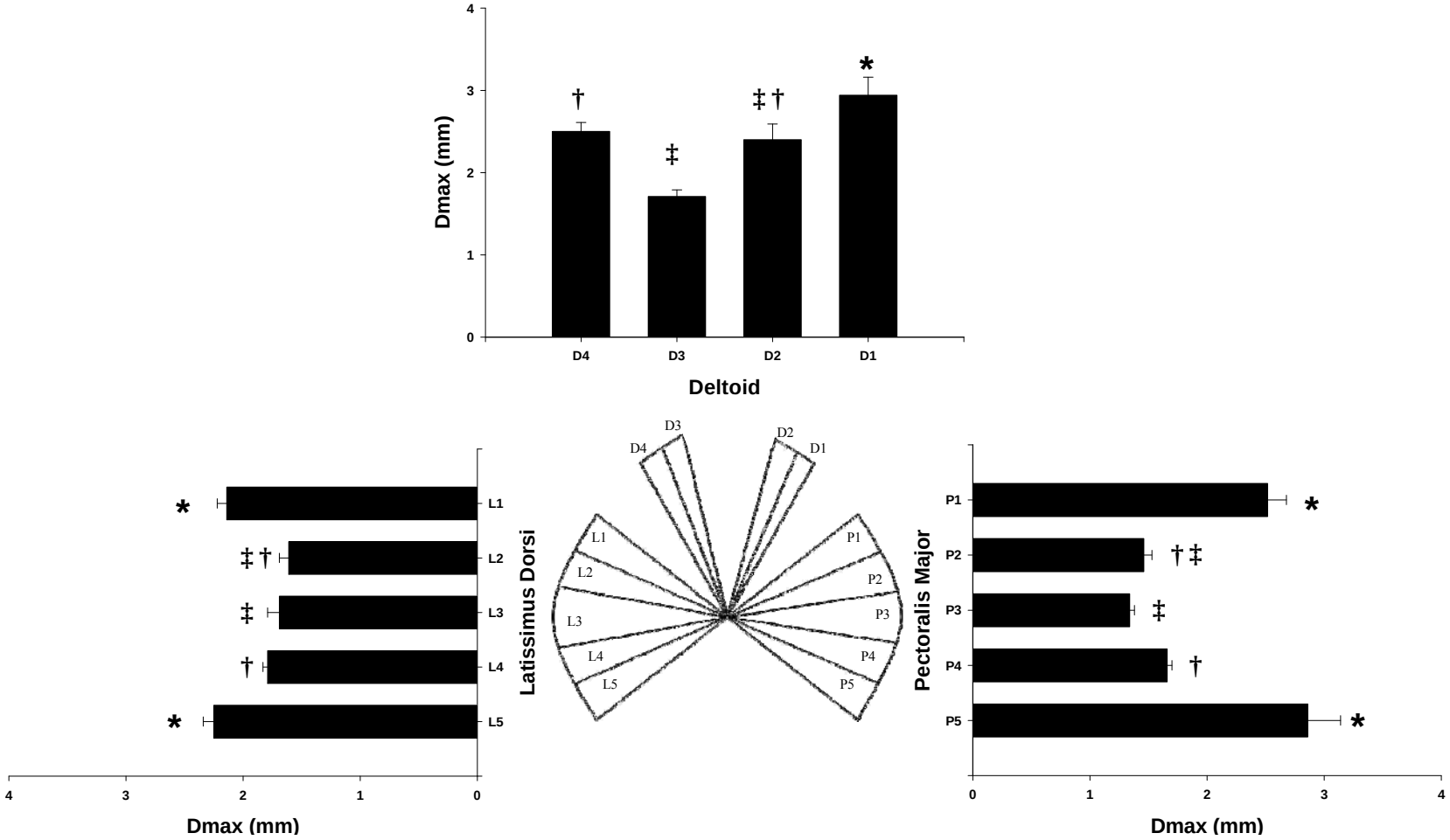

Figure 5.10 Maximal displacement (Dmax) values for each muscle segment. Located centrally is a schematic of the muscles divided into segments. Values for muscle segments located *within* individual muscles that share a common symbol **(*, †, ‡)** are not significantly different ($p<0.05$, MANOVA, $n = 12$). Group mean data (±SEM).

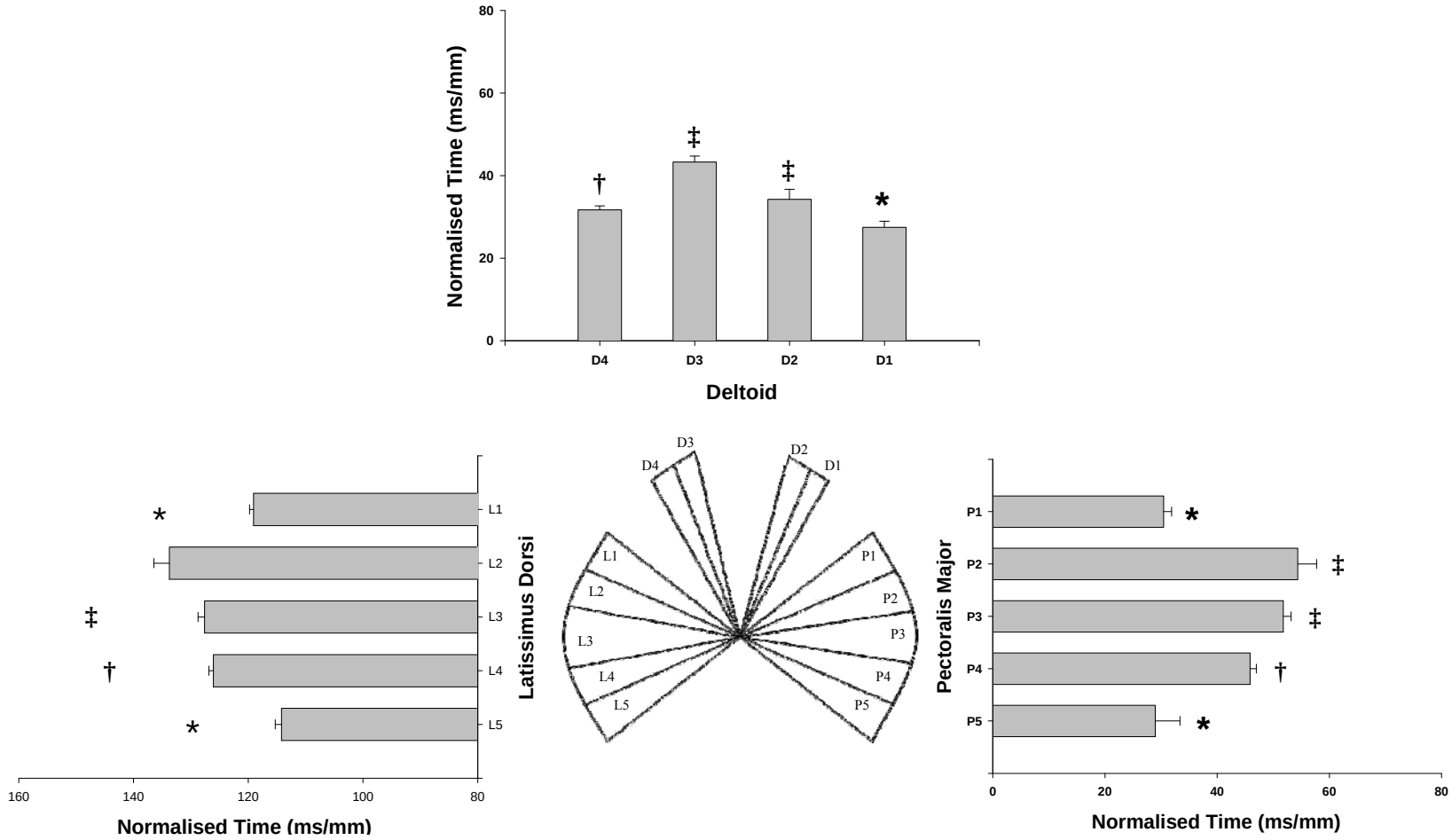

Figure 5.11 Normalised contraction time (tc*N*) for each muscle segment. Located centrally is a schematic of the muscles divided into segments. Values for muscle segments located *within* individual muscles that share a common symbol **(*, †, ‡)** are not significantly different ($p<0.05$, MANOVA, n = 12). Group mean data (±SEM).

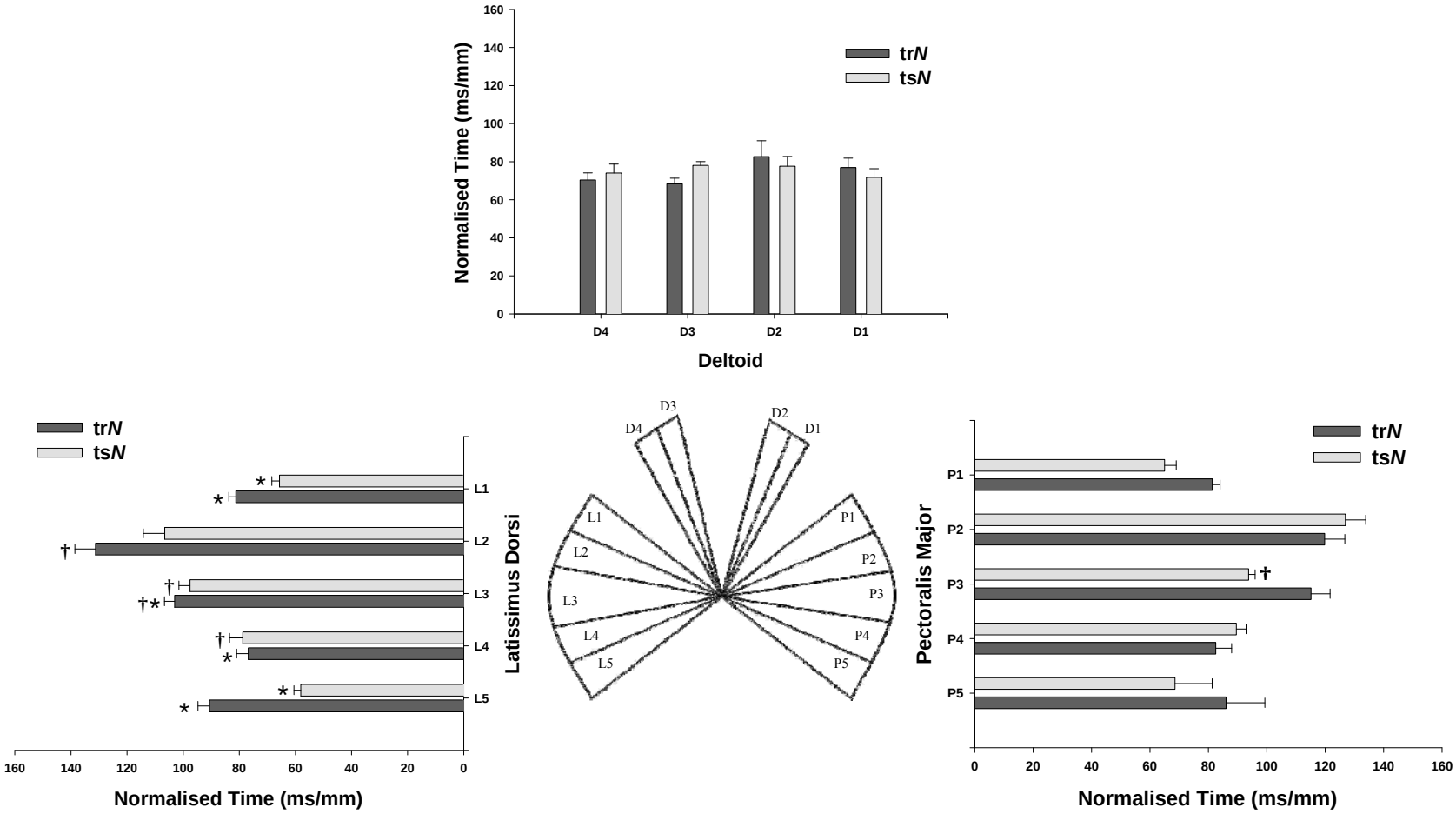

Figure 5.12 Normalised relaxation time (tr*N*) and sustain time (ts*N*) for each muscle segment. Located centrally is a schematic of the muscles divided into segments. Bars shaded the same represent a common measurement parameter. Values for muscle segments located *within* individual muscles that share a common symbol **(*, †, ‡)** are not significantly different ($p<0.05$, MANOVA, n = 12). Group mean data (±SEM)

5.4.2.2 Between segment analysis of contractile properties

Review of the data suggested that the contractile properties of the muscle segments at the periphery of each muscle investigated were significantly different ($p<0.05$) to those segments found in the centre of each muscle. Furthermore, segments that had comparable anatomical locations within individual muscles (e.g. P5 and L5) exhibited no significant differences ($p<0.05$) between contractile properties. A summary of results for all Laser-MMG variables from each muscle segment can be seen in Table 5.3.

The maximal displacement (Dmax) of each muscle segment was found to vary across the surface of the pectoralis major, deltoid and latissimus dorsi (Figure 5.10), with muscle segments located in the periphery of the muscles having significantly greater ($p<0.05$) maximal displacement (Dmax) than those segments located more centrally (Figure 5.12A). This pattern was particularly evident within the pectoralis major. Analysis of the pattern of Dmax between anterior segments and their anatomically corresponding posterior segments showed a significant correlation ($p<0.05$; $r^2 = 0.68$) (Figure 5.13B).

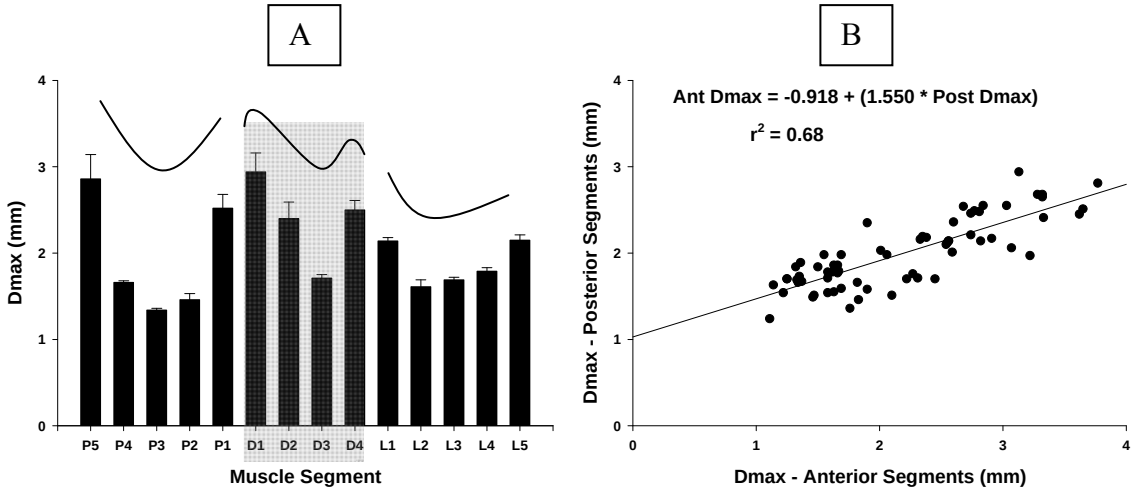

Figure 5.13 Maximal displacement (Dmax) values for all muscle segments. **A:** Group mean values for each muscle segment. Curved lines drawn on graphs are for illustration purpose only and do not represent statistical analysis. **B:** Correlation and linear regression for Dmax of the anterior and posterior segments for Dmax. n = 12 (line of best fit). Deltoid segments are highlighted in grey to aid differentiation between muscles.

To account for different absolute values of muscle belly displacement recorded from the different segments, contraction time (tc) was normalised to Dmax (now tc*N*) (Figure 5.11). The more central segments of each muscle (P2, P3, P4, D2, D3, L2, L3 and L4) were shown to have the slowest tc*N*. These were significantly slower ($p<0.05$) than the peripheral segments of each muscle (Table 5.3). Interestingly, the tc*N* values for the anteriorly located segments were correlated with the tc*N* values of similarly located posterior segments ($p<0.05$; $r^2 = 0.64$) (Figure 5.14B).

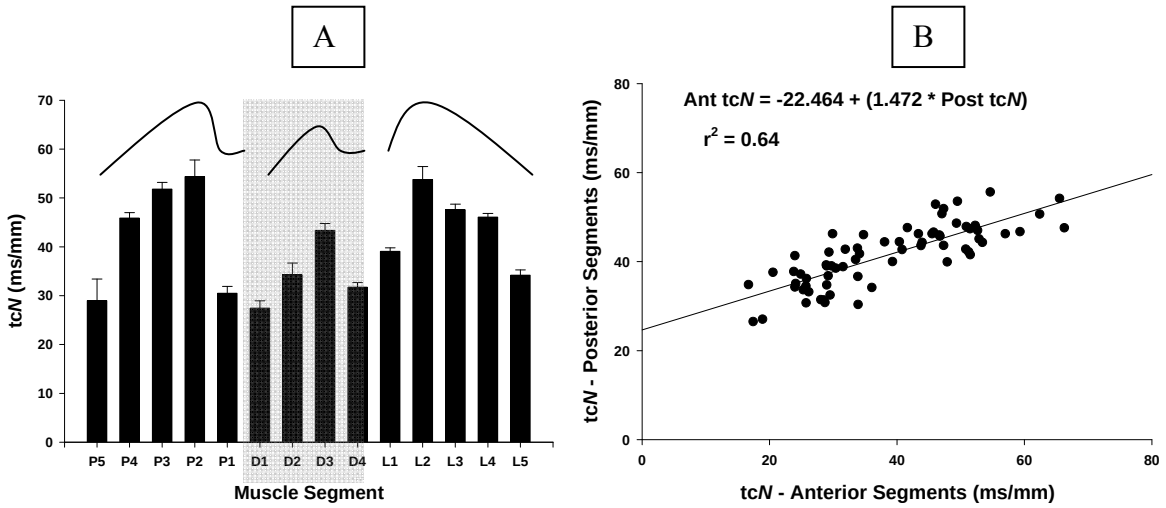

Figure 5.14 Normalised contraction times (tc*N*) for all muscle segments. **A:** Group mean values for each muscle segment. Curved lines drawn on graphs are for illustration purpose only and do not represent statistical analysis. **B:** Correlation and linear regression for tc*N* of the anterior and posterior segments for tc*N*. n = 12 (line of best fit). Deltoid segments are highlighted in grey to aid differentiation between muscles.

The normalised relaxation time (tr*N*) significantly differed ($p<0.05$) between the muscle segments of the shoulder musculature (Table 5.3). Specifically, muscle segments within pectoralis major and latissimus dorsi, but not the deltoid, were found to relax at a different rate after PNS ($p<0.05$). For the pectoralis major and latissimus dorsi, segments at the periphery of the muscle exhibited faster relaxation rates when compared to the centrally located segments. Segments within the deltoid had an average tr*N* of 74.57 ± 6.53 ms/mm, equivalent to the peripheral segments of pectoralis major and latissimus dorsi (Figure 5.12). A moderate correlation existed between the equivalent anatomically located segments ($p<0.05$; $r^2 = 0.56$) (Figure 5.15B).

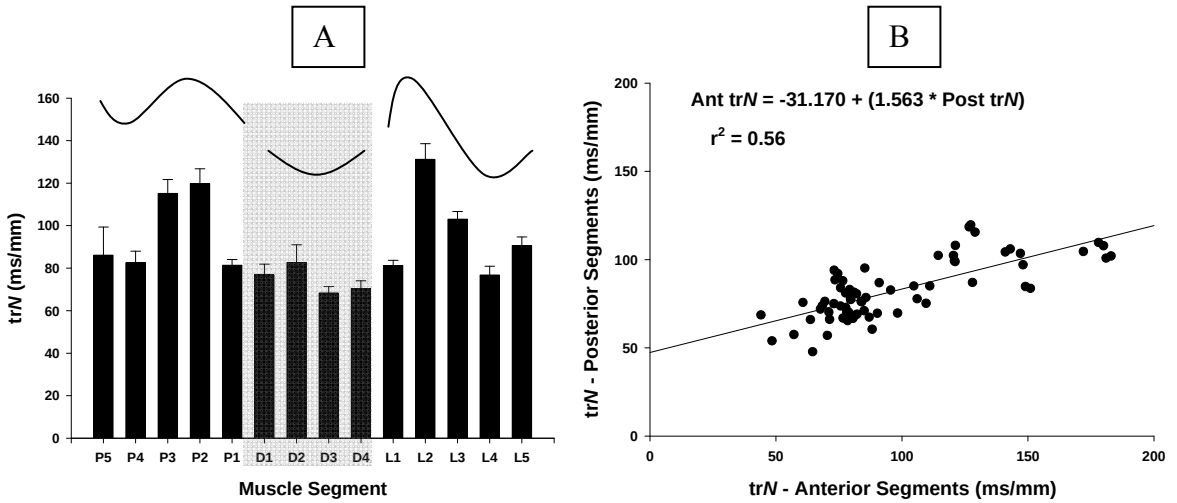

Figure 5.15 Normalise relaxation times (tr*N*) for all muscle segments. **A:** Group mean values for each muscle segment. Curved lines drawn on graphs are for illustration purpose only and do not represent statistical analysis. **B:** Correlation and linear regression for tr*N* of the anterior and posterior segments for tr*N*. n = 12 (line of best fit). Deltoid segments are highlighted in grey to aid differentiation between muscles.

Normalised sustain time (ts*N*) differed significantly ($p<0.05$) between the segments of the pectoralis major and latissimus dorsi, but not the deltoid (Table 5.3; Figure 5.16A). The contractile property ts*N* was also significantly correlated between anatomical locations (ts*N*: $p<0.05$; $r^2 = 0.69$, Figure 5.16B).

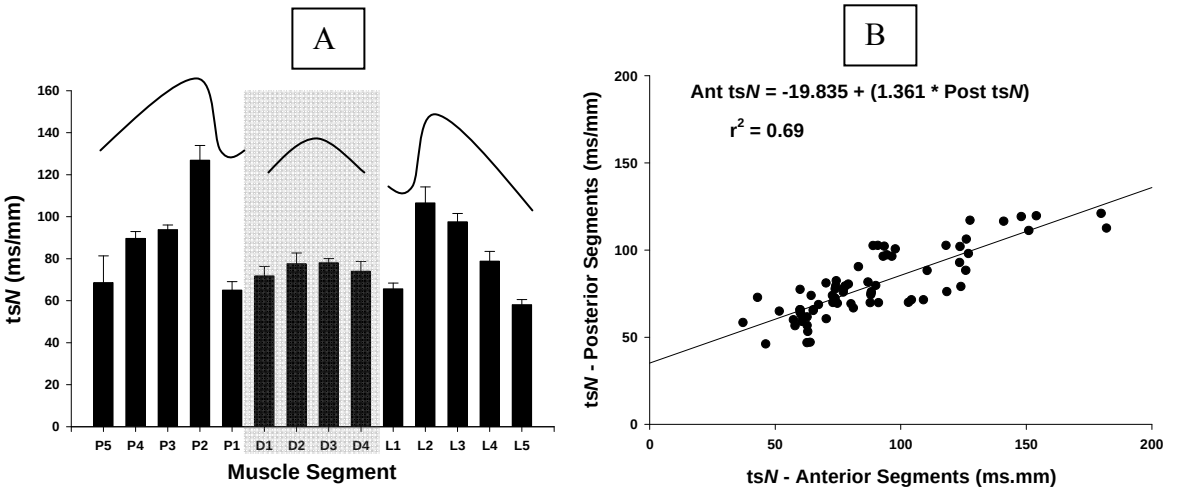

Figure 5.16 Normalised sustain times (ts*N*) for all muscle segments. **A:** Mean values for each muscle segment. Curved lines drawn on graphs are for illustration purpose only and do not represent statistical analysis. **B:** Correlation and linear regression for ts*N* of the anterior and posterior segments for ts*N*. n = 12 (line of best fit). Deltoid segments are highlighted in grey to aid differentiation between muscles.

The maximal rate of contraction (+dD/dt) and relaxation (-dD/dt) significantly differed ($p<0.05$) between segments of the superficial shoulder musculature (Table 5.3). Measures of +dD/dt for the anteriorly located segments were significantly correlated to the equivalent anatomically located segment on the posterior of the thorax ($p<0.05$; $r^2 = 0.64$) (Figure 5.17B). Similar correlations were observed for –dD/dt ($p<0.05$; $r^2 = 0.57$) (Figure 5.18B).

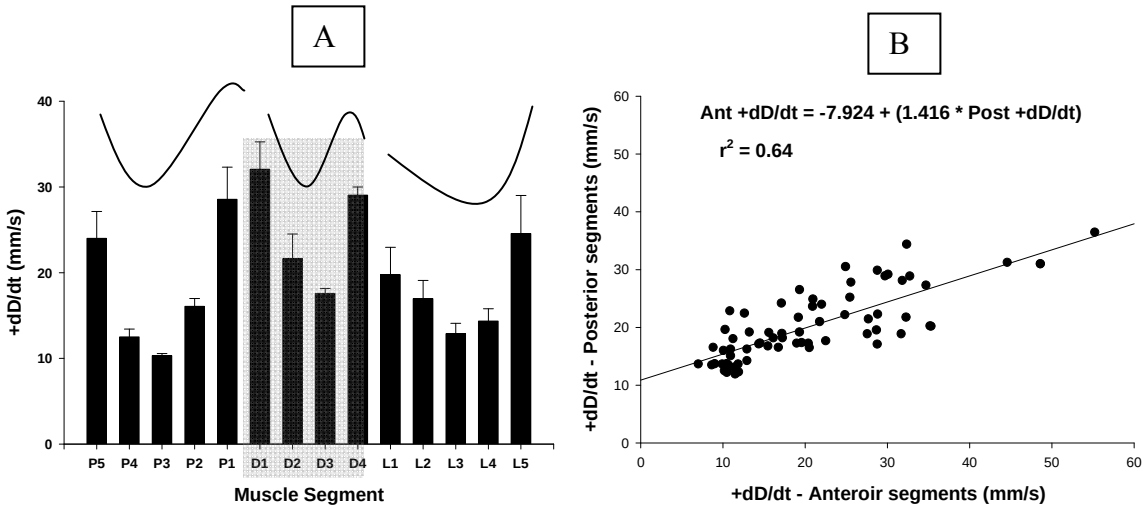

Figure 5.17 Maximal rates of contraction (+dD/dt) for all muscle segments. **A:** Group mean values for each muscle segment. Curved lines drawn on graphs are for illustration purpose only and do not represent statistical analysis. **B:** Correlation and linear regression for maximal rate of contraction of the anterior and posterior segments for ts*N*. n = 12 (line of best fit). Deltoid segments are highlighted in grey to aid differentiation between muscles.

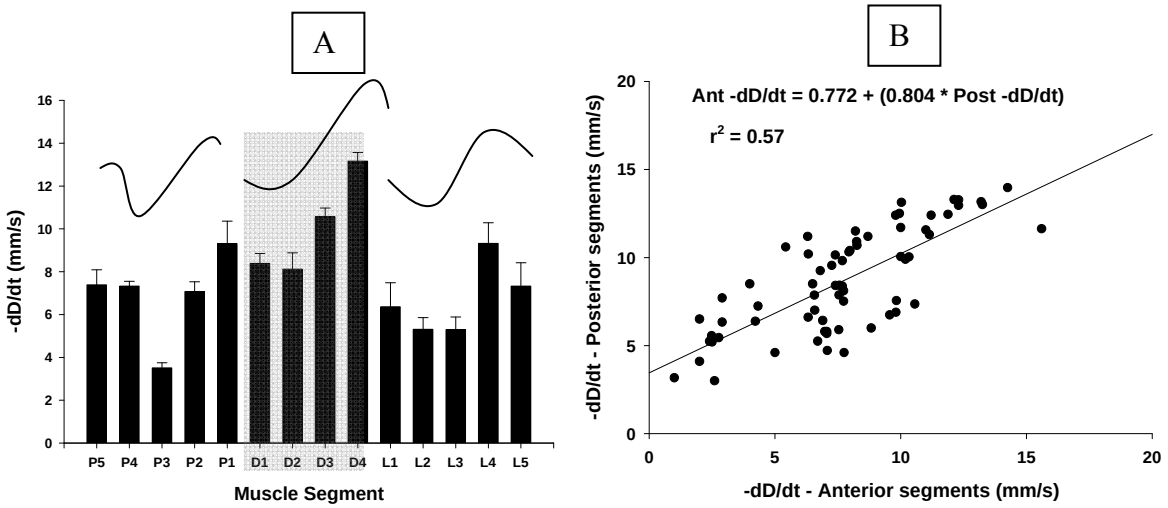

Figure 5.18 Maximal rates of relaxation (-dD/dt) for all muscle segments. **A:** Group mean values for each muscle segment. Curved lines drawn on graphs are for illustration purpose only and do not represent statistical analysis. **B:** Correlation and linear regression for maximal rate of relaxation of the anterior and posterior segments for ts*N*. n = 12 (line of best fit). Deltoid segments are highlighted in grey to aid differentiation between muscles.

Pectoralis Major

The maximal displacement (Dmax) of each segment followed a similar trend for all subjects (Figure 5.19), with the superior (P1) and inferior (P5) segments showing significantly more ($p<0.05$) lateral displacement than centrally located segments (P2/3/4).

The normalised contraction time (tc*N*) of the superior P1 and inferior P5 muscle segments was significantly shorter ($p<0.05$) than those in the centre of the muscle (P2/3/4; average 50.7 ± 4.34ms/mm) (Figure 5.11).

Normalised relaxation times (tr*N*) and sustain times (ts*N*) were also found to be significantly different ($p<0.05$) between segments. The superior P1 and inferior P4 and P5 segments had similar relaxation times (avg. 83.33 ± 2.47 ms/mm) which were, however, significantly shorter ($p<0.05$) than that found in the central segments (P2/3; avg. 117.48 ± 3.30 ms/mm) (Figure 5.12). Likewise, the superior and inferior segments (P1 and P5) also had shorter normalised sustain times (ts*N*) (avg. 66.84 ± 2.54 ms/mm) than the central segments (P3 and P4; avg. 91.71 ± 2.97 ms/mm), with segment P2 being significantly longer ($p<0.05$) than all other segments (126.94 ms/mm) (Figure 5.12).

The superior and inferior segments (P1 & P5) of the pectoralis major contracted at a significantly faster ($p<0.05$) maximal rate (avg. 26.28 ± 3.24 mm/s) than those in the centre (P2, P3, P4; avg. 12.96 ± 2.90 mm/s). The central P3 segment had the slowest ($p<0.05$) maximal rate of relaxation (P3; 2.51 mm/s) compared to the other remaining segments (P1, P2, P4 and P5; avg. 7.78 ± 1.03 mm/s).

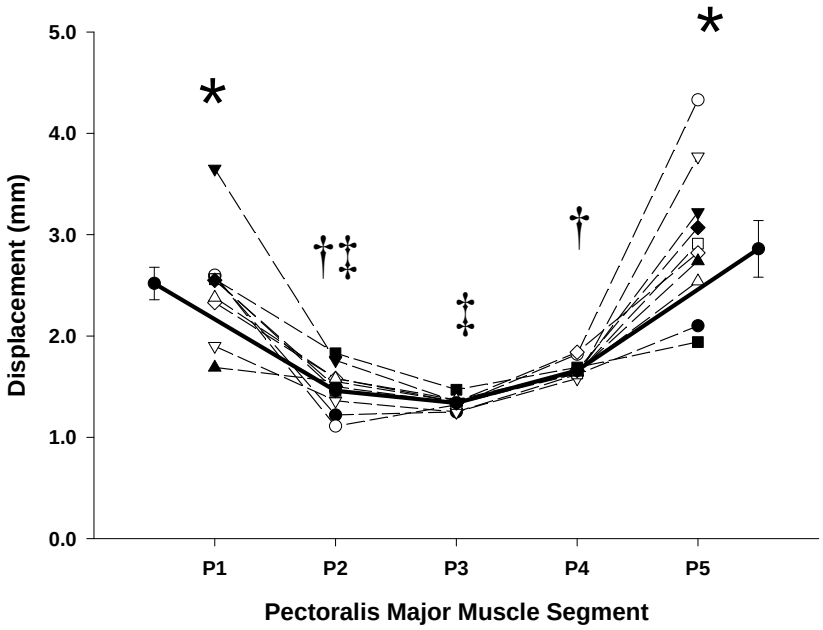

Figure 5.19 The average maximal displacement (Dmax) of each pectoralis major segment (all subjects). The superior and inferior segments of the pectoralis major displace further than the central segments. Each symbol represents an individual subject. Solid line indicates group mean ± SEM. Values sharing a common symbol (***, †, ‡**) are not significantly different ($p<0.05$, MANOVA, n = 12).

Deltoid

Significant differences ($p<0.05$) in Dmax were identified between the four segments of the deltoid muscle such that the more central segment (D3; 1.71mm) displaced significantly less ($p<0.05$) than the peripheral D1 and D4 segments of the muscle (Figure 5.20).

Normalised contraction times (tc*N*) for the anterior D1 segment were significantly shorter ($p<0.05$) than the posterior D4 segment, which itself was significantly shorter ($p<0.05$) than the more central segments D2 and D3 (Figure 5.11). Normalised relaxation times (tr*N*) for segment D2 were significantly longer ($p<0.05$) than segments D1 and D4 and sustain times (ts*N*) for segment D1 were significantly shorter ($p<0.05$) than those of segments D3 and D4, which were significantly shorter ($p<0.05$) than D2 (Figure 5.12).

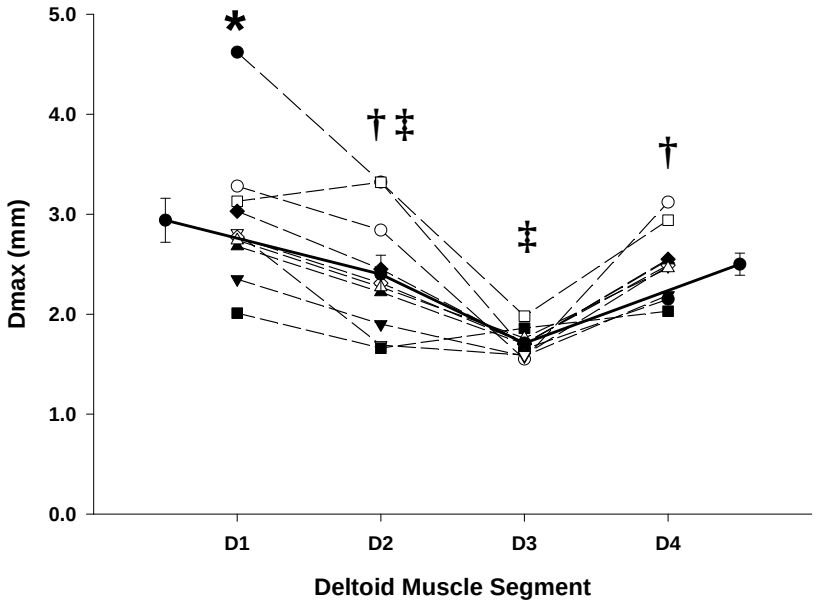

Figure 5.20 The average maximal displacement (Dmax) of each segment of the deltoid (all subjects). Each symbol represents an individual subject. Solid line indicates group mean ± SEM. Values sharing a common symbol (***, †, ‡**) are not significantly different ($p<0.05$, MANOVA, n = 12).

The maximal rate of contraction (+dD/dt) for the anterior D1 segment was significantly faster ($p<0.05$) than the remaining deltoid muscle segments (D2, D3, D4). In addition, the posterior D4 segment relaxed (-dD/dt) at a significantly faster ($p<0.05$) rate than the anterior D1 segment, which itself was faster to relax than both segment D2 or D3 (Table 5.3).

Latissimus Dorsi

Analyses of the maximal displacement (Dmax) data from all subjects indicated that, when stimulated, the superior (L1; 2.14 mm) and inferior (L5; 2.15mm) segments displaced significantly further ($p<0.05$) than the central segments (L2, L3, L4; avg. 1.70 ± 0.09 mm) (Figure 5.21).

When normalised for Dmax, segments L1 and L5 had significantly shorter normalised contraction times (tc*N*) (avg. 36.63 ± 3.44 ms/mm) than the centrally located segments (L2, L3, L4) (Figure 5.11). Additionally, segments L1, L4 and L5, when normalised for Dmax,

were found to relax (tr*N*) in a significantly shorter ($p<0.05$) time (avg. 82.88 ± 7.05 ms/mm), following PNS, than the central L2 and L3 segments (Figure 5.16).

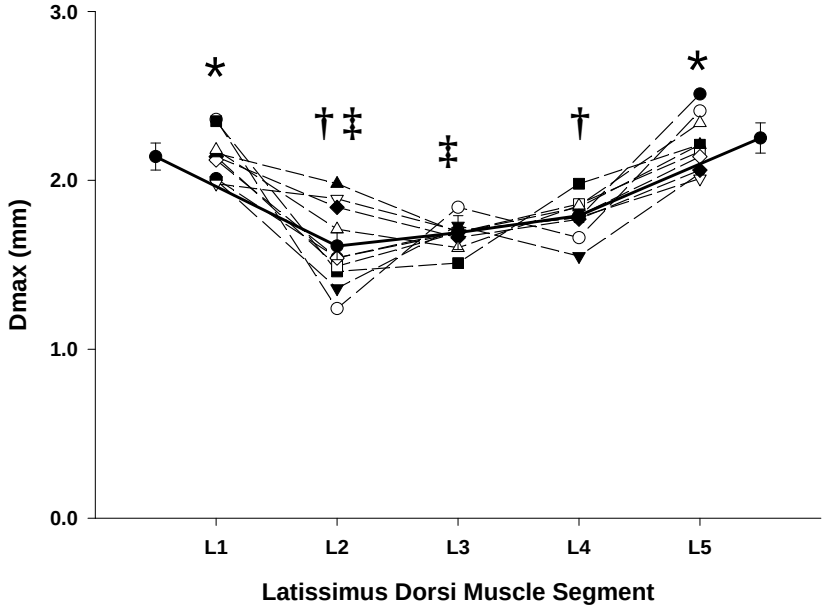

Figure 5.21 The average maximal displacement (Dmax) of each segment of the latissimus dorsi (all subjects). Each symbol represents an individual subject. Solid line indicates group mean ± SEM. Values identified by different symbols **(*, †, ‡)** are significantly different ($p<0.05$, 2-way ANOVA, n = 10).

Longer normalised sustain times (ts*N*) were observed when moving from segments near the periphery of the muscle towards segments at the centre of the muscle (Table 5.3). The superior L1 and inferior L5 segments had significantly shorter ($p<0.05$) ts*N* times than the centrally located L2, L3 and L4 segments (Figure 5.12).

The maximal rate of contraction (+dD/dt) differed ($p<0.05$) between segments (Table 5.3). The central L2, L3 and L4 segments had the slowest ($p<0.05$) maximal rate of contraction with segments L1 and L5 having the fastest (Table 5.3). Segment L3 had the slowest maximal relaxation rate (-dD/dt) with the peripheral L1, L4 and L5 segments relaxing significantly faster ($p<0.05$).

5.5 Discussion

The aim of the work presented here was to characterise the contractile properties of multiple segments within four human muscles, for the purpose of determining how muscle segment function may influence contractile properties.

With reference to the present study, the results confirm that muscle fibres within the segments of the individual muscles investigated were not homogenous with regard to their contractile properties thereby confirming the first hypothesis. Of importance was the finding that there was a directional progressive slowing in muscle fibre contraction times between segments: in a caudocephalad direction for the gluteus maximus and in a peripheral to central direction for each of the three superficial shoulder muscles. Considering that contraction time is believed homogeneous with muscle fibre type (Medler 2002), it is possible to infer that muscle fibres within the superior segment of the gluteus maximus were more predominantly type I slow-twitch than those found within the lower two segments. The whole muscle contraction times previously reported for the soleus muscle [120 ms time to peak (Buller, Dornhorst, Edwards, Kerr and Whelan 1959); 88% type I slow-twitch (Johnson, Polgar *et al.* 1973)] is comparable to the whole segment contraction time of 112 ms recorded for the upper segment of gluteus maximus. The proposition that the superior fibres of the gluteus maximus may have a more predominant type I slow-twitch muscle fibre population suggests a greater postural role for this segment, particularly for the control of hip adduction during locomotion (Basmajian and DeLuca 1985). The anatomical orientation of the muscle fibres of the superior segment, lying superior to the hip joint (Williams, Warwick *et al.* 1995) and therefore with an abductor moment arm, supports this contention. Additionally, Lyons, Perry *et al.* (1983) support this finding by showing that the upper fibres of the gluteus maximus function more like the "abductor" gluteus medius, than the "extensor" lower gluteal fibres, during both level and stair walking.

In contrast, the significantly shorter non-normalised contraction times (tc) obtained for the middle and inferior segments of the gluteus maximus suggested a higher proportion of type II fast-twitch muscle fibres within their muscle bellies. The middle segment of the gluteus

maximus had an average contraction time (tc) of 95.7 ms to peak tension which was comparable to the whole muscle contraction time of the tibialis anterior [81 ms time to peak tension (Marsh, Sale, McComas and Quinlan 1981); 73% type I slow-twitch (Johnson, Polgar *et al.* 1973)]. The inferior segment of the gluteus maximus, which had the fastest contraction time (79.1 ms time to peak tension), was similar to that reported for extensor digitorum brevis [67 ms time to peak tension (McComas and Thomas 1968); 45% type I slow-twitch (Johnson, Polgar *et al.* 1973)]. An increased proportion of type II fast-twitch muscle fibres in the lower two segments of the gluteus maximus would support a greater muscle excursion function for these two segments and support involvement in powerful extension and external rotation of the hip joint. In addition, the anatomical orientation of the muscle fibres of these two segments, positions them at or below the axis of rotation of the hip joint in the coronal plane. A higher proportion of type II fast-twitch motor units would make better use of the mechanical advantage these fibres have in providing a powerful hip extensor, external rotator and adductor force during forceful actions involving the hip joint.

Applying a similar analysis to the superficial shoulder musculature, the pectoralis major segments had average non-normalised contraction times of 74.5 ms that are comparable to the extensor digitorium brevis (45% type I slow-twitch motor units; McComas and Thomas (1968)) while the contraction time (tc) of segments within the latissimus dorsi (80.6ms) are more comparable with the tibialis anterior (73% type I slow-twitch; McComas and Thomas (1968)). Although the inter-segment differences for the shoulder muscles are not as robust as for the gluteus maximus, significantly different ($p<0.05$) contraction times were identified, in particular between the peripherally and centrally located segments. For both the pectoralis major and the latissimus dorsi, the results suggested a higher proportion of type II fast-twitch motor units within the peripheral segments.

In the current study, the contractile properties of only 4 of the 7 previously identified (Wickham and Brown 1998) deltoid segments, were assessed. The results from these 4 segments compare favourably with those of Gorelick and colleagues (2005:2007) with the more centrally located segments exhibiting slower contractile properties against those of

the faster peripheral segments. Compiling the data from the three superficial radiate muscles studied here, it appears that this organisation may be a consistent characteristic of radiate muscles. From a functional perspective, the faster and more powerful segments in the periphery of the muscle allow for the use of force-coupling to produce movements with lines of action directly through the centrally located segments. By combining the slower, less powerful central segments with the faster powerful peripheral segments, maximal force production may be enhanced.

A muscle's architecture (cross sectional area, muscle fibre length, angle of pennation etc.) is well known to have a critical impact upon muscle function (Lieber and Friden 2000) and influence the shape of the MMG waveforms following maximal PNS (Cescon, Farina *et al.* 2004). Whilst it is acknowledged that muscle segments within an individual muscle may differ in their architecture (Wickham and Brown 1998), observations of cadaveric specimens within our laboratory at macroscopic level failed to identify such differences within the pectoralis major or the latissimus dorsi muscle segments. For the deltoid, Wickham and co-workers (1998) identified architectural differences between the middle muscles segments (D3/4 – multi-pennate) and those found peripherally (D1/2 & D5/6/7 – strap). Segments D1/2/6/7 from the Wickham and Brown (1998) study were equivalent to segments D1/2/3/4 from this study. As the current study only assessed, within individual muscles, segments of similar architecture, this factor was not expected to have influenced the results. Based on results from our Laser-MMG technique, it may therefore be postulated that the proportion of type I and type II muscle fibres within the four investigated muscles, varied between their constituent segments. This variation may be related to the functional roles played by the different segments of the muscle, those being either "tonic" or "phasic" about the joint. Thus it appears possible to accept, based on this evidence, the second hypothesis that muscle segment function influences the contractile properties of each segments muscle fibres

Regarding our other results, it was not surprising to note that normalised relaxation time (tr*N*) varied significantly between segments. This parameter is related to the reuptake of calcium by the sarcoplasmic reticulum (Gillis 1985; Verburg, Thorud, Eriksen, Vollestad

and Sejersted 2001) and is characteristic of fibre type (Close 1972; Yoshitake, Shinohara *et al.* 2002). Within the gluteus maximus, the middle segment exhibited the shortest relaxation time (16.32ms/mm), coinciding with the shortest contraction time (9.87ms/mm) of all three segments. A similar pattern was observed within the shoulder musculature and found in the peripheral segments of the muscle, for example the inferior segment (P5) of pectoralis major had a tc*N* approximately 50% and a tr*N* approximately 75% of the central P3 segment.

The trend for the sustain time (ts) to be increased in the centrally located segments in all the investigated muscles, is supportive of the contention that the type I slow-twitch muscle fibre population is decreased in the centrally located segments of the shoulder musculature.

Finally, a significant difference in the absolute magnitude of segmental muscle displacement (Dmax) was observed across the muscles, with the middle segment of the gluteus maximus and the peripheral segments of the shoulder muscles displaying the greatest displacement. The MMG laser used in this study was sensitive to 0.002 mm and was therefore able to accurately detect the lateral distance displaced by the muscle following PNS. These results may reflect variations in the amount of muscle tissue available to be stimulated at each muscle segment.

A gradation of muscle contractile properties was identified across the surface of the multifunctional muscles investigated in Study D & E, hence supporting hypothesis 3. Within the gluteus maximus, the middle muscle segment displayed the fastest contractile properties across all MMG measurement variables (tc*N*, tr*N*, ts*N*, +dD/dt and –dD/dt). The adjacent cranial and caudal muscle segments were significantly slower ($p<0.05$) to contract and relax and had a reduced maximal rate of contraction and relaxation. All three superficial shoulder muscles also exhibited gradation of contractile properties across the surface of the muscle; however the direction was the reverse of that observed within the gluteus maximus. Peripheral muscle segments possessed the fastest contractile properties whilst the centrally located segments were significantly slower ($p<0.05$) to contract and relax.

Overall, our results show that the contractile properties (e.g. Dmax, tc*N*, tr*N*) of muscle fibres varied significantly between the individual segments of multifunctional muscles following maximal percutaneous neuromuscular stimulation. For the investigated muscles, normalised contraction time (tc*N*) differed significantly across the muscle, with 'slow-twitch' contractile properties found in muscle segments that have a greater 'postural' role while 'fast-twitch' contractile properties were associated with segments having a greater role in joint rotation. Together, the results indicated that these muscles were composed of muscle segments that were physiologically and anatomically designed to fulfil specific roles during everyday motor tasks.

Based on our results, it appears that the Laser-MMG waveform has the ability to quantify differences in muscle fibre type, in discrete segments of human skeletal muscle. As such, Laser-MMG waveform analysis may find utility in laboratories where non-invasive estimations of muscle fibre type are routinely required. These results also suggest caution in using biopsy samples taken from only one site to estimate the entire muscle belly fibre type populations since muscle fibre type varies both across and within the muscle itself. Finally, our results show that the Laser-MMG technique has the ability to characterise the contractile properties of small sub-volumes of muscle tissue within single muscles and allow comparisons of muscle segment performance during activation involving multi-planar joints.

Chapter 6

The influence of fiber-type on the neuromotor control of human shoulder muscle segments

6.1 Introduction

Previous work has established that the contractile properties of whole muscle are influenced by the muscle's fibre type composition (Bottinelli and Reggiani 2000; Brooke and Kaiser 1970; Simoneau and Bouchard 1989). Additionally, work presented within the present thesis has determined that muscle fibre type influences the contractile properties of individual muscle segments within the superficial muscles of the shoulder and the gluteus maximus. As seen in Chapter 5, muscle segment contractile properties are not homogenous and appear to reflect the neuromotor function that each segment performs in the production of joint movement. Given that muscle segment contractile properties vary between individual muscle segments, it would appear obvious that the CNS would need to account for these differences when planning, coordinating and executing movements requiring the activation of multiple muscle segments within individual skeletal muscles. This requirement would be particularly important when coordinating movements about a joint, such as the shoulder, which is enveloped by numerous multifunctional muscles that possess clearly established muscle segments (Wickham and Brown 1998) of variable fibre type (Chapter 5, Study E). However, to this date, there is a paucity of information available regarding how the CNS copes with non-homogenous muscle segment fibre type compositions when coordinating human skilled movement.

The objective of the work in this final experimental chapter was to determine, utilising an electromyographic (EMG) technique, whether muscle segment fibre type composition influenced how the CNS coordinated individual muscle segments during movements of the shoulder joint. To achieve this outcome, muscle segment activity was assessed at different speeds of shoulder joint movement; from very slow (1500 ms time to peak) to fast (<400 ms time to peak). This assessment was designed to determine whether increasing movement speed influenced the patterns of muscle segment activity and whether such changes were associated with fibre type composition.

It was first necessary to establish what might be considered to be 'normal' patterns of muscle segment coordination at the movement speeds investigated here. It has been clearly established that the 'pattern' of agonist and antagonist muscle activation changes as

movement speed increases from slow to ballistic . From a typically 'agonist' only pattern of muscle activation (antagonist inactive) at movement times longer than 1000 ms, a highly coordinated pattern of agonist and antagonist muscle activation gradually appears until a 'triphasic' (agonist-antagonist-agonist) electromyographic pattern is fully developed as movement times decrease below 400 ms . The more intensive biomechanical demands of ballistic movements imposes greater demands on the CNS to closely coordinate agonist and antagonist muscle activation and to recruit muscles to act as stabilisers and/or synergists to facilitate movement outcomes (Barrata 1995). Both the intensity and timing of agonist and antagonist muscle activation is influenced by movement time. For example, Angle (1977) has shown that ballistic movements produce shorter but more intensive activations of agonist muscles compared to movements performed slowly. Since single whole muscles are composed of individual muscle segments, it is most probable that these findings are applicable to individual muscle segments as well.

Given that movement speed influences neuromotor coordination of whole muscles and muscle segments, it is also necessary to consider how the CNS coordinates muscle segments with different moment arms (e.g. functions) across the joint. It is already clearly established that whole muscles are exquisitely coordinated to produce skilled movements (Scheving and Pauly 1959; Shevlin, Lehmann *et al.* 1969). In addition, many studies have now identified distinctive roles for individual segments of whole skeletal muscle, which suggests that the CNS can selectively activate segments of single skeletal muscles to produce the desired movement outcome (Brown, Solomon *et al.* 1993; Paton and Brown 1994, 1995; Riek and Bawa 1992; Ter Harr Romeny, Denier Van Der Gon *et al.* 1982; Wickham and Brown 1998). From more recent research, it has become apparent that individual muscle segments may be functionally classified according to their role in a particular movement (Wickham, Brown *et al.* 2004). Utilising functional classifications previously applied to whole skeletal muscles, Wickham and Brown (1998) have been able to classify individual muscle segments as 'prime movers', 'synergists' or 'antagonists'. Importantly, these authors have shown that a muscle segment's function determines its timing and intensity of activation. Simply stated, prime mover segments are activated first, have the longest periods of activity and the highest intensities of activation. In contrast,

synergist muscles segments have later and less intensive activations while antagonist muscle segment activation is late and variable. With regard to this study, these findings suggest that the prime mover, synergist and antagonist muscle segments will have defined periods of activation based upon their functional roles. However, how changes in muscle segment fibre type concentrations influence these patterns is unknown.

Clearly, both movement speed and muscle segment function (e.g. moment arm) have an influence on how the CNS coordinates muscle during the production of skilled movement. The objective now is to determine how these basic patterns of muscle segment coordination, as determined by the speed of movement and the function of each muscle segment, are influenced by the presence of muscle segments with varying contractile capabilities. This analysis will be valuable and instructive at the fastest possible speeds of movement (ballistic), when variations in muscle segment contractile properties would be most critical to the coordination role played by the CNS.

6.2 Aims and Hypotheses

The aim of the experiment reported here was to determine the influence of muscle segment contractile properties on neuromotor control of muscle segments in three superficial shoulder muscles.

It was hypothesised that:

1. The patterns of muscle segment activation would vary between slow and fast speeds of movement,
2. Muscle segments at all speed of movement will demonstrate activation properties consistent with their function and
3. The in-homogenous distribution of muscle segment contractile properties, across the 14 muscle segments investigated here, would result in compensatory changes in neuromotor control, particularly at the fastest (e.g. ballistic) speeds of movement.

6.3 Methods – Study F

6.3.1 Experimental design

This experiment was designed to characterise the electromyographic activity of 14 muscle segments, in three superficial shoulder muscles, during the production of an isometric shoulder adduction impulse. The impulse was performed over five different movement times (MT) (1500 ms; 1000 ms; 700 ms; 500 ms and 300 ms time to peak force). The neuromotor control (e.g. timing, intensity) of each muscle segment was characterised with a surface electromyographic technique while the isometric force impulses produced across the shoulder were recorded with a force transducer.

6.3.2 Subjects

Twelve healthy males (mean age 24.3 ± 3.7 yrs, height 177.7 ± 6.3 cm, weight 73.8 ± 6.0 kg) volunteered to participate in this experiment. The subjects had no history of neurological disorders or musculoskeletal injuries related to the shoulder complex and were all right hand dominant. All subjects had low body fat skin fold measurements (avg. 94.5mm ± 18.5mm (sum of nine sites)).

6.3.3 Muscle segment identification

Muscle segments were identified by normalising to cadaveric measures, as described in Chapter 5, Section 5.4.1.3

6.3.4 Equipment

6.3.4.1 Force transducer and amplifier

A 100 kg transducer (sensitivity: ±2mV/V at 100 kg load) quantified the force exerted by each subject. The transducer amplifier was designed and manufactured by the technical workshop of the Department of Biomedical Science (University of Wollongong) and contained a zero function to compensate for the individual weight of each subject's arm. The force transducer was calibrated according to the procedures outlined in the Chapter 2. The output from the force transducer was displayed to the subject through a force/time

software program and collected for later analysis utilising the Waveform Analysis Software Program (WASP).

6.3.4.2 Arm cast

An arm cast was produced by cutting a PVC pipe longitudinally in half. A coupling apparatus was bolted to each side of the arm cast and padding placed on the inside for the comfort of the subject (Figure 6.1). The arm cast prevented movement at the elbow joint and provided a solid and close-fitting base upon which the subject could apply force. Anchor ropes supported the arm cast to provide stabilisation during the rest periods and to eliminate movement in undesired directions.

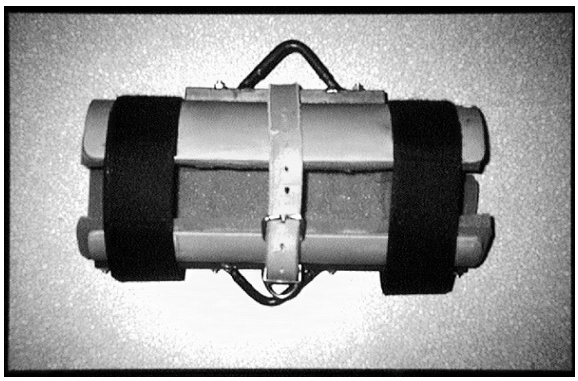

Figure 6.1 PVC arm cast with Velcro restraints and force transducer attachments.

6.3.4.3 Force/time program

Subjects viewed a computer screen that displayed a criterion force trace bordered by a ± 10% force criterion band (Figure 6.2). As the subject applied force through the arm cast to the transducer, the subject's real-time force trace scrolled across the screen. The subject controlled the level and rate of force development in order to remain within the criterion band. The program provided the subject with an indication of the desired movement time by altering the horizontal scroll speed of the trace (e.g. it took 600 ms for the trace to move from the start point (left of the screen) to the end point (right of screen) in the 300 ms to peak force movement time condition). The program received input from the force transducer amplifier, fed through a PC 30 (A-D) card (National Instruments).

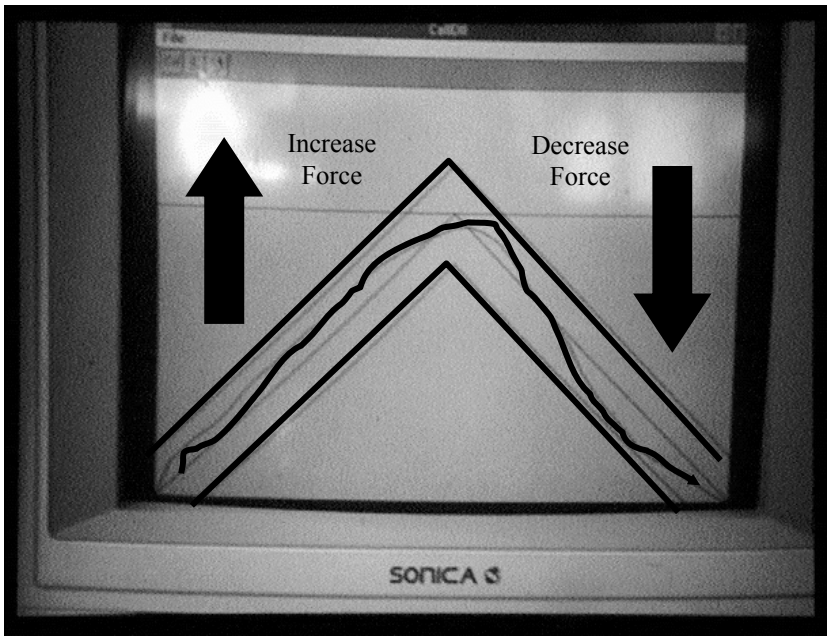

Figure 6.2 The force/time program displaying an accurate subject trial (wavy black line) bordered by the ± 10% force criterion bands and (in the centre) the ideal force line.

6.3.5 Experimental set-up

All experiments were carried out within the musculoskeletal laboratory at the University of Wollongong at a constant room temperature of 23ºC. Myoelectric electrode sites were identified as per the MMG recording sites (Chapter 5, Study E) and prepared for electromyographic recordings through alcohol bathing and abrasion with light grade sandpaper. Bipolar surface microelectrodes were attached to each of the electrode sites (Figure 6.3) and the subject seated in a straight backed upright chair. The shoulder joint was abducted to 90 degrees, as determined by goniometry, with the elbow fully extended within the supportive arm cast. The force transducer and arm cast were attached to the roof of the wire cage that surrounded the subject (Figure 6.4).

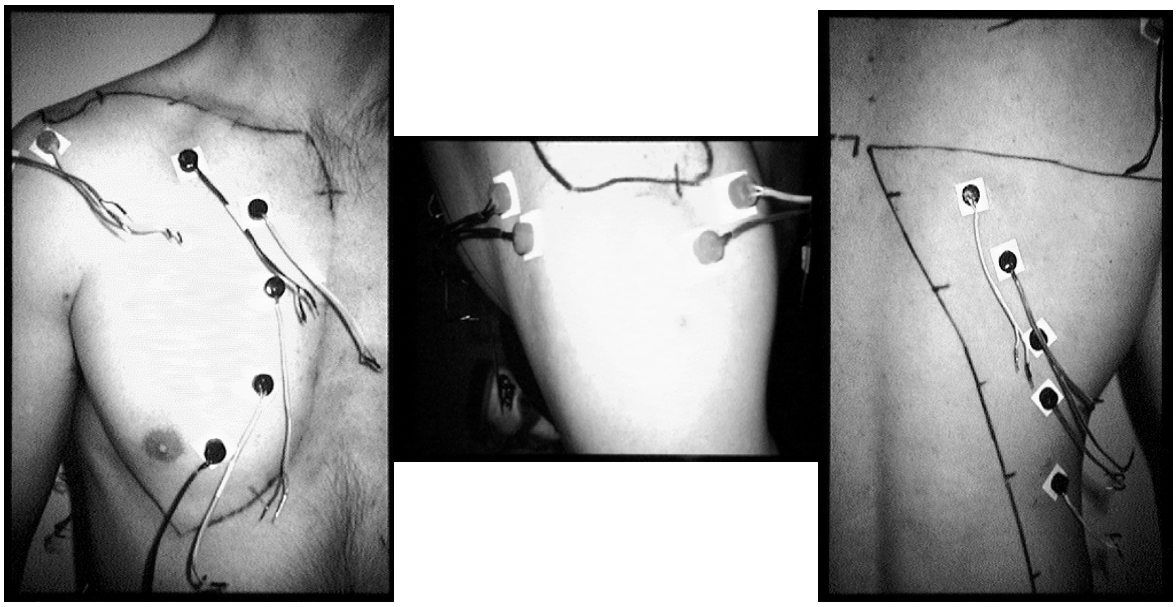

Figure 6.3 View of the pectoralis major, deltoid and latissimus dorsi muscles showing the electromyographic microelectrodes attached to a subject

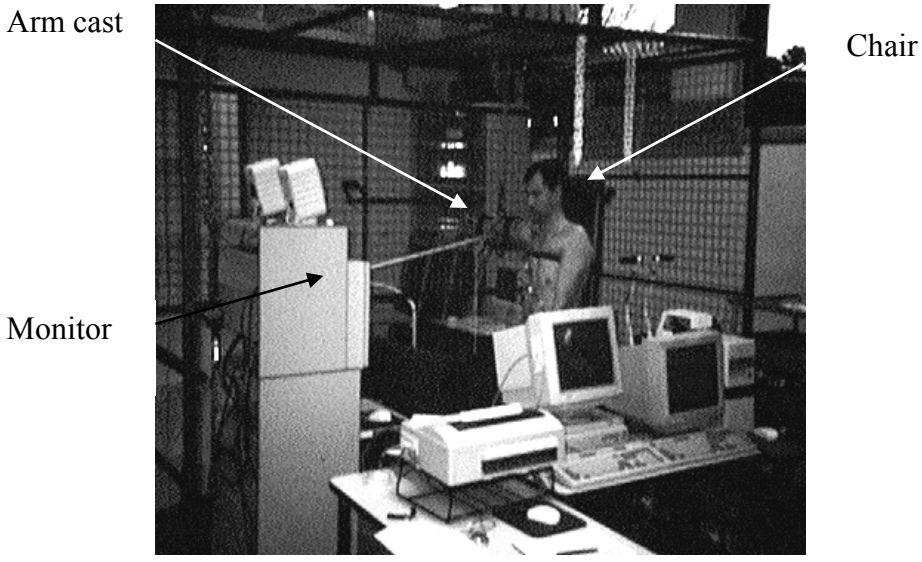

Figure 6.4 Experimental set-up showing the subject seated in the chair, arm cast and force/time monitor within the surrounding cage. The data collection computers are facing the camera.

6.3.6 Measurement of electromyographic activity and isometric force development

The subjects were given a series of 20 practise trials to allow them to familiarise themselves with the isometric shoulder adduction task and to determine appropriate electromyographic and force amplifier levels. Three static adduction maximal voluntary contractions (MVC) were then performed to determine each subject's 50% MVC level. An inter-trial interval of 60 seconds was enforced to prevent fatigue. Subjects were allowed a further 10 minute rest period prior to commencing the experimental trials.

The isometric shoulder adduction task consisted of a progressive development of force up to the 50% MVC level; the force was then decreased back to 0% MVC over an equivalent time period. The total movement times (TMT) investigated were 3000 ms, 2000 ms, 1400 ms, 1000 ms and 600 ms. The TMT equated to movement times (MT) to peak force of 1500 ms, 1000 ms, 700 ms, 500 ms, and 300 ms.

The force/time software program was triggered to start when a 2.5% threshold of maximal isometric force was exceeded and ended at the designated MT. The force/time software program displayed the subject's resultant force trace which was required to be within the prescribed ± 10% error bands for the trial to be accepted for analysis. For each subject a total of 10 accurate trials were recorded at each of the five MTs.

Electromyographic waveforms from the 14 muscle segments were recorded by differential HUMTEC pre-amplifiers and amplifiers. Electromyographic and force data was collected for 4000 ms at each trial, ensuring the collection of both pre- and post-task electromyographic activity (if present). Fast Fourier Transforms were performed on electromyographic waveforms recorded from the first and last trial from each subject. The transforms were compared to identify the presence of muscular fatigue as a result of the experimental task. No significant effects of fatigue were found within any subject ($p<0.05$).

6.3.7 Electromyographic signal analysis

Refer to Chapter 3, Section 3.4.3

6.3.8 Statistics

The mean and standard error of the mean (SEM) were calculated for the electromyographic and force variables characterising each of the 14 muscle segments at each MT. All statistics were performed using SigmaStat (SPSS Inc. USA) and Statistix 8.0 for Windows (Analytical Software. Tallahassee, FL). Data was subjected to normality and equal variance tests to confirm the normal distribution and equal spread of the data (all passed). All data presented as mean ± SEM unless otherwise stated.

The statistical significance of differences between values obtained from each muscle segment at each speed of movement was evaluated by Multivariate Analysis of Variance (MANOVA) ($p<0.05$) for subject (12 levels), muscle segment (14 levels - each segment investigated) and MT (5 levels, 1500 ms, 1000 ms, 700 ms, 500 ms, and 300 ms time to peak force). Significance of inter-condition differences of values obtained from each muscle segment and each speed of movement was evaluated by a post-hoc Bonferroni comparison ($p<0.05$). Pearson Product Moment Correlations were performed to determine the relationship between anterior and posterior segments with similar anatomical locations. Friedman Repeated Measures Analysis of Variance on Ranks was performed to determine the effect of varying movement speed on the order of segment activation. All statistics were performed on group mean data ($n = 12$).

6.4 Results

6.4.1 General muscle description and summary of results

Measurements obtained from the electromyographic activity of each muscle segment were subjected to a statistical analysis to determine significant differences ($p<0.05$) between with 14 levels of muscle segment and five levels of movement time ranging from slow to fast speeds (1500 ms, 1000 ms, 700 ms, 500 ms, and 300 ms MT to peak force). No significant effect ($p<0.05$) for subject was found, indicating a homogeneous subject sample. Statistically significant differences ($p<0.05$) were identified between muscle segments and MT (Table 6.1). For clarity of presentation, only the slow (1500 ms MT), medium (700 ms MT) and fast (300 ms MT) movements are presented in detail.

6.4.2 Effect of speed of movement (slow/medium/fast) on muscle segment activation

The influence of muscle segment fibre type on the neuromotor control of the 14 segments investigated was determined by varying the movement time from 1500 ms (slow) to 700 ms (medium) and then to 300 ms (fast). In general, varying the speed of movement significantly affected ($p<0.05$) the muscle segment activation properties of onset (On*N*) and duration (Dur*N*%), with the largest affect occurring between the ballistic (300 ms MT) and slower speeds (700 ms and 1500 ms MT).

*6.4.2.1 Muscle segment Onset (*On*N)*

In general, when the speed of movement was increased from slow (1500 ms MT) to medium (700 ms MT) and then to fast (300 ms MT), normalised onset times (On*N*) for all muscle segments occurred significantly closer ($p<0.05$) to force onset (FcOn) (1500MT avg. 180.2 ± 15.1 ms; 700MT avg. 145.9 ± 30.8 ms; 300 ms MT avg. 59.4 ± 15.0 ms). Moving in a caudocephalad direction, adjacent muscles segments exhibited significantly later ($p<0.05$) On*N* at successively slower speeds of movement (Table 6.1).

Table 6.1 Muscle segment mean values for each EMG variable at the slow (1500 ms), medium (700 ms) and fast (300 ms) MT. Values within columns that differ by greater than the t-value are significantly different ($p<0.05$) (MANOVA, n = 12) (between segment analysis). Values within rows that share a common symbol **(*, †, ‡)** are not significantly different ($p<0.05$) (MANOVA, n = 12) (between MT analysis). Deltoid segment rows are shaded in grey to aid differentiation between muscles.

			On*N* (ms)				Pk*N* (ms)			
		Segment	**1500ms**	**700ms**	**300ms**	**MT Significance**	**1500ms**	**700ms**	**300ms**	**MT Significance**
Anterior Segments	**Pectoralis Major**	**PEC 5**	-30.50 (7.31)	-37.57 (6.71)	-37.48 (3.39)	*Ns*	-159.87* (8.62)	-110.18 (8.25)	-108.64 (7.08)	*yes*
		PEC 4	94.16 (10.88)	82.08 (6.96)	79.52 (7.40)	*Ns*	-126.99 (10.76)	-115.60 (8.32)	-116.39 (11.54)	*ns*
		PEC 3	193.48* (10.34)	144.65† (2.75)	46.41‡ (8.55)	*Yes*	-142.74 (7.97)	-130.31 (11.29)	-132.72 (10.70)	*ns*
		PEC 2	221.61* (12.91)	158.53† (7.95)	44.26‡ (7.93)	*Yes*	-107.58 (10.90)	-101.82 (7.97)	-99.01 (7.05)	*ns*
		PEC 1	163.99* (11.03)	134.20† (6.08)	60.47‡ (7.59)	*Yes*	-144.54* (7.17)	-106.46 (7.71)	-95.02 (6.34)	*yes*
	Deltoid	**DELT 1**	171.45* (13.90)	296.46† (12.15)	24.38‡ (9.97)	*Yes*	37.85 (7.09)	40.26 (8.65)	-78.27* (10.17)	*yes*
		DELT 2	312.12 (10.98)	316.70 (9.80)	128.99* (13.05)	*Yes*	38.37 (8.09)	8.68 (9.87)	25.97 (9.67)	*ns*
Posterior Segments		**DELT 3**	373.75* (10.54)	284.52† (6.92)	139.83‡ (10.52)	*Yes*	43.56 (6.40)	16.57 (6.73)	-47.01* (11.79)	*yes*
		DELT 4	444.29* (12.22)	207.58† (10.09)	109.73‡ (12.05)	*Yes*	-24.44 (6.06)	-16.92 (8.60)	-66.42* (10.07)	*yes*
	Latissimus Dorsi	**LAT 1**	308.73* (5.34)	249.44† (6.37)	111.19‡ (9.10)	*Yes*	-5.45* (8.01)	-48.48 (6.92)	-57.25 (10.38)	*yes*
		LAT 2	179.28* (8.09)	117.35† (7.84)	90.50‡ (6.79)	*Yes*	-116.70 (10.79)	-85.07 (7.37)	-94.85 (10.14)	*ns*
		LAT 3	98.80 (6.55)	89.68 (7.93)	60.33* (6.50)	*Yes*	-99.77 (7.23)	-118.12 (8.61)	-59.58* (7.62)	*yes*
		LAT 4	34.26*† (3.52)	35.30† (6.21)	13.97* (7.28)	*Yes*	-176.84 (8.35)	-161.66 (8.26)	-91.45* (6.81)	*yes*
		LAT 5	-42.08 (7.66)	-36.55 (6.97)	-41.13 (6.45)	*Ns*	-162.34 (6.67)	-175.15 (6.10)	-81.33* (6.96)	*yes*
		t-value	79.40	63.32	30.90		44.93	37.22	21.24	

			Dur*N*% (%)				iEMG*N*% (%)			
		Segment	**1500ms**	**700ms**	**300ms**	**Significance**	**1500ms**	**700ms**	**300ms**	**Significance**
Anterior Segments	**Pectoralis Major**	**PEC 5**	99.50* (1.36)	120.17† (7.58)	143.80‡ (6.28)	*Yes*	90.92 (7.90)	99.05 (7.74)	81.60 (13.59)	*ns*
		PEC 4	95.08 (1.59)	109.30 (5.74)	132.17* (7.27)	*Yes*	65.52 (6.51)	65.49 (8.58)	59.63 (14.12)	*ns*
		PEC 3	91.24 (1.50)	101.09 (5.80)	107.04 (5.78)	*Ns*	40.36 (8.46)	41.62 (13.90)	28.72 (6.68)	*ns*
		PEC 2	91.33† (2.28)	106.17* (5.13)	101.02*† (4.20)	*Yes*	48.71 (5.45)	36.39 (12.88)	32.41 (11.61)	*ns*
		PEC 1	95.62* (2.97)	114.94 (5.73)	117.68 (6.77)	*Yes*	42.74 (8.51)	34.95 (16.22)	33.87 (15.97)	*ns*
	Deltoid	**DELT 1**	93.65 (2.45)	107.68 (5.64)	108.70 (7.35)	*Ns*	90.19 (11.56)	80.60 (11.21)	83.43 (16.40)	*ns*
		DELT 2	85.15 (3.74)	93.02 (3.60)	108.20* (4.56)	*Yes*	47.03 (13.22)	40.74 (9.66)	40.42 (10.40)	*ns*
Posterior Segments		**DELT 3**	88.68 (3.40)	106.20 (6.26)	177.89* (6.71)	*Yes*	68.80 (12.51)	75.05 (11.34)	67.61 (13.82)	*ns*
		DELT 4	87.43* (3.23)	109.64 (7.54)	128.89 (6.64)	*Yes*	62.72*† (6.19)	82.00* (16.04)	37.48† (10.27)	*yes*
	Latissimus Dorsi	**LAT 1**	89.28 (2.88)	95.07 (6.06)	107.94 (6.39)	*Ns*	83.05 (8.86)	53.36 (8.58)	62.48 (12.94)	*ns*
		LAT 2	92.27* (2.60)	102.42*† (5.58)	114.48† (6.27)	*Yes*	36.82 (9.18)	31.52 (6.61)	31.54 (4.78)	*ns*
		LAT 3	97.66 (1.95)	109.08 (6.41)	111.21 (7.43)	*Ns*	30.27 (4.64)	36.83 (6.51)	31.96 (13.47)	*ns*
		LAT 4	99.47* (1.91)	111.81*† (6.07)	122.22† (5.64)	*Yes*	42.80 (5.92)	52.83 (7.55)	42.52 (6.10)	*ns*
		LAT 5	102.85* (1.82)	119.74*† (6.56)	138.26† (7.76)	*Yes*	52.37 (11.49)	61.46 (15.30)	60.56 (13.93)	*ns*
		t-value	3.63	4.94	11.43		11.17	11.87	10.76	

Notably, no significant variation ($p<0.05$) existed in the On*N* times at each speed of movement for the caudal segments of the pectoralis major (P5/4) and latissimus dorsi (L5) and irrespective of the speed of movement, muscle segments P5 and L5 were the only segments to have onsets (On*N*) before the force onset (Figure 6.5).

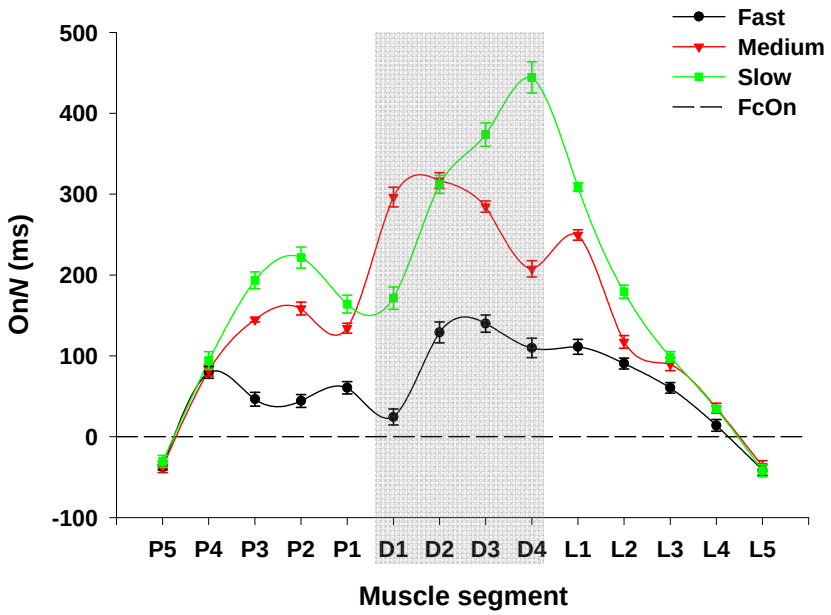

Figure 6.5 Muscle segment normalised electromyograhic onset (On*N*) at all MT. Movement times are indicated by different symbols and different coloured lines. ± SEM values are indicated only when the value exceeds the size of the symbol. Horizontal dashed line represents FcOn. Deltoid segments are shaded in grey to aid differentiation between muscles. Note the disordering of onset for muscle segments P3/2/1 during the fast movement speed.

When the order of muscle segment onset (On*N*) was compared across the different movement times (rank analysis), no significant differences ($p<0.05$) were identified. The overall order that muscle segments were activated, in relation to one another, did not change as a result of varying the speed of movement (Figure 6.5).

In order to further determine the potential change in a muscle segment's activation due to variations in the speed of movement, each muscle segments On*N* time was expressed as a percentage of the MT e.g. a -30.0 ms On*N* value would equate to -10.0% On*N*%MT for the 300 ms MT, -4.3% On*N*%MT for the 700 ms MT and -2.0% On*N*%MT for the 1500 ms MT.

Generally, when movement occurred at the fast and medium speeds, muscle segments exhibited a greater distribution of On*N*%MT measures (-13.7% to 46.6% Fast MT; -5.4% to 45.2% Medium MT) (Figure 6.6). Conversely, during the slow speed movement, muscle segment On*N*%MT values were compressed, occurring within a lesser range (-2.8% to 29.6%).

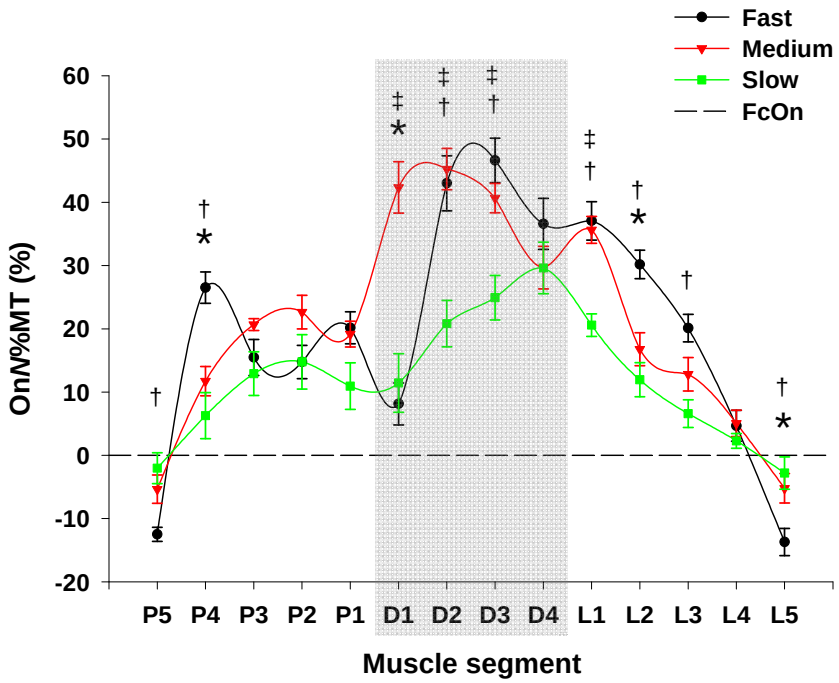

Figure 6.6 Muscle segment normalised electromyographic onset expressed as a percentage of movement time (OnN%MT) at all MT**.** Movement Times are indicated by different symbols and different coloured lines. * indicates significant difference ($p<0.05$) between fast and medium MT, † indicates significant difference ($p<0.05$) between fast and slow MT and ‡ indicates significant differences ($p<0.05$) between medium and slow MT (MANOVA, n=12). ± SEM values are indicated only when the value exceeds the size of the symbol. Horizontal dashed line indicates FcOn. Deltoid segments are shaded in grey to aid differentiation between muscles.

Muscle segments within the pectoralis major and latissimus dorsi, with the exclusion of P3/P2/P1/L4, displayed significant differences ($p<0.05$) between the fast and slow speeds of movement. Muscle segments D1/D2/D3 of the deltoid exhibited significant differences ($p<0.05$) between the fast and slow MT and also the medium and slow MT. For muscle segments P5 and L5, the prime mover segments, On*N*%MT occurred at a significantly ($p<0.05$) greater time period before force onset during the fast movement than during the slow movement. The On*N*%MT of muscle segment P4 is of particular note as there was a complete reversal of the activation order during the three movement speeds. It was

activated shortly after force onset during the slow speed and became activated sequentially later as the movements became faster. This is in direct contrast to segment P5 which was activated first during the fast movement and became activated sequentially later as the movement speed slowed.

*6.4.2.2 Muscle segment peak (*Pk*N)*

Muscle segment peaks (Pk*N*) within each muscle were affected differently by varying the speed of movement (Table 6.1 and Figure 6.7). Within the pectoralis major, only the peripheral P5 and P1 muscle segments exhibited Pk*N* times that were significantly ($p<0.05$) affected by varying the speed of movement. The Pk*N* in these muscle segments occurred prior to FcPk and significantly earlier ($p<0.05$) during the slow, as opposed to the medium and fast speed of movement. No effect of speed of movement was evident in the central P4/P3/P2 muscle segments of the pectoralis. In contrast, muscle segments D1, D3 and D4, within the deltoid, peaked significantly earlier ($p<0.05$) during the fast speed of movement than at the medium and slow speeds. The Pk*N* of muscle segment D2 was not affected by varying the speed of movement. Within the latissimus dorsi, Pk*N* at the fast speed of movement for muscle segments L5, L4 and L3 occurred significantly later ($p<0.05$) and thus closer to FcPk than during the medium and fast speeds of movement. Varying the speed of movement also affected the overall pattern of muscle segment Pk*N* within the latissimus dorsi. All muscle segments peaked (Pk*N*) at approximately the same time during the fast speed of movement; at the slower speeds the inferior segment L5 was the first to peak followed sequentially by segments L4 to L1.

*6.4.2.3 Muscle segment duration (*Dur*N*%*)*

Longer muscle segment electromyographic durations were associated with longer movement times (Figure 6.8). Paradoxically, larger muscle segment Dur*N*% measures were associated with shorter movement times (300 ms MT avg. 122.8 ± 5.5%; 700 ms MT avg. 107.6 ± 8.0%; 1500 ms MT avg. 93.5 ± 5.1%). Caudal muscle segments P5, L5, L4 were affected by varying the speed of movement with significant increases ($p<0.05$) in Dur*N*% measures associated increases in movement time. All muscle segments except the

caudal P5 and L5 segment were active for less than the movement time during the slow speed of movement.

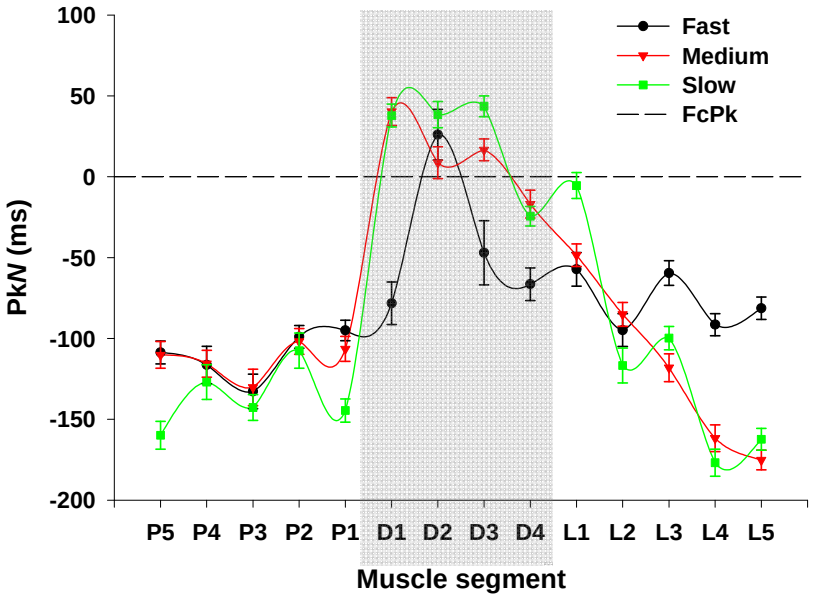

Figure 6.7 Muscle segment normalised electromyographic peak (Pk*N*) at all MT. Movement Times are indicated by different symbols and different coloured lines. ± SEM values are indicated only when the value exceeds the size of the symbol. Horizontal dashed line represents FcPk. Deltoid segments are shaded in grey to aid differentiation between muscles.

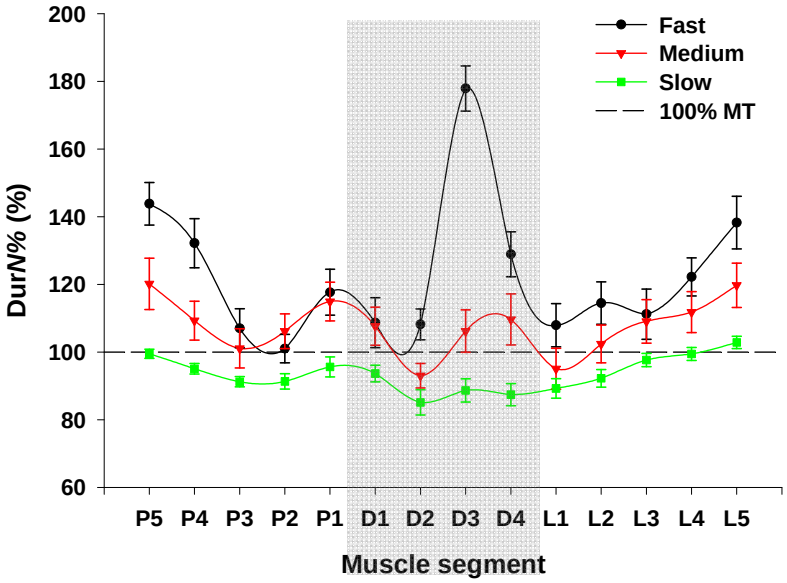

Figure 6.8 Muscle segment normalised electromyographic duration (Dur*N*%) at all MT. Movement Times are indicated by different symbols and different coloured lines. ± SEM values are indicated only when the value exceeds the size of the symbol. Horizontal dashed line represents the movement time. Deltoid segments are shaded in grey to aid differentiation between muscles.

*6.4.2.4 Muscle segment electromyographic intensity (*iEMG*N*%*)*

Muscle segment normalised electromyographic intensity (iEMG*N*%) measures were not significantly affected ($p<0.05$) by varying the movement speed. On average, muscle segments produced 54.5 ± 5.7% of their MVC levels, irrespective of movement speed (Table 6.1). Although non-significant, a trend was observed where the caudal segments of the pectoralis major and latissimus dorsi produced higher levels of electromyographic intensity, with successively cranial muscle segments producing subsequently less intensity (Figure 6.9 and 6.10). Within the agonist muscle segments, P5 produced the highest electromyographic intensity at each movement speed.

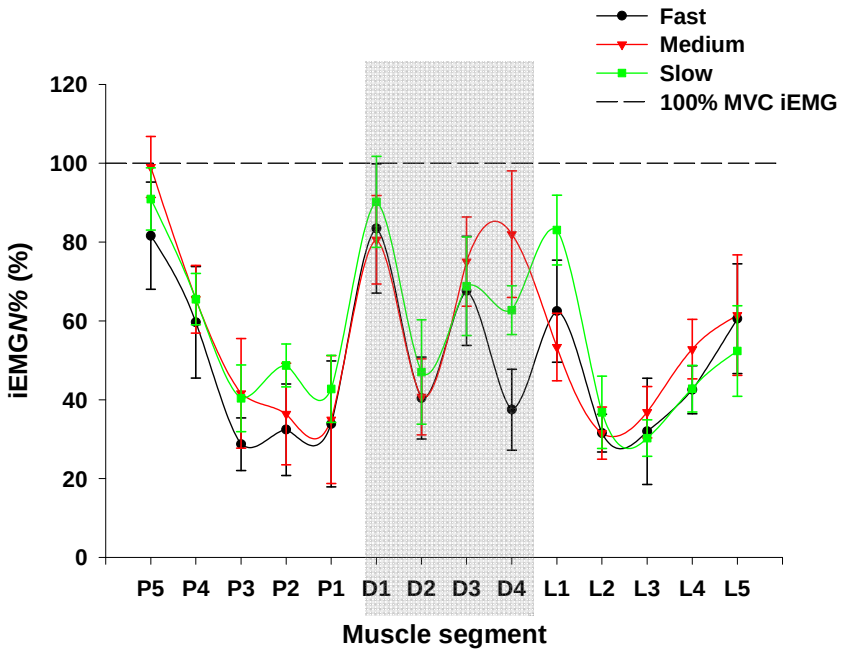

Figure 6.9 Muscle segment normalised intergrated EMG (iEMG*N*%) at all MT. Movement Times are indicated by different symbols and different coloured lines. ± SEM values are indicated only when the value exceeds the size of the symbol. Horizontal dashed line represents iEMG value at 100% MVC. Deltoid segments are shaded in grey to aid differentiation between muscles.

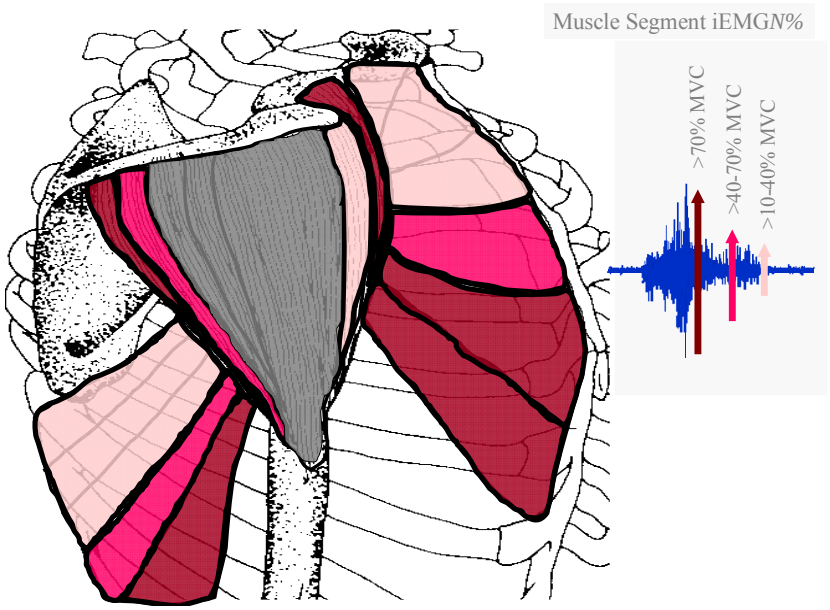

Figure 6.10 Normalised intergrated EMG (iEMG*N*%) of muscle segments averaged across all speeds of movement. Muscle segments are categorised by level of iEMG*N*% and identified by different colours (see figure key). Deltoid muscle segments shaded in grey were not examined. Maximum voluntary contraction (MVC).

6.4.3 Variation in activation properties between individual muscles

The electromyographic activity of the pectoralis major and latissimus dorsi were found to be statistically similar ($p<0.05$) with a similar pattern of onset (On*N*), peak (Pk*N*), duration (Dur*N*%) and intensity (iEMG*N*%) measures. In addition, later onsets (On) and earlier offsets (Off) in successively cranial segments were identified for both muscles (example: Figure 6.11 700 ms MT). In distinct contrast, the segments of the deltoid were activated (On*N*) at a significantly later ($p<0.05$) percentage of TMT, reached peak electromyographic activity significantly later ($p<0.05$) during the movement, at about the time of the peak of the isometric force impulse (FcPk), and displayed significantly greater ($p<0.05$) levels of intensity (iEMG*N*%) (Table 6.1).

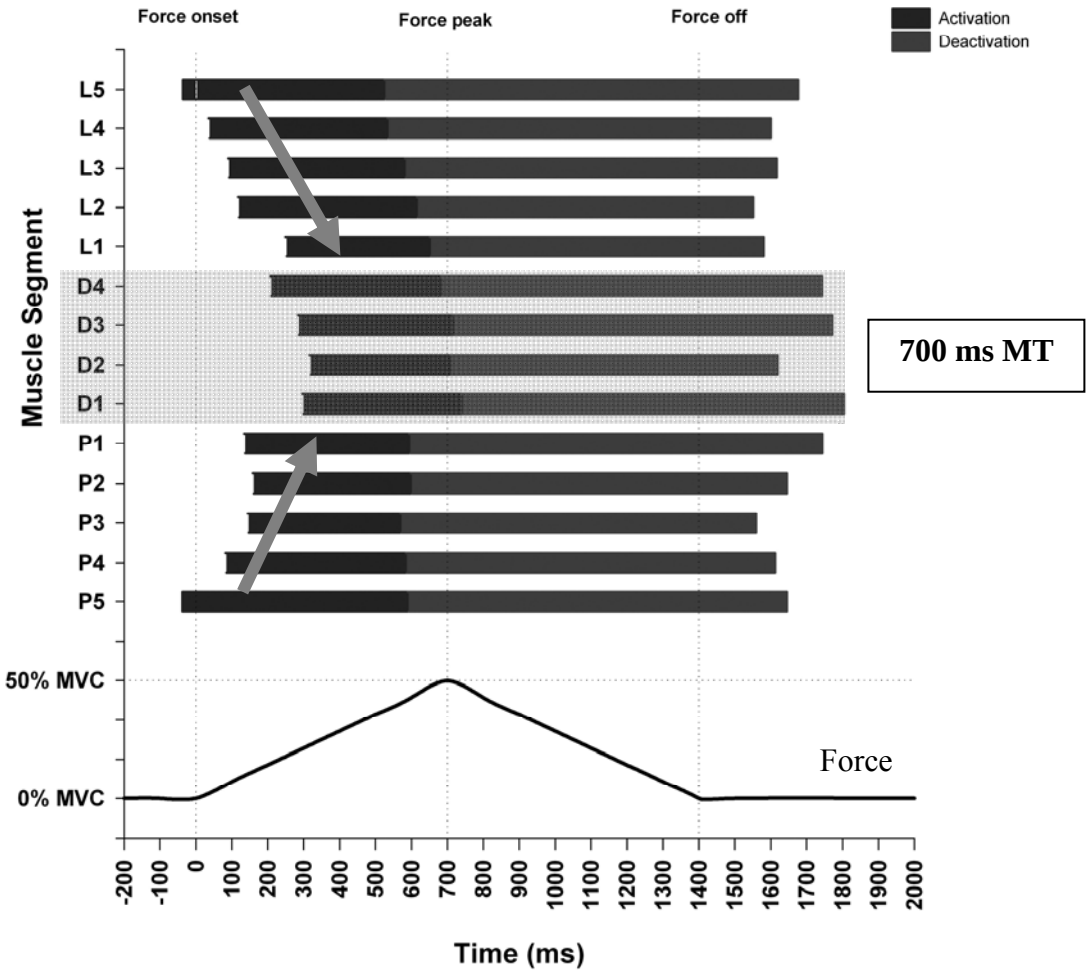

Figure 6.11 Muscle segment electromyographic onset (On), peak (Pk), duration (Dur) and offset (Off) for the 700ms MT (medium speed of movement). Darker shading on the left hand side of the horizontal bars indicates segment activation; lighter shading on the right indicates segment deactivation. Transition point between dark and light shading indicates electromyographic peak. Deltoid segments are shaded in grey to aid differentiation between muscles.

6.4.4 Variation in activation properties within individual muscles

6.4.4.1 Pectoralis Major (P1, P2, P3, P4, P5)

Across the pectoralis major, later onsets (On) and earlier offsets (Off) were identified in successively cranial segments. In the raw data, the inferior segment of the muscle was observed to activate prior to FcOn. The remaining segments within the muscle were activated post FcOn (Table 6.1 and Figure 6.5, 6.12). Unlike the latissimus dorsi, the significant differences ($p<0.05$) between muscle segments for On*N* ceased to exist above

the central segments (P3, P2, P1). Overall, muscle segment On*N* for the anterior (P1, P2, P3, P4, P5, D1 & D2) and posterior segments (L5, L4, L3, L2, L1, D4 & D3) was highly correlated ($r^2 = 0.85$) ($p<0.05$), indicating a wave of activation up the muscles.

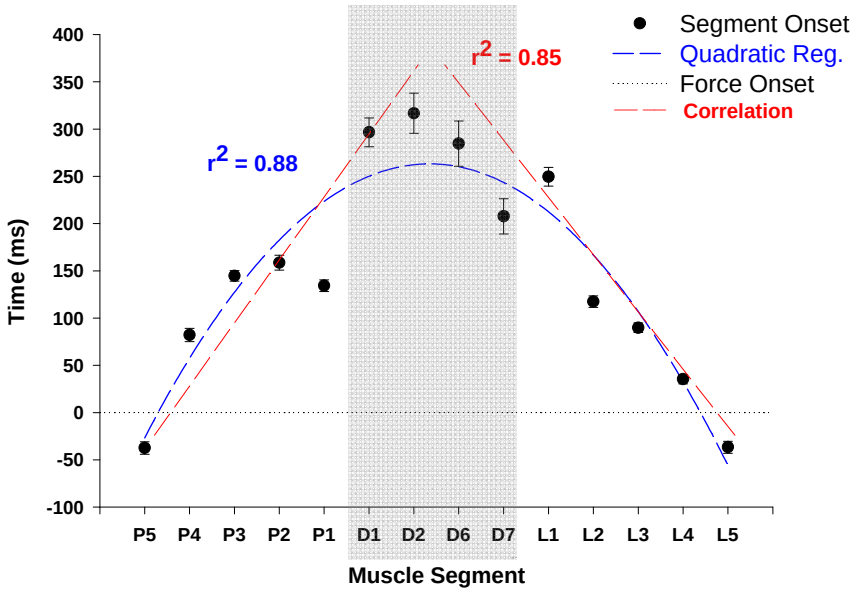

Figure 6.12 Electromyographic onset (On*N*) time for all muscle segments during the 700ms MT condition (medium speed of movement). r^2, the coefficient of determination, is shown for the fitted regression line. Force Onset = 0 ms. Deltoid segments are shaded in grey to aid differentiation between muscles. Note the wave of activation occurring, moving from the prime mover segments of the pectoralis major and latissimus dorsi to the segments of the deltoid.

All muscle segments of the pectoralis major were found to reach peak activity (Pk*N*) (avg. 112.9 ms) prior to force peak (FcPk) with no significant differences ($p=0.12$) identified between muscle segments (Table 6.1).

The duration of electromyographic activity (Dur*N*%) significantly differed ($p<0.05$) within the segments of the pectoralis major (Table 6.1). The peripheral muscle segments P5 and P1 were active longer than the central muscle segments P4, P3 and P2 (Figure 6.8). Segment P3 was the only segment with a period of activation (101%) similar to the TMT.

Normalised electromyographic discharge activity (iEMG*N*%) was observed to significantly decrease ($p<0.05$) from segment P5 to P1 (Table 6.1). Further analysis showed that muscle segment P5 had a significantly greater ($p<0.05$) iEMG*N*% than all other muscle segments with muscle segment P4 (65%) also displaying a significantly greater ($p<0.05$) iEMG*N*% then the remaining segments P3, P2 and P1 (avg. 37.7 ± 3.5%) (Figure 6.9). When the contraction intensities from each segment were summed and then averaged across the five segments, a value of 55% was achieved which closely approximated the 50% MVC level required in the experimental protocol. A quadratic regression analysis ($r^2 = 0.99$) strongly supported a relationship between muscle segment and contraction intensity (iEMG*N*%= 144.1 - (51.3 * X) + (5.9 * X^^2)).

6.4.4.2 Deltoid (D1, D2, D3, D4)

All deltoid muscle segments were activated after the onset of force (FcOn) (Figure 6.5). Segments D1, D2 and D3 were not activated until approx. 299.2 ± 16.3 ms after FcOn (700 ms MT). In contrast, segment D4 of the deltoid was activated 207.6 ms after FcOn, significantly earlier ($p<0.05$) than the other three deltoid muscle segments (Table 6.1).

Peak electromyographic activity (Pk*N*) for the deltoid muscle segments D1, D2 and D3 occurred after the force peak (FcPk) (Table 6.1). This activity is typical of antagonistic muscles. In comparison, muscle segment D4 peaked prior to the FcPk. Subsequent statistical analysis failed to establish any significant differences ($p=0.23$) between the Pk*N* measures for the deltoid muscle segments. All deltoid muscle segments peaked at approximately 30% of their duration of activation with none significantly different ($p=0.94$) from one another. Muscle segments D1, D3 and D4 were activated for durations (Dur*N*%) longer than the TMT. In contrast, D2 had a Dur*N*% less than the TMT (Table 6.1). Despite the contrast between muscle segments, no significant differences ($p=0.20$) in Dur*N*% were identified.

The intensity of electromyographic activation (iEMG*N*%) differed significantly ($p<0.05$) between muscle segments. Muscle segment D2 produced 40% of its MVC value while segments D1, D3 and D4 produced an average of 79 ± 3% of the MVC (Table 6.1). The

D2 iEMG*N*% value was significantly lower ($p<0.05$) than for the remaining muscle segments within the muscle. The average degree of all deltoid muscle segment activity (70% iEMG*N*%) was noticeably higher than that of the pectoralis major (55%) and the latissimus dorsi (47%).

6.4.4.3 Latissimus Dorsi (L1, L2, L3, L4, L5)

Muscle segment L5 was activated prior to force onset (FcOn) and significantly earlier ($p<0.05$) than the remaining muscle segments, which were activated post FcOn (Table 6.1). As the subject initially developed force, activation of muscle segments proceeded sequentially from L5 to L1, creating a wave of activation that moved from the inferior fibres of the muscle to the superior fibres (Figure 6.5 and 6.10). There was a strong linear relationship between muscle segment and activation time (On) ($r^2=0.95$).

All muscle segments reached peak electromyographic activity prior to the force peak (FcPk), a trend similar to that observed within the pectoralis major (Table 6.1). With regard to individual segments, the inferior segment L5 was the first to peak followed sequentially by segments L4 to L1 as shown by the robust correlation between muscle segment and peak activation (Pk*N*) ($r^2 = 0.98$). The results of the MANOVA suggested that while peak activation (Pk*N*) did not vary between the inferior L5 and L4 segments, all other segments (L3 to L1) showed a significant change ($p<0.05$) in this value (Table 6.1).

As can be seen in Table 6.1, all muscle segments inferior to L2 had durations of activation (Dur*N*%) that exceeded the TMT (1400 ms). Muscle segment L5, which has a line of action approximating that of the shoulder adduction impulse (Wickham, Brown *et al.* 2004), displayed the significantly longest ($p<0.05$) Dur*N*% with the remaining segments decreasing in Dur*N*% in succession towards L1 ($r^2 = 0.98$). Furthermore, statistical analysis revealed significant differences ($p<0.05$) between the individual muscle segments (Table 6.1).

The level of electromyographic activity (iEMG*N*%) differed significantly ($p<0.05$) between muscle segments (Table 6.1 and Figure 6.9). The highest level of activity was observed in

muscle segment L5 with the central muscle segments L3 and L2 having significantly lower ($p<0.05$) levels. The average iEMG*N*% activation of the combined latissimus dorsi segments was 47.2%, below that of the combined pectoralis major segment (55%), however, unlike the pectoralis major which was dominated by segment P1, no single muscle segment of the latissimus dorsi had a dominant activation.

6.5 Discussion

The objective of the work in this final experimental chapter was to determine, utilising a electromyographic (EMG) technique, whether muscle segment fibre type composition influences how the CNS coordinates individual muscle segments during movements of the shoulder joint. To achieve this outcome, muscle segment coordination was assessed at five different speeds of shoulder joint movement, from very slow to very fast. This assessment was designed to determine whether the 'normal' expected patterns of muscle segment coordination, as observed at each movement speed, were modified by the CNS to accommodate muscle segments of different fibre type compositions.

Patterns of muscle segment activation during slow and fast movement speeds

The influence of speed on muscle segment neuromotor coordination was investigated by varying the movement from a slow, feedback controlled movement (1500 ms to peak), to a near maximal speed, programmed movement (300 ms to peak). Figures 6.13 and 6.14 illustrate the overall activity of all segments as the movement time was reduced and the motor task became 'ballistic'. The analysis of each muscle segment's electromyographic activation focused on determining three pertinent points: that varying the speed of movement would significantly alter ($p<0.05$) the electromyographic onset in relation to force; that the time of muscle segment onset expressed as a percentage of the movement time would vary and that disruption would occur to the order in which muscle segments were activated during the movement.

No significant differences were identified in the On*N* of the prime mover muscle segments (P5, P4 and L5) when producing fast or slow movements. These muscle segments, located at the inferior and peripheral portion of the muscles, possessed the fastest contractile properties and were activated first, irrespective of movement speed. The remaining, more centrally located, slower muscle segments of the agonist muscles were significantly affected ($p<0.05$) by the speed of the movement. As the speed of movement was increased to the fast condition, muscle segments were successively activated closer to FcOn. Similar

activation patterns were identified in the antagonist deltoid muscle segments, although the differences were not as robust.

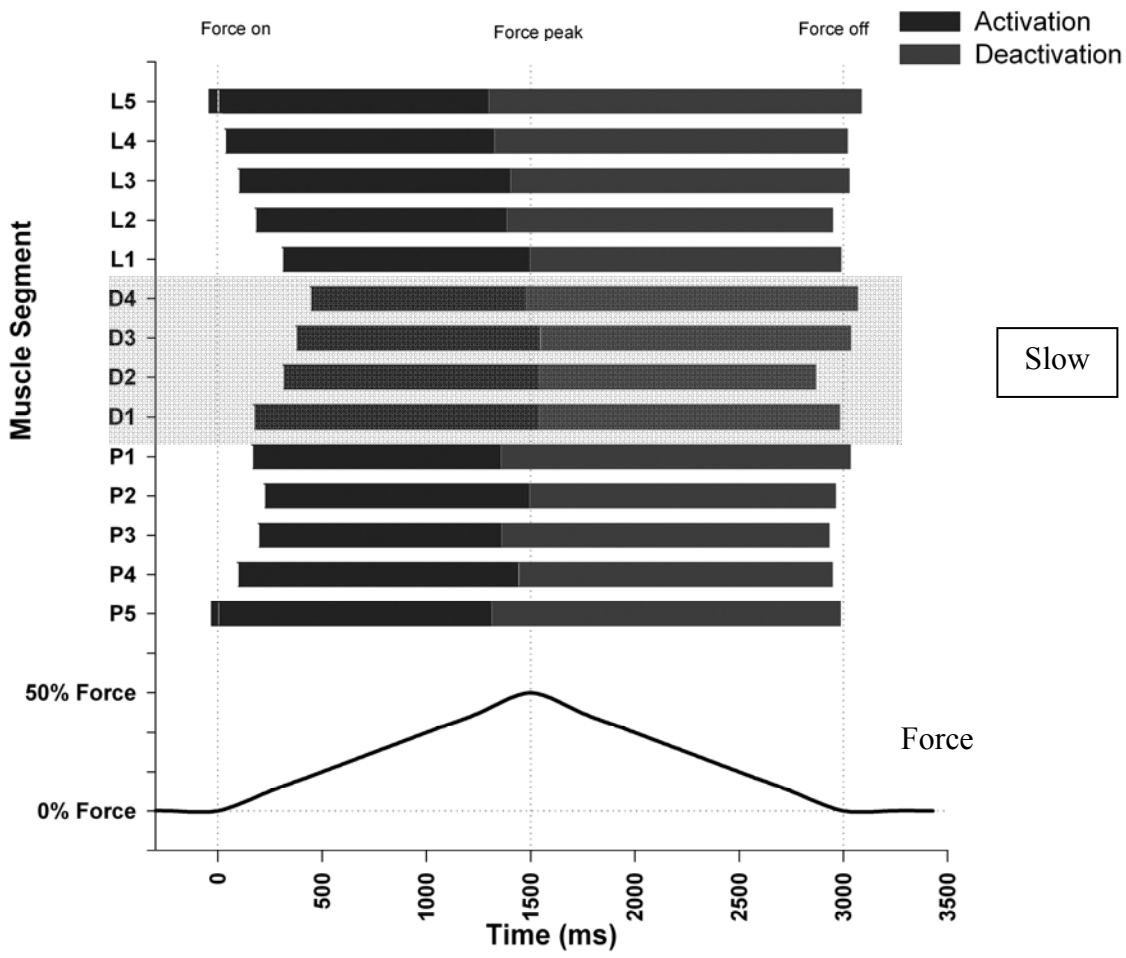

Figure 6.13 Segment onset, peak and duration compared to force onset, peak and duration for the 1500 ms MT (slow). Darker shading on the left hand side of the horizontal bars indicates segment activation; lighter shading on the right indicates segment deactivation. Transition point between dark and light shading indicates peak of electromyographic activity. Deltoid segments are shaded in grey to aid differentiation between agonist and antagonist muscles.

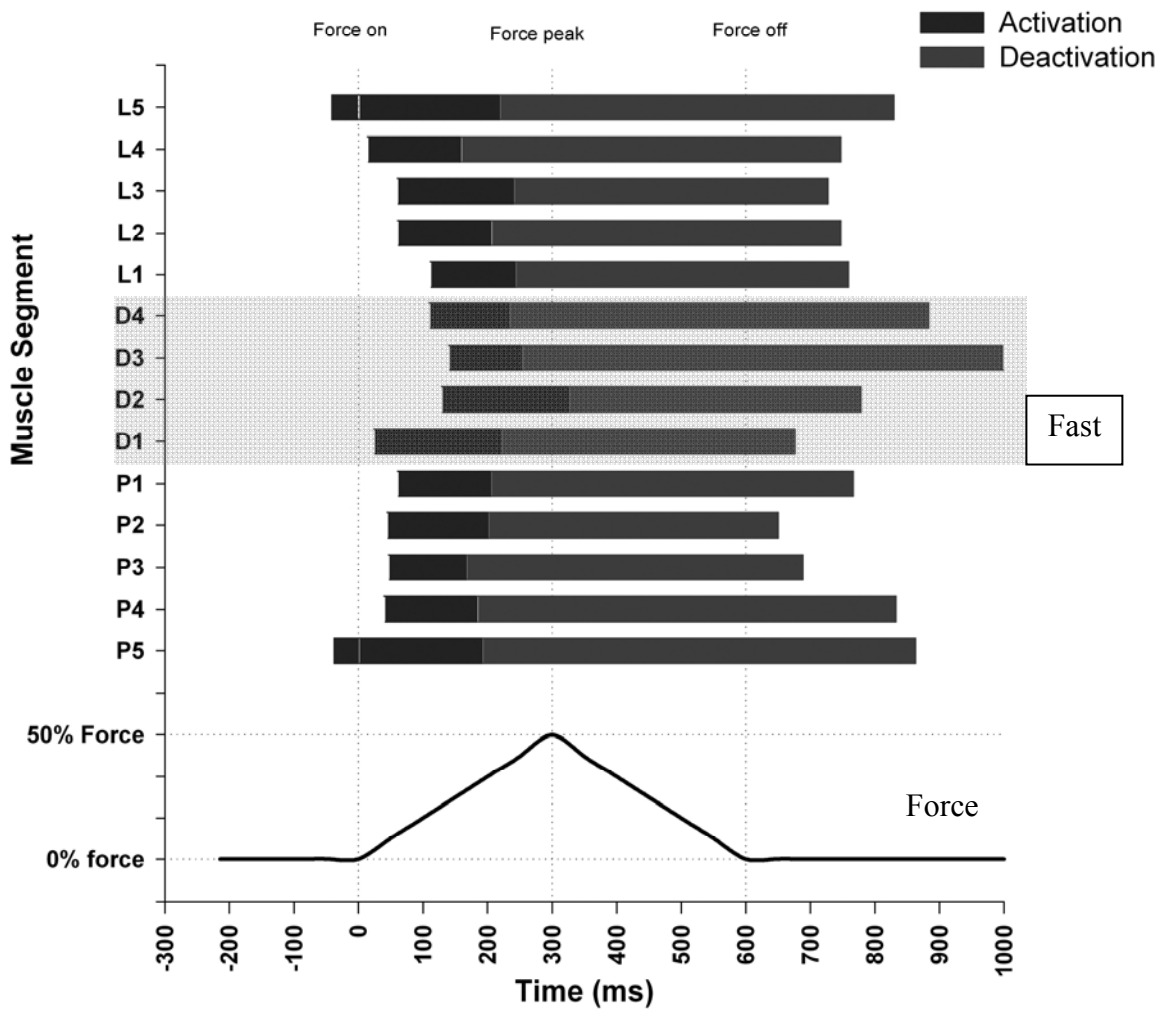

Figure 6.14 Segment onset, peak and duration compared to force onset, peak and duration for the 300 ms MT (fast). Darker shading on the left hand side of the horizontal bars indicates segment activation; lighter shading on the right indicates segment deactivation. Transition point between dark and light shading indicates peak of electromyographic activity. Deltoid segments are shaded in grey to aid differentiation between muscles.

Generally, the time period between muscle segment onsets was greater in the slow movement in comparison to the fast movement. This may be a result of the increased feedback and processing time during the slow movements during which the CNS can modify the output to the respective motor units (Christou, Shinohara and Enoka 2001; Hay and Bard 1984). In particular, the CNS can manipulate the activation of the assistant mover muscle segments in reaction to the activity of the prime mover muscle segments, which remained unchanged when variations to total movement time were made.

Muscle segments P5 and L5 were activated at a significantly lower percentage of the movement time during the fast, as opposed to the medium and slow movements. In fact, these muscle segments were activated at successively greater On*N*%MT with decreasing speeds of movement. In direct contrast, the adjacent muscle segment in the pectoralis major (P4) exhibited a direct reversal in On*N*%MT values with significant differences ($p<0.05$) observed at all speeds of movement (Figure 6.9). To better explain this, during the fast movement, muscle segment P5 was activated at the lowest percentage of movement time and muscle segment P4 the greatest. During the slow movement, muscle segment P5 was activated at the greatest percentage of movement time and muscle segment P4 the lowest. It appears that the two muscle segments alter their electromyographic onset, when expressed as a percentage of movement time, as a function of the activity in the adjacent muscle segment. During the fast movement, P5 takes the majority of the responsibility to initiate the movement, activating early in order to develop the larger amount of force required to propel the limb at the faster speed of movement. Muscle segment P4 therefore can be activated at a later stage. During the slower movements, the responsibility to develop the force appears to be shared across both muscle segments as the difference between the two in On*N*%MT is reduced (Figure 6.9). This pattern of activation was not present between the remaining muscle segments of the pectoralis major.

Within the latissimus dorsi, a similar relationship existed, with muscle segment On*N*%MT values showing a wider distribution at the fast speed and condensing during the slow speeds. Producing a fast movement places a greater requirement on the prime mover muscle segment to initiate the movement and generate the greater amounts of force to propel the limb (Angel 1977; Kido, Itoi, Lee, Neale and An 2003). In contrast, muscles segments appear to share the responsibility to a greater degree when producing the movement at slow speeds.

Muscle segment function and activation properties

Myoelectric activity recorded from the pectoralis major and the latissimus dorsi confirmed their involvement in the production of the shoulder adduction movement. Using criteria defined by Kelly (1971), both muscles could be classified as agonists and prime movers for

the shoulder adduction movement. Each muscle exhibited electromyographic activity prior to the commencement of the movement, for the duration of the movement and ceased activation at a time after the movement was completed. In contrast, the deltoid muscle, which was activated after force onset and displayed *limited* electromyographic activity, thus can be classified as an antagonist to the shoulder adduction movement. The deltoid may also have functioned as a glenohumeral joint stabiliser, reacting to the downward displacement force produced by the agonists (Kido, Itoi *et al.* 2003).

Functional muscular segments have been identified within various radiate muscles of the human through the analysis of a muscle segment's activation intensity (Paton and Brown 1994, 1995) and its contribution to the overall movement (Brown, Solomon *et al.* 1993; Pare', Stern *et al.* 1981; Riek and Bawa 1992). These analyses have identified the presence of agonist, synergist and antagonist muscle segments based on electromyographic discharge intensities recorded from each muscle segment (Paton and Brown 1995).

Based on the current literature (Brown, Wickham *et al.* 2007), it was hypothesised that muscle segments at all speeds of movement would demonstrate activation properties consistent with their function (i.e. agonist/antagonist/synergist). Results confirm the presence of individual electromyographic activation properties for muscle segments within the pectoralis major, latissimus dorsi and deltoid. Irrespective of the speed of movement, segments significantly differed ($p<0.05$) in terms of their respective onset times (On*N*), duration of electromyographic activation (Dur*N*%), and discharge intensity (iEMG*N*%).
The functional role of each muscle segment is easily demonstrable: the inferior segments of the pectoralis major (P5) and latissimus dorsi (L5) exhibited the earliest onset of electromyographic activation (an onset prior to the force onset), the longest duration of electromyographic activation and the greatest discharge intensity. Within the pectoralis major, segment P5 was identified as the prime mover segment, as it initiated the development of the muscles force output, remained active the longest duration and had the highest level of activity. Similarly, segment L5 within the latissimus dorsi can be attributed the same role. These findings concur with Buchanan, Almdale *et al.* (1986) and Paton and Brown (1995) who identified the muscle fibres that run parallel to the force direction as

fulfilling the role of agonist prime movers. Appropriately, the muscle segments P5 and L5 are the muscle segments with a line of action closest to the desired force vector for the shoulder adduction movement (Brown, Wickham *et al.* 2007; Wickham, Brown *et al.* 2004).

Muscle segments with synergistic roles were identified within the pectoralis major and the latissimus dorsi. Pectoralis major muscle segments P4, P3, P2 and P1 could be classified as synergists to the prime mover P5. Further distinction between the roles of each muscle segment is possible. Segment P1, which possesses muscle fibres that run perpendicular to the prime mover segment (P5) displayed an earlier On*N* and longer Dur*N*% with respect to P4, P3 and P2. These results indicate that segment P1 may play multiple roles when a shoulder adduction force is required: it may function in a force couple with segment P5 to generate a resultant force vector that lies between the two segments or, alternatively, it may offer a stabilising force, maintaining the integrity of the glenohumeral joint against the downward and anterior pull of the prime mover segment (P5). Assuming the proposed force couple role to be correct, muscle segment P1 would be expected to exhibit prime mover electromyographic activation properties. This was not proven in the current experiment as P1 was not activated prior to FcOn, at any of the movement speeds. The alternative role of stabilisation is therefore more probable. This action can be labelled as 'helping' synergy as the two muscle segments operate on the same joint together to achieve a movement while simultaneously neutralising the other's secondary actions (Kelly 1971).

In the previous chapter, the central muscle segments (P2/3/4) were identified as possessing slower contraction rates (tc*N*) when compared to the more peripheral muscle segments (P1/P5). Given that a relationship exists between contraction rate determined by MMG and fibre type composition (Dahmane, Djordjevic *et al.* 2005; Dahmane, Valencic *et al.* 2001), the greater concentration of slow-twitch muscle fibres in the centre of the muscle, and hence the limited force production capabilities, may prevent this portion of the muscle from acting as the prime mover segment. When this information is combined with the electromyographic activation properties, their proposed role as synergists during the experimental shoulder adduction impulse is substantiated.

The muscle segments of the latissimus dorsi did not display the same distribution of functional roles. While muscle segment L5 can be identified as the prime mover, muscle segment L1 cannot be attributed the same role as P5. Sequentially later onset times and shorter electromyographic durations were present when moving superiorly from segments L5 to L1. The lack of prime mover electromyographic activation properties from L1 indicates the absence of a force couple within the latissimus dorsi. Additional stabilising force may also have been supplied from the posterior rotator cuff muscles, which were not analysed in this study. Supraspinatus activation may have stabilised the glenohumeral joint against the downward pull of latissimus dorsi and similarly, infraspinatus activation stabilised against the internal rotation force of the latissimus dorsi muscle segments. Muscle segments L1/2/3/4 can be classified as synergists to the prime mover segment L5, as per the central pectoralis major muscle segments.

Muscle segments within the deltoid were expected to exhibit antagonistic electromyographic activation properties during the shoulder adduction impulse movement due to their global role as an abductor of the glenohumeral joint (Jenkins 1998). Our results showed muscle segments D1/D2 and D3 behaved in the expected manner however muscle segment D4 exhibited electromyographic activity that contradicts this functional role. In the experimental position (90° abducted), the posterior segment D4 was believed to have a line of action very similar to that of segment L1 (Brown, Wickham *et al.* 2007; Wickham, Brown *et al.* 2004). This, in part, may explain the similarities in electromyographic activation observed between these two segments. The remaining segments, however, displayed typical antagonistic activity with onsets occurring well into the movement, presumably reacting to the increase in force development of the agonists. With low force levels, the joint's capsular and ligamentus structures would be expected to provide support, however with an increase in force, the antagonistic muscles are required to become active and remain active until the force disperses (Angel 1977).

Do compensatory changes in neuromotor control occur as a result of the in-homogenous distribution of muscle segment contractile properties?

In Study E, the contractile properties of the same 14 muscle segments were identified through a non-invasive Laser-MMG technique. The results of the investigation determined that the muscle segments located at the periphery of the agonists (pectoralis major and latissimus dorsi) possessed the fastest contraction times (tc*N*), the highest maximal rates of contraction (+dD/dt) and the greatest magnitude of muscle segment belly displacement (Dmax) (Table 5.3). In the current study, the same peripheral muscle segments (P1 and P5; L1 and L5) were the first to be activated (On*N*) and had the longest duration (Dur*N*%) and highest intensity (iEMG*N*%) of electromyographic activation (Table 6.1). The relationship between a muscle segment's contractile properties and its electromyographic activation properties during the shoulder adduction impulse are illustrated in Figure 6.15. Each muscle segment has been categorised by tc*N* measures as possessing slow, intermediate or fast contractile properties. Overlayed is the muscle segments order of initial activation (Onset order) for the movement i.e. muscle segment L5 has fast contractile properties and was the first to be activated (indicated by the number 1).

Generally, electromyographic activation (Onset) proceeded in a wave like fashion, passing from the faster, peripheral muscle segments to the slower, more centrally located muscle segments. This pattern was consistent for both of the agonists.

The overall order that muscle segments were activated, in relation to each other, did not significantly change ($p<0.05$) as a result of varying the speed of movement. This result, in isolation, does not support the hypothesis that compensatory changes in neuromotor control would occur as a result of the in-homogenous distribution of muscle segment contractile properties. It could therefore be stated that the CNS appears not to be influence by the variation in contractile properties / muscle fibre type composition between muscle segments. However, further investigation revealed significant differences ($p<0.05$) between onset (On and On*N*%MT) values for each muscle segment and a disordering of the relative position of those significant differences as a result of varying the speed of movement.

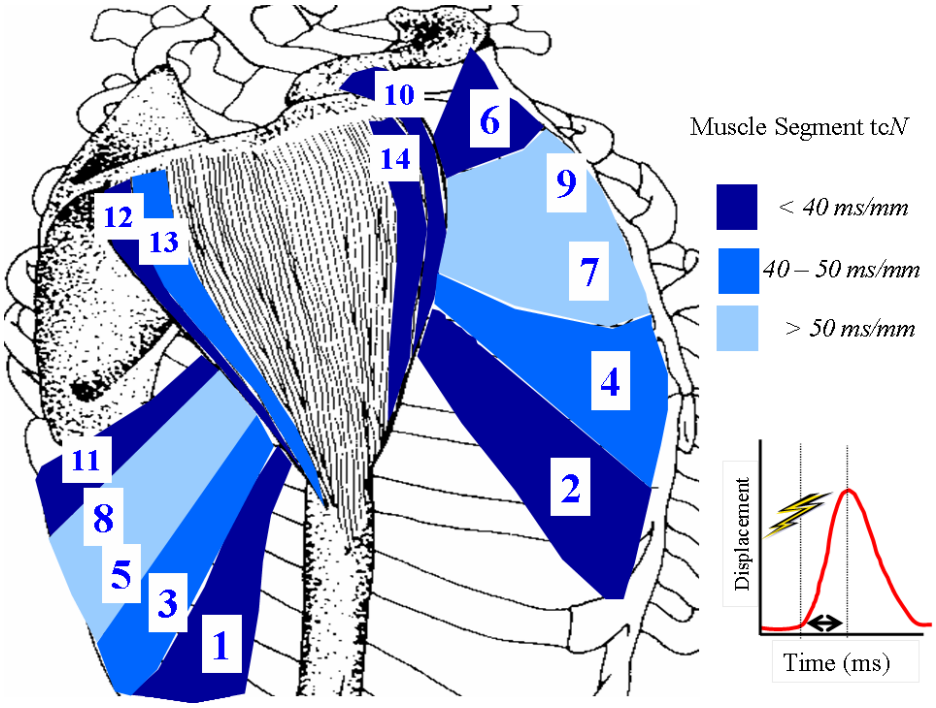

Figure 6.15 Illustration showing a muscle segments contraction time (tc*N*) and order of electromyographic activation (Onset) during the 700ms MT condition. tc*N* is identified by the relevant shade of blue (see figure key) while Onset rank is indicated by the number located on each muscle segment (ascending order).

Muscle segments within the pectoralis major were activated in a different sequence during the fast and slow movement speeds (Figure 6.16). During the slow speed of movement, as in the fast, segment P5 initiated the movement. Variation existed in the sequence of the remaining segments with muscle segments P2 and P3, which have slow contractile properties, activated earlier in the fast movement than in the slow movement. This appears to be a logical compensatory change to the activation sequence, allowing the slower segments greater time to develop maximal force. This also provides the greatest opportunity for muscle segments of variable fibre type composition to reach a common peak during the movement. The results here provide evidence of compensatory changes to the neuromotor control of muscle segments within the pectoralis major.

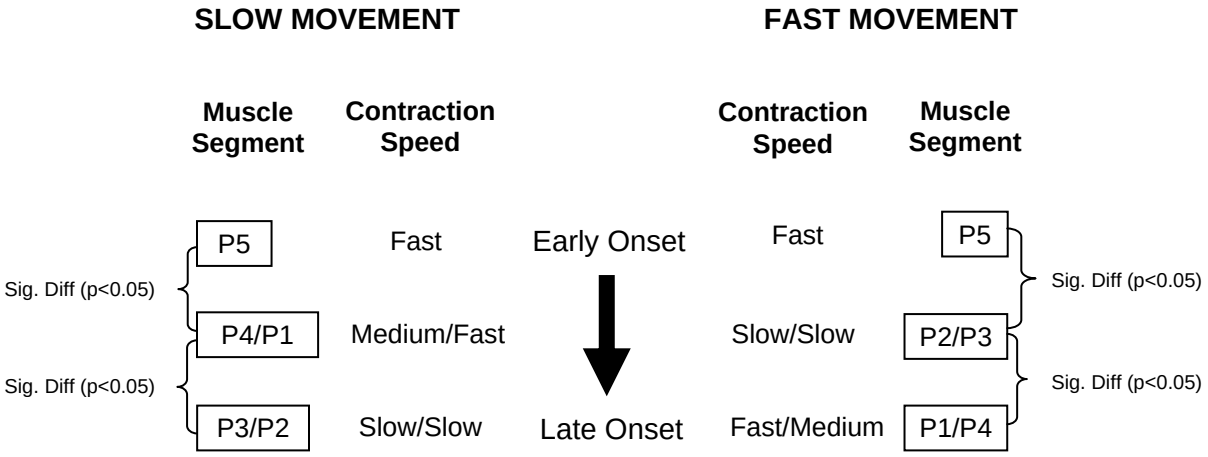

Figure 6.16 Comparison of the order of muscle segment onset within the pectoralis major at the slow and fast movement speeds. Note the variation in segment P2/P3 activation order.

Similar finding were not present within the latissimus dorsi muscle. Only segment L3 was altered due to the speed, having an onset significantly different ($p<0.05$) to its adjacent segment during the fast movement but not the slow movement. As there was no change to the activation order and onsets were relative the other segments, there was no supporting evidence of the effect of fibre type difference on the neuromotor control of the latissimus dorsi segments. The evidence supporting functional differentiation within the latissimus dorsi is therefore limited when compared to the pectoralis major. The latissimus dorsi appears to operate as a single muscle, perhaps a function of its more homogenous origin as compared to the pectoralis major with its mobile clavicular attachment.

The duration (Dur*N*%) of electromyographic activation differed between muscle segments and between movement speeds. Increases in muscle segment duration (Dur) were associated with increases in total movement time. As the speed of movement increased, muscle segment durations (Dur*N*%) became significantly longer ($p<0.05$) than the total movement time, whereas at the slow movement speed, the majority of muscle segments failed to be active for the entire movement duration. These results are to be expected as movements that take longer require longer electromyographic activations and when producing fast movements, the requirement to generate force over the entire movement is increased in order to maintain the movement speed. Varying the speed of movement

significantly affected the prime mover muscle segments, which exhibited increases in Dur*N*% measures that were associated with increases in movement speed.

The discharge intensity (iEMG*N*%) significantly varied ($p<0.05$) between adjacent muscle segments but not as a result of modulation of the movement speed. It is proposed, on the basis of the results presented here, that the CNS modulates the temporal activation properties rather than the discharge intensity of muscle segments when producing movements of different speeds.

Generally, muscle segments within the agonist muscles maintained similar electromyographic peak (Pk*N*) times. When the speed of movement was varied, only the peripheral and faster contracting P5 and L5, L4 and L3 were affected. Pk*N* at the fast speed of movement occurred significantly later ($p<0.05$) and thus closer to FcPk, than during the medium and fast speeds of movement. No effect of movement speed was evident in the central P4/P3/P2 muscle segments of the pectoralis major. Varying the speed of movement affected the overall pattern of muscle segment Pk*N* within the latissimus dorsi. At the fast speed of movement all muscle segments peaked (Pk*N*) at approximately the same time, where as at the slower speeds, the inferior segment L5 was the first to peak followed sequentially by segments L4 to L1. The results here suggest that for the pectoralis major, the CNS ensures that each muscle segment peaks at the same time, irrespective of the speed of movement, through modulation to the onset time (On), duration (Dur) and intensity (Int) properties. In comparison, muscle segments within the latissimus dorsi differed in terms of their electromyographic peak, however this only occurred at the slow speed of movement.

Significant compensatory effects ($p<0.05$) on the neuromotor control of muscle segments were evident, particularly within the pectoralis major but not so within the latissimus dorsi and deltoid. These results therefore partially support the hypothesis that the in-homogenous distribution of muscle segment contractile properties, across the 14 investigated muscle segments, would result in significant compensatory changes ($p<0.05$) in neuromotor control, particularly at the fastest (e.g. ballistic) speeds of movement. It appears, at least in this experiment at the investigated movement speeds, that the muscle

fibre type compositions as inferred by MMG do impact on when and how the CNS activates agonist muscle segments during the movement.

Chapter 7

General Discussion, Limitations and Conclusion

General Discussion

Overview

The aim of this thesis was to gain a better understanding of the structure and function of muscle segments and their influence on neuromotor control not only within a single muscle, but across a group of muscles that control a single joint. This aim was satisfied through addressing the hypotheses that motor unit contractile properties vary between the anatomical segments of a multifunctional muscle and that variations in segmental contractile properties reflects differences in the muscle segment's function and fibre type composition. Furthermore, this work attempted to show how the temporal neuromotor control characteristics of skilled movements might be influenced by variations in underlying segment contractile properties.

The results indicated that motor unit contractile properties a) did vary between muscle segments and that b) the timing and intensity of each muscle segment's activation was related to that segment's function within the motor task.

As seen in Chapter 6, prime mover (agonist) segments exhibited the earliest onsets while synergist (agonist) segments had sequentially later activations. Antagonist segments were activated significantly later and always after force onset. It was apparent that the "pattern" of activation of each muscle segment, in part, determined its "function". Furthermore, the activation pattern of each segment was influenced by its fibre type composition, as indicated by its contractile properties. It was clear that agonist segments, with lines of action most closely resembling the plane of force production (e.g. P5 and L5) (Wickham, Brown *et al.* 2004) and with fast contractile properties, were acting as prime mover segments. Generally, agonist segments with more divergent angles of force application and slower contractile properties tended to be activated later (closer to or just after the beginning of the movement) and assume a more synergistic role. Segments with antagonist lines of action opposing the movement assumed a distinct antagonist role.

The results also showed that the "pattern" of muscle segment activation becomes disrupted as movement speed changes from slow to ballistic. As tested in Chapter 6, during the

ballistic (300 ms to peak) shoulder adduction task, the order of activation of muscle segments within the pectoralis major was significantly modified compared to that seen at slower movement velocities. Interestingly, the activation of pectoralis major muscle segments during the ballistic movement appeared to preferentially activate segments with slower twitch characteristic to allow all active muscle segments time to reach a peak simultaneously, just prior to peak force. Segments within the latissimus dorsi and deltoid muscles did not exhibit any evidence of disordering when movement speed was altered.

The finding of preferential activation within muscle segments is unique, and previously un-reported, and is highly relevant to understanding the concept of a movement's degrees of freedom as espoused by Bernstein (1967). More than thirty years ago Bernstein (1967) observed that during the performance of many motor tasks, groups of muscles are recruited together as a single unit rather than as individuals. These functional groups of muscles were referred to as muscle *synergies*. Bernstein's hypothesis (1967) was that the human motor system is mechanically complex with many degrees of freedom (possible joint displacements and rotations) to achieve particular motor acts. There appears, however, to be a mismatch between the storage capabilities of the CNS and the multitude of possible movements that could be produced within the musculoskeletal system if each movement was to require its own neural circuitry. Bernstein (1967) hypothesised that to control such a system, the degrees of freedom needed to be reduced. The concept of a simplified plan of movement (motor program), developed within the higher centres of the CNS, but executed with greater complexity through the spinal cord, was one example of the attempts made to minimise the degrees of freedoms facing the neuromotor system (Bernstein 1967; Brooks 1986; Iqbal and Hemami 1996). The findings of the current thesis complicates the 'degree of freedom' problem by proposing that at the least, the CNS must program the activity of motor units within individual muscles segments rather than within whole muscles and in addition, take into account the biochemical composition of each muscle segment when planning its role in skilled movement production.

Physiological validation of the MMG technique

In order to estimate muscle segment fibre type, the thesis focused on the development of a non-invasive Laser-MMG technique to measure muscle segment contractile properties. This technique had the potential to estimate muscle segment contractile properties to allow an understanding of the spatial distribution of type I and II muscle fibres within individual muscle segments. It has been known for some time that whole muscles may exhibit strikingly heterogeneous distributions of type I and II fibres (Brooke and Kaiser 1970; Jennekens, Tomlinson *et al.* 1971; McComas and Thomas 1968) although this phenomenon has, prior to the completion of study E (Chapter 5), yet to be associated with single muscle segments. As a result scientists and clinicians may have assumed that a single muscle biopsy would be representative of the entire muscle's fibre type composition, basing deductions of muscle function and the design of rehabilitation programs on a potentially erroneous estimate of muscle fibre-type distribution. Importantly, the work presented in this thesis addresses this issue through an attempt to understand how muscle fibre-types are distributed within the segments of single skeletal muscles and furthermore, whether the CNS must account for differences in segment fibre type when producing skilled human movement.

The Laser-MMG technique, designed to measure the lateral displacement of a muscle segment's belly following PNS, was initially validated against a Tensiometric technique, which is considered to be the 'gold standard' for measuring muscle contractile properties and physiological force development. Muscle temperature and fatigue were chosen as the conditions under which the Laser-MMG was to be validated as they are well established physiological modulators of muscle fibre contractile performance (Bennett 1984, 1985; Bigland-Ritchie and Woods 1984). The simultaneous collection of Tensiometric and Laser-MMG measures allowed for sensitivity comparisons between the techniques and provided confirmation that the muscle, under experimental condition, was behaving in an acceptable, literature-proven manner.

It is well understood that muscle temperature has a measurable effect on developed tension and contraction and relaxation rates in rat muscle (Bigland-Ritchie, Thomas *et al.* 1992;

Close and Hoh 1968). In Study A (Chapter 4), the Ringers solution temperature was controlled by small ancillary heating/cooling baths in order to set the muscle temperature. In another study, as little as 2°C changes in the temperature of the Ringers solution resulted in an immediate effect on muscle fibre contractile properties, indicating that muscle temperature is highly dependent upon the temperature of the solution (Verburg, Thorud *et al.* 2001). Temperature changes in the magnitude of 5°C were used in the current investigation.

Cooling of the muscle resulted in a marked reduction in tension development and lateral displacement of the muscle's belly, as measured by Tensiometry and the Laser-MMG technique respectively. Both measurement techniques were able to detect a change in muscle contraction time (tc, tc*N*) as temperature was varied. Importantly, the Laser-MMG measures of muscle contractile properties mimicked the directional trends of Tensiometry and were found to be sensitive to temperature-induced physiological change under the current experimental conditions.

The Laser-MMG was also assessed for its ability to measure muscle contractile performance at different states of physiological fatigue. As seen in Study B (Chapter 4), whole-muscle fatigue was induced via a train of short but intensive stimulations (PNS) over a 20 second period. As with the evaluation of temperature effects, muscle contractile properties as measured by the Laser-MMG technique was compared to that derived from the Tensiometry technique. Both methods allowed identification of the decrease in maximum displacement/force production and associated slowing of the contraction time as a result of the fatigue task. Again, the Laser MMG technique was proven to produce measures of muscle contractile force similar to those detected by Tensiometry. Pearson's correlations ($r^2 = 0.73$) between the displacement/force measures of Dmax and Tmax show that the amplitude of the MMG is useful for estimating force production during fatiguing tasks when direct measures are not available. The results of this thesis are in agreement with Perry Rana, Housh *et al.* (2003) who demonstrated that MMG amplitude closely tracked the fatigue-induced decline in torque production during movements at varying velocities. Additionally, MMG displacement measures from Perry Rana, Housh *et al.*

(2003) were observed to differ between muscles, indicating that the individual contribution of each muscle to the overall force production may be quantifiable. Therefore, MMG amplitude may prove useful for detecting the relative contribution of individual muscle segments to overall muscle force production – in the same way that non-invasively obtained measures of EMG amplitude provide an objective measure of muscle force (Crosby 1978; Metral and Cassar 1981). However, it must be noted that in high-force contractions, EMG amplitude increases, whereas during sustained low force contractions, the amplitude does not always increase (Arendt-Nielsen, Mills and Forster 1989; Hansson, Strömberg, Larsson, Ohlsson, Balogh and Moritz 1992). In contrast, MMG is able to provide information about the mechanical properties of the contracting muscle and alterations in motor unit activity both during and after low-force fatiguing muscle contractions (Orizio, Gobbo *et al.* 2003; Shinohara and Sogaard 2006).

Muscle segment contractile properties

Determination of fibre type in humans currently requires a muscle biopsy - a technique that may produce results that are representative of an entire muscle's fibre type composition, rather than single muscle segment (Lexell, Taylor *et al.* 1985; Mahon, Toman *et al.* 1984; Zhao, Kawaguchi, Matsui, Kanamori and Kimura 2000). For the present study, investigations were conducted to determine whether the non-invasive Laser MMG had utility for determining muscle segment fibre type through comparison with existing invasive histological techniques.

Using a Tensiometry technique, combined with histochemical analysis in rat hind limbs, Ranatunga and Thomas (1990) concluded that the differences in twitch contraction time and shortening velocity among the investigated muscles could be explained on the basis of their respective muscle fibre-type compositions. In Study C (Chapter 4), Laser-MMG and Tensiometry measures were obtained from the red proximal (slow) and white distal (fast) regions of the rat medial gastrocnemius muscle, with fibre type confirmed through histological examination (both proximal and distal regions). Both Laser-MMG and Tensiometry techniques could be used to demonstrate the utility to distinguish the proximo-distal regionalisation of fibre types present within the muscle.

In the present study, the temporal measures of contraction time (tc, tc*N* and maximal rate of contraction +dD/dt) were identified as the most indicative of fibre type composition utilising the MMG technique. Significant differences in contraction time measures (Table 4.3) between the distal and proximal segments of the muscle confirmed the ability of the Laser-MMG technique to distinguish fibre type within different segments. These findings concur with the work of Dahmane and colleagues (Dahmane, Djordjevic *et al.* 2005; Dahmane, Valencic *et al.* 2001) who utilised an MMG technique, with fibre type identification, in human cadavers to identify a robust correlation (r=0.76) between muscle twitch contraction time and the percentage of slow-twitch muscle fibres measured at both the surface and deep within the muscle, and later confirmed with immunohistochemical identification of fibre type (Dahmane, Djordjevic *et al.* 2006). Dahmane and colleagues (2001; 2005) suggest that the MMG technique can quantify muscle fibre type both superficially and within the depth of the muscle. These findings lend support to the contention that a breadth-wise heterogeneous distribution of muscle fibre types is possible between adjacent and more distant segments within the one muscle (Study D, Chapter 5)).

After identifying in animal studies (Study A, B and C; Chapter 4) that the Laser-MMG can be used to reliably identify changes in muscle contractile properties due to physiological modulators (eg. Fatigue), the technique was applied to quantify muscle fibre type distribution in human muscle (Study D; Chapter 5). The human gluteus maximus muscle was chosen for analysis as it is a large robust and easily accessible muscle that contains at least three previously identified anatomical segments across the origin of the muscle (Lyons, Perry *et al.* 1983). While neurophysiological research (Basmajian and DeLuca 1985; Jenkins 1998) has identified distinct neuromotor functional roles (i.e. prime mover / assistant mover) for each muscle segment during movements of the hip, histological analysis of the gluteus maximus has only occurred using a single biopsy site (Johnson, Polgar *et al.* 1973). Accepting that fibre type composition can reflect the overall role that a muscle has from a fatigability point of view (postural vs. power) (Burke, Levine *et al.* 1974; Burke, Levine *et al.* 1973; Close 1965; McComas 1996; McComas and Thomas 1968; Spector, Gardiner *et al.* 1980), it is valid to assume that muscle segment fibre type

composition would reflect the overall role the muscle segment has from a fatigability point of view.

To test this assumption in the many segments of a multi-segmental muscle would normally require a multiple biopsy technique. To investigate muscle fibre type distribution in depth would require further biopsies, a method too invasive to be ethically valid. Alternative, non-invasive measures such as MMG potentially offer far more usable data. The results of Study D (Chapter 5) identified significant differences in inter-segmental contraction properties across the breadth of the human gluteus maximus. Importantly, the increasingly faster contractile properties of the muscle segments of the gluteus maximus, in a cephalo – caudal direction, were consistent with the role of the muscle segment (i.e. superior segment – postural, inferior segments – joint rotation) (Basmajian and DeLuca 1985).

There was, however, no evidence to support the notion of a length-wise (origin to insertion) change in fibre type within an individual segment (Cescon, Farina *et al.* 2004). To the author's knowledge this is the first time that muscle fibre type of multiple segments within the human gluteus maximus muscle has been demonstrated and associated with a segment's role and fatigability.

The results of Study E (Chapter 5) suggested that the contractile properties (e.g. Dmax, tc*N*, tr*N*) of muscle fibres varied significantly between the individual segments of the shoulder musculature (pectoralis major, deltoid and latissimus dorsi) following maximal PNS. Most notably, normalised contraction time (tc*N*) differed significantly across the surface of the agonist muscles, with 'slow-twitch' contractile properties found in muscle segments that have a greater role in producing movement in the coronal plane, while 'fast-twitch' contractile properties were associated with segments having more efficient moment arms to produce movement in the sagittal plane. Furthermore, a distinctive anatomical distribution of muscle fibre types was associated with each of the muscles investigated. Muscle segment contractile properties were found to be heterogeneous and their arrangement appears to reflect the most common or important joint movements. Interestingly, the muscle segments located at the periphery of all three shoulder muscles exhibited faster

contractile properties than those located in the middle of the muscle. It appears that this internal organisation may be a consistent characteristic of radiate muscles.

Together, the results of Study E (Chapter 5) indicated that the radiate muscles were composed of muscle segments that were physiologically (e.g. contractile characteristics), bio-chemically (e.g. fibre type) and anatomically (e.g. moment arm) optimised for the MOST common or important motor tasks/movements of the joint that they traverse (i.e. adduction, abduction, flexion and extension). Furthermore, there appears to be an inbuilt flexibility in the CNS control strategy to account for the pre-mentioned variations when producing less common tasks/movements. By way of example, the muscle segments within the deltoid are arranged so that the 'faster' segments are located in the anterior and posterior heads (at the periphery of the muscle), with the 'slower' segments located within the middle head (centre of the muscle) (Gorelick and Brown 2007). Functionally, this allows the deltoid to produce faster movements and theoretically higher levels of force during flexion (anterior head) and extension (posterior head) movements (i.e. movements in the sagittal plane) and conversely, maintain prolonged periods of abduction force via the middle head (i.e. movement in the coronal plane). Together with the 'faster' contracting clavicular segment of the pectoralis major (P1) (Study E), these adjacent muscle segments (D1 and P1), located within two individual muscles, can combine their actions to potentially produce a fast developing and potentially high horizontal flexion force e.g. during a bench press (Barnett, Kippers and Turner 1995). Similarly, the middle 'slower' muscle segments of the deltoid (Gorelick and Brown 2007) are optimised for the production of stabiliser forces for the glenohumeral joint and as prime movers for the production of abduction force (Wickham and Brown 1998).

Neuromotor control of muscle segments and the influence of movement speed

Having now identified that muscle segment contractile properties vary between individual muscle segments, it would appear obvious that the CNS would need to account for these differences when planning, coordinating and executing movements requiring the activation of multiple muscle segments, both within and across individual skeletal muscles.

Previous studies (Brown, Wickham *et al.* 2007; Wickham and Brown 1998; Wickham, Brown *et al.* 2004), have identified that the CNS can "fine tune" the activity of discrete muscle segments within single muscles to meet the demands of the motor task. Both within single muscles (Brown, Solomon *et al.* 1993; Wickham and Brown 1998) and across a muscle group (Brown, Wickham *et al.* 2007; Wickham, Brown *et al.* 2004), individual muscle segments may be classified according to their neuromotor function during the motor task. Prime mover segments have moment arms and lines of action that are agonistic for the movement and are the first segment activated in order to initiate the generation of force. Observations within this thesis of early activation of prime mover segments to initiate isometric force production was consistent with the findings of Flanders and Soechting (1990) who reported that the first "peak" of muscle activation was always within motor units close to the optimal line of action of the muscle. Those agonist muscle segments with more divergent lines of action (smaller rotatory force components) were activated after the prime mover segments and were termed "synergists" (Wickham and Brown 1998). Muscle segments with antagonist moment arms and lines of action were generally activated late; these segments being termed "antagonists". Such functional classifications of muscle segments have been found to be appropriate both within, and between muscles grouped around a particular joint (Brown, Wickham *et al.* 2007; Wickham, Brown *et al.* 2004).

With reference to Table 6.1, significant differences were identified in muscle segment activation times (On*N*), both between and within the muscles investigated. Notably, the inferior segments of the pectoralis major (P5) and latissimus dorsi (L5) (Fig. 6.5) were the first activated, irrespective of movement speed. Adjacent segments followed a wave of sequential activation, in a superior direction, through the agonist pectoralis major and latissimus dorsi muscles and even into the antagonistic D1 segment of the deltoid.

What functional conclusions maybe drawn from this result? Although segmental moment arm data was not calculated for this thesis, reference to classical descriptions of whole muscle function (Kapandji 1982; Williams, Warwick *et al.* 1995), simple observation of cadaveric segment mechanical lines of action (the angle of insertion onto the humerus for these muscle segments approximates 90 degree) and the shoulder moment arm data of

Wickham and Brown (2004) and estimates of Brown, Wickham *et al.* (2007), suggest that P5 and L5 had agonist moment arms for shoulder adduction from a position of 90 degrees of shoulder abduction. In contrast, the centrally located segments of the deltoid (D2, D3) would all play an antagonist role (Basmajian and DeLuca 1985; Kapandji 1982). It may be concluded that the inferior segments within the pectoralis major and latissimus dorsi function together as prime movers for shoulder adduction. Their collective time of activation, generally 40 ms prior to force generation, was within the 30-100 ms electromechanical delay window reported by Cavanagh and Komi (1979) and Norman and Komi (1979) confirming their functional role in movement initiation and their prime mover status. In contrast, the significantly later and sequential activation times (Table 6.1) of adjacent segments P4 – P2 and L4 – L1 would suggest that these segments were synergist muscle segments.

Muscle segment P1 was activated earlier than the adjacent P2 and P3 segments during slower movement speeds. This segment is located at the opposite extremity of the muscle and has an almost perpendicular fibre direction (in 90° shoulder abduction position) to the prime mover P5. Its role in the adduction movement may hypothetically be that of joint support and stability or alternatively, as a synergist to P5. It has been observed that maximising the mechanical advantage (i.e. selecting the muscle with the greatest moment arm), is not the only factor used by the CNS to determine the appropriate muscle activation pattern required to drive joint rotation (Flanders and Soechting 1990; Vasavada, Peterson and Delp 2002). Using neck muscles, Vasavada, Peterson *et al.* (2002) illustrated that sternocleidomastoid may be more strongly activated in flexion than in lateral bending because there are fewer muscles available to generate the flexion moment. In contrast, during lateral bending, sternocleidomastoid may be required to counteract the extension moment of splenius capitus (Vasavada, Peterson *et al.* 2002). These findings suggest that a muscle may not receive preferential activation over other available muscles simply because it has the optimal moment arm for a movement. In the context of the current investigation, segment P1 may be activated earlier to stabilise the joint whereas during the fast movement there is little time to stabilise and segments P2 and P3 are required to be activated early in order to generate the rapid force requirements.

Comparison of the timing of muscle segment myoelectric peak intensity (Pk) to force peak (FcPk) clearly showed that the prime mover muscle segments (P5 and L5), as well as the synergist segments (P4-P1 and L4-L1), all reached maximal motor unit activity at least one electromechanical delay period before force peak was achieved (Table 6.1). In contrast, the antagonist segments (D1-D3) all reached peak myoelectric activity significantly later and after force peak. These findings were consistent with those of Brown and Cooke (1990) who showed AG1 muscle burst activity to begin >30 ms prior to movement onset. During the fast movement, both segments D1 and D4 peaked prior to FcPk. This indicates that either the force generated by the agonists required rapid stabilisation from the D1 and D4 segments or that the D1 and D4 segments that are adjacent to the agonist P1 and L1, contributed to the adduction movement. The waves of sequential segment activation appeared to ignore the anatomical boundaries between whole muscles, suggesting that the CNS coordinated individual muscle segments rather than the whole muscle as one unit, to complete this motor task. This further complicates the process of controlling motor tasks as there appears to be no defined limits of muscles to which discrete functions can be applied. To the author's knowledge, this finding has not been previously described in the scientific literature.

It should not be concluded that the 14 muscle segments identified in this study represent the definitive muscle segment design imposed by the CNS. Following convention (Brown, Solomon *et al.* 1993; Johnson and Bogduk 1994; Manueddu, Blanc *et al.* 1989; Pare', Stern *et al.* 1981; Paton and Brown 1994, 1995; Soderberg and Dostal 1978; Wickham and Brown 1998; Wickham, Brown *et al.* 2004; Wickham, Brown *et al.* 2004), the analysis was based upon the arbitrary anatomical subdivision of each muscle and was not based on anatomical parameters such as fascicle length, direction or innervation and did not reference each muscle's neuromuscular compartments (English and Weeks 1984; English, Wolf *et al.* 1993). It is possible that a muscle segment could be simplified down to the level of a single motor unit and its associated muscle fibres and that those muscle fibres may in fact be spread across multiple anatomical muscle segments. It is probable that similar findings to the results of this thesis would have been found if fewer, or more, muscle segments had been investigated.

The results obtained here identified significant differences in the neuromotor activation of muscle segments. Within a given muscle, functional differentiation existed as evidenced by differences in muscle segment onsets, durations and intensities, indicating that the CNS has the capability to independently control muscle segments. This conclusion is not new, but rather a reinforcement of those found in previous studies (Brown, Solomon *et al.* 1993; Brown, Wickham *et al.* 2007). What is new however is the detection of the orderly recruitment (*wave of activation*) of the adjacent segments as the movement proceeded, starting at the prime mover and dispersing to the synergists. This result concurs to some extent with English and Weeks (1984) who postulated that when a muscle has multiple force vectors, "….*the mechanical arrangement of muscle units is such that strict orderly recruitment occurs in terms of force for the direction requiring most precision"* (English and Weeks 1984). In the context of the current thesis, the activation of muscle segments occurred in an order that provided for the greatest amount of force and precision for the required shoulder adduction motor task.

With regard to the effect of movement speed, no gross disordering of the muscle segments onset was identified within any of the investigated muscles regardless of the speed of muscle contraction. However, when muscle segment onsets were expressed as a percentage of the movement time (On*N*%MT), the pectoralis major exhibited altered relative timing between the segments. This was particularly evident during the fast movement (Figure 6.5 and 6.6). The sequential "wave of activation" present during the slow movements became disordered as movement speed was increased. During fast movements, the assistant mover segments within pectoralis major were activated significantly later than the prime mover segments changing the relative timing of their activation. In contrast to the spreading out of segment onset times, On*N*%MT values were compressed during the slow speed movement. This indicates that the CNS may initially prioritise the activation of only the essential (i.e. prime mover) muscle segments to commence the movement during ballistic movements, perhaps due to the imposed time constraints. It is the author's opinion that this form of relative disordering is a direct reflection of the differences in muscle segment fibre type composition and hence the neuromotor control of the muscle segments involved in producing the movement. Most notably, variation to the control of muscle segment onset

measures existed in the more centrally located muscle segments that exhibit slower segment contractile properties. This finding appears logical when coupled with the finding of homogeneous myoelectric peak activity. The CNS must manipulate the onset of these slower contracting segments, especially during fast movements, in order to allow enough time for all segments to achieve a uniform peak of muscle activity that occurs just prior to force peak.

When movement speed is varied, from slow to fast, a morphing of the electrical activation pattern occurs, changing from a single burst pattern to a triphasic burst pattern. This morphing has been identified to occur on a gradual basis as the movements become faster, rather than at a set movement speed (Brown and Gilleard 1991). All components of the triphasic EMG pattern (AG1 / ANT / AG2) are observable during ballistic movement (movements taking less than <400ms to complete). The presence of triphasic EMG patterns from individual muscle segments has been reported by Wickham (2002), showing that two non-continuous EMG bursts were present within the agonist prime movers segments, but not the assistant mover segments, during ballistic shoulder adduction movements. The EMG traces of the prime mover segments investigated within this study exhibited burst patterns resembling those of Wickham (2002), although this was only assessed through a qualitative approach.

The presence of variations in displacement properties, myoelectric properties and EMG burst patterns between adjacent muscle segments from within the same skeletal muscle confirms the notion that the CNS considers individual muscle segments as sub-volumes of muscle tissue that require individual neuromotor control – that they are, in effect, muscles within muscles.

Limitations

The results of the thesis need to be interpreted with full regard to the limitations of the studies. Firstly, in reference to the MMG experiments, the contractions were electrically induced rather than voluntarily performed. Furthermore, the size and placement of the surface stimulation electrodes, as well as the voltage delivered, meant that adjacent muscle segments often received some stimulation. While we cannot discount the possibility that the mechanical movement of adjacent muscle tissue may have influenced a particular segment's Laser-MMG waveforms, it appeared unavoidable if we were to ensure that the particular segment being investigated was fully stimulated. Attempts to minimise the spread of the PNS current, by using smaller electrodes and inter-electrode distances, resulted in discomfort for the subject and the practice was discontinued. Further work is warranted to determine the specific effects of movement within adjacent muscle segments on the Laser-MMG waveform.

Secondly, the thesis specifically addressed the effects of external stressors (e.g. temperature and fatigue) on the MMG waveforms obtained from animal muscle. In the human muscle experiments that followed, protocols designed to limit such effects were put in place. These protocols specified restricted physical activity prior to testing and controlled laboratory temperatures. Whilst levels of subject physical activity, and hence fatigue status prior to testing was strictly controlled, intramuscular temperature monitoring was beyond the capabilities of the laboratory.

Thirdly, the effects of factors such as subcutaneous fat, on the derived Laser-MMG waveforms, have not been assessed in this data set. While our own observations that increased subcutaneous fat attenuates MMG waveforms are in agreement with published reports (Beck, Housh *et al.* 2005), the relatively homogenous somatotype of our subjects may have negated this as a confounding variable.

Fourthly, the problem of crosstalk between adjacent bipolar electrode pairs needs to be addressed. If detectable levels of crosstalk were present, the ability to differentiate between

the activities of adjacent muscle segments would be compromised. Considerable effort, in line with Winter, Fuglevand *et al.*(1994), was made to minimise the effects of electrode crosstalk. The bipolar electrodes were specifically designed to have small active plates (1.6 mm in diameter) and inter-electrode distances (6.5 mm). This electrode design, using the crosstalk "rule of thumb" reported by Basmajian and DeLuca (1985), would suggest meaningful pickup of muscle fibre activity only within approximately 6.5 mm of each bipolar electrode pair. Adjacent bipolar electrode pairs were generally spaced more than 1 cm from each other so as to minimise, as much as practicable, electrode crosstalk. It is considered that, regardless of possible electrode crosstalk, the results presented here provide strong evidence of the sequential activation of adjacent muscle segments to control the isometric adduction task. It would have been expected that high levels of electrode crosstalk would have negated the possibility of this result.

Finally, the association between a muscle segment's contractile properties and its fibre type composition is only inferred. Due to ethical restrictions on human experimentation, multiple muscle biopsies to determine actual muscle fibre type compositions for each muscle segment investigated were not performed. Assumptions with regards to fibre type composition were made on the basis of the work of Dahmane, Djordjevic *et al.* (2005; 2006), who showed significant correlations between the percentage of type I muscle fibres and contraction time, both at the surface and within deep regions of the muscle.

Conclusion

The results of this investigation suggest that individual muscle segments could be functionally classified as prime movers, synergists and antagonists, that the functional role of an individual segment is reflected by its contractile properties and that segmental motor unit activation is not homogenous across the breadth of the human gluteus maximus, pectoralis major, deltoid and latissimus dorsi muscles. These results also supported the contention that individual skeletal muscles are composed of discrete sub-volumes (segments) of muscle tissue which may be independently controlled by the CNS to produce the desired motor outcome. The timing of muscle segment activation was highly coordinated both within and between muscles and specifically for the pectoralis major, varying the speed of movement has disordering effects on muscle segment activation, creating implications for the neuromotor control of movement by the CNS. These findings are important in that they suggest that the degrees of freedom problem in motor control is more complex given that individual muscle segments within a single muscle may show different patterns of muscle activation, both when producing different movements and during the same movement when performed at different speeds.

REFERENCES

Abernethy, P., Wilson, G. and Logan, P. (1995). Strength and power assessment. *Sports Medicine* **19**: 401-417.

Akataki, K., Mita, K., Itoh, K., Suzuki, N. and Watakabe, M. (1996). Acoustic and electrical activities during voluntary isometric contraction of biceps brachii muscles in patients with spastic cerebral palsy. *Muscle and Nerve* **19**: 1252-1257.

Akataki, K., Mita, K., Watakabe, M. and Itoh, K. (2003). Mechanomyographic responses during voluntary ramp contractions of the human first dorsal interosseus muscle. *European Journal of Applied Physiology* **89**: 520-525.

Allen, D. (2004). Skeletal muscle function: Role of ionic changes in fatigue, damage and disease. *Clinical and Experimental Pharmacology and Physiology* **31**: 485-493.

Allen, D., Lannergren, J. and Westerblad, H. (1995). Muscle cell function during prolonged activity: cellular mechanisms of fatigue (Review). *Experimental Physiology* **80**(4): 497-527.

Angel, R.W. (1977). Antagonist muscle activity during rapid arm movements: central versus proprioceptive influences. *Journal of Neurology, Neurosurgery and Psychiatry* **40**: 683-686.

Angel, R.W. (1981). Electromyographic patterns during ballistic movements in normals and hemiplegic patients. *Progress in Clinical Neurophysiology* **9**: 347-357.

Arendt-Nielsen, L., Mills, K.R. and Forster, A. (1989). Changes in muscle fiber conduction velocity, mean power frequency, and mean EMG voltage during prolonged submaximal contractions. *Muscle and Nerve* **12**: 493-497.

Ariano, M.A., Armstrong, R.B. and Edgerton, V.R. (1973). Hindlimb muscle fiber populations of five mammals. *Journal of Histochemistry and Cytochemistry* **21**(1): 51-55.

Asmussen, E. (1979). Muscle fatigue. *Medicine and Science in Sports* **11**(4): 313-321.

Asmussen, G. and Gaunitz, U. (1981). Mechanical properties of the isolated inferior oblique muscle of the rabbit. *Pflugers Archives* **392**: 183-190.

Asmussen, G. and Gaunitz, U. (1989). Temperature effects on isometric contractions of slow and fast twitch muscles of various rodents dependence on fibre type composition: a comparative study. *Biomedica Biochimica Acta* **48**: 536-541.

Barany, M. (1967). ATPase activity of myosin correlated with speed of muscle shortening. *Journal of General Physiology* **50**: 197-218.

Barnett, C., Kippers, V. and Turner, P. (1995). Effects of variations of the bench press exercise on the EMG activity of five shoulder muscles. *Journal of Strength and Conditioning Research* **9**: 222-227.

Barrata, R. (1995). Architecture-based force-velocity models of load-moving skeletal muscles. *Clinical Biomechanics* **10**(3): 149-155.

Barry, D.T., Leonard, J.A., Gitter, A.J. and Ball, R.D. (1986). Acoustic myography as a control signal for an externally powered prosthesis. *Archives of Physical Medicine and Rehabilitation* **67**(4): 267-269.

Basmajian, J.V. and DeLuca, C.J. (1985). Muscle Alive; Their Functions Revealed by Electromyography. Williams & Wilkins, Sydney.

Beck, T.W., Housh, T.J., Cramer, J.T., Weir, J.P., Johnson, G.O., Coburn, J.W., Malek, M.H. and Mielke, M. (2005). Mechanomyographic amplitude and frequency responses during dynamic muscle actions: a comprehensive review. *Biomedical Engineering Online* **4**: 67.

Bellemare, F., Woods, J.J., Johansson, R. and Bigland-Ritchie, B. (1983). Motor-unit discharge rates in maximal voluntary contractions of three human muscles. *Journal of Neurophysiology* **50**: 1380-1392.

Bennett, A.F. (1984). Thermal dependence of muscle function. *American Journal of Physiology* **247**: 217-229.

Bennett, A.F. (1985). Temperature and muscle. *Journal of Experimental Biology* **115**(1): 333-344.

Berardelli, A., Hallett, M., Rothwell, J.C., Agostino, R., Manfredi, M., Thompson, P.D. and Marsden, C.D. (1996). Single-joint rapid arm movements in normal subjects and in patients with motor disorders. *Brain* **119**(2): 661-674.

Bern, R.M. and Levy, M.N. (1990). Principles of Physiology. The C.V. Mosby Company, St Louis.

Bernstein, N.A. (1967). The coordination and regulation of movements. Pergamon, New York.

Bershitsky, S.Y. and Tsaturyan, A.K. (2002). The elementary force generation process probed by temperature and length perturbations in muscle fibres from the rabbit. *Journal of Physiology (London)* **540**(3): 971-988.

Bichler, E. and Celichowski, J. (2001a). Mechanomyographic signals generated during unfused tetani of single motor units in the rat medial gastrocnemius muscle. *European Journal of Applied Physiology* **85**: 513-520.

Bichler, E. and Celichowski, J. (2001b). Changes in the properties of mechanomyographic signals and in the tension during the fatigue test of rat medial gastrocnemius muscle motor units. *Journal of Electromyography and Kinesiology* **11**: 387-394.

Bigland-Ritchie, B., Thomas, C.K., Rice, C.L., Howarth, J.V. and Woods, J.J. (1992). Muscle temperature, contractile speed, and motoneuron firing rates during human voluntary contractions. *Journal of Applied Physiology* **73**(6): 2457-61.

Bigland-Ritchie, B.R. and Woods, J.J. (1984). Changes in muscle contractile properties and neural control during human muscle fatigue. *Muscle and Nerve* **7**: 691-699.

Binder, M.C., Bawa, P., Ruenzel, P. and Henneman, E. (1983). Does orderly recruitment of motoneurons depend on the existence of different types of motor units? *Neuroscience Letters* **36**(1): 55-58.

Bonner, J. and Pollard, J.A. (2003). Myosin ATPase Staining Procedure: Nerve and Muscle Staining Manual. Institute of Clinical Neurosciences, Royal Price Alfred Hospital, Sydney.

Bottinelli, R. and Reggiani, C. (2000). Human skeletal muscle fibres: molecular and functional diversity. *Progress in Biophysics and Molecular Biology* **73**: 195-262.

Brooke, M. and Kaiser, K. (1970). Muscle fibre types: How many and what kind? *Archives of Neurology* **23**: 369-379.

Brooks, G., Fahey, T., White, T. and Baldwin, K. (2000). Exercise Physiology: Human bioenergetics and its applications. Mayfield Publishing Company, California, USA.

Brooks, V.B. (1986). The Neural Basis of Motor Control. Oxford University Press, USA.

Brown, J.M.M. and Gilleard, W. (1991). Transition from slow to ballistic movement: development of triphasic electromyogram patterns. *European Journal of Applied Physiology* **63**(5): 381-386.

Brown, J.M.M., Solomon, C. and Paton, M. (1993). Further evidence of functional differentiation within biceps brachii. *Electromyography and Clinical Neurophysiology* **33**: 1-8.

Brown, J.M.M., Wickham, J.B., McAndrew, D.J. and Huang, X.-F. (2007). Muscles within muscles: Coordination of 19 muscle segments within three shoulder muscles during isometric motor tasks. *Journal of Electromyography and Kinesiology* **17**: 57-73.

Buchanan, T.S., Almdale, D.P., Lewis, J.L. and Rymer, W.Z. (1986). Characteristics of synergic relations during isometric contractions of human elbow muscles. *Journal of Neurophysiology* **56**(5): 1225-1241.

Bull, M.L., De Freitas, V. and Vitti, M. (1989). Electromyographic study of the trapezius (pars superior) and serratus anterior (pars inferior) muscles in free movements of the shoulder. *Electromyography and Clinical Neurophysiology* **29**: 119-125.

Bull, M.L., Vitti, M. and De Freitas, V. (1990). Electromyographic study of the trapezius (pars superior) and serratus anterior (pars inferior) in free movements of the arm. *Annals of Anatomy* **171**: 125-133.

Buller, A.J., Dornhorst, A.C., Edwards, R., Kerr, D. and Whelan, R.F. (1959). Fast and slow muscles in mammals. *Nature* **183**: 1516-1517.

Burke, R.E. (1978). Motor Units: Physiological/Histochemical Profiles, Neural Connectivity and Functional Specializations. *American Zoologist* **18**(1): 127-134.

Burke, R.E., Levine, D.N., Salcman, M. and Tsairis, P. (1974). Motor units in cat soleus muscle: physiological, histochemical and morphological characteristics. *Journal of Physiology* **238**(3): 503-14.

Burke, R.E., Levine, D.N., Tsairis, P. and Zajac, F.E. (1973). Physiological types and histochemical profiles in motor units of the cat gastrocnemius. *Journal of Physiology* **234**(3): 723-48.

Burke, R.E., Levine, D.N. and Zajac, F.E. (1971). Mammalian motor units: Physiological-histochemical correlation in three types in cat gastrocnemius. *Science* **174**: 709-712.

Burke, R.E. and Tsairis, P. (1973). Anatomy and innervation ratios in motor units of cat gastrocnemius. *Journal of Physiology* **234**: 749-765.

Burnham, R., Martin, T., Stein, R., Bell, G., MacLean, I. and Steadward, R. (1997). Skeletal muscle fibre type transformation following spinal cord injury. *Spinal Cord* **35**(2): 86-91.

Cady, E., Elshove, H., Jones, D. and Moll. (1989b). The metabolic causes of slow relaxation in fatigued human skeletal muscle. *Journal of Physiology* **418**: 327-37.

Cady, E., Jones, D., Lynn, J. and Newham, D. (1989a). Changes in force and intracellular metabolites during fatigue of human skeletal muscles. *Journal of Physiology* **418**: 311-25.

Cavanagh, P.R. and Komi, P.V. (1979). Electromechanical delay in human skeletal muscle under concentric and eccentric contractions. *European Journal of Applied Physiology* **42**: 159-163.

Cescon, C., Farina, D., Gobbo, M., Merletti, R. and Orizio, C. (2004). Effect of accelerometer location on mechanomyogram variables during voluntary, constant force contractions in three human muscles. *Medical and Biological Engineering and Computing* **42**: 121-127.

Christou, E.A., Shinohara, M. and Enoka, R.M. (2001). The changes in EMG and steadiness with variation in movement speed for concentric and eccentric contractions. 25th American Society of Biomechanics, San Diego, CA.

Close, R. (1965). The relation between intrinsic speed of shortening and duration of the active state of muscle. *Journal of Physiology (London)* **180**: 542-559.

Close, R. (1972). Dynamic properties of mammalian skeletal muscles. *Physiological Reviews* **52**(1): 129-183.

Close, R. and Hoh, J.F.Y. (1968). Influence of temperature on isometric contractions of rat skeletal muscles. *Nature* **217**(5134): 1179-1180.

Crosby, P. (1978). Use of surface electromyography as a measure of dynamic force in human limb muscles. *Medical & Biological Engineering & Computing* **16**: 519-524.

Crouch, J.E. (1985). Functional Human Anatomy. Lea & Febiger, Philadelphia.

Dahmane, R., Djordjevic, S., Simunic, B. and Valencic, V. (2005). Spatial fiber type distribution in normal human muscle: Histochemical and tensiomyographical evaluation. *Journal of Biomechanics* **38**(12): 2451-2459.

Dahmane, R., Djordjevic, S. and Smerdu, V. (2006). Adaptive potential of human biceps femoris muscle demonstrated by histochemical, immunohistochemical and mechanomyographical methods. *Medical & Biological Engineering & Computing* **44**(11): 999-1006.

Dahmane, R., Valencic, V., Knez, N. and Erzen, I. (2001). Evaluation of the ability to make non-invasive estimation of muscle contractile properties on the basis of the muscle belly response. *Medical and Biological Engineering and Computing* **39**(1): 51-55.

De la Barrera, E.J. and Milner, T.E. (1994). The effects of skinfold thickness on the selectivity of surface EMG. *Electroencephalography and Clinical Neurophysiology* **93**: 91-99.

De Ruiter, C.J. (1996). Blood flow occlusion, maximal force production and EMG in two rat gastrocnemius muscle compartments. *European Journal of Physiology* **433**: 166-173.

De Ruiter, C.J., De Haan, A. and Sargeant, A.J. (1995a). Repeated force production and metabolites in two medial gastrocnemius muscle compartments of the rat. *Journal of Applied Physiology* **79**(6): 1855-1861.

De Ruiter, C.J., De Haan, A. and Sargeant, A.J. (1995b). Physiological characteristics of two extreme muscle compartments in gastrocnemius medialis of the anesthetized rat. *Acta Physiologica Scandinavica* **153**(4): 313-324.

De Ruiter, C.J., De Haan, A. and Sargeant, A.J. (1996). Fast twitch muscle unit properties in different rat medial gastrocnemius muscle compartments. *Journal of Neurophysiology* **75**(6): 2243-2254.

Desmedt, J.E. and Godaux, E. (1981). Spinal motoneuron recruitment in man: deordering with direction but not with speed of voluntary movement. *Science* **214**: 933-936.

Djordjevic, S., Valencic, V. and Jurcic-Zlobec, B. (2001). The comparison of dynamic characteristics of skeletal muscles in two groups of sportsmen - sprinters and cyclists. *Biomedical Engineering* **3**: 1 - 4.

Emanuel, M. (1972). Mechanomyography of the external urethral sphincter. *Journal of Urology* **107**(5): 795-801.

English, A.W. and Weeks, O.I. (1984). Compartmentalization of single muscle units in cat lateral gastrocnemius. *Experimental Brain Research* **56**: 361-368.

English, A.W., Wolf, S.L. and Segal, R.L. (1993). Compartmentalisation of muscles and their motor nuclei: The partitioning hypothesis. *Physical Therapy* **73**(12): 857-67.

Esposito, F., Orizio, C. and Veicsteinas, A. (1998). Electromyogram and mechanomyogram changes in fresh and fatigued muscle during sustained contraction in men. *European Journal of Applied Physiology* **78**: 494-501.

Ettema, G.J.C., Styles, G. and Kippers, V. (1998). The moment arms of 23 muscle segments of the upper limb with varying elbow and forearm positions: Implications for motor control. *Human Movement Science* **17**(2): 201-220.

Flanders, M. and Soechting, J.F. (1990). Arm muscle activation for static forces in three-dimensional space. *Journal of Neurophysiology* **64**: 1818–1836.

Frangioni, J.V., Kwan-Gett, T.S., Dobrunz, L.E. and McMahon, T.A. (1987). The mechanism of low-frequency sound production in muscle. *Biophysical Journal* **51**(5): 775-83.

Gillis, J.M. (1985). Relaxation of vertebrate skeletal muscle. A synthesis of the biochemical and physiological approaches. *Biochimica Et Biophysica Acta* **811**(2): 97-145.

Gollnick, P.D., Piehl, K., Saubert, C.W.t., Armstrong, R.B. and Saltin, B. (1972). Diet, exercise, and glycogen changes in human muscle fibers. *Journal of Applied Physiology* **33**(4): 421-5.

Gorelick, M. (2005). Location of Injury Site in Chronic Low Back Pain Patients: An Electromyographic and Mechanomyographic Analysis. Department of Biomedical Science. University of Wollongong. Wollongong. PhD.

Gorelick, M.L. and Brown, J.M.M. (2007). Mechanomyographic assessment of contractile properties within seven segments of the human deltoid muscle. *European Journal of Applied Physiology* **100**(1): 35-44.

Gottlieb, G.L., Corcos, D.M. and Agarwal, G.C. (1989). Organising principles for single joint movement: A speed-insensitive strategy. *Journal of Neurophysiology* **63**: 625-636.

Guyton, A.C. and Hall, J.E. (2000). Textbook of medical physiology. W.B. Saunders Company, Philadelphia, Pennsylvania.

Hansson, G.-Å., Strömberg, U., Larsson, B., Ohlsson, K., Balogh, I. and Moritz, U. (1992). Electromyographic fatigue in neck/shoulder muscles and endurance in women with repetitive work. *Ergonomics* **35**: 1341-1352.

Hay, L. and Bard, C. (1984). The role of movement speed in learning a visuo-manual coordination in children. *Psychological Research* **V46**(1): 177-186.

Hebel, R. and Stromberg, M.W. (1986). Anatomy and Embryology of the Laboratory Rat. BioMed Verlag, Worthsee, FRG.

Henneman, E. and Mendell, L.M. (1981). Functional organisation of motoneuron pool and its inputs. Handbook of Physiology. The nervous system II. B. MD. The American Physiological Society**:** 423-507.

Henneman, E., Somjen, G. and Carpenter, D.O. (1965). Excitability and inhibitability of motoneurons of different sizes. *Journal of Neurophysiology* **28**: 599-620.

Henneman, E., Somjen, G. and Carpenter, D.O. (1965a). Functional significance of cell size in spinal motoneurons. *Journal of Neurophysiology* **28**: 560-581.

Henriksson-Larsen, K., Lexell, J.K. and Sjostrom, M. (1983). Distribution of different fibre types in human skeletal muscle. 1. Method for the preparation and analysis of cross-sections of the whole tibialis anterior. *Histochemical Journal* **15**: 167-178.

Heslinga, J.W. and Huijing, P.A. (1990). Effects of growth on architecture and functional characteristics of adult rat gastrocnemius muscle. *Journal of Morphology* **206**: 119-132.

Hodgson, J.A. (1983). The relationship between soleus and gastrocnemius muscle activity in conscious cats - a model for motor unit recruitment? *Journal of Physiology* **337**: 553–562.

Hoffer, J.A., Loeb, G.E., Marks, W.B., O'Donovan, M.J., Pratt, C.A. and Sugano, N. (1987). Cat hindlimb motoneurons during locomotion. I. Destination, axonal conduction velocity, and recruitment threshold. *Journal of Neurophysiology* **57**(2): 510-529.

Hoffer, J.A., Loeb, G.E., Marks, W.B. and Sugano, N. (1983). Orderly recruitment of cat hindlimb motoneurons during locomotion. *Electroencephalography and Clinical Neurophysiology* **56**(3): S100-S101.

Hoffer, J.A., Loeb, G.E., Sugano, N., Marks, W.B., O'Donovan, M.J. and Pratt, C.A. (1987). Cat hindlimb motoneurons during locomotion. III. Functional segregation in sartorius. *Journal of Neurophysiology* **57**(2): 554-562.

Hoffer, J.A., Sugano, N., Loeb, G.E., Marks, W.B., O'Donovan, M.J. and Pratt, C.A. (1987). Cat hindlimb motoneurons during locomotion. II. Normal activity patterns. *Journal of Neurophysiology* **57**(2): 530-553.

Hortobagyi, T., Dempsey, L., Fraser, D., Zheng, D., Hamilton, G., Lambert, J. and Dohm, L. (2000). Changes in muscle strength, muscle fibre size and myofibrillar gene expression after immobilization and retraining in humans. *Journal of Physiology* **524**(1): 293-304.

Huijing, P., Van Lookeren Campagne, A. and Koper, J. (1989). Muscle architecture and fibre characteristics of rat gastrocnemius and semimembranosus muscles during isometric contractions. *Acta Anatomica* **135**(1): 46-52.

Huijing, P.A., Nieberg, S.M., vd Veen, E.A. and Ettema, G.J. (1994). A comparison of rat extensor digitorum longus and gastrocnemius medialis muscle architecture and length-force characteristics. *Acta Anatomica* **149**(2): 111-20.

Iqbal, K. and Hemami, H. (1996). An investigation into the execution of human skilled movements. 3rd International conference on signal processing, Beijing, China.

Jenkins, D.B. (1998). Hollinshead's Functional Anatomy of the Limbs and Back. W. B. Saunders Company, Philadelphia.

Jennekens, F., Tomlinson, B. and Walton, J. (1971). Data on the distribution of fibre types in five human limb muscles: An autopsy study. *Journal of Neurological Sciences* **14**: 245-257.

Johnson, G. and Bogduk, N. (1994). Anatomy and actions of the trapezius muscle. *Clinical Biomechanics* **9**: 44-50.

Johnson, M.A., Polgar, J., Weightman, D. and Appleton, D. (1973). Data on the distribution of fibre types in thirty six human muscles: an autopsy study. *Journal of the Neurological Sciences* **18**: 111-129.

Kanda, K., Burke, R.E. and Walmsley, B. (1977). Differential control of fast and slow twitch motor units in the decerebrate cat. *Experimental Brain Research* **29**(1): 57-74.

Kanda, K. and Hashizume, K. (1992). Factors causing difference in force output among motor units in the rat medial gastrocnemius muscle. *Journal of Physiology* **448**: 677-95.

Kapandji, I.A. (1982). The Physiology of the Joints: Upper Limb. Churchill Livingstone.

Kelly, D.L. (1971). Kinesiology: Fundamentals of Motion Description. Prentice-Hall Inc., New Jersey.

Kido, T., Itoi, E., Lee, S., Neale, P.G. and An, K. (2003). Dynamic stabilizing function of the deltoid muscle in shoulders with anterior instability. *American Journal of Sports Medicine* **31**(3): 399-403.

Kimura, T., Hamada, T., Massako Ueno, L. and Moritani, T. (2003). Changes in contractile properties and neuromuscular propagation evaluated by simultaneous mechanomyogram and electromyogram during experimentally induced hypothermia. *Journal of Electromyography and Kinesiology* **13**(5): 433-40.

Koh, T.J. and Gradiner, M.D. (1993). Evaluation of methods to minimise crosstalk in surface electromyography. *Journal of Biomechanics* **26**(Supp 1): 151-157.

Kouzaki, M., Shinohara, M. and Fukunaga, T. (1999). Non-uniform mechanical activity of quadriceps muscle during fatigue by repeated maximal voluntary contraction in humans. *European Journal of Applied Physiology* **80**: 9-15.

Kraemer, W.J., Staron, R.S., Gordon, S.E., Volek, J.S., Koziris, L.P., Duncan, N.D., Nindl, B.C., GÃmez, A.L., Marx, J.O., Fry, A.C. and Murray, J.D. (2000). The effects of 10 days of spaceflight on the shuttle Endeavour on predominantly fast-twitch muscles in the rat. *Histochemistry and Cell Biology* **114**(5): 349-355.

Kuo, K.H.M. and Clamann, H.P. (1981). Coactivation of synergistic muscles of different fibre types in fast and slow contractions. *American Journal of Physical Medicine* **60**(5): 219-238.

Lannergren, J. and Westerblad, H. (1991). Force decline due to fatigue and intracellular acidification in isolated fibres from the mouse skeletal muscle. *Journal of Physiology* **434**: 307-322.

Larrson, L., Sjodin, B. and Karlsson, J. (1978). Histochemical and biochemical changes in human skeletal muscle with age in sedentary male age 22-65 years. *Acta Physiologica Scandinavica* **103**: 31-39.

LeBozec, S. and Maton, B. (1987). Differences between motor unit firing rates, twitch characteristics and fibre type composition in an agonistic muscle group in man. *European Journal of Applied Physiology & Occupational Physiology* **56**(3): 350-5.

Lexell, J.K., Henriksson-Larsen, K. and Sjostrom, M. (1983a). Distribution of different fibre types in human skeletal muscle- Effects of aging studied in the whole cross sections. *Muscle and Nerve* **6**: 85-100.

Lexell, J.K., Henriksson-Larsen, K. and Sjostrom, M. (1983b). Distribution of different fibre types in human skeletal muscles: A study of cross sections of whole muscle vastus lateralis. *Acta Physiologica Scandinavica* **117**: 115-122.

Lexell, J.K., Taylor, C. and Sjostrom, M. (1985). Analysis of sampling errors in biopsy techniques using data from whole muscle cross-sections. *Journal of Applied Physiology* **59**(4): 1228-1235.

Lieber, R.L. and Friden, J. (2000). Functional and clinical significance of skeletal muscle architecture. *Muscle and Nerve* **23**: 1647-1666.

Linder, A., Dag, S., Marti-Korff, S., Quiroz-Rothe, E., Rivero, J. and Drommer, W. (2002). Effects of repeated biopsying on muscle tissue in horse. *Equine Veterinary Journal* **34**(6): 619-624.

Loeb, G.E. (1985). Motoneurone task groups: coping with kinematic heterogeneity. *Journal of Experimental Biology* **115**: 137-46.

Loeb, G.E. (1987). Hard lessons in motor control from the mammalian spinal cord. *Trends in the Neurosciences* **10**: 108-113.

Loughlin, M. (1993). Muscle Biopsy, A Laboratory Investigation. Butterworth-Heinemann Ltd, Oxford, England.

Lynn, P.A., Bettles, N.D., Hughes, A.D. and Johnson, S.W. (1978). Influence of electrode geometry on bipolar recordings of the surface electromyogram. *Medical & Biological Engineering & Computing* **16**: 651-660.

Lyons, K., Perry, J., Gronley, J., Barnes, L. and Antonelli, D. (1983). Timing and relative intensity of hip extensor and abductor muscle action during level and stair ambulation. *Physical Therapy* **64**: 1597-1606.

MacConaill, M.A. and Basmajian, J.V. (1977). Muscles and Movements: A Basis for Human Kinesiology. Robert E. Krieger Publishing Co. Inc., New York.

MacDougall, J.D., Elder, G.C., Sale, D.G., Moroz, J.R. and Sutton, J.R. (1980). Effects of strength training and immobilization on human muscle fibres. *European Journal of Applied Physiology & Occupational Physiology* **43**(1): 25-34.

MacIntosh, B.R. (2003). Role of Calcium Sensitivity Modulation in Skeletal Muscle Performance. *News in Physiological Sciences* **18**(6): 222-225.

Mahon, M., Toman, A., William, P. and Bagnall, K. (1984). Variability of histochemical and morphometric data from needle biopsy specimens of the quadriceps femoris muscle. *Journal of the Neurological Sciences* **63**: 85-100.

Malinchik, S., Xu, S. and Yu, L.C. (1997). Temperature-induced structural changes in the myosin thick filament of skinned rabbit psoas muscle. *Biophysical Journal* **73**: 2304-2312.

Mannion, A.F. (1999). Fibre type characteristics and function of the human paraspinal muscles: normal values and changes in association with lower back pain (Review). *Journal of Electromyography and Kinesiology* **9**: 363-377.

Mannion, A.F., Dumas, G.A., Cooper, R.G., Espinosa, F.J., Faris, M.W. and Stevenson, J.M. (1997). Muscle fibre size and type distribution in thoracic and lumbar regions of erector spinae in healthy subjects without low back pain: normal values and sex differences. *Journal of Anatomy* **190**: 505-513.

Mannion, A.F., Kaser, L., Weber, E., Rhyner, A., Dvorak, J. and Muntener, M. (2000). Influence of age and duration of symptoms on fibre type distribution and size of the back muscle in chronic low back pain patients. *European Spine Journal* **4**: 273-81.

Mannion, A.f., Meier, M., Grob, D. and Muntener, M. (1998). Paraspinal muscle fibre type alterations associated with scoliosis: an old problem revisited with new evidence. *European Spine Journal* **7**: 289-293.

Mannion, A.F., Weber, B., Dvorak, J., Grob, D. and Muntener, M. (1997). Fibre type characteristics of the lumbar paraspinal muscles in healthy subjects and in patients with low back pain. *Journal of Orthopaedic Research* **15**: 881-887.

Manueddu, C., Blanc, W. and Taillard, W. (1989). Study of the functioning of the gluteus medius and maximus: an electromyographic analysis. *Ann. Kinesither* **16**: 193-201.

Marsh, E., Sale, D., McComas, A.J. and Quinlan, J. (1981). Influence of joint position on ankle dorsiflexion in humans. *Journal of Applied Physiology* **51**: 160-167.

Martini, F., Timmons, M. and McKinley, M. (2000). Human Anatomy. Prentice Hall, New Jersey, USA.

Maton, B. and Gamet, D. (1989). The fatigability of two agonistic muscles in human isometric voluntary submaximal contraction : an EMG study. *European Journal of Applied Physiology* **58**: 369-374.

McAndrew, D.J. and Brown, J.M.M. (2004). Muscles Within Muscles, Inter- and Intra-Muscle Segment Coordination. Australian Association of Exercise and Sports Science Inaugural Conference, Brisbane, Australia.

McAndrew, D.J., Rosser, N. and Brown, J.M.M. (2006). Mechanomyographic measures of muscle contractile properties are influenced by the duration of the stimulatory pulse. *Journal of Applied Research* **6**(2): 142-152.

McComas, A.J. (1996). Skeletal Muscle: Form and Function. Human Kinetics, Champaign.

McComas, A.J. and Thomas, H.C. (1968). Fast and slow twitch muscles in man. *Journal of the Neurological Sciences* **7**: 301-307.

Medler, S. (2002). Comparative trends in shortening velocity and force production in skeletal muscles. *American Journal of Physiology: Regulatory Integrative Comparative Physiology* **283**: 368 - 378.

Metral, S. and Cassar, G. (1981). Relationship between force and integrated EMG activity during voluntary isometric anisotonic contraction. *European Journal of Applied Physiology* **46**: 185-198.

Mirka, G.A. (1991). The quantification of emg normalization error. *Ergonomics* **34**(3): 343-352.

Miyamoto, N. and Oda, S. (2003). Mechanomyographic and electromyographic responses of the triceps surae during maximal voluntary contractions. *Journal of Electromyography and Kinesiology : Official Journal of the International Society of Electrophysiological Kinesiology* **13**(5): 451-9.

Nagesser, A.S., van der Laarse, W.J. and Elzinga, G. (1993). ATP formation and ATP hydrolysis during fatiguing, intermittent stimulation of different types of single muscle fibres from Xenopus laevis. *Journal of Muscle Research and Cell Motility* **14**: 608-618.

Nonaka, H., Mita, K., Akataki, K., Watakabe, M. and Yabe, K. (2000). Mechanomyographic investigation of muscle contractile properties in preadolescent boys. *Electromyography and Clinical Neurophysiology* **40**(5): 287-93.

Norman, R.W. and Komi, P.V. (1979). Electromechanical delay in skeletal muscle under normal movement conditions. *Acta Physiologica Scandinavica* **106**: 241–248.

Orizio, C. (1993). Muscle sound: bases for the introduction of a mechanomyographic signal in muscle studies. *Critical Reviews in Biomedical Engineering* **21**(3): 201 - 243.

Orizio, C., Baratta, R.V., Zhou, B.H., Solomonow, M. and Veicsteinas, A. (1999). Force and surface mechanomyogram relationship in cat gastrocnemius. *Journal of Electromyography and Kinesiology* **9**(2): 131-40.

Orizio, C., Baratta, R.V., Zhou, B.H., Solomonow, M. and Veicsteinas, A. (2000). Force and surface mechanomyogram frequency responses in cat gastrocnemius. *Journal of Biomechanics* **33**(4): 427-33.

Orizio, C., Baratta, R.V., Zhou, B.H., Solomonow, M. and Veicsteinas, A. (2000). Force and surface mechanomyogram relationship in cat gastrocnemius. *Journal of Biomechanics* **9**: 131 - 140.

Orizio, C., Diemont, B., Esposito, F., Alfonsi, E., Parrinello, G., Moglia, A. and Veicsteinas, A. (1999). Surface mechanomyogram reflects the changes in the mechanical properties of muscle at fatigue. *European Journal of Applied Physiology & Occupational Physiology* **80**(4): 276-84.

Orizio, C., Gobbo, M., Diemont, B., Esposito, F. and Veicsteinas, A. (2003). The surface mechanomyogram as a tool to describe the influence of fatigue on biceps brachii motor unit activation strategy. Historical basis and novel evidence. *European Journal of Applied Physiology* **90**: 326-336.

Orizio, C., Gobbo, M., Veicsteinas, A., Baratta, R.V., Zhou, B.H. and Solomonow, M. (2003). Transients of the force and surface mechanomyogram during cat gastrocnemius tetanic stimulation. *European Journal of Applied Physiology and Occupational Physiology* **88**(6): 601-6.

Orizio, C., Liberati, D., Locatelli, C., De Grandis, D. and Veicsteinas, A. (1996). Surface mechanomyogram reflects muscle fibres twitches summation. *Journal of Biomechanics* **29**(4): 475-81.

Pare', E.B., Stern, J.R. and Schwartz, J.M. (1981). Functional differentiation within the tensor fascia latae; a telemetered electromyographic analysis of its locomotor roles. *Journal of Bone and Joint Surgery* **63a**(9): 1457-1471.

Paton, M.E. and Brown, J.M.M. (1994). An electromyographic analysis of functional differentiation in human pectoralis major muscle. *Journal of Electromyography and Kinesiology* **4**(3): 161-169.

Paton, M.E. and Brown, J.M.M. (1995). Functional differentiation within latissimus dorsi. *Electromyography & Clinical Neurophysiology* **35**(5): 301-9.

Perry Rana, S.R., Housh, T.J., Johnson, G.O., Bull, A.J. and Cramer, J.T. (2003). MMG and EMG responses during 25 maximal, eccentric, isokinetic muscle actions. *Medicine and Science in Sports and Exercise* **35**(12): 2048-2054.

Perry-Rana, S.R., Housh, T.J., Johnson, G.O., Bull, A.J., Berning, J.M. and Cramer, J.T. (2002). MMG and EMG responses during fatiguing isokinetic muscle contractions at different velocities. *Muscle and Nerve* **26**: 367-373.

Phillips, K. (2005). Muscles within muscle: A laser-based mechanomyographic analysis of contractile properties within the segments of the rat medial gastrocnemius muscle. Department of Biomedical Science. University of Wollongong. Wollongong. B.Sc. (Hons)

Piacentini, S.C. and Berzin, F. (1989). Electromyographic study of the upper, middle and lower portion of the trapezius in the circumduction movement of the arm on a shoulder wheel apparatus. *Electromyographic and Clinical Neurophysiology* **29**: 315-319.

Prezant, D.J., Richner, B., Valentine, D.E., Aldrich, T.K., Fishman, C.L., Nagashima, H., Chaudhry, I. and Cahill, J. (1990). Temperature dependence of rat diaphragm muscle contractility and fatigue. *Journal of Applied Physiology* **69**(5): 1740-1745.

Prodanov, D., Thil, M., Marani, E., Delbeke, J. and Holsheimer, J. (2005). Three-dimensional topography of the motor endplates of the rat gastrocnemius muscle. *Muscle & Nerve* **32**(3): 292-302.

Ranatunga, K.W. and Thomas, P.E. (1990). Correlation between shortening velocity, force-velocity relation and histochemical fibre-type composition in rat muscles. *Journal of Muscle Research & Cell Motility* **11**(3): 240-50.

Riek, S. and Bawa, P. (1992). Recruitment of motor units in human forearm extensors. *Journal of Neurophysiology* **68**(1): 100-107.

Rivero, J.-L.L., Talmadge, R.J. and Edgerton, V.R. (1999). Interrelationships of myofibrillar ATPase activity and metabolic properties of myosin heavy chain-based fibre types in rat skeletal muscle. *Histochemistry and Cell Biology* **111**(4): 277-287.

Rosser, N., McAndrew, D.J. and Iverson, D.C. (2005). Mechanomyography; Lasers for non-invasive quantification of muscle recovery from exercise induced fatigue. Australian Conference of Sports Medicine, Melbourne, Australia.

Sacks, R. and Roy, R. (1982). Architecture of the hind limb muscles of cats: functional significance. *Journal of Morphology* **173**(2): 185-95.

Sandstedt, P. (1981). Representativeness of a muscle specimen for the whole muscle. *Acta Neurologica Scand* **64**: 427-437.

Sandstedt, P., Nordell, L. and Henriksson, K. (1982). Quantitative analysis of muscle biopsies from volunteers and patients with neuromuscular disorders. *Acta Physiologica Scandinavica* **66**: 130-144.

Scheving, L.E. and Pauly, J.E. (1959). An electromyographic study of some muscles acting on the upper extremity of man. *Anatomical Record* **135**: 239-245.

Schuenke, M., Schulte, E. and Schumacher, U. (2006). Thieme Atlas of Anatomy. Thieme, New York.

Segal, R.L., Wolf, S.L., DeCamp, M.J., Chopp, M.T. and English, A.W. (1991). Anatomical partitioning of three multiarticular muscles. *Acta Anatomica* **142**: 261-266.

Shevlin, M.G., Lehmann, J.F. and Lucci, J.A. (1969). Electromyographic study of the function of some muscles crossing the glenohumeral joint. *Archives of Physical Medicine and Rehabilitation* **50**(5): 264-270.

Shinohara, M. and Sogaard, K. (2006). Mechanomyography for studying force fluctuations and muscle fatigue. *Exercise & Sport Sciences Reviews* **34**(2): 59-64.

Simoneau, J.-A. and Bouchard, C. (1989). Human variation in skeletal muscle fibre type proportion and enzyme activity. *American Journal of Physiology* **257**: E567-E572.

Snelson, L. (2003). Does muscle belly displacement correlate to physiological changes in the muscle? Department of Biomedical Science. University of Wollongong. Wollongong. B.SC. (Hons)

Soderberg, G.L. and Dostal, W.F. (1978). Electromyographic study of three parts of the gluteus medius muscle during functional activities. *Physical Therapy* **58**(6): 360-368.

Solomonow, M., Baratta, R., Bernardi, M., Zhou, B., Lu, Y., Zhu, M. and Acierno, S. (1994). Surface and wire EMG crosstalk in neighbouring muscles. *Journal of Electromyography and Kinesiology* **4**: 131-14.

Spector, S., Gardiner, P., Zernick, R., Roy, R. and Edergerton, V. (1980). Muscle Architecture and force-velocity characteristics of cat soleus and medial gastrocnemius: implications for motor control. *Journal of Neurophysiology* **44**(5): 951-60.

Staron, R.S., Kraemer, W.J., Hikida, R.S., Fry, A.C., Murray, J.D. and Campos, G.E.R. (1999). Fiber type composition of four hindlimb muscles of adult Fisher 344 rats. *Histochemistry and Cell Biology* **111**(2): 117-123.

Stephenson, D.G. and Williams, D.A. (1985). Temperature-dependent calcium sensitivity changes in skinned muscle fibres of rat and toad. *The Journal of Physiology (London)* **360**(1): 1-12.

Sugiura, M. and Kanda, K. (2004). Progress of age-related changes in properties of motor units in the gastrocnemius muscle of rats. *Journal of Neurophysiology* **92**: 1357-1365.

Ter Harr Romeny, B.M., Denier Van Der Gon, J.J. and Gielen, C.C.A.M. (1982). Changes in recruitment order of motor units in the human biceps muscle. *Experimental Neurology* **78**: 360-368.

Thomas, C.K., Sesodia, S., Erb, D.E. and Grumbles, R.M. (2003). Properties of medial gastrocnemius motor units and muscle fibers reinnervated by embryonic ventral spinal cord cells. *Experimental Neurology* **180**(1): 25-31.

Thomas, J.S., Schmidt, E.M. and Hambrecht, F.T. (1978). Facility of motor unit control during tasks defined directly in terms of unit behaviors. *Experimental Neurology* **59**(3): 384-97.

Ustunel, I., Akkoyunlu, G. and Demir, R. (2003). The effect of testosterone on gastrocnemius muscle fibres in growing and adult male and female rats: a histochemical, morphometric and ultrastructural study. *Anatomia, Histologia, Embryologia: Veterinary Medicine Series C* **32**(2): 70-9.

Valencic, V. and Djordjevic, S. (2001). Influence of acute physical exercise on twitch response elicited by stimulation of skeletal muscle in man. *Biomedical Engineering* **2**: 1 - 4.

Valencic, V., Knez, N. and Simunic, B. (2001). Tenziomyography (TMG): Detection of skeletal muscle response by means of radial muscle belly displacement. *Biomedical Engineering* **1**: 1 - 10.

Van Leeuwen, J.L. and Spoor, C.W. (1993). Modelling the pressure and force equilibrium in unipennate muscles with in-line tendons. *Philosophical transactions of the Royal Society of London- Series B: Biological Science* **342**(1302): 321-33.

Vasavada, A.N., Peterson, B.W. and Delp, S.L. (2002). Three-dimensional spatial tuning of neck muscle activation in humans. *Experimental Brain Research* **147**: 437-448.

Verburg, E., Thorud, H.M., Eriksen, M., Vollestad, N.K. and Sejersted, O.M. (2001). Muscle contractile properties during intermittent nontetanic stimulation in rat skeletal muscle. *American Journal of Physiology - Regulatory Integrative & Comparative Physiology* **281**(6): R1952-1965.

Wang, L.C. and Kernell, D. (2000). Proximo-distal organisation and fibre type regionalisation in rat hind limb muscles. *Journal of Muscle Research and Cell Motility* **21**(6): 587 - 598.

Wang, L.C. and Kernell, D. (2001). Quantification of fibre type regionalisation: an analysis of lower hindlimb muscles in the rat. *Journal of Anatomy* **198**(3): 295-308.

Watakabe, M., Mita, K., Akataki, K. and Itoh, K. (2003). Reliability of the mechanomyogram detected with an accelerometer during voluntary contractions. *Medical and Biological Engineering and Computing* **41**(2): 198-202.

Weeks, O.I. and English, A.W. (1985). Compartmentalisation of the cat lateral gastrocnemius motor nucleus. *Journal of Comparative Neurology* **235**(2): 255-67.

Westerblad, H., Allen, D.G., Bruton, J.D., Andrade, F.H. and Lannergren, J. (1998). Mechanisms underlying the reduction of isometric force in skeletal muscle fatigue. *Acta Physiologica Scandinavica* **162**: 253-260.

Westerblad, H., Bruton, J.D., Allen, D.G. and Lannergren, J. (2000). Functional significance of Ca^{2+} in long lasting fatigue of skeletal muscle. *European Journal of Applied Physiology* **83**: 166-174.

Wickham, J. and Brown, J.M.M. (1998). Muscles within muscles: the neuromotor control of intra-muscular segments. *European Journal of Applied Physiology* **78**: 219-225.

Wickham, J., Brown, J.M.M., Green, R. and McAndrew, D.J. (2004). Muscles within muscles: the classical triphasic EMG burst and its applicability to segments of large radiate agonist/antagonist muscles. *Journal of Musculoskeletal Research* **8**(2&3): 107-117.

Wickham, J.B. (2002). Muscles within Muscles: The neuromotor activation patterns of intramuscular segments. Department of Biomedical Science. University of Wollongong. Wollongong. Ph.D.

Wickham, J.B., Brown, J.M.M. and McAndrew, D.J. (2004). Muscles within muscles: anatomical and functional segmentation of selected shoulder joint musculature. *Journal of Musculoskeletal Research* **8**(1): 57-73.

Williams, P.L., Warwick, R., Dyson, M. and Bannister, L.H., Eds. (1995). Gray's Anatomy. Sydney, Churchill Livingston.

Winter, D.A., Fuglevand, A.J. and Archer, S.E. (1994). Crosstalk in surface electromyography: theoretical and practical estimates. *Journal of Electromyography and Kinesiology* **4**(1): 15-26.

Woittiez, R., Huijing, P. and Rozendal, R. (1983). Influence of muscles architecture on the length-force diagram of mammalian muscle. *Pflugers Archives - European Journal of Physiology* **399**(4): 275-9.

Wolf, S. and Kim, J. (1997). Morphological analysis of the human tibialis anterior and medial gastrocnemius muscle. *Acta Anatomica* **158**(4): 287-295.

Xu, S., Offer, G., Gu, J., White, H.D. and Yu, L.C. (2003). Temperature and ligand dependence of conformation and helical order in myosin filaments. *Biochemistry* **42**: 390-401.

Yoshitake, Y., Shinohara, M., Ue, H. and Moritani, T. (2002). Characteristics of surface mechanomyogram are dependent on development of fusion of motor units in humans. *Journal of Applied Physiology* **93**(5): 1744-1752.

Yoshitake, Y., Ue, H., Miyazaki, M. and Moritani, T. (2001). Assessment of lower-back muscle fatigue using electromyography, mechanomyography, and near-infrared spectroscopy. *European Journal of Applied Physiology and Occupational Physiology* **84**(3): 174-9.

Zhao, W.-P., Kawaguchi, Y., Matsui, H., Kanamori, M. and Kimura, T. (2000). Histochemistry and morphology of the multifidus muscle in lumbar disc herniation. *Spine* **25**(17): 2191-2199.

Zuurbier, C.J. and Huijing, P.A. (1993). Changes in geometry of actively shortening unipennate rat gastrocnemius muscle. *Journal of Morphology* **218**(2): 167-80.

APPENDIX A

MMG laser site and Microelectrode site identification

Pectoralis Major

1. Identify the Clavicle, marking the inferior border.
2. Identify the Sternal muscular attachment down to the Xiphoid Process.
3. Identify the lower rib leaving the Sternum. Immediately above this, identify the Intercostal space and the middle of the superior rib.
4. Mark from the Xiphoid Process to the muscular fold, along the superior rib.
5. Identify the intermuscular space between the Clavicular Head of pectoralis major and the anterior Head of the deltoid. This should be approximately 2/3 of the length of the Clavicle, moving laterally. Mark point A.
6. Measure from point A to the Sternoclavicular joint, mark point B. Mark 50% of this distance. This point is **P1**
7. Measure from point B inferiorly to the lateral aspect of the muscular fold, following the origin of the pectoralis major. Mark this point C. This is done by moulding solder wire to the shape of the muscles origin.
8. Cut the solder wire to this length and then divide this distance into four equal compartments.
9. Identify the middle of each individual compartment, marking the points on the solder wire. Mould the solder wire back onto the origin, and then mark the points **P2**, **P3**, **P4**, and **P5**, moving inferiorly.
10. Identify the insertion of the pectoralis major onto the Humerus. Mark point D.
11. Mark lines from each of the points (**P1**) to the insertion point.
12. Calculate 25% of each line, measuring from the origin to the insertion. Mark these distances on the lines for sites. 25% was chosen as it corresponded with the most appropriate site for assessment. Data to support this was obtained via inspection of cadaveric specimens and based on muscle bulk, muscle to tendon proportions and unrestricted access to the muscle i.e. no bone or adjacent muscle overlying the site.

Deltoid

The microelectrode placement sites utilised for the deltoid muscle correspond to those of Wickham & Brown (1998).

1. Identify the inferior border of the Clavicle.
2. Continue around the outer edge of the Acromion Process, marking the angle and down the inferior aspect of the spine of the Scapula.
3. Mould solder wire around the drawn line and cut to length.
4. Calculate 37 % of wire length for point ****D1****, mark on wire.
5. Calculate 51 % of wire length for point ****D2****, mark on wire.
6. Calculate 76 % of wire length for point ****D3****, mark on wire.
7. Calculate 83 % of wire length for point ****D4****, mark on wire.
8. Mould solder wire back onto line and mark points (****D1****).
9. Identify the deltoid Tuberosity on the Humerus. Mark point A
10. Identify the intermuscular space between the anterior head of the deltoid and the Clavicular head of the pectoralis major. Mark point F on the Clavicle.
11. Along this line measure 10 mm from the deltoid Tuberosity towards the Clavicle. Mark this point B.
12. Mark a line from the deltoid Tuberosity to the medial aspect of the Spine of the Scapula. Mark point E.
13. Along this line measure 10 mm from the deltoid Tuberosity towards the medial aspect of the Spine of the Scapula. Mark this point C.
14. Join points ****D1**** and ****D2**** to point B.
15. Join points ****D3**** and ****D4**** to point C.
16. Calculate 25% of each line, measuring from the origin to the insertion. Mark these distances on the lines for electrode placement. 25% was chosen as it corresponded with the most appropriate site for assessment. Data to support this was obtained via inspection of cadaveric specimens and based on muscle bulk, muscle to tendon proportions and unrestricted access to the muscle i.e. no bone or adjacent muscle overlying the site.

Latissimus Dorsi

1. Identify the Spinous Process of C7.
2. Count down to identify the Spinous Process of T7. Mark point A.
3. Identify the most superior point of the Illiac crest. Mark point B.
4. Identify the muscles insertion point on the Humerus. Mark point C.
5. Join point A to point B. Join both points to point C, creating a triangle.
6. Measure the distance between point A and point B.
7. Divide the distance into five equidistant compartments.
8. Identify the 50% point of each individual compartment, marking the points ****L1****, ****L2****, ****L3****, ****L4****, ****L5****, moving inferiorly.
9. Join the points (****L1****) to point C.
10. Calculate 25% of each line, measuring from the origin to the insertion. Mark these distances on the lines for electrode placement. 25% was chosen as it corresponded with the most appropriate site for assessment. Data to support this was obtained via inspection of cadaveric specimens and based on muscle bulk, muscle to tendon proportions and unrestricted access to the muscle i.e. no bone or adjacent muscle overlying the site.